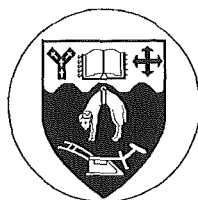


Photonitration of Aromatic Compounds by Tetranitromethane

A thesis presented
for the Degree of
Doctor of Philosophy in Chemistry
in the
University of Canterbury
by
Craig P. Butts



University of Canterbury
Christchurch
New Zealand
1996

Abstract

This thesis describes the photochemical reactions of aromatic substrates with tetranitromethane. These reactions are known to proceed *via* the initial formation of a triad of species; the aromatic radical cation, trinitromethanide ion, and nitrogen dioxide. The chemistry of these systems involves the recombination of this triad.

This thesis consists of five major parts. In the first (Chapter 2), the photochemical reactions of 1,5-dimethylnaphthalene with tetranitromethane are described. The initial step in the recombination of the triad is the reaction of trinitromethanide ion with the aromatic radical cation and this work highlights the importance of the resultant carbon radical stability to the reaction pathway. The isolation of a number of nitro-trinitromethyl adducts **221-224**, **228-229**, and hydroxy-trinitromethyl adducts **225-227**, in addition to the thermal allylic rearrangement of adduct **228** to adduct **221** is documented.

The second part (Chapter 3), discusses the photochemical reactions of 1-methoxynaphthalene with tetranitromethane. The effect of the methoxy substituent on the aromatic substrate is examined and the likely mode of formation of the trinitromethyl aromatic compound **309** and the nitro aromatic compound **306** *via* highly unstable intermediate adduct species is described. The identification of two labile nitro-trinitromethyl adducts **314** and **315** is also documented.

The third part of this thesis (Chapter 4) describes the photochemical reactions of 4-methylanisole with tetranitromethane. A solvent induced change in the regiochemistry of trinitromethanide ion attack on the radical cation is rationalised in terms of the stabilisation of the trinitromethanide ion by more polar solvent environments. Evidence was obtained indicating that the nitro-trinitromethyl adducts **423** and **424** are formed *via* an allylic rearrangement of initially formed adducts **435** in competition with the formation of the observed nitro aromatic compound **420**.

The fourth part of this thesis (Chapters 5 and 6) describes the photochemical reactions of 2-methylanisole, 2,4-dimethylanisole, 4-fluoroanisole, and 4-fluoro-3-methylanisole with tetranitromethane. The effect of

substitution of the aromatic substrate was explored and nitro-trinitromethyl adducts **518-519**, **521-522**, **617-623**, and **634-636** identified.

The final section of this thesis (Chapter 7) examines the effect of ethanol in the photolysis medium. The photochemical reactions of tetranitromethane with 1,2-dimethoxybenzene, 1,4-dimethoxybenzene, and 1,2-methylenedioxybenzene are described in addition to re-examination of the photochemical reactions of tetranitromethane with 1-methoxynaphthalene and 2-methylanisole in the presence of ethanol in the photolysis solution. Ethanol solvation of the trinitromethanide ion appears to retard nucleophilic attack on the aromatic radical cation in addition to introducing a sterically mediated change in the regiochemistry of trinitromethanide ion attack on the radical cation. A final feature of interest, the identification of highly labile nitro-trinitromethyl adducts **724** and **725** in the photolysis product mixtures of 1,4-dimethoxybenzene and tetranitromethane is also documented.

Contents

Chapter One - General Introduction.....	3
Aromatic Nitration	3
Electrophilic vs Electron Transfer Nitration.....	4
Electron Donor-Acceptor complexes	8
ArH-Tetranitromethane Systems	13
Triad recombination.....	21
Adduct formation as a general phenomena.....	25
References	37
Chapter 2 - Photolysis of 1,5-Dimethylnaphthalene.....	42
Introduction.....	42
Results	45
Discussion	63
Summary	71
References	72
Chapter 3 - Photolysis of 1-Methoxynaphthalene	73
Introduction.....	73
Results	76
Discussion	85
Summary	93
References	94
Chapter 4 - Photolysis of 4-Methylanisole.....	96
Introduction.....	96
Results	102
Discussion	111
Summary	119
References	120

Chapter 5 - Photolysis of 2-methylanisole and 2,4-dimethylanisole.....	121
Introduction.....	121
Results	124
Discussion	136
Summary	142
References	143
Chapter 6 - Photolysis of 4-Fluoroanisole and 4-Fluoro-3-methylanisole	144
Introduction.....	144
Results	147
Discussion	167
Summary	176
References	178
Chapter 7 - Photolysis in the Presence of Ethanol.....	179
Introduction.....	179
Results	181
Discussion	199
Summary	219
References	220
Experimental	221
Experimental Data Relating to Chapter 2	223
Experimental Data Relating to Chapter 3	231
Experimental Data relating to Chapter 4	238
Experimental Data Relating to Chapter 5	244
Experimental Data Relating to Chapter 6	252
Experimental Data Relating to Chapter 7	265
Crystallography	278
References	296

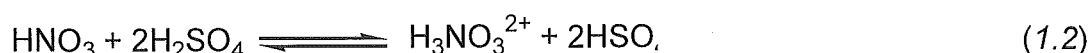
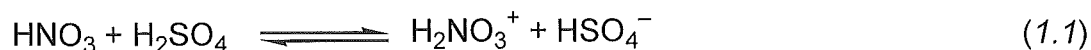
Chapter One

Introduction

Aromatic Nitration

Aromatic nitration has been one of the keystones of organic mechanistic studies in the past. Despite the extensive research into this area, questions still remain over key features of the reaction mechanism. By 1960, the nitronium ion (NO_2^+) was generally accepted¹ as the active nitrating species under “normal” nitration reaction conditions, e.g. nitric acid in sulphuric acid or organic solvents. The nitronium ion was first suggested by Euler² in 1903, and in later years a number of techniques were employed to implicate it in nitration reaction mixtures, however its existence was not demonstrated conclusively until 1946 by Ingold *et al.*³

In 1908 Hantzsch performed a cryoscopic investigation of sulphuric acid solutions.⁴ Nitric acid was one of the solutes used in this study and was assumed to be protonated in one of two ways, as shown in Equations (1.1) and (1.2).

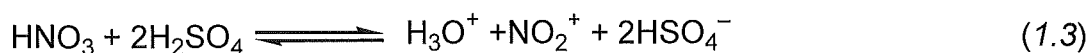


A study of the freezing point depressions induced by the nitric acid solute gave a van't Hoff *i*-factor of 3 (three-fold depression) indicating that nitric and sulphuric acids formed three ionic species on mixing. Hantzsch thence concluded that Equation (1.2) was the dominant reaction, and $\text{H}_3\text{NO}_3^{2+}$ the principal nitrating species in nitric/sulphuric acid mixtures. His findings were qualitatively supported by Robles and Moles.⁵

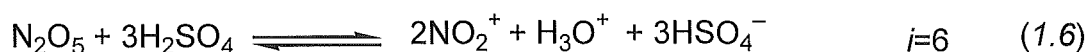
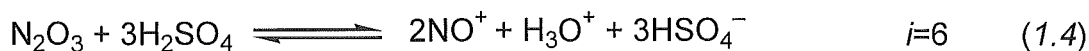
In 1934 Médard⁶ observed two frequencies, 1050 and 1400 cm^{-1} , in Raman spectra of nitric-sulphuric acid mixtures but had no reasonable explanation for these features, subsequently Chédin observed these same frequencies for anhydrous nitric acid solutions.⁷ Dinitrogen pentoxide (N_2O_5) was proposed as the source of the signals, however he obtained entirely different spectra on examining solutions of N_2O_5 in aprotic solvents. The idea

was presented⁸ that in acidic solutions dinitrogen pentoxide was ionised to form nitronium ion (NO_2^+) and nitrate ion (NO_3^-). These speculations were supported by further spectroscopic study,³ and the two Raman frequencies were eventually assigned to these two ionic species.

The advent of improved cryoscopic techniques by Hammett⁹ led Ingold *et al.*³ to re-examine Hantzsch's work. Using these new methods, a van't Hoff *i*-factor of 3.82 was measured which, when adjusted for the presence of an equilibrium in the system, became an exactly 4-fold depression. This was interpreted as arising from the reaction described in Equation (1.3).



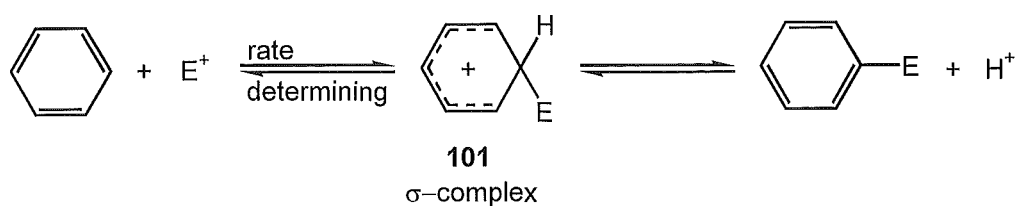
Similar experiments performed on dinitrogen trioxide, tetroxide, and pentoxide gave *i*-factors of 5.85, 5.84, and 5.85 respectively. Allowing for equilibrium conditions these factors became exactly 6. These cryoscopic results were interpreted as arising as a result of the equilibria given in Equations (1.4), (1.5), and (1.6) respectively.



Nitronium ion, NO_2^+ was consequently accepted as the active nitrating species in these reactions, particularly as its electrophilic nature made it a reasonable candidate as a reactive species given analogous reactions known at that time.

Electrophilic vs Electron Transfer Nitration

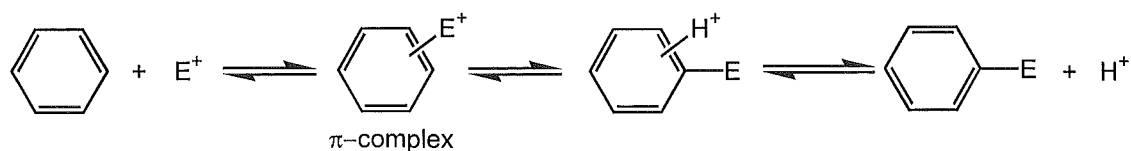
As no kinetic isotope effect is observed in many electrophilic aromatic substitution reactions, the generally accepted mode of reaction is a two-step mechanism proceeding *via* a Wheland intermediate or σ -complex **101** (Scheme 1.1).¹⁰



Scheme 1.1

The addition of the electrophile (E^+) is thus the rate limiting step and the subsequent proton loss has no kinetic significance. In the case of nitration however, there are difficulties with this mechanism. For aromatic compounds more reactive than toluene, the rate of nitration is encounter limited and thus all such aromatics react at the same rate.¹¹ The encounter limited rate implies that NO_2^+ reacts instantly with any aromatic molecule it encounters and would also, if the mechanism described in Scheme 1.1 were to hold true, react non-selectively, *i.e.* at the nearest site on the aromatic ring. This would lead to a statistical distribution of NO_2 substitution at all carbon positions around a substituted aromatic. Contrary to this, regioselectivity *is* observed on nitration of substituted aromatics, *e.g. para* and *ortho* substitution predominate in nitration of toluene by solutions of mixed nitric and sulphuric acids.¹² These two contradictory results imply a deficiency in the proposal in Scheme 1.1 when applied to nitration.

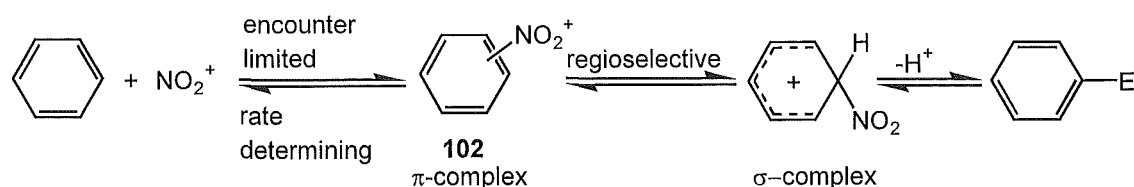
Dewar suggested the importance of π -complexes in electrophilic aromatic substitution reactions in 1946 (Scheme 1.2).¹³



Scheme 1.2

Subsequently Olah and co-workers¹² invoked this theory on finding that the relative rates of nitration by nitronium salts resembled the relative stability of the loose π -complexes formed by aromatic compounds with weak electrophiles

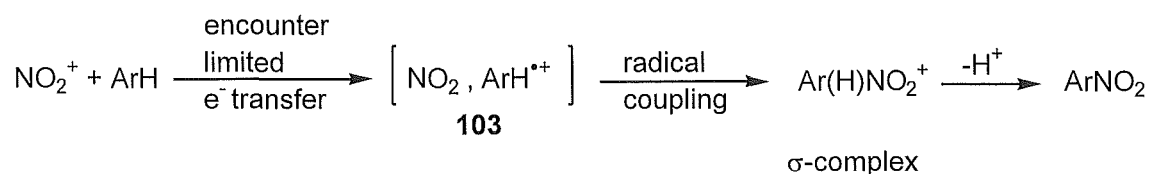
(Br₂, I₂).¹⁴ The suggestion was that formation of the π -complex **102** between NO₂⁺ and the aromatic π -system occurred prior to addition and generation of the σ -complex **101** (Scheme 1.3).



Scheme 1.3

The second (regioselective) step is thus independent of the first, rate determining, step, allowing both encounter limited reaction rates and regiospecific substitution. This proposal became the focus of discussion in the mechanistic debate, and questions were raised regarding Olah's experimental technique among other matters.^{1,15,16}

In 1978, Perrin¹⁶ questioned the ability of NO₂⁺ to be regioselective when in a π -complex and not when free in solution. As an alternative to Olah's ideas he resurrected an earlier theory regarding the mode of formation of the σ complex. This mechanism, first proposed by Kenner¹⁷ and Weiss,¹⁸ involved initial electron transfer between NO₂⁺ and the aromatic (Scheme 1.4, overleaf).



Scheme 1.4

This electron transfer mechanism replaces the intermediate π -complex **102** of Scheme 1.3 with the radical - radical cation pair **103** which still allows differentiation between intermolecular and intramolecular (regiochemical) selectivity. Perrin suggested that as the \cdot NO₂ species involved in intramolecular selectivity is different from the NO₂⁺ involved in the first (intermolecular) step then the paradox of selectivity can be explained. To support this postulate, he

reported electrochemical experiments with naphthalene. In these experiments a mixture of naphthalene and $\cdot\text{NO}_2$ in CH_3CN was electrochemically oxidised at anodic potentials able to oxidise naphthalene to naphthalene $^{+\cdot}$ but insufficient to also oxidise $\cdot\text{NO}_2$. The products from this supposed reaction of $\cdot\text{NO}_2$ and naphthalene $^{+\cdot}$ were then analysed and found to be a mixture of 1- and 2-nitronaphthalenes, with a 1-/2- substitution ratio of 9.2.1 which Perrin compared with the 10.9 ratio for the nitration of naphthalene with $\text{HNO}_3/\text{H}_2\text{SO}_4/\text{urea}$ in CH_3CN . He claimed that these results were equal within experimental error and thus the reaction pathway in both cases was likely to be the same, *i.e.* nitric acid nitration involved the same intermediates, $\cdot\text{NO}_2$ and naphthalene $^{+\cdot}$, as the electrochemical nitration and consequently must involve an initial electron transfer step.

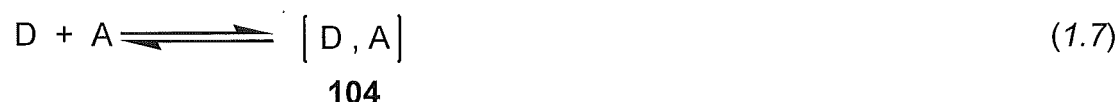
These findings were criticised by Ebersson and co-workers¹⁹ because of deficiencies in the experimental methods employed by Perrin. Rate measurements made on control reactions of Perrin's electrochemical experiments, using only $\cdot\text{NO}_2$ and naphthalene without anodic oxidation, revealed that at least 40-60% of the reaction products seen under oxidising conditions were independent of the generation of the radical cation, *i.e.* they were derived from the thermal reaction of $\cdot\text{NO}_2$ and naphthalene. Ebersson also observed an entirely different 1-/2- substitution ratio (*ca.* 20) when performing the electrochemical experiment, but he was not able to rationalise the difference between his and Perrin's ratio. In addition, Ebersson noted that anodic oxidation could not avoid the formation of H^+ at the anode, and that the thermal reactions of $\cdot\text{NO}_2$ and naphthalene were promoted by acid. Thus the measurements in the control reactions gave merely a lower limit to the rate of $\cdot\text{NO}_2$ -naphthalene reaction in the electrochemical experiments. These results led Ebersson to state that Perrin's observations were almost exclusively the result of $\cdot\text{NO}_2$ -naphthalene reactions, and that the electron transfer mechanism, while not completely excluded, was not supported by the existing experimental evidence.

In 1986, Kochi *et al.*²⁰ claimed the formation of a genuine solvent caged radical - radical cation pair similar to **103**, consisting of anthracene $^{+\cdot}$ and $\cdot\text{NO}_2$, in the presence of a weakly nucleophilic species, trinitromethanide ion

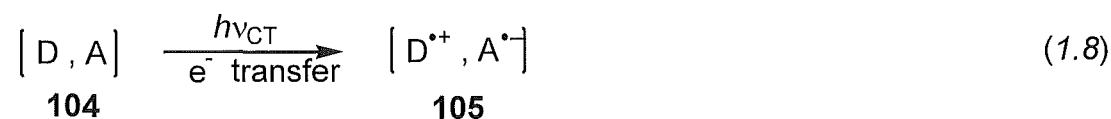
$[\text{C}(\text{NO}_2)_3^-]$. This was achieved this by specific irradiation of the charge transfer band of the electron donor-acceptor (EDA) complex generated when tetranitromethane $[\text{C}(\text{NO}_2)_4]$ and an aromatic species are mixed.

Electron Donor-Acceptor complexes

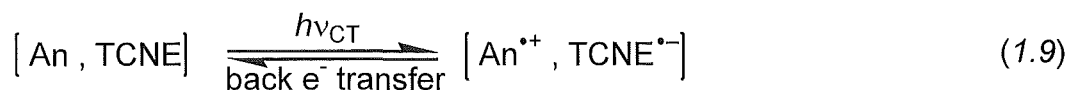
EDA complexes have been recognised as intermediates in many reaction processes.²¹ When they have been characterised as such, they exist as the weakly bound species **104** in equilibrium with the parent components^{22,23} [Equation (1.7)].



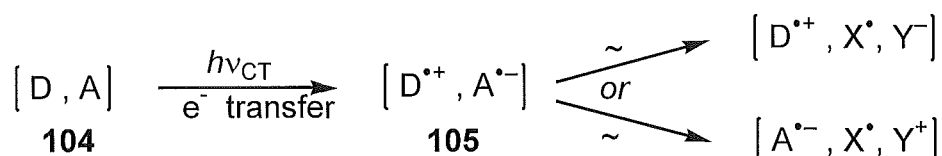
Accompanying the formation of EDA complexes is the generation of often intense colour which Mulliken²³ assigned to the charge transfer transition of an electron from an occupied molecular orbital of the donor to an unoccupied orbital localised on the acceptor. Irradiation at wavelengths corresponding to the absorption bands of species **104** will induce electron transfer, resulting in the formation of a radical cation - radical anion pair **105** [Equation (1.8)], examples of which have been observed by time-resolved spectroscopy and identified by the absorption characteristics of the two individual components, $\text{D}^{\bullet+}$ and $\text{A}^{\bullet-}$.²⁴



For cases where both the anion and cation are structurally stable, **105** undergoes rapid back electron transfer to the EDA complex **104**. One such system is the anthracene (An) - tetracyanoethylene (TCNE) donor acceptor complex [Equation (1.9)],²⁴ where the high rate of back electron transfer means that no significant concentration of the ion pair is achieved and consequently no photochemistry is observed in this system, even on prolonged irradiation.



In contrast, formation of a sufficiently unstable cation or anion can preclude back electron transfer by fragmentation of one or other of the components (Scheme 1.5). Recombination of these fragments leads to efficient charge transfer photochemistry.²⁵



Scheme 1.5

An example of this occurs for the acceptor tetranitromethane, which pulse radiolysis studies²⁶ have shown yields an unstable radical anion on electron capture and subsequent rapid fragmentation of the radical anion to give $\cdot\text{NO}_2$ and $\text{C}(\text{NO}_2)_3^-$.

Kochi *et al.* examined the charge transfer processes in the photochemistry of substituted anthracene - tetranitromethane EDA complexes²⁷ by pico-second absorption spectroscopy. Charge transfer absorption spectra (Figure 1.1, overleaf) of the EDA complex of anthracene and tetranitromethane (in dichloromethane) demonstrate that although the absorption maxima of the EDA complex is below 400 nm, it does absorb above this. In contrast, the two individual components of the EDA complex, TNM and anthracene, do not absorb significantly above approximately 410 nm. Thus irradiation of the anthracene -tetranitromethane electron donor acceptor complex at wavelengths longer than 410 nm will excite the complexes while not altering the energies of the individual components.

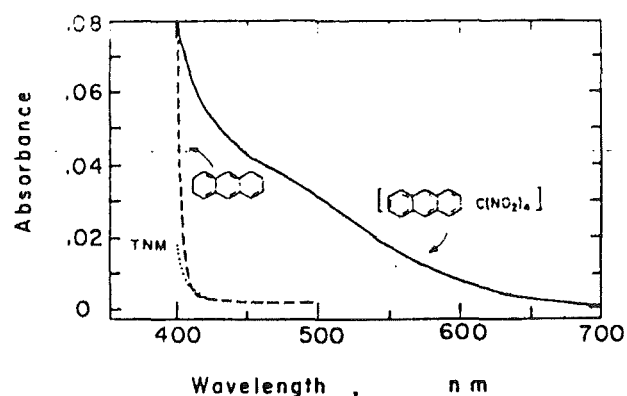


Figure 1.1 - Charge transfer absorption spectra of the EDA complex of anthracene and tetranitromethane.

Specific irradiation of the charge transfer bands of EDA complexes between various substituted anthracenes and tetranitromethane with light of 532 nm wavelength, generated the arene radical cations as expected. The identity of the radical cation absorption spectra were confirmed by comparison with absorption spectra of radical cations generated by anodic oxidation (Figure 1.2).

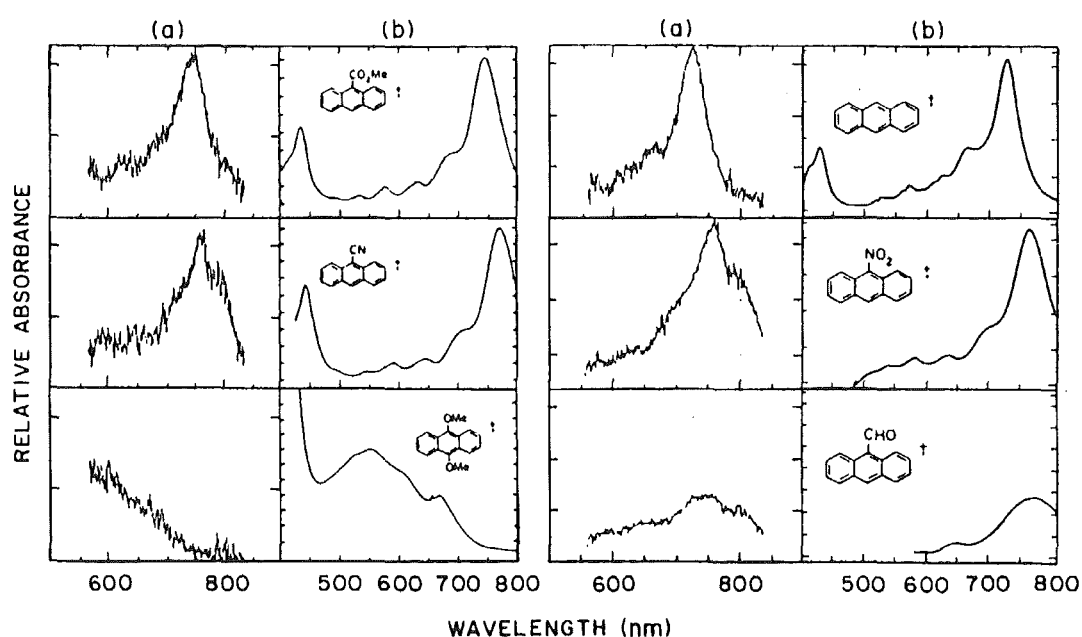
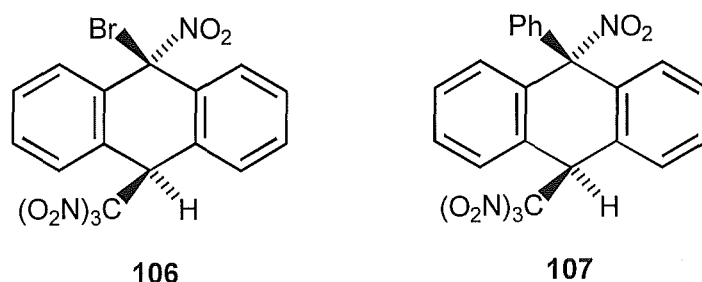
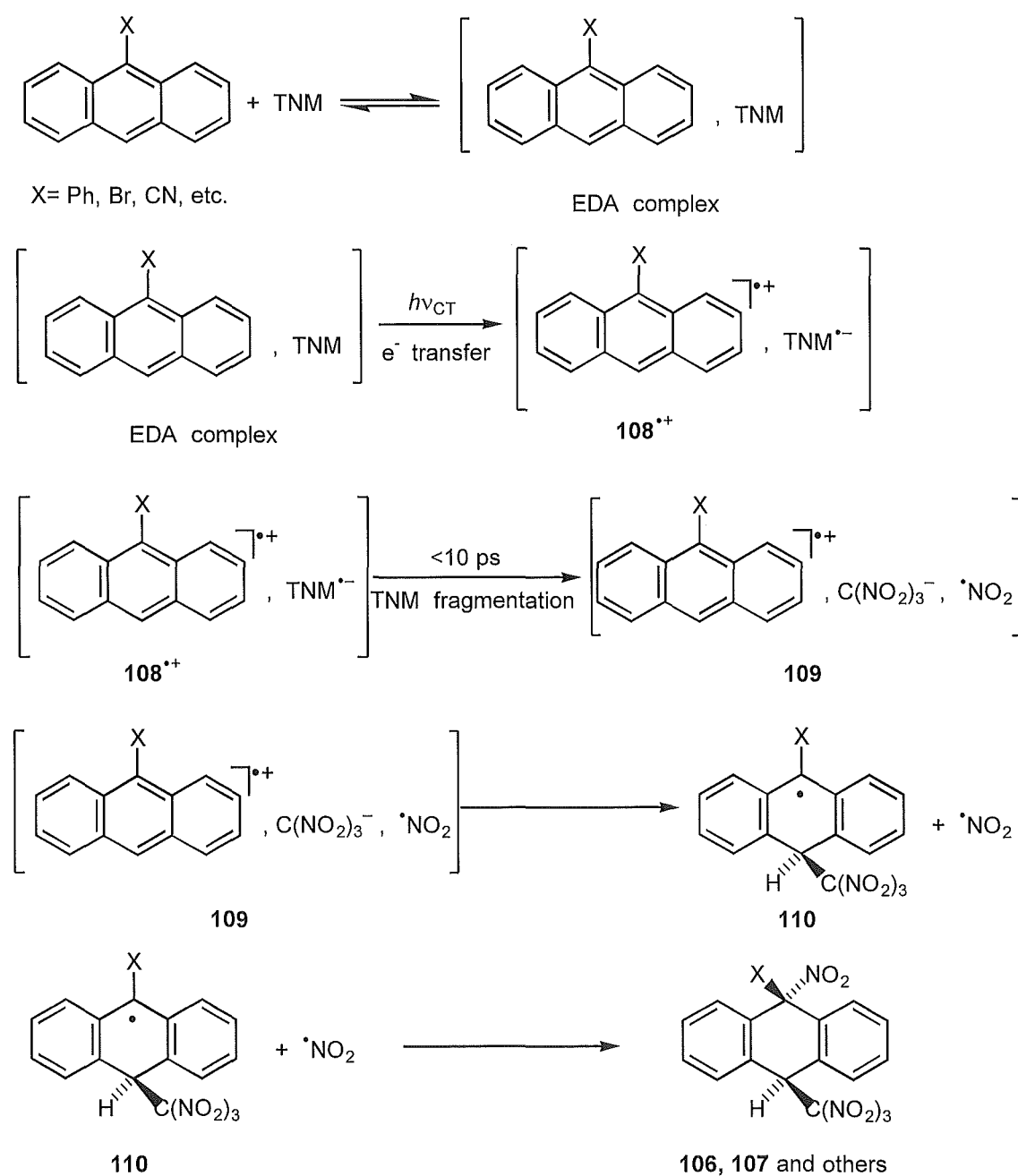


Figure 1.2 - Absorption spectra of radical cations generated by (a) Irradiation of the EDA complex between the aromatic compound and tetranitromethane, and (b) by anodic oxidation.

The lifetimes of these radical cations were found to be substantially longer than those generated using TCNE as the acceptor, and photoproducts were generated in the mixture with a high quantum yield (*ca.* 0.8),²⁸ demonstrating the relatively low rate of back electron transfer in these systems. The structures of the principal photoproducts from photolysis of the 9-bromo- and 9-phenyl-anthracenes with tetranitromethane, **106** and **107** respectively, were established by X-ray crystallography.



The addition of trinitromethyl and nitro moieties to the central ring of the anthracene arene system demonstrates the fragmentation of the tetranitromethanide radical anion. Kochi and co-workers further confirmed the previous pulse radiolysis studies²⁶ of the tetranitromethanide radical anion fragmentation by irradiating solutions of hexamethylbenzene and tetranitromethane and observing simultaneously the generation of trinitromethanide ion, $C(NO_2)_3^-$ and the hexamethylbenzene radical cation within a 25 ps laser pulse. The inability to detect tetranitromethanide radical anion in the experiment led Kochi to propose that it decayed in less than 10 ps (the resolution of the experiment). Given these results, Kochi outlined a complete mechanistic hypothesis (Scheme 1.6, overleaf) for the electron transfer, fragmentation, and subsequent recombination reactions of anthracenes with tetranitromethane.



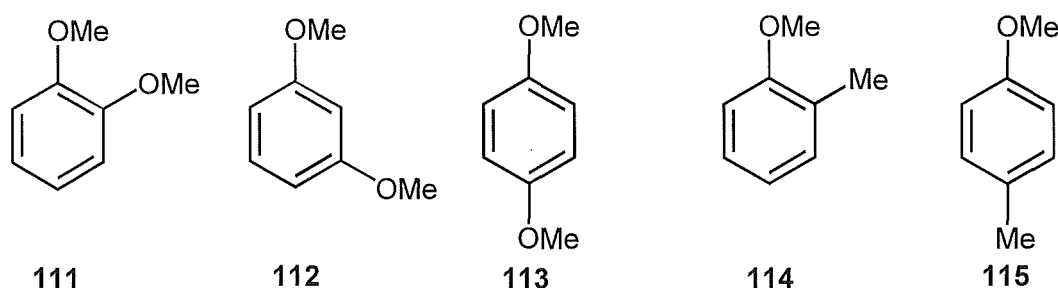
Scheme 1.6

The three components **109** in Scheme 1.6 were termed the “triad” and on the basis of the rapid time-scale of their formation, it was assumed that they were solvent caged and recombined independently of other triads in the solution. Kochi observed the decay of absorption bands due to **108^{•+}** between 100 ps and 4 ns after irradiation and simultaneously a rise in a new band near 550 nm which was assigned, by comparison with related spectra,²⁹ as belonging to hydranthryl radical **110**. The regiospecificity of the trinitromethanide ion addition in this step was stated as being consistent with formation of the stable *meso*

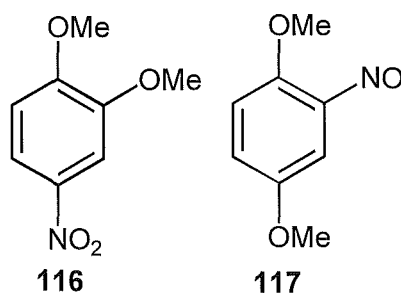
radical, from which photoadducts **106**, **107**, and others are formed by addition of $\cdot\text{NO}_2$.

ArH-Tetranitromethane Systems

Kochi and Sankararaman extended the study of the photochemistry of tetranitromethane with aromatic substrates by using various methoxybenzenes as donors.³⁰ They examined the reactions of 1,2-dimethoxybenzene **111**, 1,3-dimethoxybenzene **112**, 1,4-dimethoxybenzene **113**, 2-methylanisole **114**, and 4-methylanisole **115**.

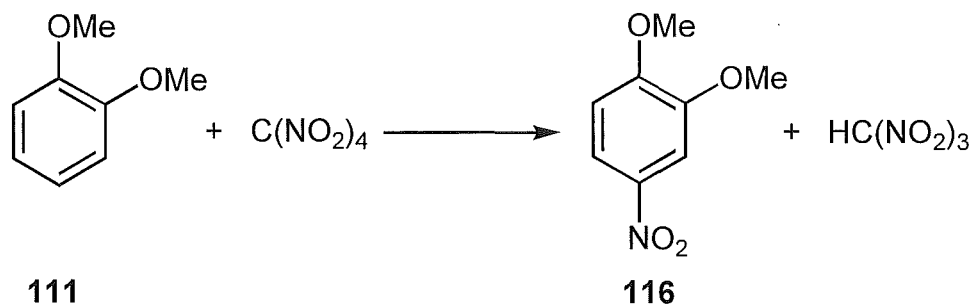


Examination of photoproducts formed on irradiation of the charge transfer band of the EDA complexes of tetranitromethane with the various methoxybenzenes revealed two distinct product types. GC-MS analysis of mixtures derived from photolysis of solutions of tetranitromethane with dimethoxybenzenes **111** and **113** showed in near quantitative conversion into nitro aromatic species **116** (98%) and **117** (92%) respectively.



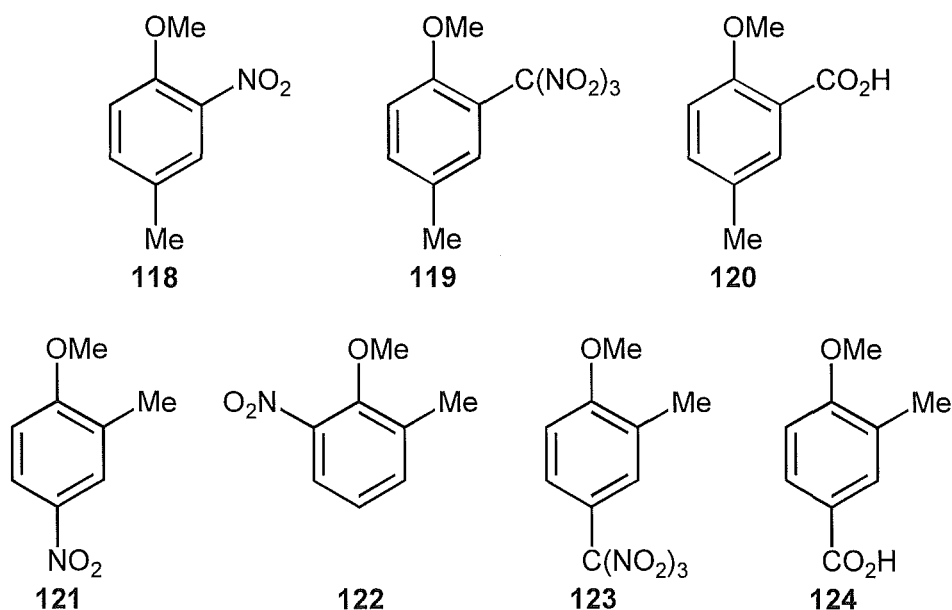
For these reactions, the trinitromethanide ion is converted into nitroform $[\text{C}(\text{NO}_2)_3]$ in molar equivalence to the nitro aromatic compounds formed. The stoichiometry of the reaction was consequently assigned typically as shown in

Scheme 1.7. Similar experiments using 1,3-dimethoxybenzene as the donor resulted in formation of only one nitro aromatic compound and at least three further unidentified products of higher molecular mass.

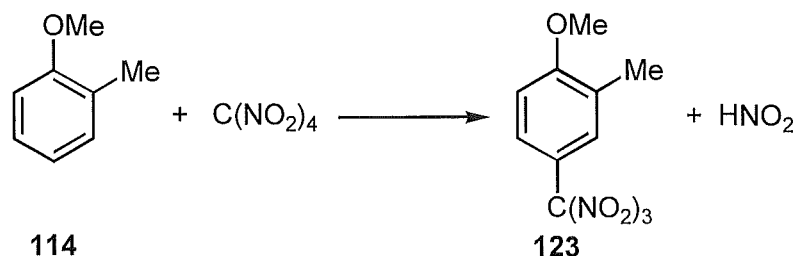


Scheme 1.7

In contrast to the predominant nitration observed for these dimethoxybenzenes, photolysis of a solution of tetranitromethane and 4-methylanisole **115**, yielded less than 5% (by GC) of the nitro aromatic compound **118** while the majority of the mixture (70%) was found to be trinitromethyl derivative **119**. The latter compound, **119**, was characterised by hydrolysis to the known carboxylic acid **120**. Similarly, photolysis of a solution of 2-methylanisole **114** and tetranitromethane, yielded only small amounts of nitro aromatic compounds **121** and **122**, (10% and 6% respectively) and much higher yields of the trinitromethyl compound **123** (60%), again identified by hydrolysis to the corresponding carboxylic acid **124**.

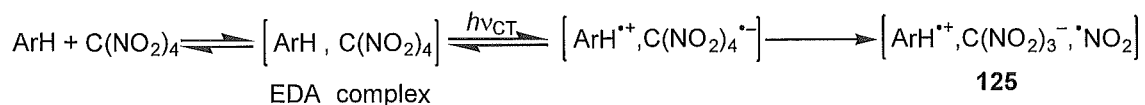


In these reactions Kochi suggested that the third member of the triad, $\cdot\text{NO}_2$, was converted into one equivalent of the unstable nitrous acid, e.g. Scheme 1.8.



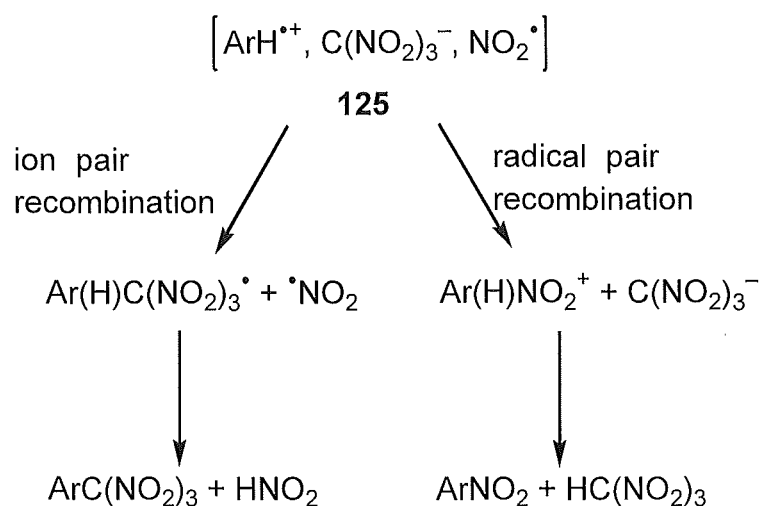
Scheme 1.8

Kochi rationalised these results by assuming that all of the EDA complexes underwent the same initial steps, forming the triad **125** (Scheme 1.9).



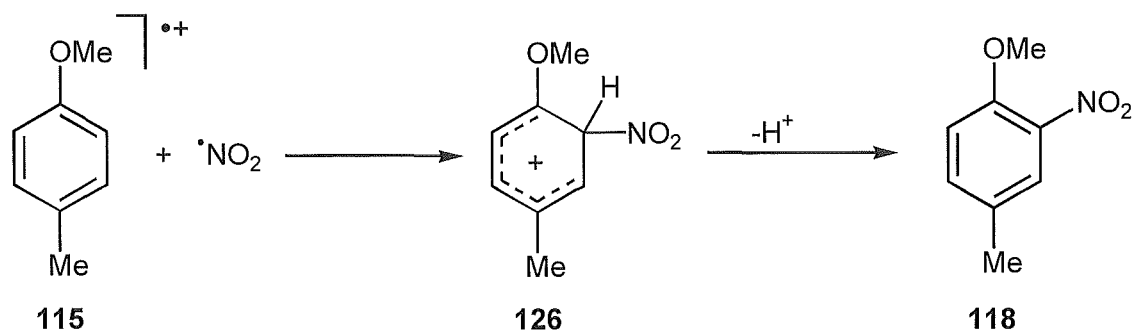
Scheme 1.9

The recombination of this triad to yield the photoproducts occurs in subsequent reaction steps. He assumed that product formation from the recombination of **125**, simply involved competition between radical pair ($\cdot\text{NO}_2$, $\text{ArH}^{\bullet+}$) recombination and ion pair $[\text{C}(\text{NO}_2)_3^{\bullet-}, \text{ArH}^{\bullet+}]$ recombination (Scheme 1.10).



Scheme 1.10

The radical pair recombination was assumed to proceed *via* a σ -complex species which could subsequently undergo proton loss to yield the nitro aromatic compound, as shown in Scheme 1.11 for 4-methylanisole.



Scheme 1.11

The regioselectivity of $\bullet\text{NO}_2$ addition in the initial radical pair collapse was rationalised in terms of the higher stability of the Wheland intermediate **126** in which one resonance form (denoted **126a** in Figure 1.3, overleaf) is substantially stabilised by the methoxy group. The alternative regiochemistry would be derived from Wheland intermediate **127** for which the methyl group stabilises the position of positive charge in one resonance structure (**127a**).

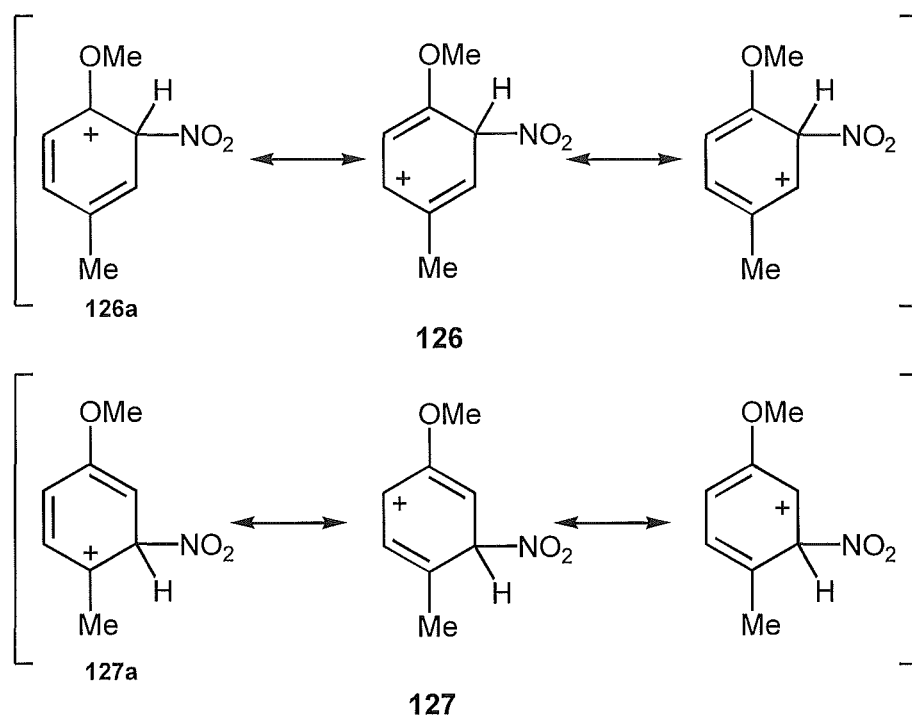
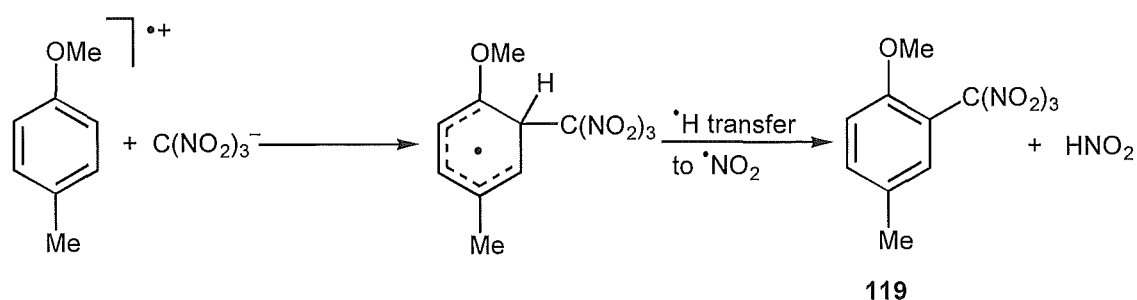


Figure 1.3

Kochi was less clear regarding the sequence of events following ion pair collapse, describing it as “ionic annihilation” and comparing it to previous studies of anodic methoxylation and cyanation.³¹ However, the extent of his mechanistic interpretation of the process is summarised in Scheme 1.12.

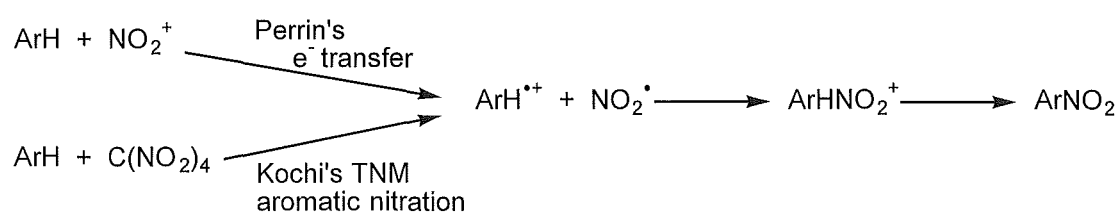


Scheme 1.12

In this case Kochi stated that the regioselectivity of trinitromethanide ion addition was governed by spin (charge) density in the LUMO of the radical cation, *i.e.* high charge density at a given site on the radical cation would lead to preferred bond formation at this site. No justification was presented at this

point for the change from nitration of dimethoxybenzenes to trinitromethylation of the corresponding methylanisoles.

Having stated that nitration of the dimethoxybenzenes by tetranitromethane proceeded *via* radical pair collapse ($\cdot\text{NO}_2 + \text{ArH}^{\cdot+}$) within the triad and was independent of the “spectator” trinitromethanide ion, Kochi and co-workers claimed that these³⁰ and related aromatic ether systems³² were models for the intermediate steps of the electron transfer mode of aromatic nitration which Perrin had proposed earlier (Scheme 1.13).



Scheme 1.13

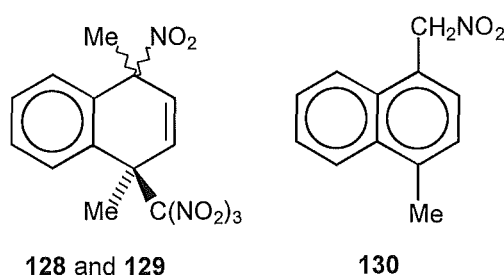
To extend the support for Perrin's theory, Kochi compared³³ the product yields of various thermal nitrations of naphthalene and methyl substituted naphthalenes with the corresponding photochemical charge transfer nitrations using tetranitromethane. In the case of naphthalene he claimed that Perrin's¹⁶ and Ebersson's¹⁹ use of 1-/2- nitro substitution patterns was invalid given the very small quantities of 2-nitronaphthalene formed. His explanation was that small changes in 2-nitro yield, particularly those due to experimental error, would have a magnified effect on the ratio calculated and consequently Kochi quoted only absolute yields in this work (Table 1.1).

Table 1.1 - Thermal and Photochemical Nitrations of Naphthalene

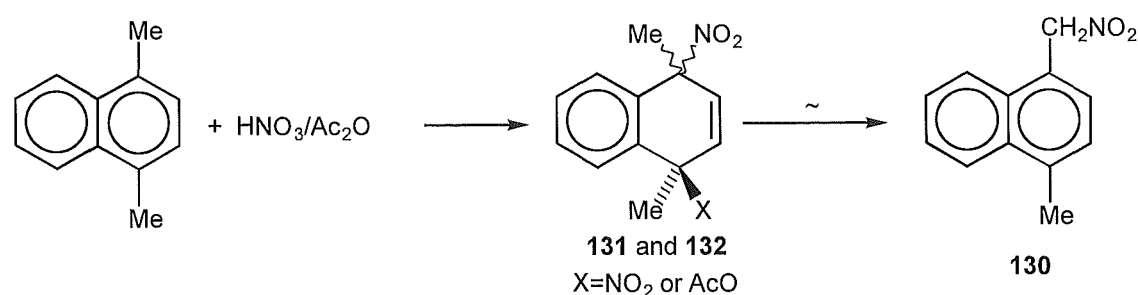
Method	Reagent	Solvent	T/°C	1-NO ₂ (mol%)	2-NO ₂ (mol%)
Thermal	HNO ₃	Ac ₂ O	0	94	6
Thermal	PyNO ₂ ⁺ BF ₄ ⁻	MeCN	25	89	9
Thermal	HNO ₃ /NaN ₃	Ac ₂ O	0	95	4
Charge Transfer	pyNO ₂ ⁺ BF ₄ ⁻	MeCN	-40	83	15
Charge Transfer	C(NO ₂) ₄	MeCN	25	82	11

Kochi's interpretation of this data was that the yields in each case were essentially the same, thus supporting his postulate that thermal nitrations involved the same intermediate species ($\cdot\text{NO}_2$ and $\text{ArH}^{\cdot+}$) as the charge-transfer experiments.

The study of the photonitration of methylnaphthalenes with tetranitromethane, in particular 1,4-dimethylnaphthalene, was hindered by the generation of significant quantities (45% in CH_2Cl_2 at 0°C) of *ipso* adducts **128** and **129** of the type previously seen²⁸ in anthracene-TNM systems.



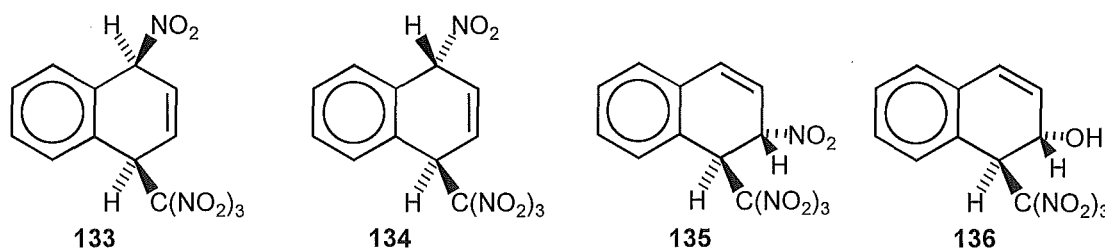
These adducts were observed in ^1H n.m.r. spectra of crude reaction mixtures in a 1:4 *cis:trans* ratio in dichloromethane and the structure of the *trans*-isomer was confirmed by X-ray crystallography. This adduct was also observed to rearrange cleanly to the side chain nitro aromatic **130** when left in solution at room temperature. Kochi compared the *ipso* adducts to those found by Fischer and Wilkinson³⁴ on reaction of 1,4-dimethylnaphthalene with $\text{HNO}_3/\text{Ac}_2\text{O}$ nitrating mixtures where adducts **131** and **132** were also known to rearrange to the side chain nitro aromatic **130** (Scheme 1.14).



Scheme 1.14

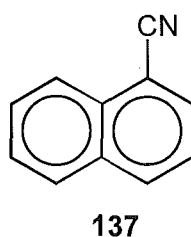
As the formation of these adducts, and their subsequent rearrangements, made the exact origin of any observed nitro aromatic in this system unclear, Kochi stated that, for the 1,4-dimethylnaphthalene system in particular, it was not possible to differentiate between electrophilic ($\text{NO}_2^+ + \text{ArH}$) and charge transfer ($^{\bullet}\text{NO}_2 + \text{ArH}^{\bullet+}$) nitration.

In response to these findings, Ebersson *et al.* provided evidence³⁵ that Kochi's naphthalene data was similarly flawed and the use of GC product analysis in this case had obscured the results. Ebersson found that 85-95% of the products formed in the photochemical reaction between naphthalene and tetranitromethane were trinitromethyl-nitro- or trinitromethyl-hydroxy-dihydronaphthalene adducts **133-136**.



The cis 1-nitro-4-trinitromethyl adduct **133** was isolated in pure form and fully characterised by ^1H , ^{13}C and heteronuclear n.m.r. techniques.

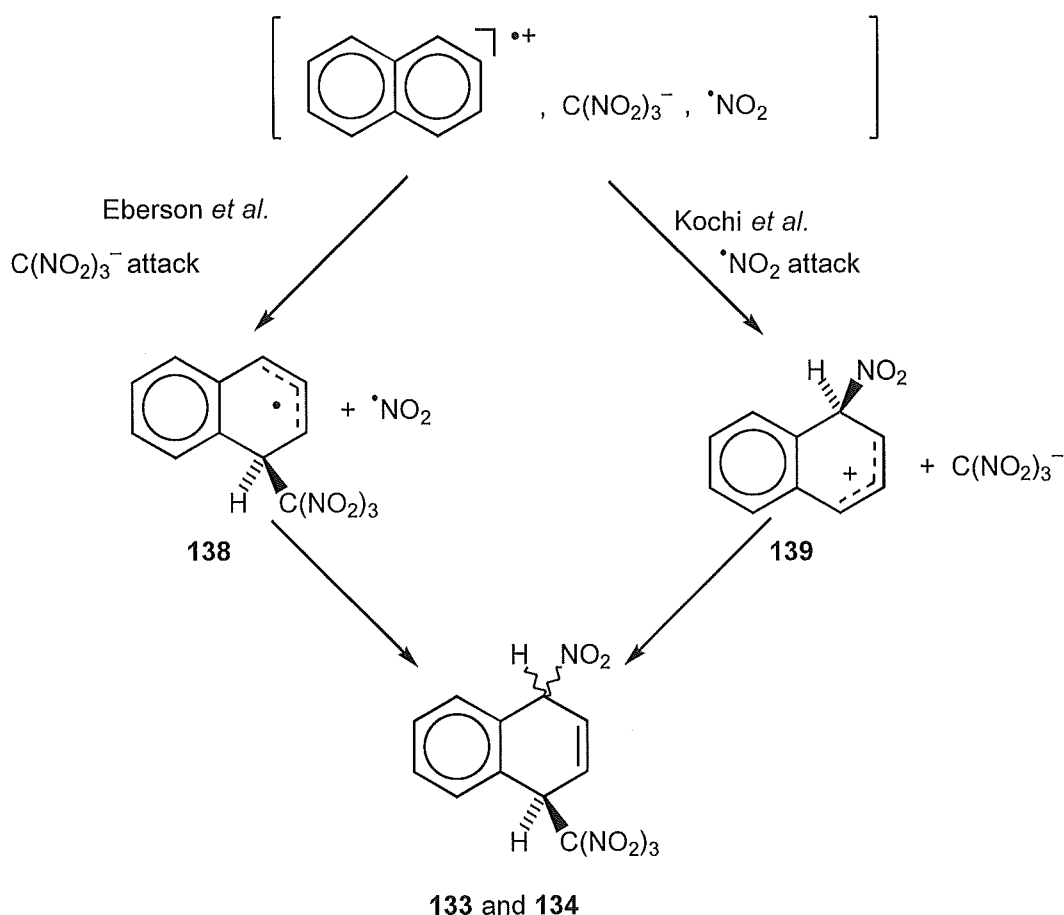
It was noted that Kochi's product analysis of naphthalene-TNM photolysis mixtures (where he claimed no adducts were present) was performed by GC (with injection port temperatures of 100°C), and injection of pure **133** into GC apparatus at various injection port temperatures revealed its clean decomposition into 1-nitronaphthalene at temperatures between 100 and 200°C . Above this temperature, the product composition became a mixture of naphthalene, 1- and 2-nitronaphthalenes, and small quantities of 1-naphthonitrile **137**.



Eberson also observed the spontaneous decomposition of adduct **133** to 1-nitronaphthalene by loss of nitroform, when left in solution (both CD₃CN and CD₃OD) for any length of time. This, coupled with the GC results showed that care was necessary when examining the system as the formation of these unstable intermediates could be a major pathway to the observed 1-nitronaphthalene. A similar nitroform elimination from **135** was proposed as one source of the 2-nitronaphthalene observed by Kochi *et al.* and further, Eberson claimed that most, if not all, of the products previously identified by Kochi in the photochemical reactions of naphthalene and tetranitromethane were derived from an addition-elimination mechanism. As the details of this mechanism were as yet unclear, it was stated that "this makes the nitro isomer distributions from the tetranitromethane induced photonitration of aromatics of limited use for mechanistic discussions of electrophilic nitration by nitronium ion."³⁵

Triad recombination

The main feature of the addition-elimination mechanism of tetranitromethane-ArH photochemistry which was not clearly understood was the first step in the recombination of the components of the triad. Contrary to their previous statements²⁸ regarding the mechanism of formation of adducts in anthracene-tetranitromethane systems, Kochi *et al.*³³ asserted that, for 1,4-dimethylnaphthalene-tetranitromethane photolysis systems, *radical* pair bond formation was the first step of the triad recombination. Eberson *et al.*³⁶ on the other hand, examined the effect of added acid to photolysis systems and concluded that trinitromethanide anion - aromatic cation coupling was the initiating step of triad recombination. These two competing views are illustrated for the case of naphthalene in Scheme 1.16 (overleaf).



Scheme 1.16

Ebersson argued that Kochi's Wheland intermediate **139** would be more likely to lose a proton than to couple with the trinitromethanide ion, however hydrogen atom transfer from the delocalised radical **138** would be less favourable than the competing $\cdot\text{NO}_2$ addition. To support the theory of initial trinitromethanide ion attack, Ebersson *et al.* noted that added acid would reduce the nucleophilicity of the trinitromethanide ion in the triad by protonation to give the less nucleophilic nitroform $[\text{HC}(\text{NO}_2)_3]$,³⁷ resulting in slower or no reaction of trinitromethanide ion with the radical cation in the triad. Thus if the reaction proceeds by Ebersson's mechanism in Scheme 1.16, the rate of triad recombination will be reduced and given the longer lifetime of the radical cation its observation might be possible by e.p.r. in at least some ArH-tetranitromethane systems. To test this hypothesis, Ebersson *et al.* examined the e.p.r. spectra of a large number of aromatic species generated on photolysis with tetranitromethane in dichloromethane, with and without added acid.

Trifluoroacetic acid (TFA) was judged to be a suitable protic acid for these studies as it was found to be only approximately 0.5 p*K* unit weaker than nitroform in dichloromethane. The addition of a tenfold excess of TFA to trinitromethanide ion would therefore be sufficient to reduce trinitromethanide ion concentrations to <1% of their original value.

The e.p.r. spectra were measured under three sets of photolysis conditions:-

Solution 1: Standard reaction conditions - ArH (20-40 mmol dm⁻³), TNM (0.8 mol dm⁻³), dichloromethane and irradiation for 6 minutes.

Solution 2: Standard reaction conditions + trifluoroacetic acid (0.4 mol dm⁻³).

Solution 3: Control reaction, as for (2) but without tetranitromethane.

Results for these experiments are shown in Table 1.2. The ratio tabulated was calculated from the relative increase in spectral intensity between Solution 1 and Solution 2 studies.

Table 1.2 - E.p.r. spectral intensities on photolysis of ArH/TNM solutions with and without added trifluoroacetic acid

ArH	e.p.r. spectral Intensity			Ratio
	Soln 1	Soln 2	Soln 3	
	C(NO ₂) ₄	C(NO ₂) ₄ + TFA	TFA	
Naphthalene	<2	<2	<2	1
1-Methylnaphthalene	<2	<2	<2	1
1,4-Dimethylnaphthalene	<2	10	<1.5	>5
1,2-Dimethylnaphthalene	<2.5	54	<2	>22
1,8-Dimethylnaphthalene	<2	16	4	>8
1,4,6,7-Tetramethylnaphthalene	<.7	52	4	>74
1,4,5,8-Tetramethylnaphthalene	<1.8	100	5	>55
1,3,5,8-Tetramethylnaphthalene	<2	44	2.6	>22
1,4-Dimethoxybenzene	<2	540	<2	>270
9-Phenylanthracene	<1.8	100	8	>56
9,10-Diphenylanthracene	2.6	300	6.5	115
Perylene	8	230	25	106
Tris(4-bromophenyl)amine	19	181	3.2	9.5
9,10-Dimethylantracene	<1	600	4.6	>600

These data show that only a few of the substrates exhibited measurable e.p.r. activity under solution 1 conditions but addition of trifluoroacetic acid (Solution 2) to the system caused nearly all of the substrates studied to exhibit significantly increased e.p.r. activity; the resulting spectra were positively identified as the appropriate radical cation (or dimer radical cation $(ArH)_2^{*+}$) in most cases. Control reactions with only trifluoroacetic acid and the aromatic substrate present (Solution 3) were performed to ensure that the radical cations observed were not the result of oxidation of the substrate by the acid. In most cases this oxidation was not significant. The large increase in e.p.r. activity on addition of the acid supported Ebersson's theory regarding the increase in the lifetime of the aromatic radical cation, and that this prolonged lifetime was a direct result of reduced trinitromethanide ion activity. Consequently the remaining pathway available to the triad involved nitrogen dioxide - aromatic radical cation radical coupling. This was demonstrated in the product analysis of naphthalene/tetranitromethane/trifluoroacetic acid photolysis mixtures (Table 1.3), where significantly reduced adduct yields were observed. The high 1-/2-nitronaphthalene product ratios (up to 63) obtained are typical for this *NO_2 /radical cation coupling reaction in naphthalene.¹⁹

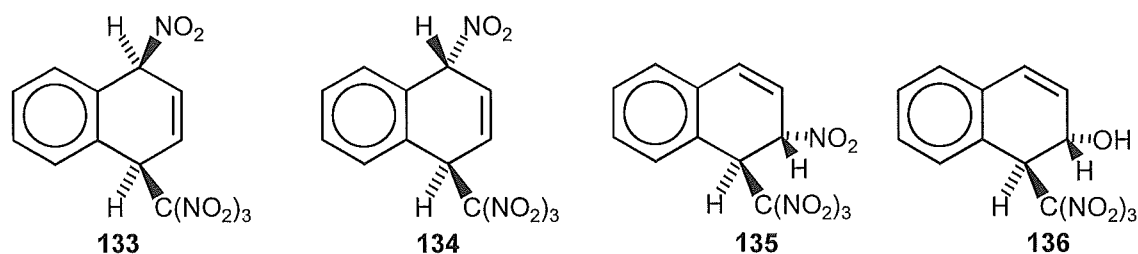
Table 1.3 - Product yields on photolysis of naphthalene/tetranitromethane/trifluoroacetic acid solutions.

TFA (mol dm ⁻³)	Relative yields (%) of			1-:2-NO ₂ ratio	Conversion (%)
	1-NO ₂	2-NO ₂	Σ Adducts		
0	11	0.4	89	28	69
0.5	68	1.9	30	36	57
1.0	80	1.5	19	53	50
1.5	82	1.3	16	63	40
2.0	82	1.6	16	51	37

Eberson *et al.* stated that the reduction in adduct yields and the high 1-/2-nitronaphthalene ratios observed on addition of trifluoroacetic acid, when coupled with the e.p.r. data, gave incontrovertible proof of trinitromethanide ion involvement in the first step of triad recombination under standard photolysis conditions.

Adduct formation as a general phenomena

Having established the intermediacy of the trinitromethanide ion in the photochemical reactions of tetranitromethane with naphthalene, Eberson and Hartshorn examined the products formed on photolysis of other aromatic substrates with tetranitromethane in both dichloromethane and acetonitrile solutions.^{38a-z,39a-f,43} Eberson's earlier studies³⁵ of the photolysis of naphthalene with tetranitromethane had shown that most (85-95%) of the initial products formed were dihydronaphthalenes **133-136** and that the first step in their formation, following generation of the triad, was trinitromethanide ion addition to the aromatic radical cation.



It appears reasonable that the regiochemistry of trinitromethanide ion attack on a radical cation might be affected by two major features:

- (1) the distribution of the positive charge in the radical cation, and
- (2) the relative stabilities of the resultant radicals $\text{Ar(H)C(NO}_2)_3^\bullet$.

In this later connection two features of the structure, $\text{Ar(H)C(NO}_2)_3^\bullet$, must be considered. These are first the inherent energy of the carbon radical system itself, and second the steric interaction introduced between the trinitromethyl group and the remainder of the molecule.

The calculated (AM1) cationic charge distribution for the naphthalene radical cation is shown in Figure 1.4, overleaf.

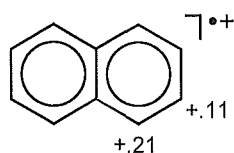
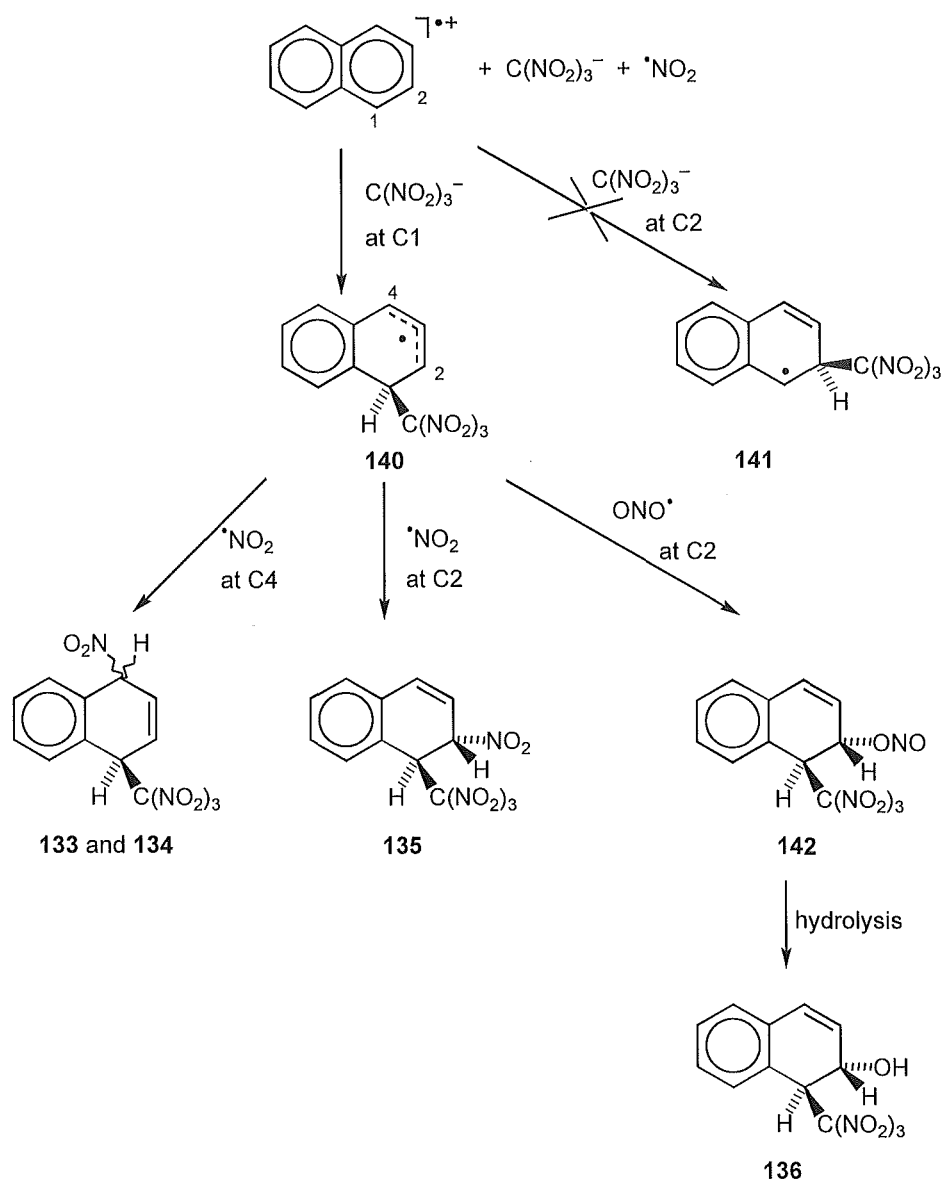


Figure 1.4

The charge distribution at C1 would clearly favour trinitromethanide ion attack at this position, as would the formation of the more stable phenyl-allylic radical **140** (Scheme 1.17). It should be noted that products formed from the less stable, localised, phenyl radical **141** are not seen among the reaction products.



Scheme 1.17

Coupling of nitrogen dioxide with delocalised radical **140** at C4 would give the two epimeric 1,4-trinitromethyl-nitro adducts **133** and **134**. In contrast, two modes of nitrogen dioxide coupling are observed at C2; C-N bond formation *trans* to the bulky trinitromethyl group results in the formation of **135** while C-O coupling yields hydroxy adduct **136** via the nitrito intermediate **142**. Nitrogen dioxide addition via C-O bond formation is known to occur in circumstances of steric compression around the reaction site^{40a} and where the neighbouring groups are electron withdrawing.^{40b} The subsequent hydrolysis of **142** to **136** could either occur during the reaction or the work-up procedure.

Similarly, adducts **144-151** were found in yields of up to 70% in the reaction mixtures resulting from photolysis of solutions of 1-methylnaphthalene **143**^{38m} with tetranitromethane. The calculated charge distribution in radical cation **143**^{•+} and the products identified are shown in Figure 1.5.

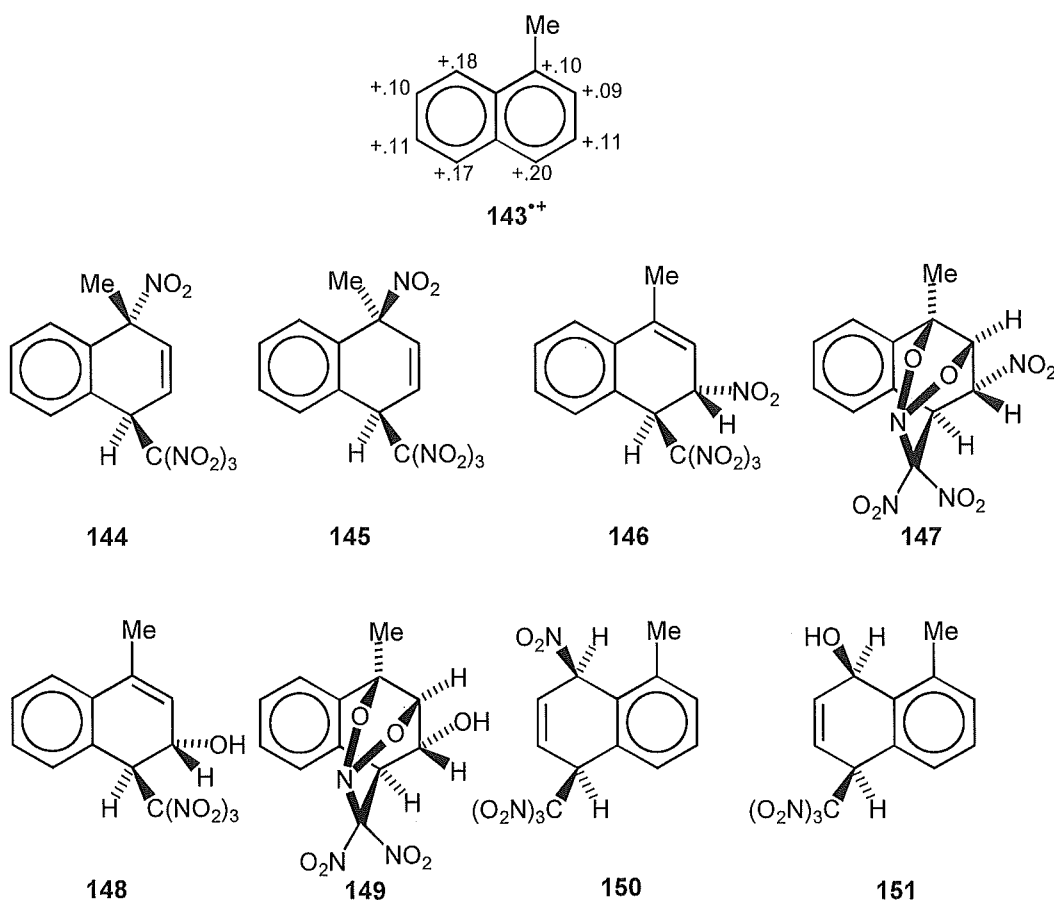
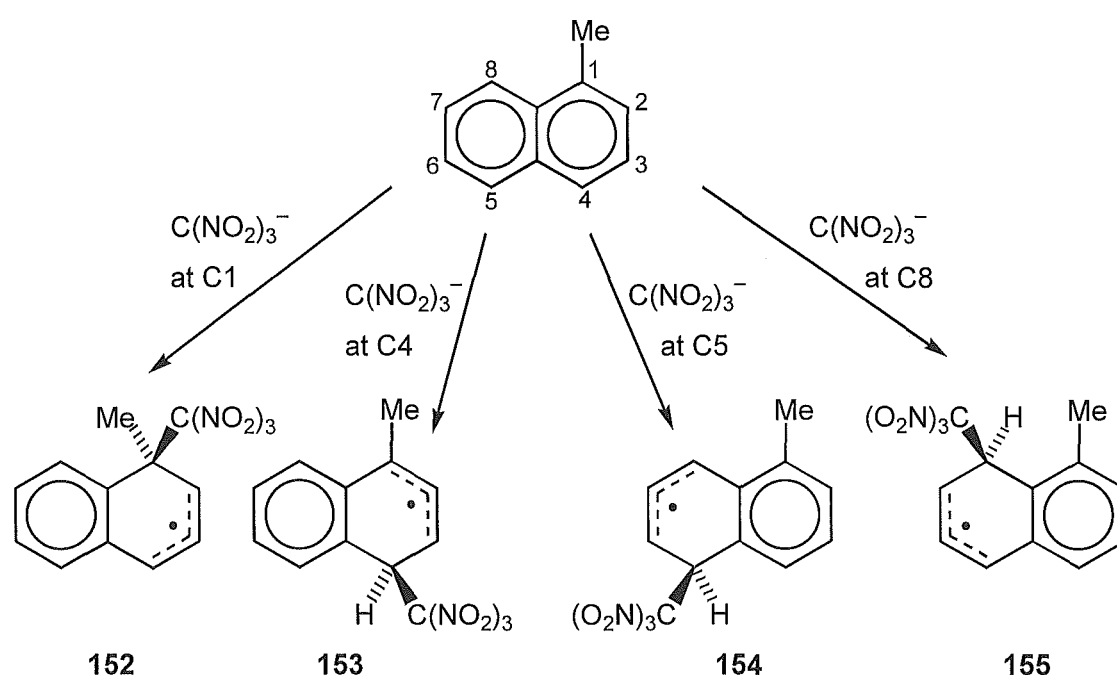


Figure 1.5 - Products isolated from the photolysis reactions of 1-methylnaphthalene and tetranitromethane.

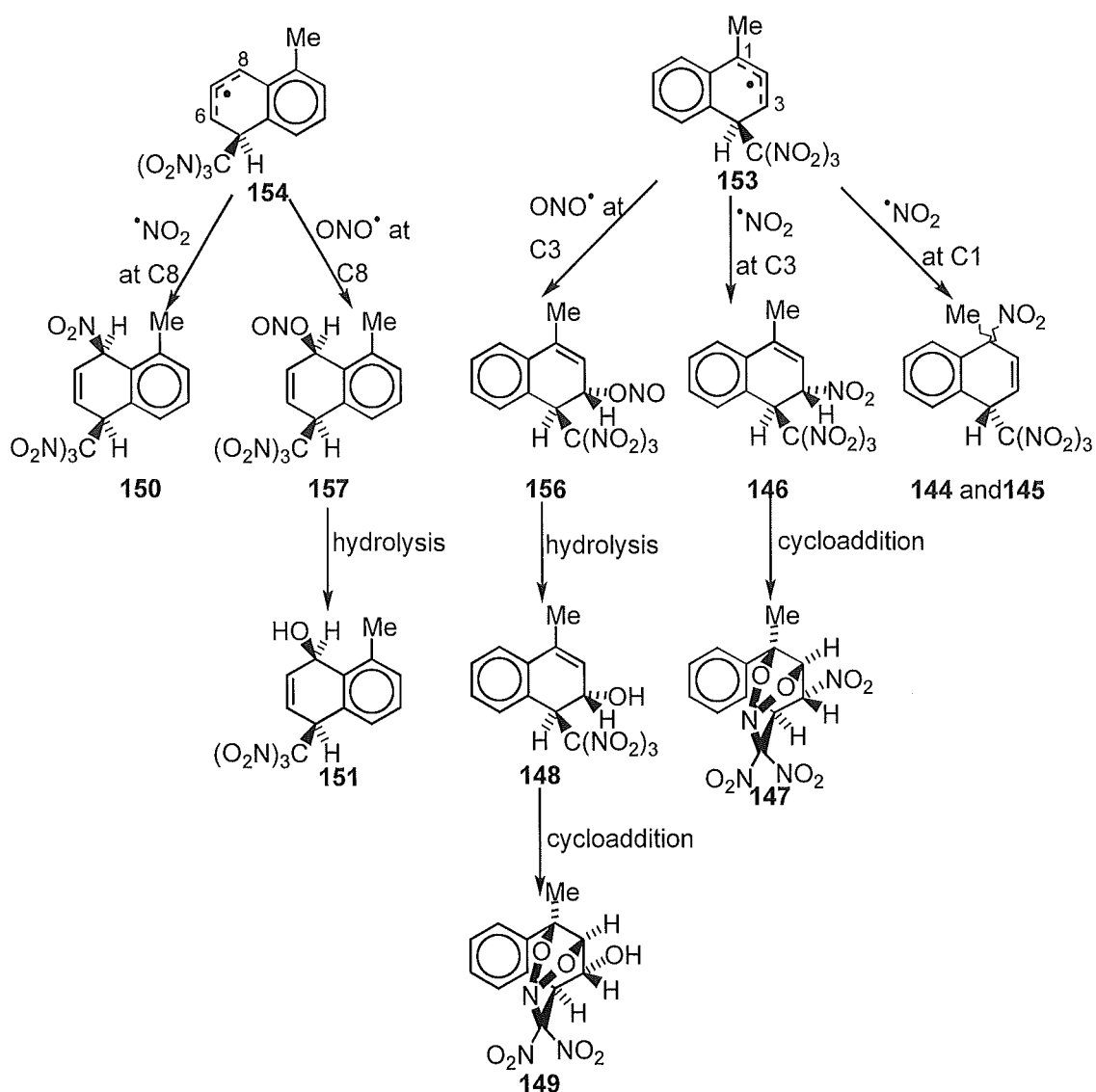
Trinitromethanide ion addition to **143**^{•+} could occur at any of the eight ring positions but as demonstrated for naphthalene, low charge density or the formation of a high energy localised radical is disfavoured; consequently trinitromethanide ion attack at any of the β positions of 1-methylnaphthalene is inhibited by both these factors. The remaining α -positions C1, C4, C5, and C8 are therefore the most likely sites for trinitromethanide ion attack (Scheme 1.18).



Scheme 1.18

The lower charge density at C1 or the inherent strain of the *ipso* interactions of the trinitromethyl and methyl substituents in radical **152**, formed by trinitromethanide ion attack at this position, inhibit addition at this site. Similarly trinitromethanide ion attack at C8, although appearing reasonable given the high charge distribution at this site, is disfavoured by the *peri* interactions of the methyl and trinitromethyl substituents in the resultant radical **155**. In line with these facts, the products isolated from photolysis reactions of 1-methylnaphthalene with tetranitromethane are not derived from these two species.

Adducts **150** and **151**, formed *via* trinitromethanide ion attack at C5, were observed in yields totalling no more than 10% of identified products in either dichloromethane or acetonitrile. This can be rationalised by comparing the relative stabilities of the two radical intermediates **153** and **154** which lead to product formation. Structure **153** is a 1-methyl-phenyl-allylic radical where the delocalised radical is stabilised by the 1-methyl substituent whereas **154** is simply a phenyl-allylic radical. Given these conditions, **153** would be expected to be the less energetic and the more favoured intermediate for adduct formation. In the event approximately 90% of identified products were derived from this intermediate (Scheme 1.19).



Scheme 1.19

Nitrogen dioxide coupling at C8 in the delocalised carbon radical **154** through C-N and C-O bond formation would give rise to **150** and **151** (via the nitrito adduct **157**) respectively. Radical **153** was seen to couple with nitrogen dioxide in three ways; the epimeric pair **144** and **145** arose from $\cdot\text{NO}_2$ addition to C1, while C-N bond formation at C3 yielded **146** and C-O bond formation at this same site would form nitrito adduct **156** which on hydrolysis would yield hydroxy adduct **148**. Adduct **148** was not observed in the reaction mixtures due to its propensity to undergo a novel thermal intramolecular cycloaddition of one nitro group of the trinitromethyl substituent to the internal 1,2-alkene system, giving rise to **149**. The analogous nitro adduct **146**, which was isolated and identified by X-ray crystallography, was seen to undergo a similar cycloaddition to give the cycloaddition to **147**. Related cycloadditions of nitro groups to unsaturated systems are known to occur both photochemically⁴¹ and thermally.⁴²

The study of the photolysis of 2,3-dimethylnaphthalene³⁸ⁿ **158** with tetranitromethane further demonstrated the influence of steric interactions in the trinitromethyl radical intermediate on the reaction pathway. As in 1-methylnaphthalene, adducts were isolated in yields of up to 75% in both dichloromethane and acetonitrile reaction solutions. For the 2,3-dimethylnaphthalene radical cation **158**^{•+} the charge distribution was calculated as being shown in Figure 1.6

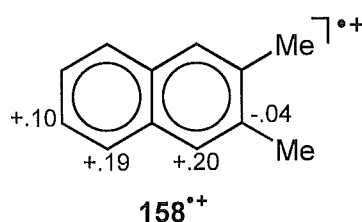
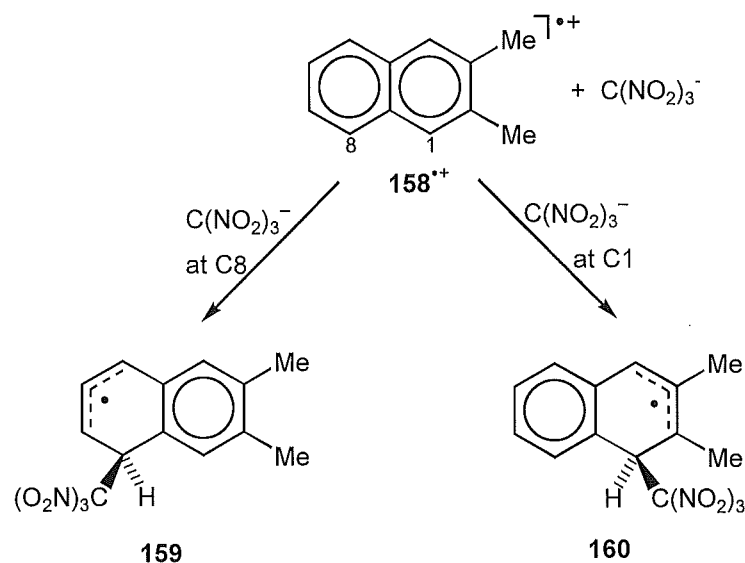


Figure 1.6 - Calculated (AM1) charge distribution on the radical cation of 2,3-dimethylanisole.

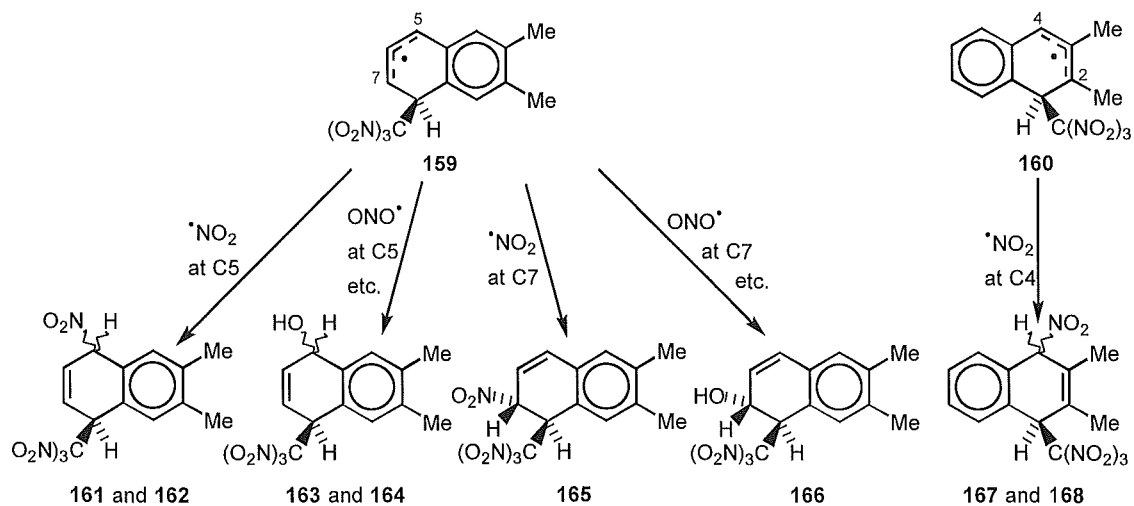
On the basis of the charge distribution and the formation of stable allylic radical intermediates, trinitromethanide ion attack appears likely either at C1 or C8 of

the radical cation of 2,3-dimethylnaphthalene, affording the two delocalised radicals **159** and **160** (Scheme 1.20).



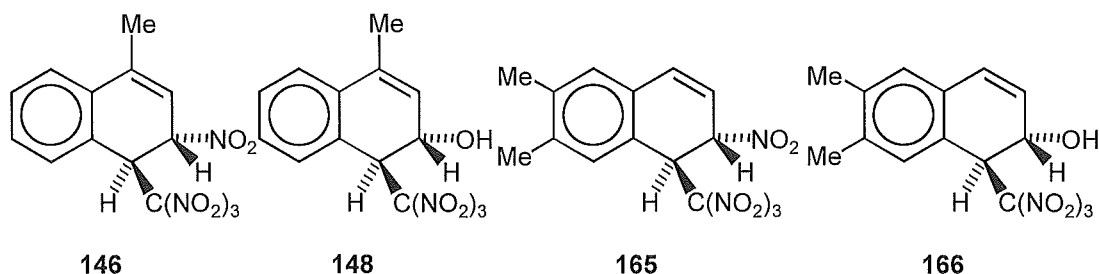
Scheme 1.20

The formation of the unsubstituted, phenyl allylic radical **159** would seem to be less likely given the results for 1-methylnaphthalene where methyl substituted delocalised radicals were favoured. However, steric interactions between the bulky trinitromethyl group and the buttressed methyl substituent in **160** would raise the energy of this intermediate species. In the event, the majority of trinitromethanide addition (*ca.* 80% of identified products) was observed at C8 (Scheme 1.21).



Scheme 1.21

Subsequent coupling of NO₂ to C4 of **160** would yield the two epimeric 1,4-nitro-trinitromethyl adducts **167** and **168**. In contrast, nitrogen dioxide addition at C5 of **159** proceeded both *via* C-N coupling, to give **161** and **162**, and C-O coupling, to afford **163** and **164**. Similarly, radical coupling at C7 through C-N and C-O bond formation, *trans* to the adjacent bulky trinitromethyl group, would give rise to **165** and **166** respectively. No cycloaddition of the 1-trinitromethyl-2-X-dihydronaphthalene adducts **165** and **166** was seen on the time-scale of the photolysis. However, impure samples of **165** and **166** were observed to undergo cycloaddition in solution with half lives of 138 hours and 38 hours respectively. The lack of the electron donating methyl groups on the alkene moieties of **165** and **166**, which were present in the analogous 1-methylnaphthalene cycloadduct precursors **146** and **148**, is believed to be responsible for this slower cycloaddition. The methyl groups increase the electron availability of the unsaturated system and thus increase the driving force for cycloaddition by the electron deficient nitro groups.



Similarly the slower rate of cycloaddition of nitro precursor **165**, as compared to its hydroxy counterpart **166**, was rationalised by the greater electron withdrawing effect of the nitro group on the alkene system, thus reducing the electron availability in the alkene system. The predominance of products formed by trinitromethanide ion attack at C8 of the 2,3-dimethylnaphthalene radical cation (*via* **159**) rather than C1 (*via* **160**), demonstrates that intermediate species such as **160** suffer energetically from the steric interaction between the buttressed methyl group and the adjacent trinitromethyl group, despite the accompanying methyl stabilisation of the allylic radical system.

The study of the photolysis of 1,4-dimethylnaphthalene with tetranitromethane⁴³ further illustrates the importance of the resultant radical

stability in determining the regiochemistry of trinitromethanide ion attack. The calculated charge distribution for the radical cation of the substrate is shown in Figure 1.7.

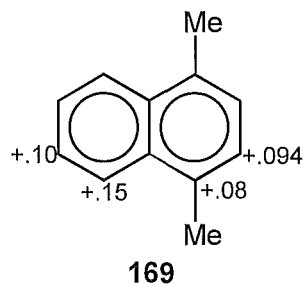
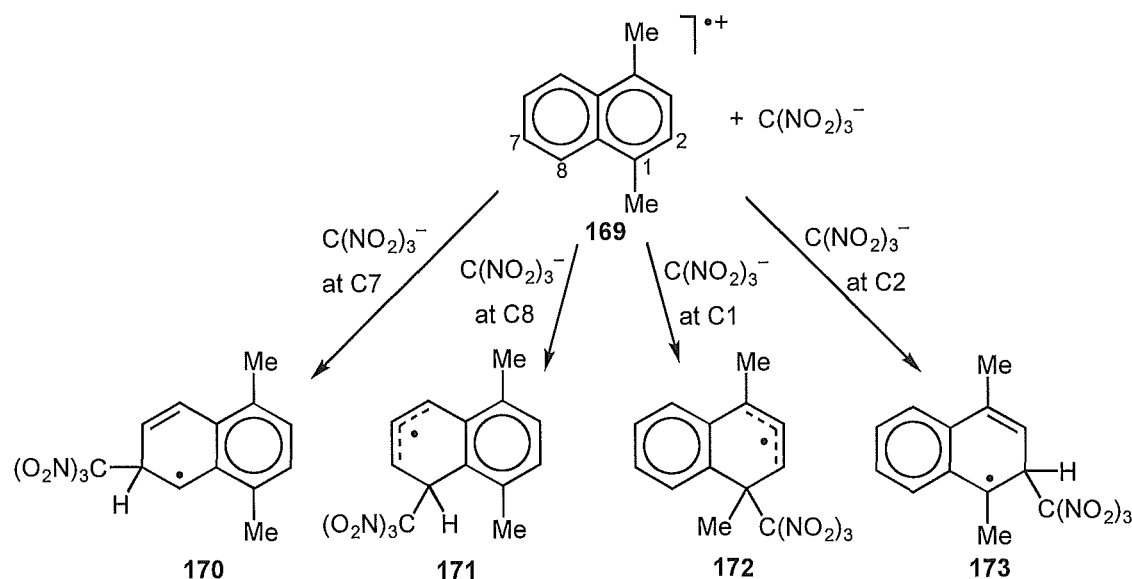


Figure 1.7 - Calculated (AM1) charge distribution on the 1,4-dimethylnaphthalene radical cation.

The charge distribution on this molecule is unusual as it has relatively high positive charge distributions at all four carbon positions. The radicals resulting from trinitromethanide ion attack at these carbons are shown in Scheme 1.22.

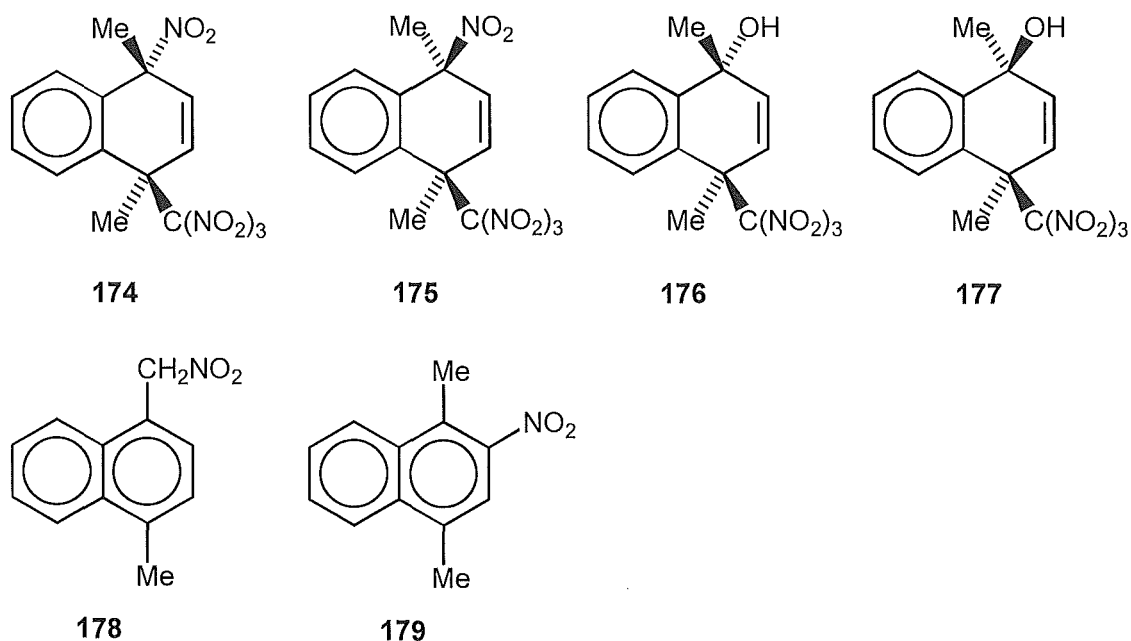


Scheme 1.22

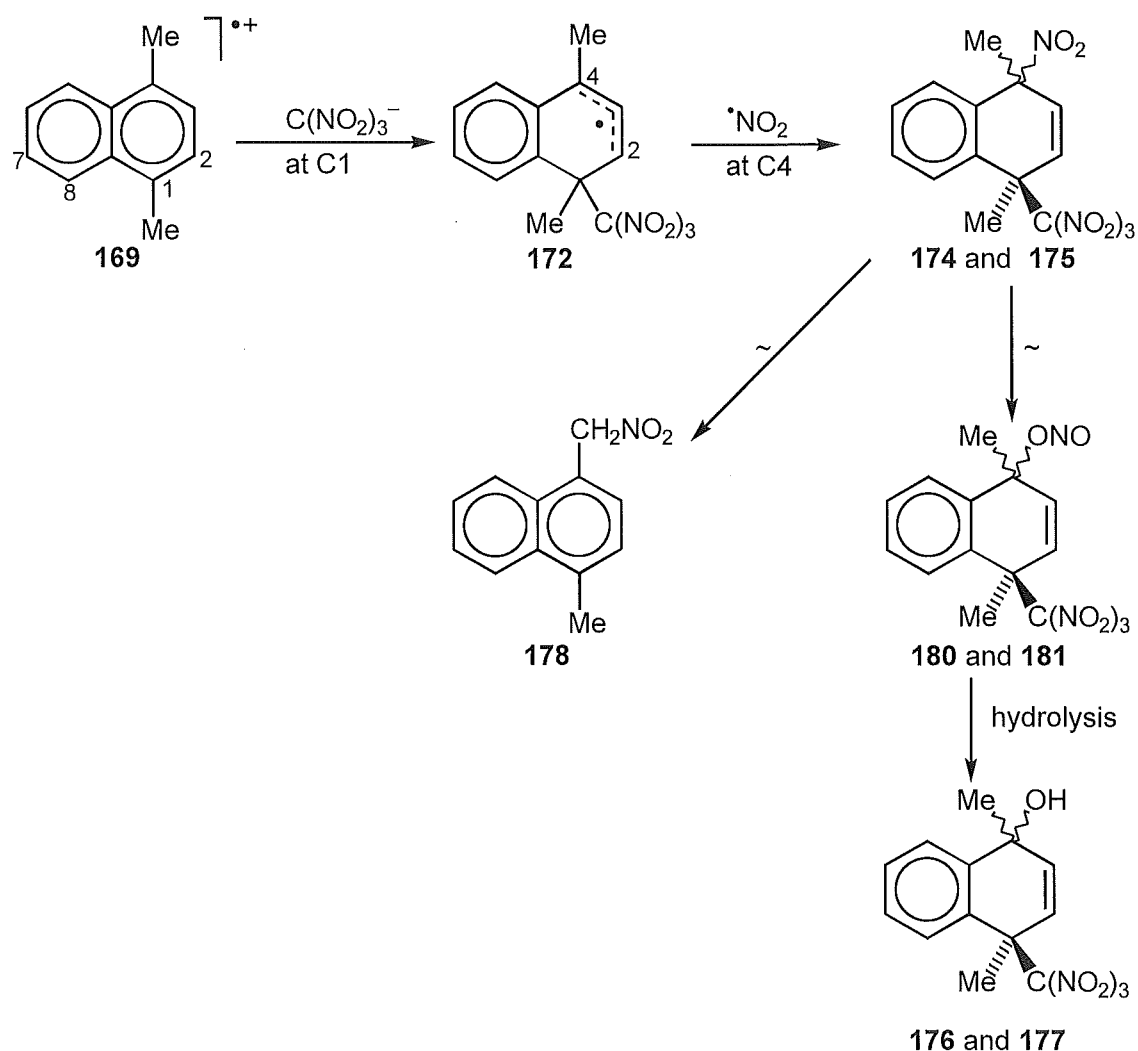
Only C8 has a marginally higher charge density than the other carbon positions but trinitromethanide ion attack at this reaction site would give rise to delocalised carbon radical **171** which possesses a destabilising *peri* interaction

between the trinitromethyl substituent and the methyl group on the adjacent ring. As the other three ring positions have approximately equal charge density it appears that the factor which determines the operative reaction pathway is the relative resultant radical stability. Structure **170** which would result from trinitromethanide ion addition to C7 is a benzylic secondary radical which is free of steric interaction. In contrast, **173** has a tertiary benzylic radical centre but suffers steric compression between the trinitromethyl and methyl groups. Finally, **172** has the stabilised character of a phenyl-1-methylallyl radical; however the *ipso* trinitromethyl substitution in this radical introduces steric compression which will raise its energy somewhat.

The photolysis of solutions of 1,4-dimethylnaphthalene with tetranitromethane again showed predominant adduct formation, compounds **174** and **175** constituting >95% of all products when the reaction was performed at -50° in dichloromethane. The side-chain nitro compound **178** was shown to arise by rearrangement of adducts **174** and **175**.



Adducts **174-177** are derived from **172** *via* trinitromethanide ion attack at C1 (Scheme 1.23). The nitro aromatic compound **179** was formed only in small amounts in acetonitrile photolysis solutions by an unspecified mechanism.



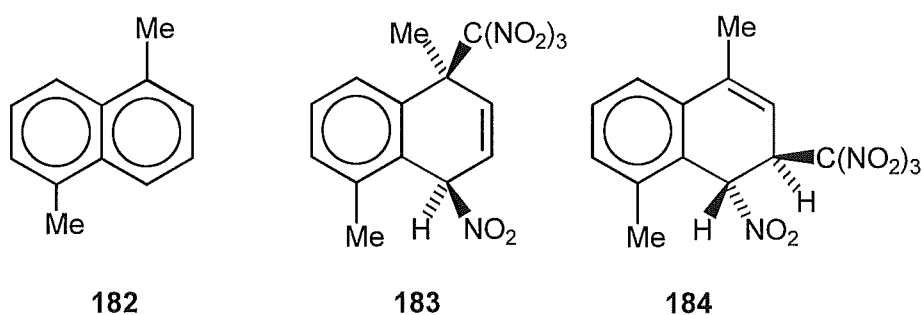
Scheme 1.23

The isolation of **174** from a reaction mixture allowed observation of its thermal and acid induced rearrangements. An array of compounds were observed including epimerisation to **175**, nitro to nitrito rearrangement to give **180** and **181**, and even elimination of tetranitromethane to regenerate the starting material 1,4-dimethylnaphthalene. Rearrangement to the nitromethyl compound **178** was the major pathway, as seen previously³³.

It thus appears that although a significant amount of research has been carried out looking into the photochemical reactions of aromatics with tetranitromethane, there are still unanswered questions regarding the origin of many of the compounds which have been observed in previous studies. It now seems clear that the relative stability of the intermediate $\text{Ar}(\text{H})\text{C}(\text{NO}_2)_3^\cdot$ provides a more satisfying rationale for the regiochemistry of attack of trinitromethanide

ion on the radical cations of naphthalene derivatives. The use of a wider variety of aromatic systems may provide greater insight into this observation.

In this thesis are described the results of further photolysis reactions of aromatic compounds with tetranitromethane. In Chapter 2 the reaction chemistry of 1,5-dimethylnaphthalene **182** is discussed, including the observation of a facile allylic rearrangement of an initially formed adduct, 1,5-dimethyl-*r*-1-nitro-*t*-4-trinitromethyl-1,4-dihydronaphthalene **183**, to give the rearranged product **184**.



In subsequent Chapters, the results of photolysis reactions of a series of methoxy compounds with tetranitromethane are described. In particular, these studies reveal the marked influence of the methoxy function on the regiochemistry of trinitromethanide ion attack on these radical cations, and also further reactions of trinitromethyl substituted aromatic compounds.

References

- ¹ Ingold, C.K., "Structure and Mechanism in Organic Chemistry", 2nd ed., Cornell University Press, Ithaca, N.Y., 1969, Chapter VI.
- ² Euler, H., *Ann.*, 1903, **330**, 280.
- ³ Ingold, C.K., Millen, D.J., and Poole, H.G., *Nature*, 1946, **158**, 480.
- ⁴ Hantzsch, A., *Z., physik. Chem.*, 1908, **65**, 41.
- ⁵ De Robles, C.R., and Moles, E., *Anales fís. Y quím.*, 1935, **32**, 474.
- ⁶ Médard, L., *Compt. rend.*, 1934, **199**, 1615.
- ⁷ Chédin. J., *Compt. rend.*, 1935, **200**, 1397; Chédin. J., *Compt. rend.*, 1935, **201**, 552, 714; Chédin. J., *Compt. rend.*, 1936, **202**, 220, 1067; Chédin. J., *Compt. rend.*, 1936, **203**, 772, 1509; Chédin. J., *Ann. chim.*, 1937, **8**, 243.
- ⁸ Bennett, G. M., Brand, C. D., and Williams, G., *J. Chem. Soc.*, 1946, 869.
- ⁹ Hammett, *J. Am. Chem. Soc.*, 1933, **55**, 1900; Hammett, *J. Am. Chem. Soc.*, 1937, **59**, 1708.
- ¹⁰ As stated, for example, by Ingold, C. K., "The Transition State", *Spec. Publ. Chem. Soc.*, 1962, **No. 16**, 119.
- ¹¹ Coombes, R. G., Moodie, R. B., and Schofield, K., *J. Chem. Soc. B*, 1968, 800; Hartshorn, S. R., Moodie, R. B., Schofield, K., and Thompson, M. J., *ibid.*, 1971, 2447.
- ¹² Olah, G. A., *Acc. Chem. Res.*, 1971, **4**, 240 and references cited within.
- ¹³ Dewar, M. J. S., *J. Chem. Soc.*, 1946, **406**, 777; Dewar, M. J. S., *Nature (London)*, 1954, **176**, 784.; Dewar, M. J. S., "The Electronic Theory of Organic Chemistry", Oxford University Press, London, 1949.
- ¹⁴ Olah, G. A., Kuhn, S. J., and Flood, S. H., *J. Am. Chem. Soc.*, 1961, **83**, 4571; Olah, G. A., Kuhn, S. J., and Flood, S. H., *ibid.*, 1961, **83**, 4581;
- ¹⁵ Rithchie, C. D., and Win, H., *J. Org. Chem.*, 1964, **29**, 3093; Tolgyesi, W. S., *Can. J. Chem.*, 1965, **43**, 343; Ridd, J. D., "Studies on Chemical Structure and Reactivity", Methuen, London, p. 152; Brown, H. C., and Wirkkala, *J. Am. Chem. Soc.*, 1966, **88**, 145; Cerfontain, H., and Telder, A., *Recl. Trav. Chim. Pays-Bas*, 1967, **86**, 377; Caille, S. W., and Corriu, J. P., *Chem. Commun.*, 1967, 1251; Caille, S. W., and Corriu, J. P., *Tetrahedron*, 1969, **25**, 2005;
- ¹⁶ Perrin, C. L., *J. Am. Chem. Soc.*, 1977, **99**, 5516.

-
- ¹⁷ Kenner, J., *Nature*, 1945, **156**, 369.
- ¹⁸ Weiss, J., *Trans Faraday Soc.*, 1946, **42**, 116.
- ¹⁹ Ebersson, L., and Radner, F., *Acta Chem Scand. Ser. B*, 1980, **34**, 739.
- ²⁰ Sankararaman, S., Haney, W. A., and Kochi, J.K., *J. Am. Chem. Soc.*, 1987, **109**, 5235-5249
- ²¹ Epiotis, N. D., *J. Am. Chem. Soc.*, 1972, **94**, 1924; Fukui, K., *Acc. Chem. Res.*, 1971, **4**, 57; Houk, K. N., *J. Am. Chem. Soc.*, 1973, **95**, 4092; Dewar, M. J. S., *Angew. Chem. Int. Ed. Engl.*, 1971, **10**, 761 and references therein.
- ²² Foster, R., "Organic Charge-Transfer Complexes", Academic Press, New York, 1969; Andrews, L. J., Keefer, R. Y., "Molecular Complexes in Organic Chemistry", Holden-Day, San Francisco, 1964; Briegleb, G., "Electron Donator-Acceptor Komplexe", Springer-Verlag, Berlin, 1961; Kochi, J. K., "Organometallic Mechanisms and Catalysis", Academic Press, New York, 1978.
- ²³ Mulliken, R. S., *J. Am. Chem. Soc.*, 1952, **74**, 811; Mulliken, R.S., and Person, W.B., "Molecular Complexes: A Lecture and Re.p.r.int Volume", Wiley, New York, 1969.
- ²⁴ Hilinski, E.F., Masnovi, J. M., Amatore, C., Kochi, J.K., and Rentzepis, P. M., *J. Am. Chem. Soc.*, 1983, **106**, 6167; Hilinski, E.F., Masnovi, J.M., Kochi, J.K., and Rentzepis, P. M., *Ibid.*, 1984, **106**, 8071.
- ²⁵ Jones, G. H., Becker, W. G., and Chiang, S. H., *J. Am. Chem. Soc.*, 1983, **105**, 1269; Jones, G. H., and Becker, W. G., *ibid.*, 1983, **105**, 1276; Mukai, T., Sato, K., and Yamashita, Y. *J. Am. Chem. Soc.*, 1981, **103**, 670.
- ²⁶ Chaudhuri, S. A., and Asmus, K. D., *J. Phys Chem.*, 1972, **76**, 26.
- ²⁷ Masnovi, J. M., Huffman, J. C., Kochi, J. K., Hilinski, E. F., and Rentzepis, P. M., *Chem. Phys. Lett.*, 1984, **106**, 20.
- ²⁸ Masnovi, J.M., and Kochi, J.K., *J. Org. Chem.*, 1985, **50**, 5245.
- ²⁹ Chu, T. L., and Weissman, S. I., *J. Chem. Phys.*, 1954, **22**, 21; Dallinga, G., Mackor, E. L., and Stuart, A. A. V., *Mol. Phys.*, 1958, **1**, 123; Kerimov, Maksytov, E. M., Milonich, A. I., and Slovetskii, V. I., *Izv. Akad. Navk. SSR*, 1979, 632 and references therein.

-
- ³⁰ Sankararaman, S., and Kochi, J. K., *Recl Trav Chim. Pays-Bas*, 1986, **105**, 278.
- ³¹ Yoshida, K., "Electrooxidation in Organic Chemistry", Wiley, New York, 1984.
- ³² Sankararaman, S., Haney, W. A., and Kochi, J. K., *J. Am. Chem. Soc.*, 1987, **109**, 5235.
- ³³ Sankararaman S., and Kochi, J. K., *J. Chem. Soc. Perkin Trans. 2*, 1991, 1.
- ³⁴ Fischer, A., and Wilkinson, F., *Can. J. Chem.*, 1972, **50**, 3988.
- ³⁵ Ebersson, L., Hartshorn, M. P., and Radner, F., *J. Chem. Soc. Perkin Trans. 2*, 1992, 1793.
- ³⁶ Ebersson, L., Hartshorn, M. P., Radner, F., and Svensson, J. O., *J. Chem. Soc. Perkin Trans. 2*, 1994, 1719.
- ³⁷ Ebersson, L., Hartshorn, M. P., and Svensson, J. O., *J. Chem. Soc. Chem. Commun.*, 1993, **21**, 1614.
- ³⁸ (a) Ebersson, L., Hartshorn, M. P., Radner, F., Merchán, M., and Roos, B. O., *Acta Chem. Scand.*, 1993, **47**, 176; (b) Ebersson, L., Hartshorn, M. P., Radner, F., and Robinson, W.T., *J. Chem. Soc. Chem. Commun.*, 1992, **7**, 566; (c) Ebersson, L., Hartshorn, M. P., and Radner F., *J. Chem. Soc. Perkin Trans 2.*, 1992, 1793; (d) Ebersson, L., and Hartshorn, M. P., *J. Chem. Soc. Chem. Commun.*, 1992, 1563. (e) Ebersson, L., Hartshorn, M. P., Radner, F., and Robinson, W. T., *Acta Chem. Scand.*, 1993, **47**, 410; (f) Ebersson, L., Hartshorn, M. P., and Svensson, J. O., *Acta Chem. Scand.*, 1993, **47**, 925; (g) Ebersson, L., Calvert, J. L., Hartshorn, M. P., and Robinson W.T., *Acta Chem. Scand.*, 1993, **47**, 1025; (h) Butts, C. P., Calvert, J. L., Ebersson, L., Hartshorn, M. P., and Robinson, W.T., *J. Chem. Soc. Chem. Commun.*, 1993, **19**, 1513; (i) Ebersson, L., Hartshorn, M. P., and Svensson, J. O., *J. Chem. Soc. Chem. Commun.*, 1993, **21**, 1614; (j) Butts, C. P., Calvert, J. L., Ebersson, L., Hartshorn, M. P. Maclagan, R. G. A. R., and Robinson, W. T., *Aust. J. Chem.*, 1994, **47**, 1087; (k) Ebersson, L., Calvert, J. L., Hartshorn, M. P., and Robinson, W. T., *Acta Chem. Scand.*, 1994, **48**, 347; (l) Calvert, J. L., Ebersson, L., Hartshorn, M. P., Maclagan, R. G. A. R., and Robinson, W. T., *Aust. J. Chem.*, 1994, **47**, 1211; (m) Calvert, J. L., Ebersson, L., Hartshorn, M. P., Maclagan, R. G. A. R., and Robinson, W. T.,

Aust. J. Chem., 1994, **47**, 1591; (n) Butts, C. P., Calvert, J. L., Ebersson, L., Hartshorn, M. P., Radner, F., and Robinson, W. T., *J. Chem. Soc. Perkin Trans. 2*, 1994, 1485; (o) Calvert, J. L., Ebersson, L., Hartshorn, M. P., Robinson, W. T., and Timmerman-Vaughan, David, J., *Acta Chem. Scand.*, 1994, **47**, 1087; (p) Ebersson, L., Hartshorn, M. P., Persson, O., Robinson, W. T., and Timmerman-Vaughan, D. J., *Acta Chem. Scand.*, 1995, **49**, 482; (q) Ebersson, L., Hartshorn, M. P., Robinson, W. T., and Timmerman-Vaughan, D. J., *Acta Chem. Scand.*, 1995, **49**, 571; (r) Butts, C. P., Ebersson, L., Foulds, G. J., Fulton, K. L., Hartshorn, M. P., and Robinson, W. T., *Acta Chem. Scand.*, 1995, **49**, 76; (s) Butts, C. P., Ebersson, L., Hartshorn, M. P., Robinson, W. T., Timmerman-Vaughan, D. J., and Young, D. A. W., *Acta Chem. Scand.*, 1996, **50**, 29; (t) Svensson, J. O., *Acta Chem. Scand.*, *in press* (u) Butts, C. P., Ebersson, L., Hartshorn, M. P., Robinson, W. T., and Wood, B. R., *Acta Chem. Scand.*, *in press*; (v) Butts, C. P., Ebersson, L., Fulton, K. L., Hartshorn, M. P., Jamieson, G. B., and Robinson, W. T., *Acta Chem. Scand.*, *in press*; (w) Butts, C. P., Ebersson, L., Fulton, K. L., Hartshorn, M. P., and Robinson, W. T., *Aust. J. Chem.*, *in press*; (x) Butts, C. P., Ebersson, L., Fulton, K. L., Hartshorn, M. P., Robinson, W. T., and Timmerman-Vaughan, D. J., *Acta Chem. Scand.*, *submitted*; (y) Ebersson, L., Hartshorn, M. P., and Timmerman-Vaughan, D. J., *Acta Chem. Scand.*, *submitted*; (z) Ebersson, L., Hartshorn, M. P., and Svensson, J. O., *Acta Chem. Scand.*, *Submitted*.

³⁹ (a) Butts, C. P., Ebersson, L., Hartshorn, M. P., Persson, O., and Robinson, W. T., *Acta Chem. Scand.*, 1995, **49**, 253; (b) Butts, C. P., Ebersson, L., Hartshorn, M. P., and Robinson, W. T., *Acta Chem. Scand.*, 1995, **49**, 389; (c) Butts, C. P., Ebersson, L., Hartshorn, M. P., and Robinson, W. T., *Acta Chem. Scand.*, 1996, **50**, 122; (d) Butts, C. P., Ebersson, L., Hartshorn, M. P., and Robinson, W. T., *Aust. J. Chem.*, 1995, **48**, 1989; (e) Butts, C. P., Ebersson, L., Hartshorn, M. P., and Robinson, W. T., *J. Chem. Soc. Perkin Trans. 2*, *in press*; (f) Butts, C. P., Ebersson, L., Hartshorn, M. P., Robinson, W. T., and Timmerman-Vaughan, D. J., *Acta Chem. Scand.*, *in press*;

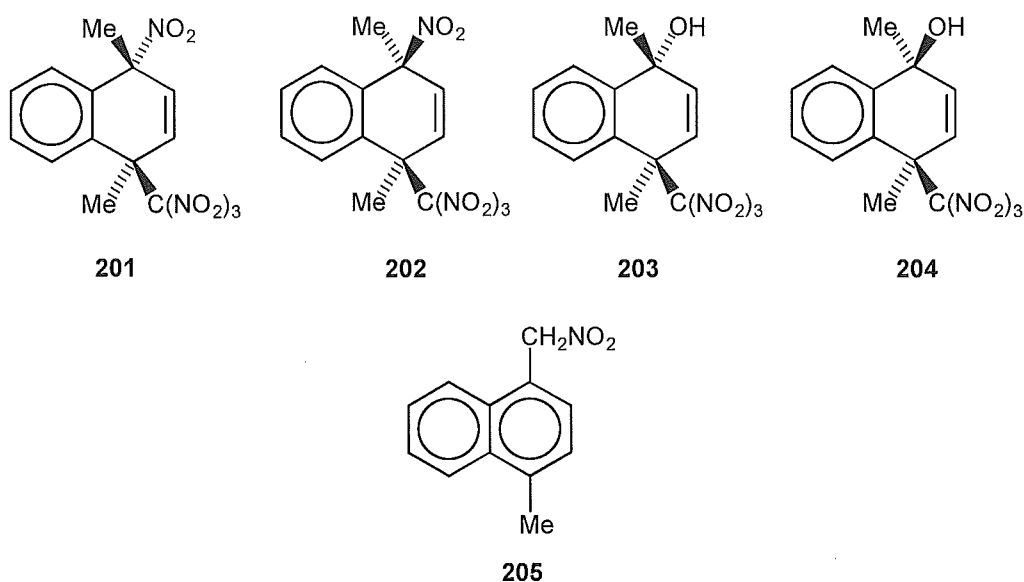
⁴⁰ (a) Blunt, J. W., Hartshorn, M. P., Jensen, R. G., Walker, A. G., and Wright, G. I., *Aust. J. Chem.*, 1989, **42**, 675, and papers cited therein; (b)

- Hartshorn, M. P., Readman, J. M., Robinson, W. T., Vaughan, J., and Whyte, A. R., *Aust. J. Chem.*, 1985, **38**, 1693.
- ⁴¹ Buchi, G., and Ayer, D. E., *J. Am. Chem. Soc.*, 1956, **78**, 689; Schienbaum, M. L., *J. Org. Chem.*, 1964, **29**, 2200; Charlton, J. L., Liao, C., and de Mayo P., *J. Am. Chem. Soc.*, 1971, **93**, 2463; Maki, Y., Izuta, K., and Suzuki, M., *Tetrahedron Lett.*, 1972, 1973; Bouchet, P., Coquelet, C., Elguero, J., and Jacquier, R., *Tetrahedron Lett.*, 1973, 891; Maki, Y., Suzuki, M., Hosokami, M. T., and Furuta, T., *J. Chem. Soc. Perkin Trans. 2*, 1974, 1354; Saito, I, Takami, M., and Matsuera, T., *Bull. Chem. Soc. Jpn.*, 1975, **48**, 2865; Mattes, S. L., and Farid, S., *J. Chem. Soc. Chem. Commun.*, 1980, 126.
- ⁴² (a) Simonyan, L. A., Gambaryan, N. P., Petrovski, P. V., and Knunyants, I. L., *Bull. Acad. Sci. USSR (Engl. transl.)*, 1968, 357; (b) Leitich, J., *Angew Chem.*, 1976, **88**, 416; (c) Balczewski, P., Beddoes, R., and Joule, J. A., *J. Chem. Soc. Chem. Commun.*, 1991, 559.
- ⁴³ Ebersson, L. , Hartshorn, M. P., and Radner F., *J. Chem. Soc. Perkin Trans. 2*, 1992, 1799.

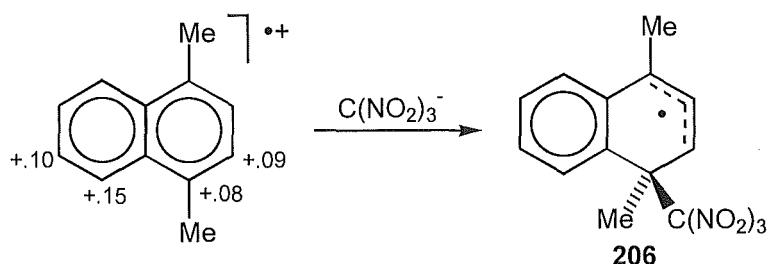
Chapter 2

Introduction

The various mechanistic interpretations of the photochemical reactions of aromatic substrates with tetranitromethane were outlined in Chapter 1. The crucial step in photoproduct formation in these systems was shown to be the recombination of the triad fragments; the aromatic radical cation, trinitromethanide ion $[\text{C}(\text{NO}_2)_3]^-$ and nitrogen dioxide, and it was demonstrated¹ that trinitromethanide ion attack on the aromatic radical cation is the predominant initiating process in this triad recombination. Photolysis of 1,4-dimethylnaphthalene with tetranitromethane resulted² in the predominant formation of trinitromethyl-nitro adducts **201** and **202** (ca. 90% yield) and smaller quantities of the analogous hydroxy adducts **203** and **204** at -50° in dichloromethane. Rearrangement of **201** and **202** resulted in significant yields of the nitromethyl aromatic **205** at higher reaction temperatures.

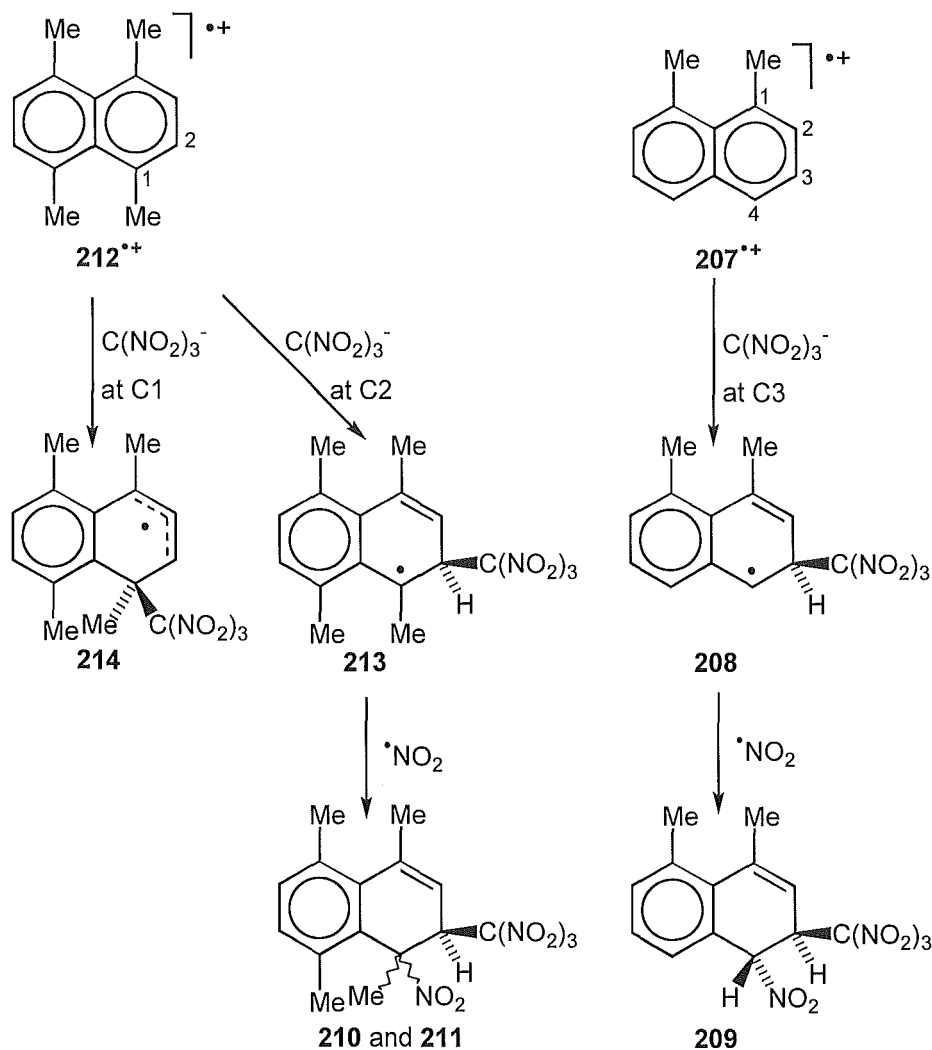


The unstable adducts are formed *via* initial trinitromethanide ion attack at C1 of the 1,4-dimethylnaphthalene radical cation and subsequent nitrogen dioxide coupling *via* either C-NO₂ or C-ONO bond formation. Attack of trinitromethanide at C1 occurs despite the low charge density at this position of the radical cation of 1,4-dimethylnaphthalene because the resultant radical species is the relatively stable 1-methyl-phenyl-allylic radical **206** (Scheme 2.1).



Scheme 2.1

The formation of allylic radicals such as **206** appears to be a feature in mechanisms leading to product formation in tetranitromethane-ArH photolysis reactions. Only adducts **209** from the photolysis reactions with tetranitromethane of 1,8-dimethylnaphthalene **207**,³ and **210** and **211** from similar reactions of 1,4,5,8-tetramethylnaphthalene **212**,⁴ appear to be derived from benzylic radical intermediates (denoted **208** and **213** in Scheme 2.2).



Scheme 2.2

The formation of the localised radical **213** might be rationalised as a reasonable alternative to the formation of the radical species **214** by trinitromethanide ion addition to C1 of the radical cation of 1,4,5,8-tetramethylnaphthalene. The combination of *ipso* and *peri* interactions between the trinitromethyl group and the two methyl substituents in structure **214** would create a highly congested and unstable species, despite the presence of the phenyl-allylic radical system. Structure 13, although requiring attack of the trinitromethanide ion β to a methyl group, is a tertiary benzylic radical.

Adduct **209** was formed only in small quantities and might be rationalised by the relatively high charge distribution at C3 of the radical cation of 1,8-dimethylnaphthalene **207^{•+}** (Figure 2.1) and the lack of any steric congestion within the intermediate species **208**.

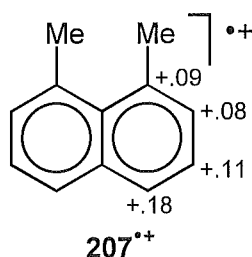
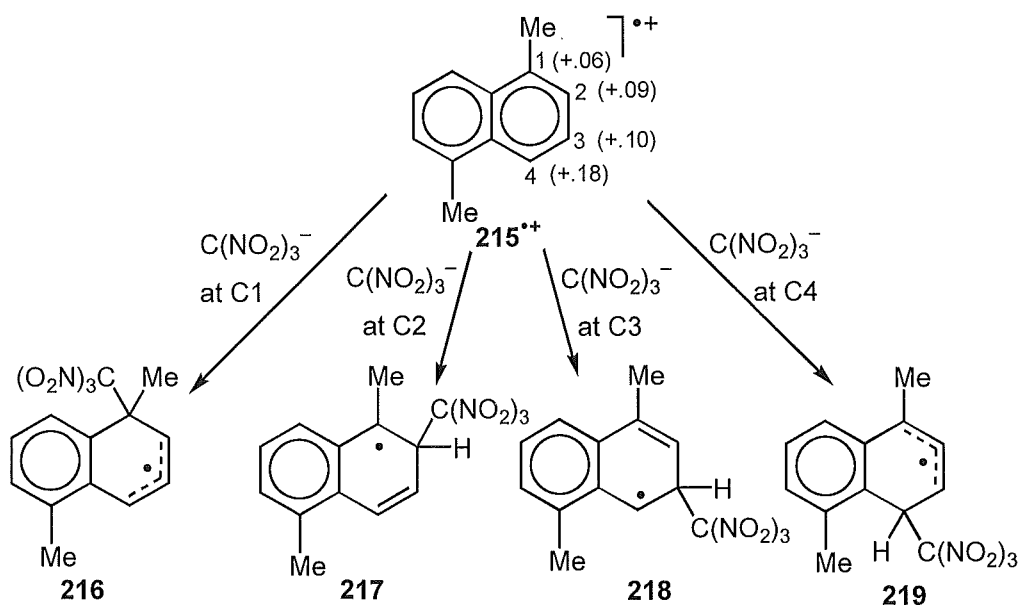


Figure 2.1 - Calculated (AM1) charge distribution the 1,8-dimethylnaphthalene radical cation

Given these apparent exceptions to the preferred formation of allylic radicals, it was considered that study of 1,5-dimethylnaphthalene would further clarify the relative importance of radical cation charge distribution and intermediate radical stability in the regiochemistry of trinitromethanide ion attack on aromatic radical cations. The charge distribution on the 1,5-dimethylnaphthalene radical cation **215^{•+}** and the structures of the four potential intermediate radical species **216-219** resulting from trinitromethanide ion attack at each carbon position are shown in Scheme 2.3, overleaf.



The position of highest positive charge is C4 but the 1-methyl-phenyl-allylic radical species **219** resulting from trinitromethanide ion attack at this position will be destabilised by the *peri* interaction between the trinitromethyl and methyl substituents. Similarly, the second allylic radical **216**, formed by trinitromethanide ion addition to C1 of the radical cation of 1,5-dimethylnaphthalene will suffer from the steric compression of the *ipso* trinitromethyl and methyl groups. However, given the results for the photolysis of 1,4-dimethylnaphthalene where *ipso* adducts were observed, this species might be expected to form despite the low positive charge at C1. Alternatively, product formation could proceed *via* trinitromethanide ion attack at C2 or C3 of the aromatic radical cation to give benzylic radical species **217** or **218**, in a similar manner to the apparent formation of **208** and **213** in the cases of 1,8-dimethylnaphthalene and 1,4,5,8-tetramethylnaphthalene.

Results

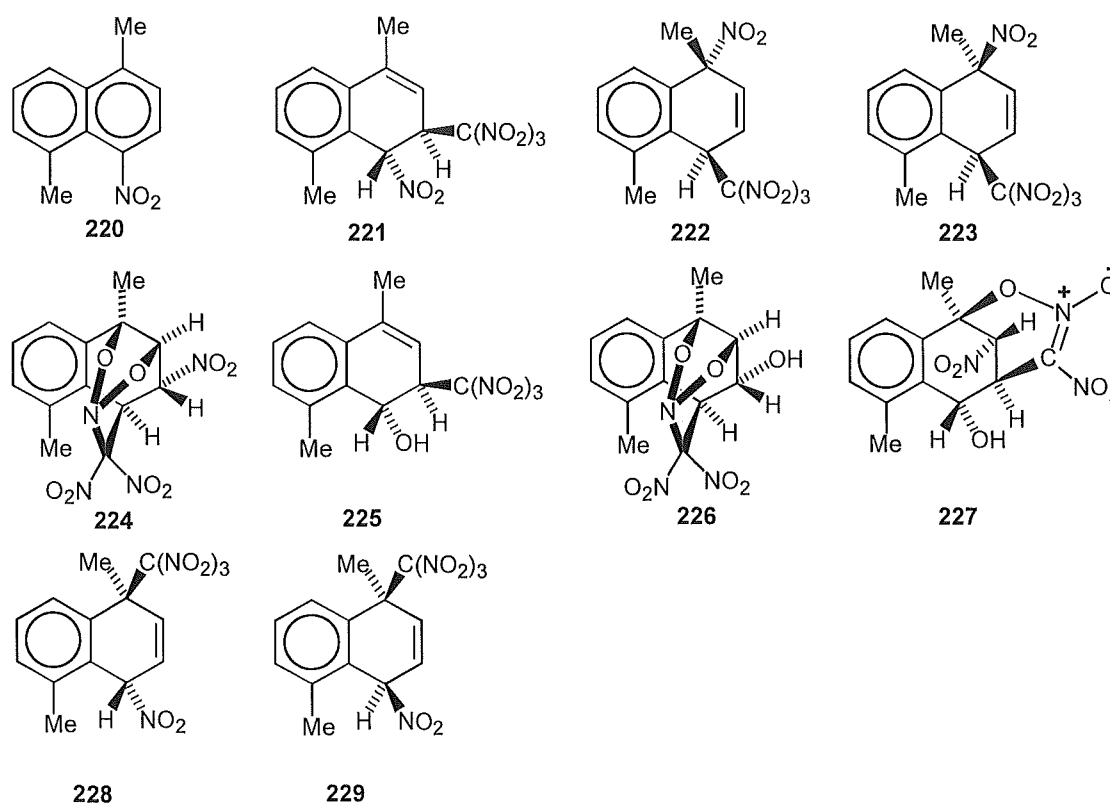
General procedure for the photolysis of 1,5-dimethylnaphthalene with tetranitromethane.

A solution of 1,5-dimethylnaphthalene (500 mg, equal to a 0.4 mol l⁻¹ solution) and tetranitromethane (0.8 mol l⁻¹) in dichloromethane (at +20°, -20°, -50°, or -78°) or acetonitrile (20° or -20°) was irradiated with filtered light (λ

cut-off at 435 nm). Aliquots were withdrawn from the reaction mixture at appropriate time intervals, the volatile material removed rapidly under reduced pressure at $\leq 0^\circ$, and the product composition determined by ^1H n.m.r. spectral analysis (for details see Experimental Section; Table 8.2.1). A summary of the results is given in Table 2.4 later in this chapter.

Photolysis of 1,5-dimethylnaphthalene and tetranitromethane in dichloromethane at 20° .

A solution of 1,5-dimethylnaphthalene (0.4 mol l^{-1}) and tetranitromethane (0.8 mol l^{-1}) was irradiated at $+20^\circ$ for 1.5 hours and the composition of the mixture was monitored by withdrawing samples for ^1H n.m.r. at appropriate intervals (Tables 2.4 and 8.2.1). Removal of volatile material under reduced pressure at $\leq 0^\circ$ gave a mixture of adducts **221-229**, 1,5-dimethyl-4-nitronaphthalene **220** and small quantities of unknown aromatic compounds. Separation of the mixture by h.p.l.c on a cyanopropyl column using hexane-dichloromethane solvent mixtures achieved partial separation of some of these components.



The first compound eluted from the column was the principal aromatic species, identified as 1,5-dimethyl-4-nitronaphthalene **220** by its mass spectrum and melting point⁵ in combination with ¹H n.m.r. and n.O.e. spectral data. In particular, the presence of four doublet resonances in the aromatic region of the ¹H n.m.r indicates either 2- or 4-nitro substitution on one of the aromatic rings; the observation of only one n.O.e. between the methyl resonance at δ 2.55 and an aromatic proton which was coupled to a triplet proton resonance, supports the 4-nitro substitution pattern (Figure 2.2).

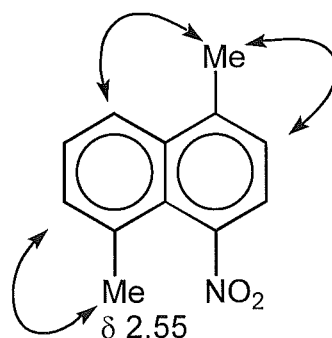


Figure 2.2 - Observed nuclear Overhauser enhancements for methyl ¹H resonances of **220** (see the experimental section for details)

The structure of the first adduct **221** eluted from the h.p.l.c column was determined by single-crystal X-ray analysis. A perspective drawing of 4,8-dimethyl-*r*-1-nitro-*t*-2-trinitromethyl-1,2-dihydronaphthalene **221**, C₁₃H₁₂N₄O₈, m.p. 68-70° (decomp.), is presented in Figure 2.3 (overleaf), and the corresponding atomic coordinates are given in Table 9.6.2.

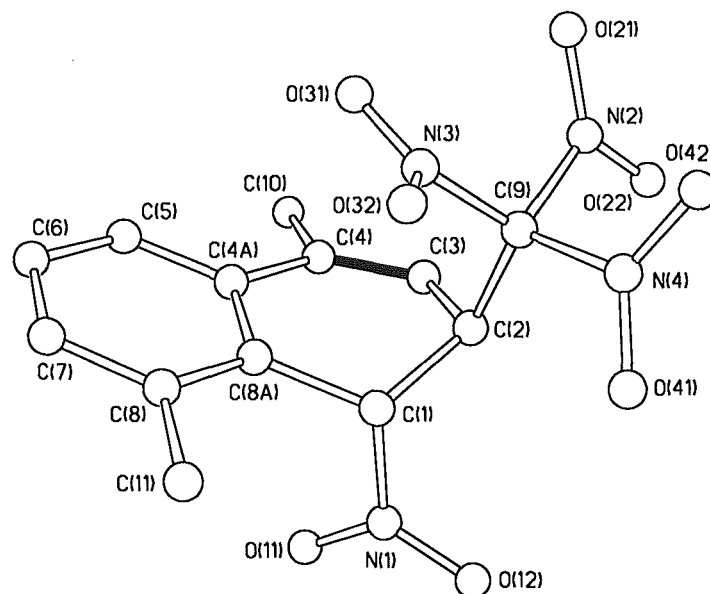


Figure 2.3 - Perspective drawing of adduct **221**

In the solid state the conformation of the alicyclic ring is such that the nitro and trinitromethyl substituents are close to *anti* to each other, with the C1-NO₂ bond close to perpendicular to the plane of the aromatic ring [torsional angles: N(1)-C(1)-C(2)-C(9) -153.3(4)°; N(1)-C(1)-C(8A)-C(8) 88.8(6)°]. The spectroscopic data for adduct **221** in solution were in accord with the established solid state structure. In particular, the CH-C(NO₂)₃ resonance appeared at δ 40.8, and the CH-NO₂ resonance appeared at δ 78.8, these assignments being confirmed by reverse detected heteronuclear correlation spectra (HMQC). The ¹H n.m.r. couplings were in agreement with the solid state conformation of the molecule; the appearance of the ¹H n.m.r. resonance for H1 (br s) is consistent with the torsional angle H(1)-C(1)-C(2)-H(2) 80.7(2)° and similarly the torsional angle H(2)-C(2)-C(3)-H(3) -34.2(0)° fits with the observed ¹H coupling constant J_{H_2,H_3} 5.9Hz.

Adducts **222** and **223** were eluted next from the h.p.l.c. column and in that order. While adduct **223** could not be obtained in a pure state, its epimer **222** gave crystals of adequate quality for its structure determination by single-crystal X-ray analysis. A perspective drawing of 1,5-dimethyl-*r*-1-nitro-*t*-4-

trinitromethyl-1,4-dihydronaphthalene **222**, $C_{13}H_{12}N_4O_8$, m.p. 84-86° (decomp.), is presented in Figure 2.4, and the corresponding atomic coordinates in Table 8.2.3.

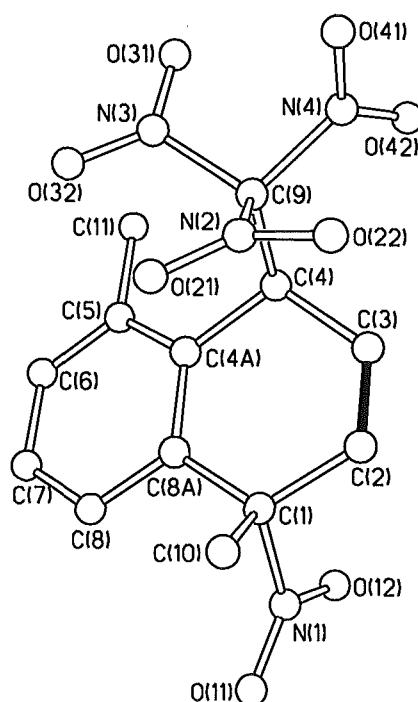


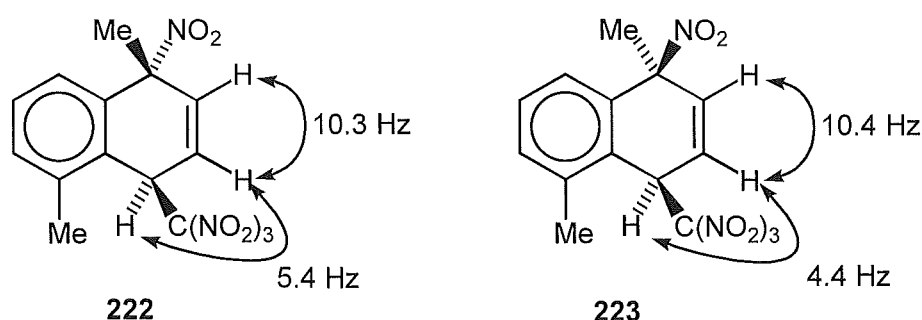
Figure 2.4 - Perspective drawing of adduct **222**

The structure consists of an enantiomeric pair of molecules, in which the magnitude of related torsional angles differ but not in a chemically significant manner. In the solid state the alicyclic ring exists in a distorted boat conformation, with the C(4)-C(NO₂)₃ bond close to perpendicular to the plane of the aromatic ring, but with the C(1)-C(10) and C(1)-N(1) bonds more evenly displaced from the plane of the aromatic ring [torsional angles: C(5)-C(4A)-C(4)-C(9) 79.6(8)° {enantiomer, -81.9(8)°}; C(8)-C(8A)-C(1)-C(10) -64.3(9)° {57.1(8)°}; C(8)-C(8A)-C(1)-N(1) 52.2(8)° {-59.1(7)°}]. The spectroscopic data for adduct **222** were consistent with the established structure. The structure of the epimeric adduct **223** was assigned on the basis of a comparison of its obtainable spectroscopic data with that of adduct **222**. The relevant data for both **222** and **223** is shown in Table 2.1, overleaf.

Table 2.1 Comparison of n.m.r. chemical shift data for epimeric adducts **222** and **223**

	222		223	
	¹ H	δ	¹ H	δ
¹ H n.m.r. data	1-CH ₃	2.03	1-CH ₃	1.98
	5-CH ₃	2.22	5-CH ₃	2.28
	H2	6.32	H2	6.52
	H3	6.40	H3	6.52
	H4	5.78	H4	5.78
¹³ C n.m.r. data	1-CH ₃	27.9	1-CH ₃	31.1
	5-CH ₃	19.9	5-CH ₃	19.1
	C4	42.5	C4	42.4
	C3	122.4	C3	124.5/135.5
	C2	135.6	C2	124.5/135.5
	C1	88.3	C1	86.6

The ¹³C n.m.r. chemical shifts for adduct **223** for C1 (δ 86.6), C4 (δ 42.4), and C2/C3 (δ 124.5, 135.5) point to the same connectivity in the alicyclic ring as for adduct **222**, leaving its epimeric nature as the structural difference. The ¹H n.m.r. coupling data (Figure 2.5), in conjunction with the observed n.O.e. between the 1-Me and H2 protons in both adducts **222** and **223** also support the assignment of their structural and stereochemical relationship.

Figure 2.5 - Comparison of the relevant ¹H n.m.r. coupling patterns for adducts **222** and **223**.

Previous studies⁶ have demonstrated that *trans*-1,4-nitro-trinitromethyl adducts are eluted from the h.p.l.c. column before their *cis* counterparts, thus the elution order of the epimeric nitro/trinitromethyl adducts **222** and **223** is consistent with their identification as the *r*-1-nitro-*t*-4-trinitromethyl and *r*-1-nitro-*c*-4-trinitromethyl isomers respectively.

The remaining four adducts were eluted in the order: nitro cycloadduct **224**, 4,8-dimethyl-*t*-2-trinitromethyl-1,2-dihydronaphthalen-*r*-1-ol **225**, hydroxy cycloadduct **226**, nitronic ester **227**, but here for simplicity the evidence for structural assignments will be presented for pairs of compounds, **224** and **226**, and **225** and **227**. The structures of the nitro cycloadduct **224** and the hydroxy cycloadduct **226** were determined by single-crystal X-ray analysis. A perspective drawing of the nitro cycloadduct **224**, C₁₃H₁₂N₄O₈, m.p. 168-170° (decomp.), is presented in Figure 2.6, and the corresponding atomic coordinates are given in Table 8.2.4.

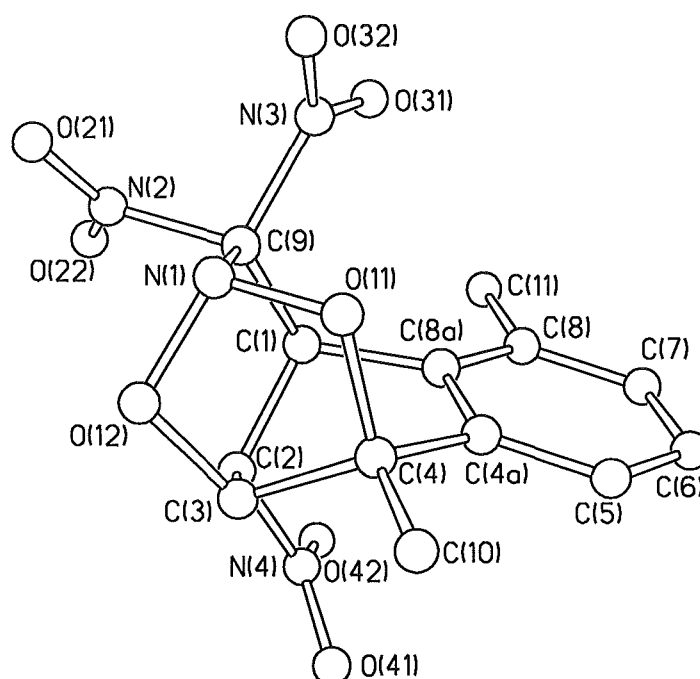


Figure 2.6 - Perspective drawing of cycloadduct **224**

Similar information is presented for the hydroxy cycloadduct **226**, $C_{13}H_{13}N_3O_7$, m.p. 171-173° (decomp.), in Figure 2.7 and Table 8.2.5. Not surprisingly, given the common dominant features of the heterocyclic cage structures and the aromatic ring in the two compounds, the solid state structures of the two cycloadducts **224** and **226** are closely similar.

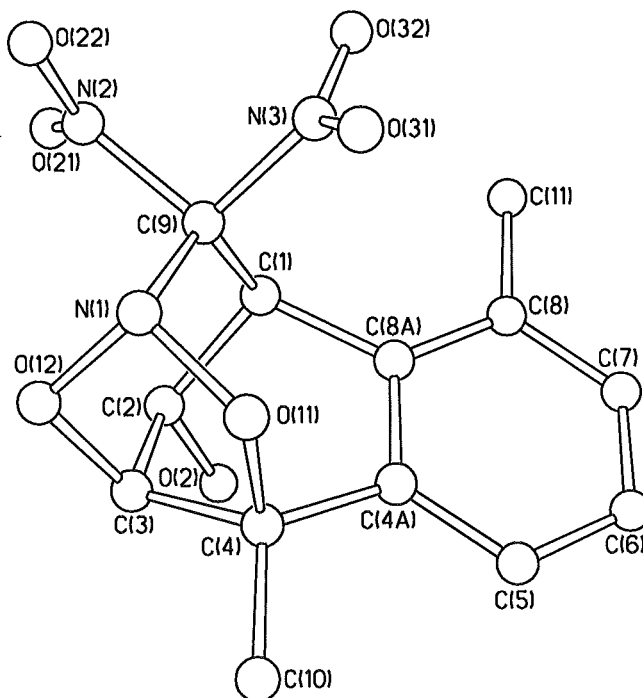


Figure 2.7 - Perspective drawing of cycloadduct **226**

Within the heterocyclic cage of each cycloadduct the N(1) atom is trigonal pyramidal and the C(9)-N(1) bond length [1.482(3) Å for cycloadduct **224**, 1.486(3) Å for **226**] is significantly shorter than the corresponding C(9)-N(2) 1.553(3) Å [1.531(3) Å for **226**] and C(9)-N(3) 1.532(3) Å [1.521(3) Å for **226**] bond lengths, similar to those observed earlier for analogous cage structures. In both structures the C(1)-C(9) bond is close to *anti* to the C(2)-X bond [torsional angles: for **224**, C(9)-C(1)-C(2)-N(4) -173.0(2)°; for **226** C(9)-C(1)-C(2)-O(2) -167.6(2)°], the plane of the C(2)-NO₂ group in nitro cycloadduct **224** being close to eclipsed with the C(2)-C(3) bond [torsional angle: C(3)-C(2)-N(4)-O(41) 12.0(3)°]. In the two structures there are minor differences in the orientations of

the C9-nitro groups, but this presumably reflects optimum crystal packing in the two structures and has no chemical significance. For both cycloadducts **224** and **226** the spectroscopic data were consistent with the established structures. In particular, the crucial ^{13}C n.m.r. resonances for **224**, $\text{CH-C}(\text{NO}_2)_2\text{R}$ (δ 41.3) and CH-NO_2 (δ 79.4), and **226**, $\text{CH-C}(\text{NO}_2)_2\text{R}$ (δ 44.7) and CH-OH (δ 67.0) were identified, and the ^1H n.m.r. coupling patterns observed in each adduct were essentially identical (Figure 2.8), as expected given the rigid polycyclic cage structure of the substituted ring system.

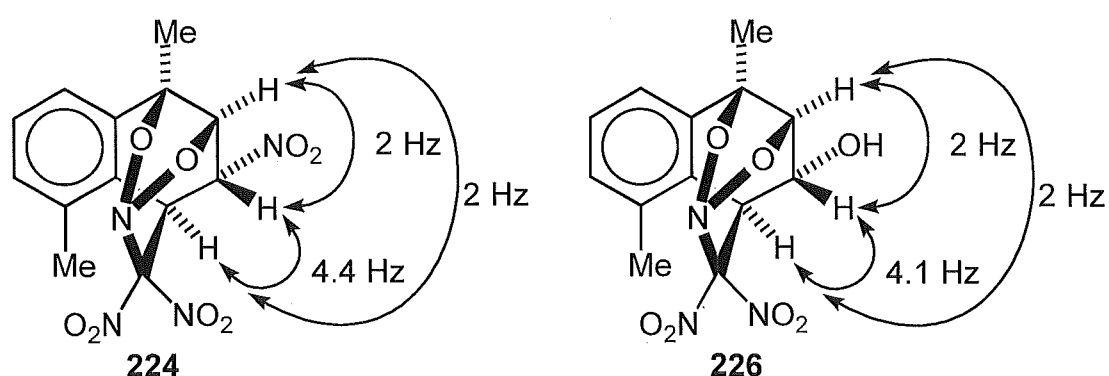


Figure 2.8 - ^1H n.m.r. H-H coupling constants for cycloadducts **224** and **226**

The observed ^1H n.m.r. coupling constants are consistent with the solid state configurations; $J_{\text{H}_1,\text{H}_2}$ 4.4 Hz for **224** and 4.1 Hz for **226** fit torsional angles $\text{H}(1)\text{-C}(1)\text{-C}(2)\text{-H}(2)$ $-51.1(1)^\circ$ and $-50.3(1)^\circ$ respectively, as does $J_{\text{H}_2,\text{H}_3}$ 2 Hz (for both **224** and **226**) with torsional angles $\text{H}(2)\text{-C}(2)\text{-C}(3)\text{-H}(3)$ $75.3(1)^\circ$ and $73.1(1)^\circ$.

4,8-Dimethyl-*t*-2-trinitromethyl-1,2-dihydronaphthalen-*r*-1-ol **225** could be isolated only as an impure oil and its structural assignment is based on a consideration of its spectroscopic data and its conversion in high yield on reaction with a solution of nitrogen dioxide in dichloromethane into the nitronic ester **227**, the structure of which was determined by single-crystal X-ray analysis. A perspective drawing of the nitronic ester **227**, $\text{C}_{13}\text{H}_{13}\text{N}_3\text{O}_7$, m.p. $157\text{-}159^\circ$ (decomp.), is presented in Figure 2.9 and the corresponding atomic coordinates are given in Table 8.2.6.

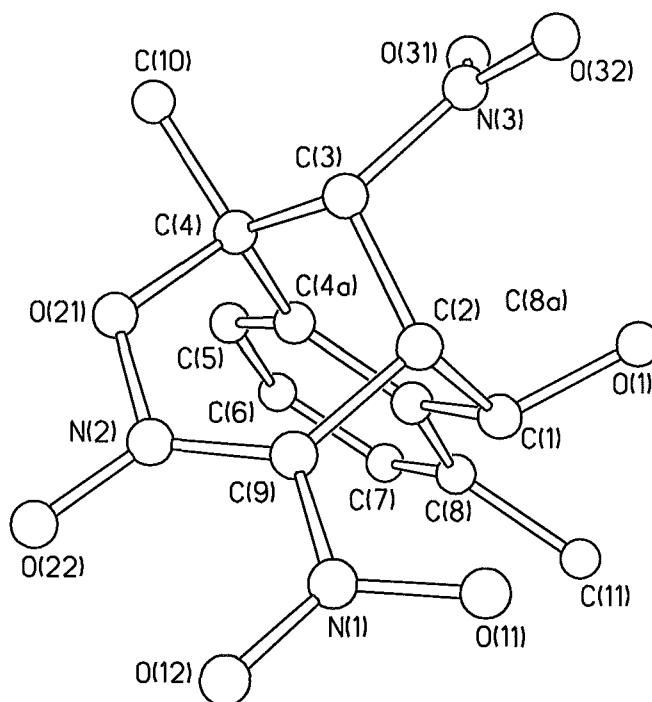


Figure 2.9 - Perspective drawing of nitronic ester **227**.

The partial double bond character of the C(9)-N(1) bond [bond length C(9)-N(1) 1.43(5) Å *c.f.* C(3)-N(3) 1.50(9) Å and C(9)-N(2) 1.32(0) Å] holds the N(1) nitro group close to eclipsed with the C(9)-N(2) bond [torsional angle O(12)-N(1)-C(9)-N(2) -4.1(5)°]. The spectroscopic data for the nitronic ester **227** were in accord with established structure. In particular, the ¹H n.m.r. coupling constants J_{H_1, H_2} 2.4 Hz and J_{H_2, H_3} 3.9 Hz are consistent with the solid state torsional angles H(1)-C(1)-C(2)-H(2) 76.3(1)° and H(2)-C(2)-C(3)-H(3) -59.4(1)° respectively. The connectivity in the hydroxy adduct **225** was defined by a combination of observations of its ¹H n.m.r. spectrum and related nuclear Overhauser enhancement experiments; the results of which are summarised in Figure 2.10, overleaf.

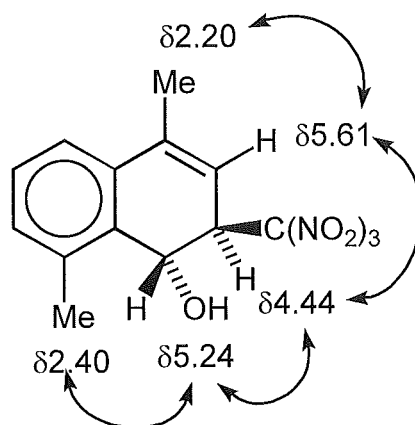


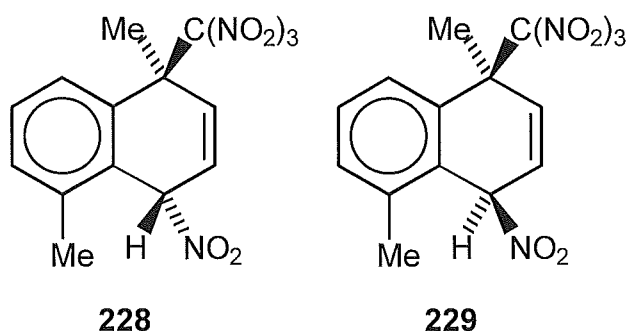
Figure 2.10 - Observed nuclear Overhauser enhancements in adduct **225**

The assignment of the ^1H n.m.r. spectrum allowed unequivocal identification of the protonated carbon resonances *via* reverse detected heteronuclear correlation spectra (HMQC). Thus it became clear that the hydroxy adduct **225** had a 4,8-dimethyl-2-trinitromethyl-1,2-dihydronaphthalen-1-ol structure with the significant ^{13}C n.m.r. resonances being δ 46.1 [$\text{C2-C}(\text{NO}_2)_3$], δ 63.4 [C1-OH], and δ 110.85 [$\text{C3} = \text{C4}$].

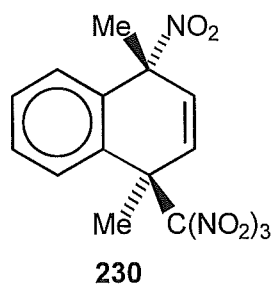
The formation of the nitronic ester **227** from the hydroxy adduct **225** by a nitro-denitro-cyclisation reaction on treatment with nitrogen dioxide in dichloromethane is somewhat unusual. However, a number of analogous nitronic esters have been isolated from the photolysis of the charge transfer complex of 1,2,3-trimethylbenzene with tetranitromethane⁷, and it is clear that these too were formed by nitro-denitro-cyclisation of intermediate nitro/trinitromethyl- and hydroxy/trinitromethyl- cyclohexa-1,3-dienes in a similar manner to the formation of **225**. The single-crystal X-ray analysis for the nitronic ester **227** resolves the remaining structural uncertainty in the hydroxy adduct **225** - namely the *r*-1-hydroxy-*t*-2-trinitromethyl stereochemical feature.

Photolysis of 1,5-dimethylnaphthalene and tetranitromethane in dichloromethane at -20°

The photolysis of the charge transfer complex of 1,5-dimethylnaphthalene and tetranitromethane at -20° for 1.5 h gave a mixture of products (Tables 2.4 and 9.6.1) including increased amounts of the epimeric 4,8-dimethyl-1-nitro-4-trinitromethyl adducts **228** (20%) and **229** (2%).



Adducts **228** and **229** were partially separated from this mixture by h.p.l.c. The *r*-1-nitro-*t*-4-trinitromethyl adduct **228** was eluted with 4,8-dimethyl-*r*-1-nitro-*t*-2-trinitromethyl-1,2-dihydronaphthalene **221** and could not be isolated in a pure state. The *r*-1-nitro-*c*-4-trinitromethyl epimer **229** was eluted later in admixture with 1,5-dimethyl-*r*-1-nitro-*c*-4-trinitromethyl-1,4-dihydronaphthalene **223**, the elution order being consistent with the assignment of adduct **228** as the *r*-1-nitro-*t*-4-trinitromethyl epimer and adduct **229** as the *r*-1-nitro-*c*-4-trinitromethyl epimer. These stereochemical assignments are further supported by the observation that in (D)-chloroform or (D₂)-dichloromethane the *r*-1-nitro-*t*-4-trinitromethyl epimer **228** is transformed with retention of stereochemistry into 4,8-dimethyl-*r*-1-nitro-*t*-2-trinitromethyl-1,2-dihydronaphthalene **221**, the structure of which has been established, earlier, by single-crystal X-ray analysis. The lability of the *r*-1-nitro-*t*-4-trinitromethyl epimer **228** prevented the full n.m.r. characterisation of this compound, but the ¹H n.m.r. data were consistent with its structural assignment as being epimeric with adduct **229** and structurally similar to the *r*-1-nitro-*t*-4-trinitromethyl adduct **230**, formed on photolysis of 1,4-dimethylnaphthalene with tetranitromethane, which was identified by single crystal X-ray analysis.



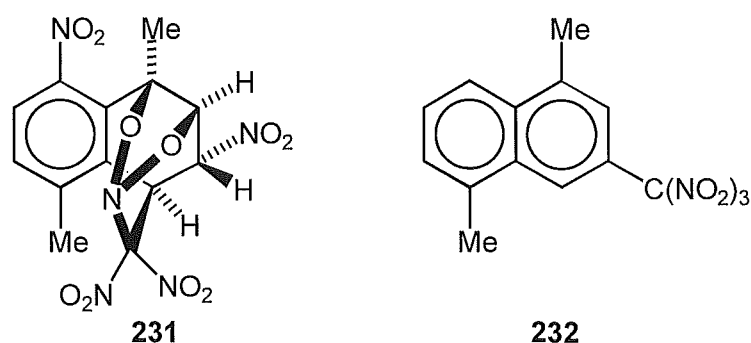
A comparison of the ^1H n.m.r. chemical shift data for adducts **228**, **229**, and **230** is shown in Table 2.2.

Table 2.2 Comparison of ^1H n.m.r. chemical shift data for adducts **228-230**

	228	229	230
	δ	δ	δ
4-CH ₃	2.19	2.05	2.11
H3	6.70	6.70	6.68/6.26
H2	6.48	6.79	6.68/6.26
H1	6.26	6.03	N/A

Although much spectroscopic data for the *r*-1-nitro-*c*-4-trinitromethyl epimer **229** were obscured by being in a mixture with adduct **223**, the crucial ^{13}C n.m.r. resonances for the alicyclic ring of adduct **229** could be identified by reverse detected heteronuclear correlation spectra (HMQC/HMBC). In particular, signals at δ 49.1 [Me-C4-C(NO₂)₃], 78.75 [C1-NO₂], 126.5 [C3], and 131.9 [C2] indicated clearly the connectivity in the *r*-1-nitro-*c*-4-trinitromethyl epimer **229**.

Chromatography of the mixture of products on a silica gel Chromatotron plate allowed the isolation of small amounts of two further materials, **231** and **232**, neither of which were present in the mixture prior to chromatography.



The structure of the dinitro cycloadduct **231**, C₁₃H₁₁N₅O₁₀, m.p. 120°, was determined by single-crystal X-ray analysis, a perspective drawing is presented in Figure 2.11 (overleaf), and corresponding atomic coordinates are given in Table 8.2.7.

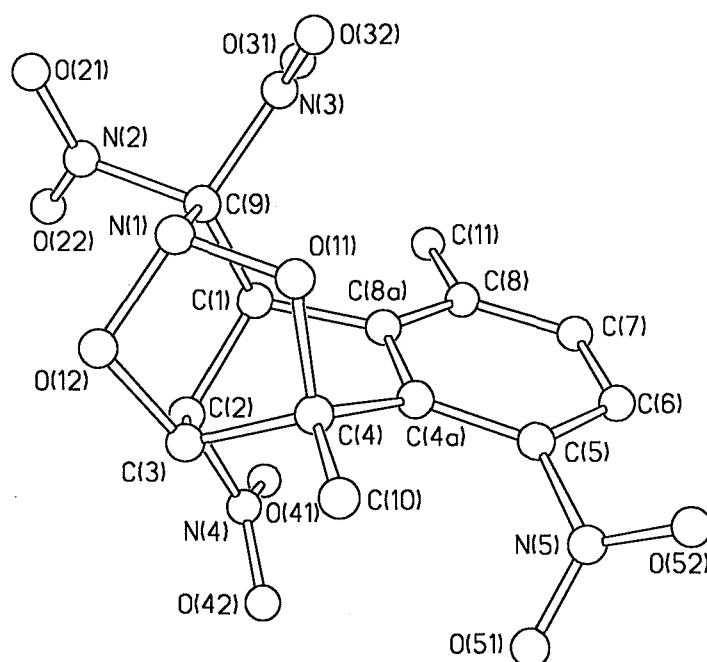


Figure 2.11 - Perspective drawing of dinitro cycloadduct **231**

With the exception of the additional nitro group at C(5), the structure is closely similar to that of the nitro cycloadduct **224**, above. Here again the nitrogen atom in the heterocyclic cage structure is clearly trigonal pyramidal, a similar pattern of bond length differences C(9)-N(1) 1.471(3), C(9)-N(2) 1.533(3), C(9)-N(3) 1.514(3) Å is evident, and the orientation of the C(2)-NO₂ group is indicated by the torsional angles: C(9)-C(1)-C(2)-N(4) -173.3(2)°; C(3)-C(2)-N(4)-O(42) 14.8(3)°. The spectroscopic data which were obtainable with limited amounts of material were consistent with the established structure. The ¹H n.m.r. chemical shift data of the two nitro cycloadducts **224** and **231** is compared in Table 2.3, overleaf.

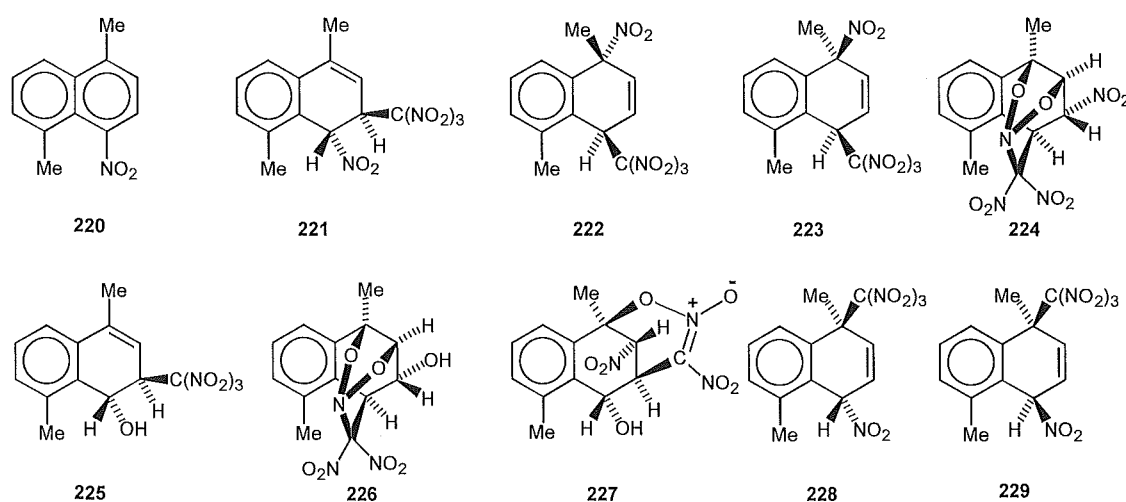
Table 2.3 Comparison of ^1H n.m.r. data for nitro cycloadducts **224** and **231**

^1H	224 δ	231 δ
4- CH_3	1.95	2.03
H3	5.51	5.45
H2	5.70	5.68
H1	5.64	5.55

The 4,8-dimethyl-2-trinitromethylnaphthalene structure **232** was assigned on the basis of its accurate mass which pointed to a molecular formula $\text{C}_{13}\text{H}_{11}\text{N}_3\text{O}_6$, and the appearance of two singlet resonances in the aromatic region of the ^1H n.m.r. spectrum which indicated a 1,3-substitution pattern in one of the aromatic rings.

Photolysis in dichloromethane at -50° and -78° .

The photolysis of the charge transfer complex of 1,5-dimethylnaphthalene and tetranitromethane in dichloromethane at -50° or -78° resulted in the formation of adducts **221**, **222**, **228**, and **229**, and some unidentified adducts; the formation of adducts **223-227** was suppressed under these reactions conditions. A summary of the product yields in these reactions is given in Table 2.4 later in this chapter.



Photolysis in acetonitrile at 20° and -20°.

Photolysis of the charge transfer complex of 1,5-dimethylnaphthalene and tetranitromethane in acetonitrile at 20° for 2.5 h gave a high yield of 4,8-dimethyl-1-nitronaphthalene **220** (50%) and the three nitro/trinitromethyl adducts **221** (15%), **222** (14%), and **223** (4%) (Table 2.4, overleaf). In a comparable reaction, but at -20°, the yields of 4,8-dimethyl-1-nitronaphthalene **220** (38%) and the nitro/trinitromethyl adduct **221** (10%) were somewhat lower, and significant amounts of the epimeric 4,8-dimethyl-1-nitro-4-trinitromethyl adducts **228** (11%) and **229** (2%) were formed. In neither reaction were adducts **224**, **225**, **226** and **227** formed. A summary of the product yields in these reactions is given in Table 2.4, overleaf.

Photolysis in dichloromethane containing trifluoroacetic acid (0.7 M).

The photolysis of the charge transfer complex of 1,5-dimethylnaphthalene and tetranitromethane in dichloromethane at 20° containing trifluoroacetic acid (0.7 M) for 3 h resulted in the formation of small amounts of adducts **228** (1 %) and **221** (3 %), unidentified adducts (total 2 %), and 4,8-dimethyl-1-nitronaphthalene **220** (93 %) (Table 2.4, overleaf).

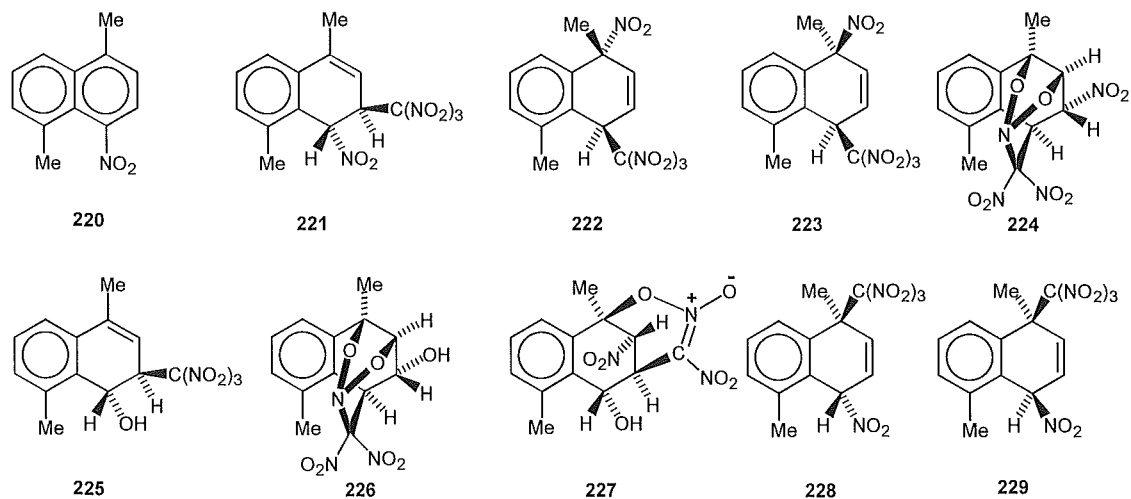
Photolysis in 1,1,1,3,3,3-hexafluoropropan-2-ol.

The photolysis of the charge transfer complex of 1,5-dimethylnaphthalene and tetranitromethane in 1,1,1,3,3,3-hexafluoropropan-2-ol at 20° for 3 h resulted in the formation of substantial amounts of adduct **221** (20 %) and 4,8-dimethyl-1-nitronaphthalene **220** (74 %) as the major product (Table 2.4, overleaf).

The product yields for all the photolysis reaction conditions employed are displayed in Table 2.4, overleaf.

Table 2.4 - Overview of yields of products from the photolysis of 1,5-dimethylnaphthalene (0.4 mol l^{-1}) and tetranitromethane (0.8 mol l^{-1})

Reaction Conditions	t/h	Conversion %	Yields (%)									Adducts ^A	220	ArX ^A
			221	222	223	224	225	226	227	228	229			
DCM/+20°	1	62	23.3	9.2	2.3	9.1	16.2	7.7	2.3	2.7	1.5	74.3	20.2	25.7
	1.5	80	22.4	8.3	1.5	8.8	14.2	8.0	1.5	5.8	1.3	71.8	19.8	28.2
DCM/-20°	1	61	11.1	5.8	2.0	-	1.2	<.5	<.5	16.1	1.6	42.0	48.8	58.0
	1.5	85	13.6	6.1	1.7	-	0.9	<.5	<.5	19.8	1.8	44.9	46.2	54.8
DCM/-50°	1	65	12.1	10.5	-	-	-	-	-	30.5	4.5	69.9	24.4	30.1
	2	c. 100	12.0	10.8	-	-	-	-	-	28.3	4.5	68.4	20.3	31.6
DCM/-78°	1	85	9.1	17.2	-	-	-	-	-	28.6	6.7	76.7	14.9	23.3
	2	97	9.2	16.3	-	-	-	-	-	26.7	4.3	73.6	15.7	26.4
AN/+20	1.5	82	16.3	14.3	4.6	-	-	-	-	-	-	35.8	53.4	64.1
	2.5	c. 100	15.4	13.8	4.1	-	-	-	-	-	-	38.6	50.4	61.4
AN/-20	1.5	80	7.2	10.6	3.9	-	-	-	-	10.7	1.9	52.6	35.8	47.4
	2.5	c. 100	9.5	10.6	5.0	-	-	-	-	10.6	1.8	48.3	37.7	51.7
DCM/TFA/ +20°	1	48	2.7	-	-	-	-	-	-	1.3	-	6.3	91.8	93.7
	1.5	58	2.7	-	-	-	-	-	-	1.0	-	5.7	92.5	94.3
	3	84	2.7	-	-	-	-	-	-	1.2	-	6.2	92.5	1.3
HFP/+20°	1	32	14.6	-	-	-	-	-	-	-	-	17.4	76.8	82.6
	1.5	42	16.5	-	-	-	-	-	-	-	-	19.4	75.2	80.6
	3	69	19.7	-	-	-	-	-	-	-	-	23.6	73.7	76.3

^Atotal

Rearrangement studies of the epimeric 4,8-dimethyl-1-nitro-4-trinitromethyl-1,4-dihydronaphthalenes **228** and **229**.

The mixture of products from the photolysis of 1,5-dimethylnaphthalene and tetranitromethane for 2 h in dichloromethane at -50° (Table 2.4) was dissolved in (D)-chloroform and the ^1H n.m.r. spectrum of the solution monitored at appropriate time intervals. Under these reactions conditions adducts **222** and **223**, and the unidentified adducts were stable, but adduct **228** was converted into adduct **221** (Figure 2.12).

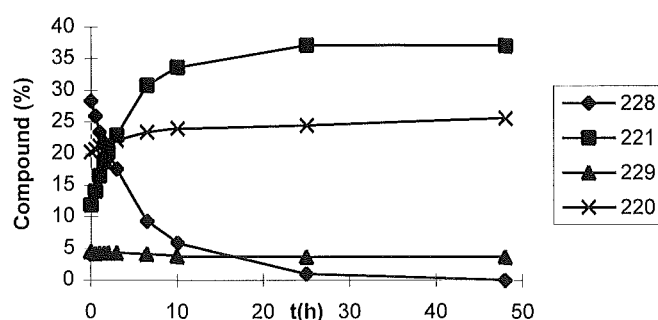
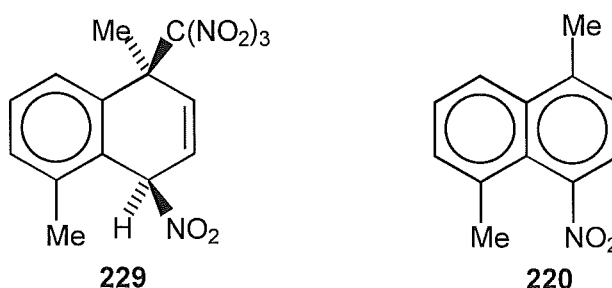


Figure 2.12 - Rearrangement study of adduct **228** in (D)-chloroform

In a similar experiment, but in (D₂)-dichloromethane, a more rapid conversion of adduct **228** into adduct **221** occurred, with some concurrent formation of 4,8-dimethyl-1-nitronaphthalene **220** (Figure 2.13). At longer reaction times (48 h) it was clear that adduct **229** slowly decomposed to give the nitro compound **220**.



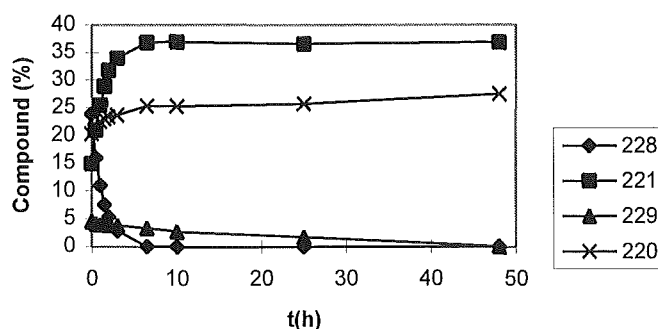
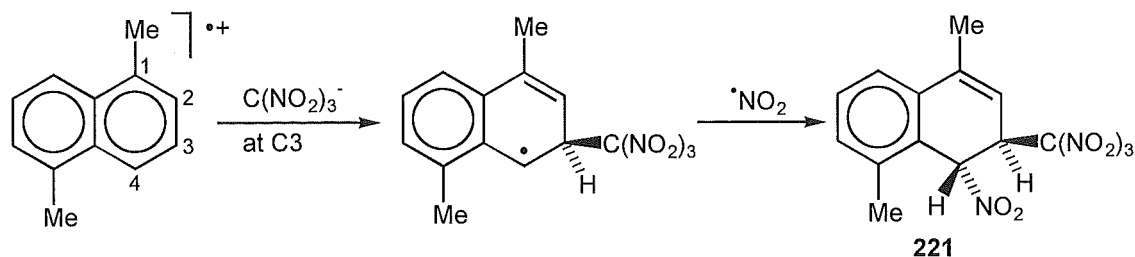


Figure 2.13 - Rearrangement study of adducts **228** and **229** in (D₂)-dichloromethane

Discussion

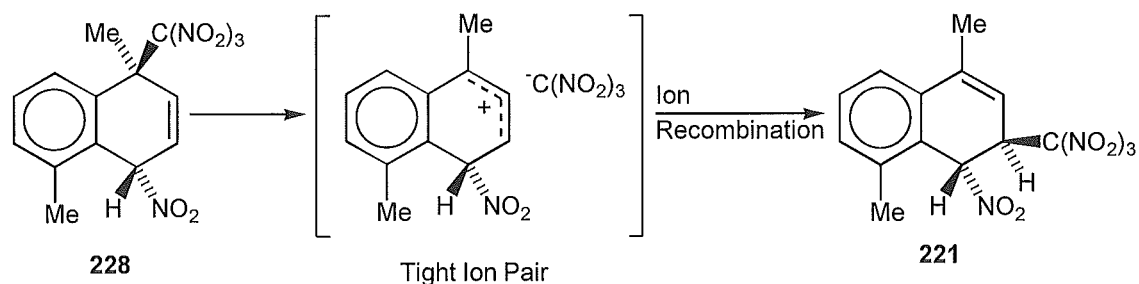
The regiochemistry of trinitromethanide ion attack on the radical cation of 1,5-dimethylnaphthalene.

A discussion of the regiochemistry of trinitromethanide ion attack on the radical cation of 1,5-dimethylnaphthalene is complicated by the observation that 4,8-dimethyl-*r*-1-nitro-*t*-4-trinitromethyl-1,4-dihydro-naphthalene **228** undergoes allylic rearrangement in dichloromethane solution at 22° to give 4,8-dimethyl-*r*-1-nitro-*t*-2-trinitromethyl-1,2-dihydronaphthalene **221**. In photolysis reactions at 20° there seems to be little doubt that much of adduct **221** is produced by a thermal rearrangement of adduct **228** formed initially in the photochemical reaction. For photolysis reactions at lower temperatures (-20 to -78°) there remains the probability that some of the rearranged adduct **221** detected among the products (Table 2.4) is formed from adduct **228** during the isolation procedure and the acquisition of ¹H n.m.r. spectra. However, the possibility can not be excluded that minor amounts (up to 5% yield) of 4,8-dimethyl-*r*-1-nitro-*t*-2-trinitromethyl-1,2-dihydronaphthalene **221** are formed directly by initial attack of trinitromethanide ion at C3 in the radical cation of 1,5-dimethylnaphthalene (Scheme 2.4, overleaf).



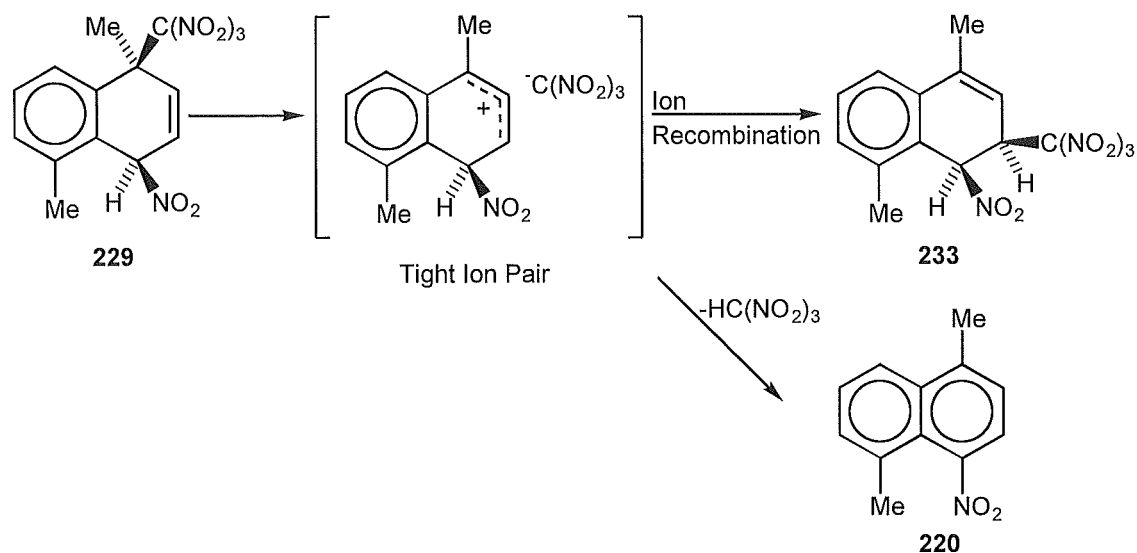
Scheme 2.4

In sharp contrast to the lability of the *r*-1-nitro-*t*-4-trinitromethyl adduct **228** towards allylic rearrangement, the *r*-1-nitro-*c*-4-trinitromethyl adduct **229** is relatively stable and, when it does react, it yields the product of elimination, 4,8-dimethyl-1-nitronaphthalene **220**. This is presumably an indication that the allylic rearrangement of adduct **228** proceeds *via* a tight ion pair; for the rearrangement of adduct **228** this would lead stereospecifically to the *r*-1-nitro-*t*-2-trinitromethyl adduct **221** (Scheme 2.5),



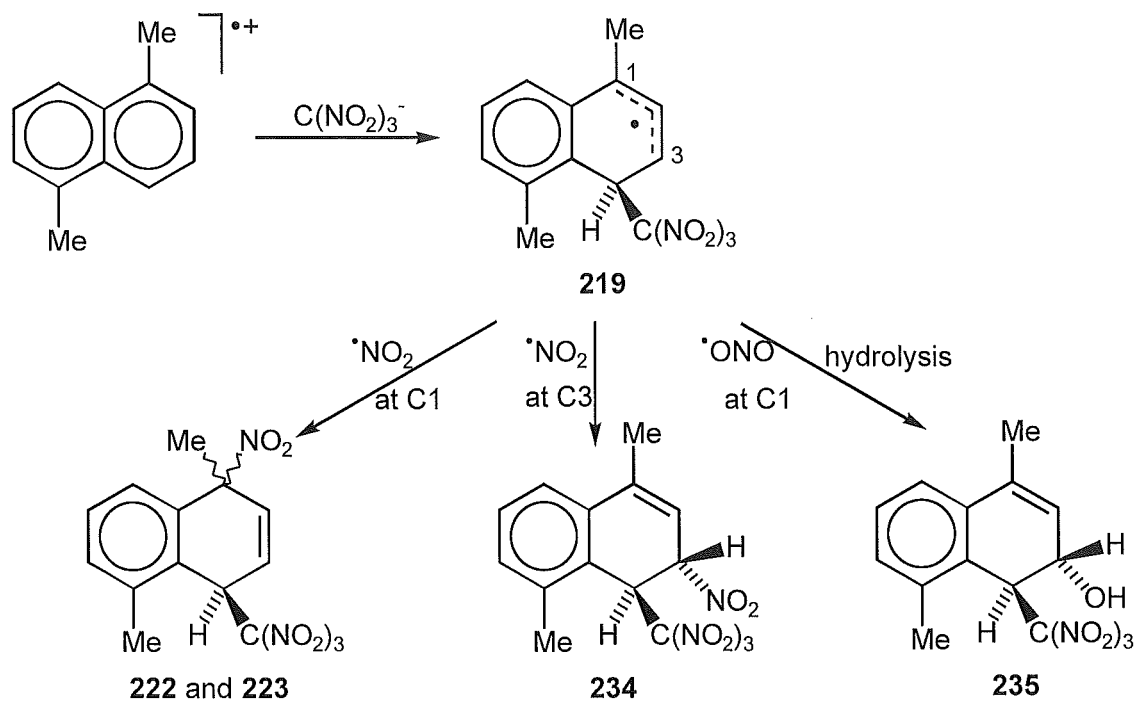
Scheme 2.5

but analogous rearrangement of adduct **229** would give the sterically compressed *cis*-epimer **233** (Scheme 2.6, overleaf). The nature of the driving force(s) for the rearrangement of adduct **228** to give adduct **221** is uncertain, but two possibilities appear reasonable. Apart from the release of the steric compression inherent in the location of a trinitromethyl group *ipso* to a substituent larger than hydrogen, it seems possible that the attainment of styrene-type conjugation in the product may be significant.



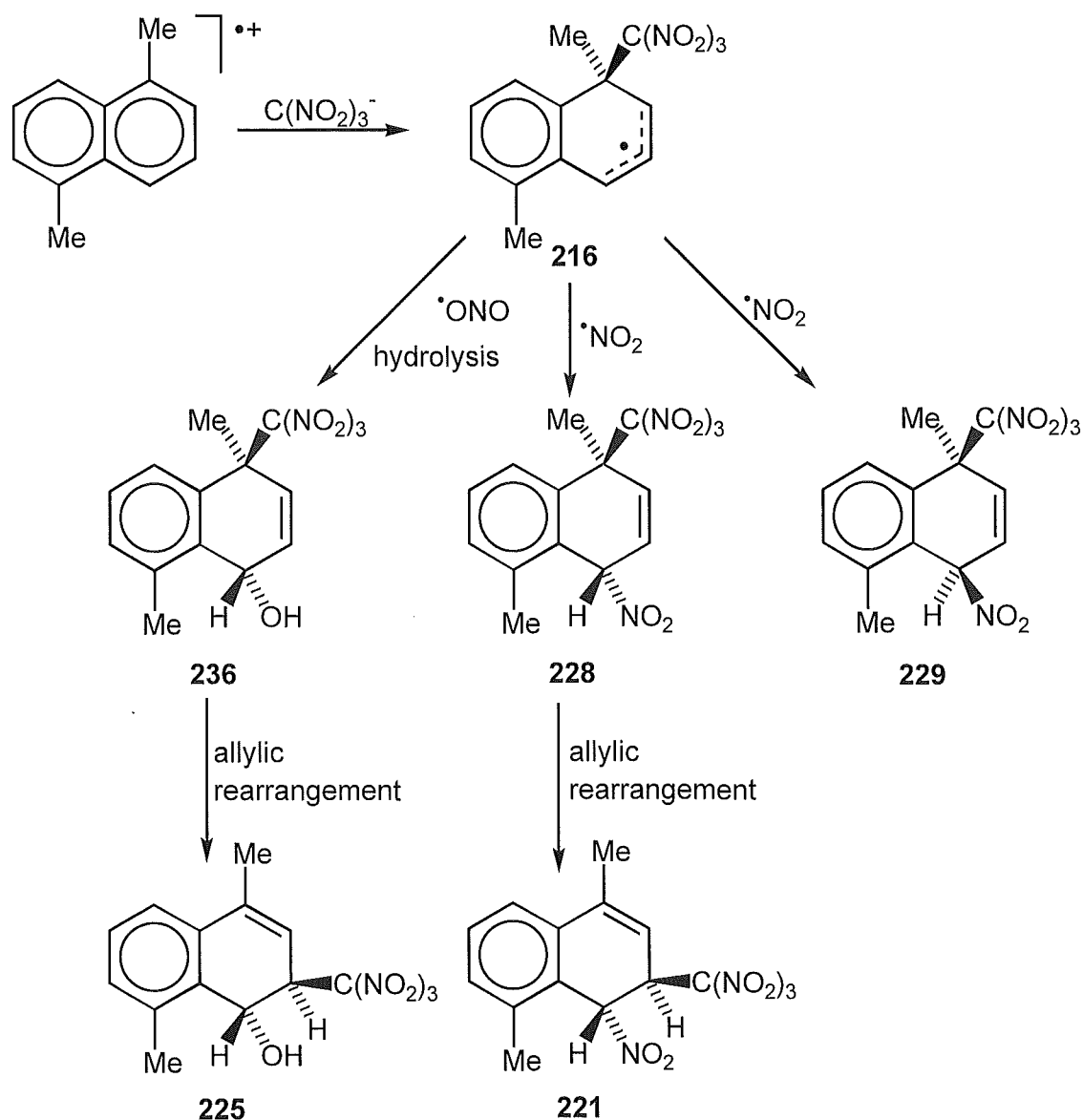
Scheme 2.6

Adducts **222** and **223**, and the precursors **234** and **235** to nitro cycloadduct **224** and hydroxy cycloadduct **226** respectively, arise from initial attack of trinitromethanide ion at C4 in the radical cation of 1,5-dimethylnaphthalene (Scheme 2.7).



Scheme 2.7

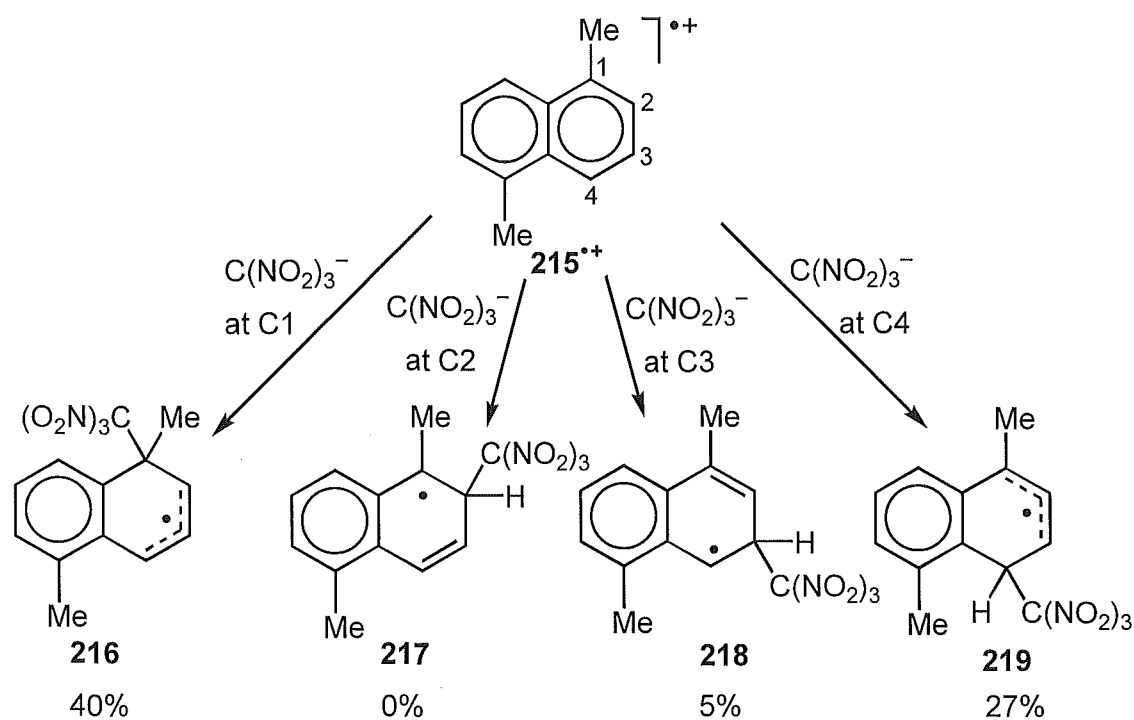
Adducts **228** and **229** arise from initial attack of trinitromethanide ion at C1 in the radical cation of 1,5-dimethylnaphthalene to give the phenyl-allylic radical **216** (Scheme 2.8). Subsequent radical coupling of nitrogen dioxide at C4 in the phenyl-allylic radical would give the epimeric adducts **228** and **229**. Although the formation of 4,8-dimethyl-*t*-2-trinitromethyl-1,2-dihydronaphthalen-*r*-1-ol **225**, and thence the nitronic ester **227**, can not be accounted for on the basis of the thermal rearrangement of the nitro/trinitromethyl adduct **228** in (D₂)-dichloromethane, adduct **225** could arise by allylic rearrangement of the structurally related hydroxy/trinitromethyl adduct **236**.



Scheme 2.8

This adduct **236** would be formed by hydrolysis of the nitrite ester formed by radical reaction of the phenyl-allylic radical **219** with nitrogen dioxide. Given the difference in the electron-withdrawing properties of hydroxy and nitro groups, it appears likely that the allylic rearrangement of the hydroxy/trinitromethyl adduct **236** would occur more rapidly than that of the nitro/trinitromethyl adduct **228**.

On the basis of the above discussion, adducts **221**, **225**, **227**, **228** and **229** are formed either totally, or in the case of **221** substantially, by attack of trinitromethanide ion *ipso* to a methyl group at C1 in the radical cation of 1,5-dimethylnaphthalene to give the phenyl-allylic radical **216** (total ca. 40 % in dichloromethane at 20°; see Scheme 2.9 below). Adducts **222**, **223**, **224** and **226** are formed by attack of trinitromethanide ion *peri* to a methyl group at C4 in the radical cation of 1,5-dimethylnaphthalene to give the 1-methyl-1-phenyl-allylic radical **219** (total c. 27 % in dichloromethane at 20°). Only a minor amount (say c. 5 %) of adduct **221** arises by attack of trinitromethanide ion at C3 in the radical cation of 1,5-dimethylnaphthalene to give the benzylic radical **218** and none at C2 to give the tertiary benzylic radical **217**.



Scheme 2.9

These data are consistent with the premise that the regiochemistry of trinitromethanide ion attack on a radical cation is determined by the relative stabilities of the delocalised carbon radicals which result from reaction at the various positions in that radical cation. In the present context, the 1-methyl-1-phenylallylic radical **219** is destabilised by the significant *peri* steric interaction between the bulky trinitromethyl group and the proximate methyl group, while the alternative phenyl-allylic radical **216** is subject only to the steric compression resulting from *ipso* attachment of the trinitromethyl group. It appears that trinitromethanide ion attack at the β positions of the radical cation of 1,5-dimethylnaphthalene is highly disfavoured, despite the relatively high charge distribution at these sites.

The photochemistry of 1,5-dimethylnaphthalene and tetranitromethane in dichloromethane containing trifluoroacetic acid or in 1,1,1,3,3,3-hexafluoropropan-2-ol.

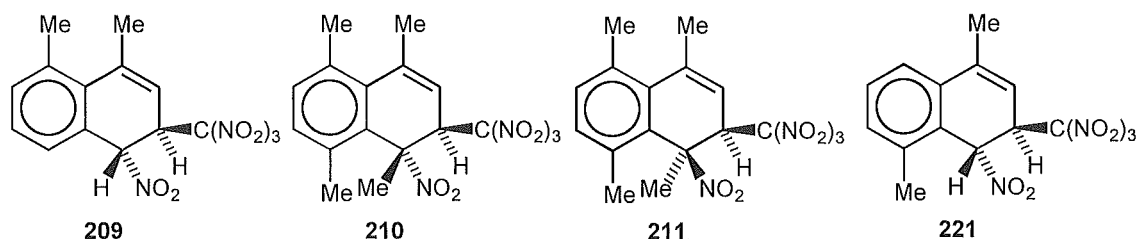
The photolysis of the charge transfer complex of 1,5-dimethylnaphthalene and tetranitromethane in dichloromethane at 20° gives mainly adducts (total 72 %) which arise by initial attack of trinitromethanide ion on the radical cation of 1,5-dimethylnaphthalene. In the presence of trifluoroacetic acid (0.7 M), the trinitromethanide ion will be converted into the less nucleophilic nitroform by protonation, and this is reflected in the reduction in total adduct yield (to 6 %), with a concomitant increase in the product of radical coupling of nitrogen dioxide with the radical cation of 1,5-dimethylnaphthalene to give the 4,8-dimethyl-1-nitronaphthalene **220**.

The photolysis of aromatic substrates with tetranitromethane in 1,1,1,3,3,3-hexafluoro-propan-2-ol has been reported⁸ to suppress the normal reaction pathways leading to the formation of adducts in dichloromethane, presumably resulting from extreme deactivation of radical cation reactivity towards nucleophiles in the former solvent by either protonation or, more likely, hydrogen bonding of the nucleophilic species. In the study of the reactions of 1,5-dimethylnaphthalene it is clear that this deactivation is less effective, adducts (ca. 24 %) formed by initial trinitromethanide ion attack on the radical cation of 1,5-dimethylnaphthalene accompanying the product of radical

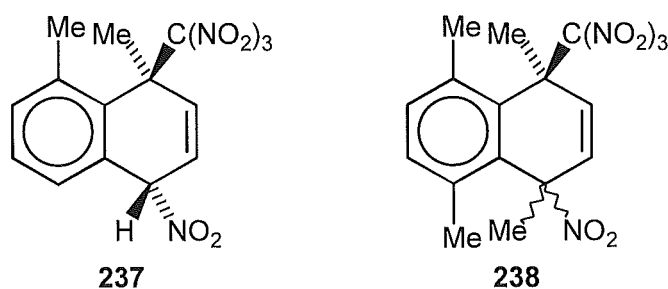
coupling of nitrogen dioxide with the radical cation, 4,8-dimethyl-1-nitronaphthalene **220** (74 %).

*The possible implications of the allylic rearrangement of 4,8-dimethyl-r-1-nitro-t-4-trinitromethyl-1,4-dihydronaphthalene **228** to give 4,8-dimethyl-r-1-nitro-t-2-trinitromethyl-1,2-dihydronaphthalene **221** for other reaction systems.*

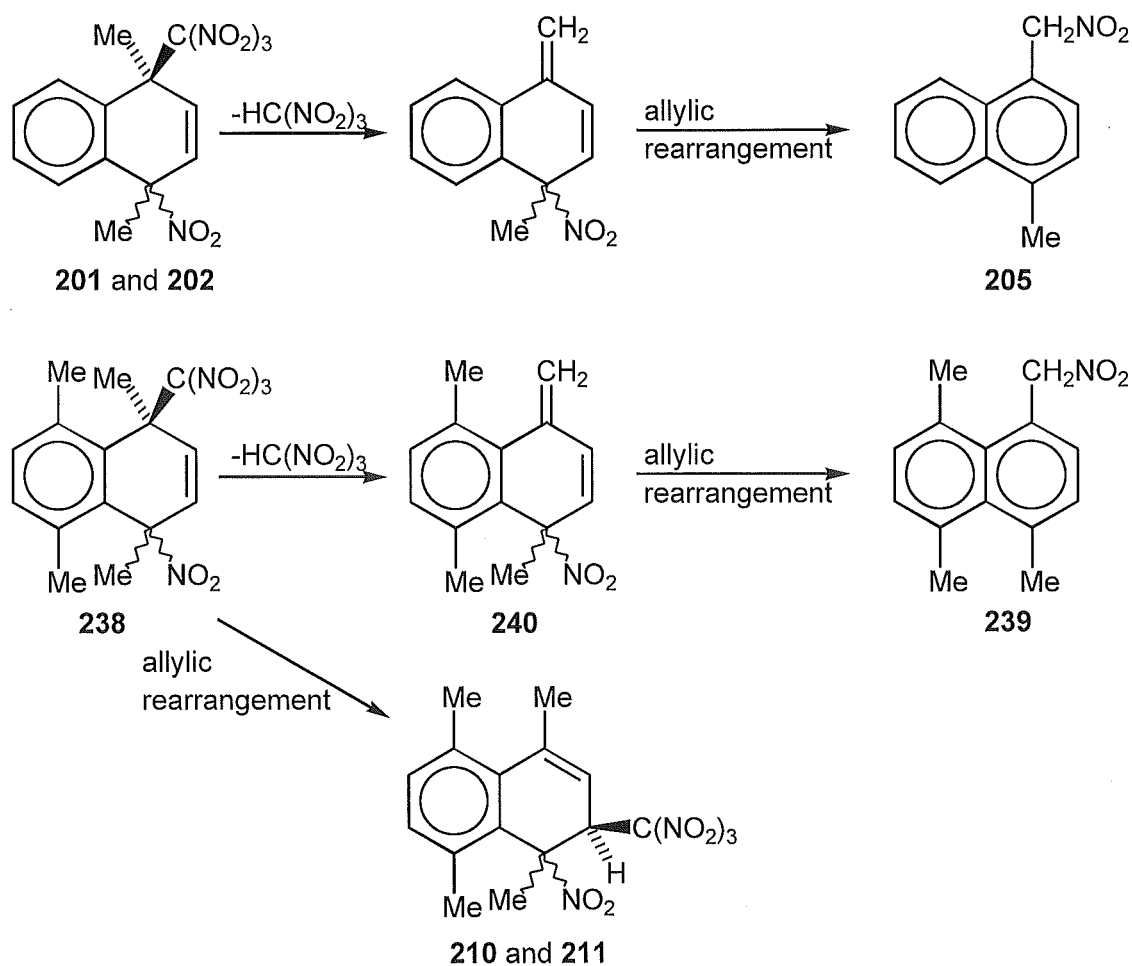
The allylic rearrangement of 4,8-dimethyl-r-1-nitro-t-4-trinitromethyl-1,4-dihydronaphthalene **228** accounts for much, if not all, of the formation of 4,8-dimethyl-r-1-nitro-t-2-trinitromethyl-1,2-dihydronaphthalene **221**. As discussed earlier, 1-nitro-2-trinitromethyl adducts **209-211** were also observed as the major products in the photolysis mixtures of tetranitromethane with 1,8-dimethylnaphthalene and 1,4,5,8-tetramethylnaphthalene respectively.⁴ These adducts were formed despite the presumed intermediacy of localised carbon radicals in their formation.



Given the common features of adducts **209-211** with adduct **221**, in particular the 4-methyl-substituent in each case, and the now recognised mode of formation of **221** being predominantly *via* allylic rearrangement of the sterically congested 1-trinitromethyl-4-nitro adduct **228**, it is reasonable to envisage a similar source of adducts **209-211**, *i.e.* *via* allylic rearrangement of initially formed 1-nitro-4-trinitromethyl adducts **237** and **238** respectively.



This theory is supported by the formation of 4,5,8-trimethyl-1-nitromethylnaphthalene **239** as the major product on photolysis of the charge transfer complex of 1,4,5,8-tetramethylnaphthalene with tetranitromethane.⁴ By analogy with the mode of formation of 4-methyl-1-nitromethylnaphthalene **205** on rearrangement of the adducts **201** and **202** (Scheme 2.10) from 1,4-dimethylnaphthalene proposed by Ebersson *et al.*,² it is clear that 4,5,8-trimethyl-1-nitromethylnaphthalene **239** can be formed by similar rearrangement of the 1,4,5,8-tetramethyl-1-nitro-4-trinitromethyl-1,4-dihydronaphthalenes **238** via the intermediate **239**.



Scheme 2.10

On the basis of the foregoing, it appears most likely that adducts **238**, in parallel with the formation of the nitromethyl compound **239**, also undergo allylic rearrangement to yield the 1,4,5,8-tetramethyl-1-nitro-2-trinitromethyl-1,2-dihydronaphthalenes **210** and **211**.

Summary

This analysis resolves the apparent enigma of trinitromethanide ion attack on the radical cations of both 1,4,5,8-tetramethylnaphthalene and 1,8-dimethylnaphthalene to form a localised benzylic radical - this form of attack does not occur. Rather, the operative pathway in trinitromethanide ion attack on an aromatic radical cation is guided by the formation of the most stable intermediate radical species, and it appears that, for the various substituted naphthalene substrates at least, radical cation charge distribution at best a secondary factor in their reactions with tetranitromethane.

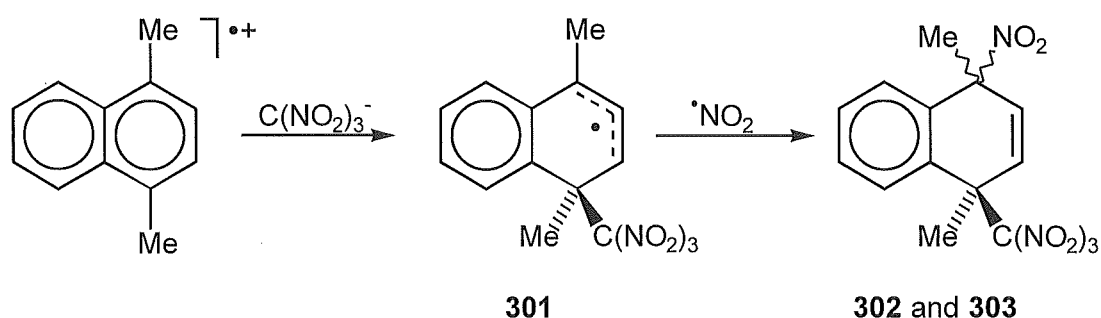
References

- ¹ Eberson, L., Hartshorn, M. P., Radner, F., and Svensson, J. O., *J. Chem. Soc. Perkin Trans. 2*, 1994, 1719.
- ² Eberson, L., Hartshorn, M. P., and Radner, F., *J. Chem. Soc. Perkin Trans. 2*, 1992, 1799.
- ³ Calvert, J. L., Eberson, L., Hartshorn, M. P., Maclagan, R. G. A. R., and Robinson, W. T., *Aust. J. Chem.*, 1994, **47**, 1211.
- ⁴ Eberson, L., Calvert, J. L., Hartshorn, M. P., and Robinson W.T., *Acta Chem. Scand.*, 1993, **47**, 1025.
- ⁵ Davies, A., and Warren, K. D., *J. Chem. Soc. B*, 1969, 873.
- ⁶ Butts, C. P., Calvert, J. L., Eberson, L., Hartshorn, M. P., Radner, F., and Robinson, W. T., *J. Chem. Soc. Perkin Trans. 2*, 1994, 1485.
- ⁷ Butts, C. P., Eberson, L., Hartshorn, M. P., Robinson, W. T., Timmerman-Vaughan, D. J., and Young, D. A. W., *Acta Chem. Scand.*, 1996, **50**, 29.
- ⁸ Eberson, L., Hartshorn, M. P., Persson, O., *Angew. Chem., Int. Ed. Engl.*, 1995, **34**, 2268.

Chapter 3

Introduction

The photonitration of aromatic compounds with tetranitromethane has been shown to proceed *via* the formation of a triad of species; the aromatic radical cation, trinitromethanide ion $[\text{C}(\text{NO}_2)_3]^-$, and nitrogen dioxide. The recombination of these species is the crucial step in the formation of photoproducts in these systems. It was demonstrated¹ that trinitromethanide ion attack on the radical cation is the initiating process in this triad recombination. For naphthalene derivatives, trinitromethanide ion attack occurs almost exclusively at the α positions of the radical cation to form allylic radicals such as **301** in Scheme 3.1, formed on photolysis of 1,4-dimethylnaphthalene with tetranitromethane.

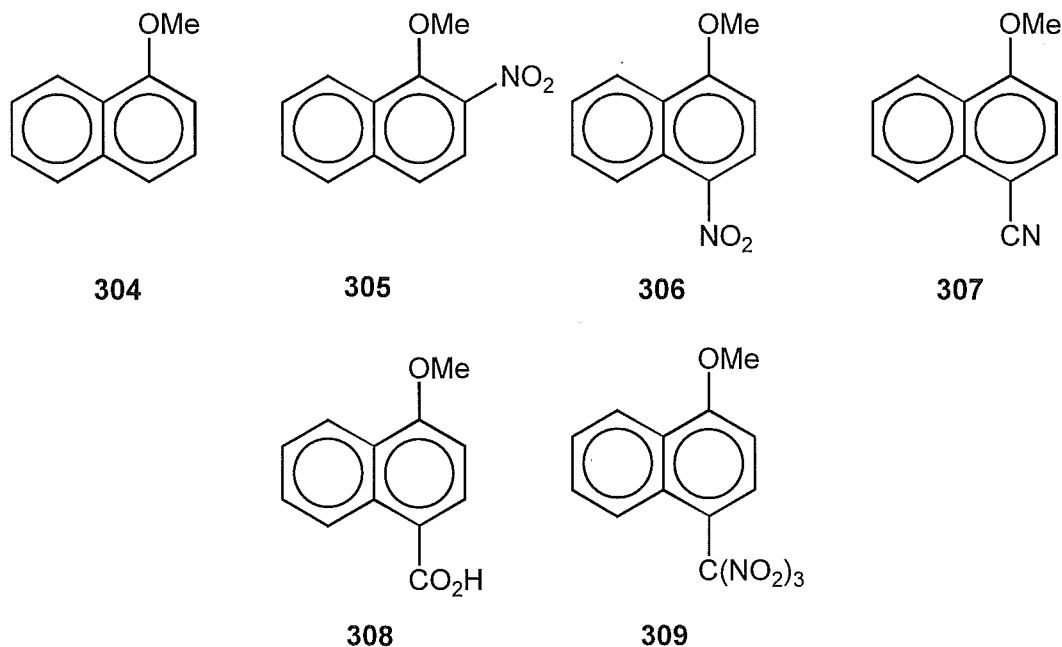


Scheme 3.1

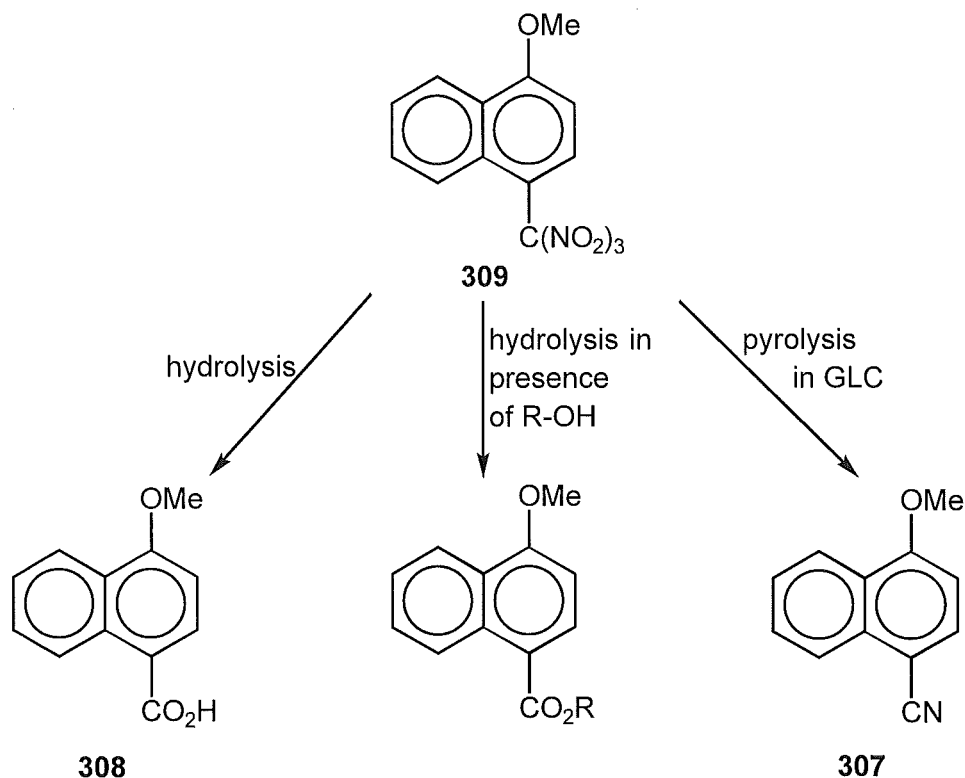
Subsequent $\cdot\text{NO}_2$ coupling to allylic radical **301** gives the epimeric nitro-trinitromethyl dihydronaphthalene adducts **302** and **303**.

Methyl substituted naphthalenes² and methoxybenzene derivatives³ have been the main focus of study of ArH-tetranitromethane photolysis reactions. However, direct comparison of the results for these two types of aromatic compounds is difficult given the uncertain influence of methoxy substituents on these reactions. It was considered that an understanding of the role of the methoxy group on the formation of photoproducts was necessary before a comparison could be made. 1-Methoxynaphthalene **304** was deemed

to be an appropriate aromatic substrate as a comparison of its reactivity with the reactivity of the better understood methyl substituted naphthalenes would allow the influence of the methoxy group to be examined.



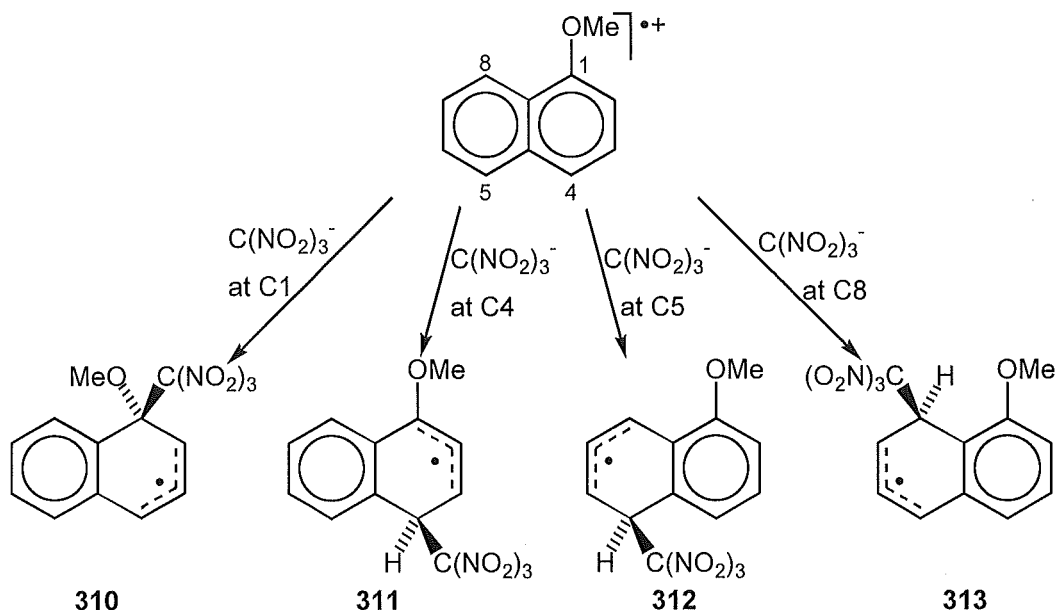
An earlier study of the photolysis reactions of tetranitromethane with 1-methoxynaphthalene by Ebersson and Radner⁴ used GLC analysis of the resultant product mixtures and found high yields of 2-nitro- and 4-nitro-1-methoxynaphthalenes **305** and **306** with small amounts (<5%) of 4-methoxy-1-naphthonitrile **307**. In addition, 4-methoxy-1-naphthoic acid **308** precipitated during or after photolysis; in the presence of a variety of alcohols 4-methoxy-1-naphthoic acid **308** no longer precipitated from reaction mixtures, but the corresponding esters were formed in yields of up to 47%. The formation of 4-methoxy-1-naphthoic acid **308** (or its esters), and the detection of 4-methoxy-1-naphthonitrile **307** on GLC analysis, were seen as evidence that 1-methoxy-4-trinitromethylnaphthalene **309** was present in the reaction mixture. Subsequent hydrolysis in the prevailing acidic conditions of the reaction medium would give carboxylic acid **308** (or ester in the presence of an alcohol) or pyrolysis in the GLC inlet system could give the substituted naphthonitrile **307** (Scheme 3.2, overleaf).



Scheme 3.2

Although no direct evidence of the formation of nitro-trinitromethyl adducts was obtained, such adducts were suggested as labile intermediates in the formation of the postulated 1-methoxy-4-trinitromethylnaphthalene **309** precursor. Given the use of GLC techniques in the study described above to identify products, and the known thermal instability of dihydronaphthalene adducts in analyses of these types^{2(c)} it seems reasonable that adduct formation may provide a pathway to the observed aromatic products.

The mode of formation of these labile adducts is of interest. Given the preferred formation of allylic radical intermediates in these systems, trinitromethanide ion attack on the radical cation of 1-methoxynaphthalene could be expected at C1, C4, C5 or C8 of the radical cation, giving radical species **310-313** respectively (Scheme 3.3, overleaf)



Trinitromethanide ion attack at C1 of the radical cation would give the phenyl-allylic radical **310** which suffers from steric compression of the geminal trinitromethyl and methoxy substituents. Structure **313** formed by trinitromethanide ion addition to C8 of the radical cation possesses a destabilising *peri* interaction between the adjacent bulky substituents. Intermediates **311** and **312**, formed by trinitromethanide ion attack at C4 and C5 respectively, are both free of steric interactions, but the 1-methoxy-phenyl allylic nature of radical **311** should be more stable. Given this analysis, it was expected that products derived from **311** would predominate.

Results

General procedure for the photolysis of 1-methoxynaphthalene with tetranitromethane.

A solution of 1-methoxynaphthalene **304** (500 mg, equal to 0.4 mol l⁻¹) and tetranitromethane (0.8 mol l⁻¹) in dichloromethane (at 20°, -20°, -50°, or -78°) or acetonitrile was irradiated with filtered light (λ cut-off at 435 nm). Aliquots were withdrawn from the reaction mixture at appropriate time intervals, the volatile material removed rapidly under reduced pressure at $\leq 0^\circ$, and the

product composition determined by ^1H n.m.r. spectral analysis (for details see Experimental Section; Tables 8.3.1 - 8.3.3)

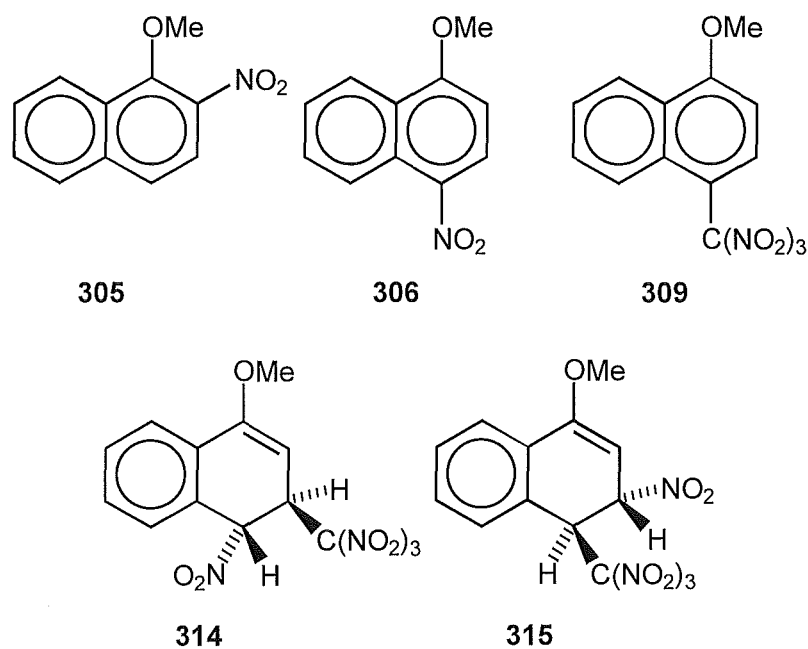
Photolysis of 1-methoxynaphthalene and tetranitromethane in dichloromethane at 20°.

A solution of 1-methoxynaphthalene (0.4 mol l^{-1}) and tetranitromethane (0.8 mol l^{-1}) in dichloromethane was irradiated at 20°. The composition of the reaction mixture was monitored by withdrawing samples for ^1H n.m.r. spectral analysis (Table 3.1; Table 8.3.1).

Table 3.1 - Overview of yields from the photolysis of 1-methoxynaphthalene (0.4 mol l^{-1}) and tetranitromethane (0.8 mol l^{-1}) in dichloromethane at 20°.

t/h	Conversion(%)	Yield (%)							Unknowns
		305	306	308	309	314	315	319	
0.25	36.5	2.0	38.2	-	41.3	7.4	11.0	-	-
0.5	68.2	3.0	41.7	-	41.7	6.2	7.7	-	-
1	~100	5.2	50.4	-	34.6	6.3	3.3	-	-
2	100	7.3	57.4	4.8	24.1	6.5	-	-	-

The solution after 1 h (conversion ca. 100%), after work-up, contained the 1-methoxy-2-nitronaphthalene **305** (5%), 1-methoxy-4-nitronaphthalene **306** (50%), 1-methoxy-4-trinitromethyl-naphthalene **309** (35%), and the two unstable adducts **314** (6%) and **315** (3%). The aromatic compounds were separated by chromatography on a silica gel Chromatotron plate and the nitro derivatives of 1-methoxynaphthalene **305** and **306** were identified by comparison with authentic material.



The structure of 1-methoxy-4-trinitromethylnaphthalene **309**, $C_{12}H_9N_3O_7$, m.p. 192-194°, was determined by single crystal X-ray analysis; a perspective drawing is presented in Figure 3.1, and corresponding atomic coordinates are given in Table 8.3.4.

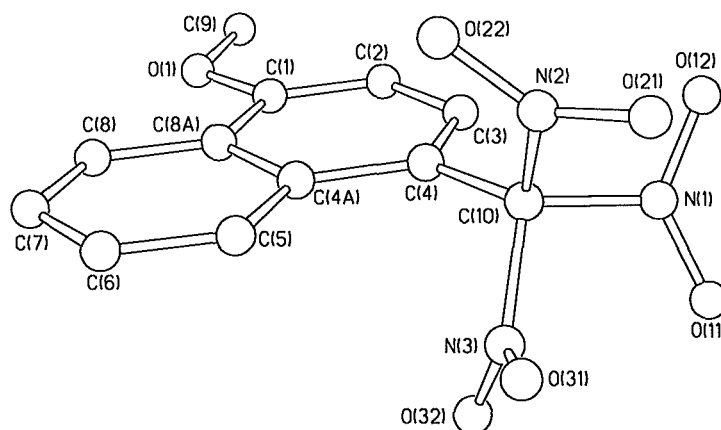
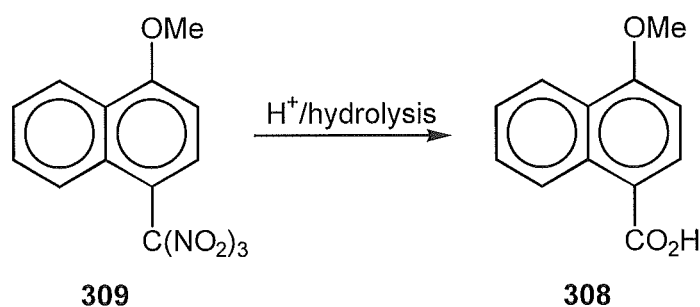


Figure 3.1 - Perspective drawing of **309**

The structure consists of two crystallographically independent molecules. Comparison of torsional angles for the two molecules reveals that for both molecules the methoxy group lies in the plane of the naphthalene ring system with the O(1)-C(9) and O(1')-C(9') bonds eclipsed with the C(1)-C(2) and C(1')-

C(2') bonds respectively. The differences between the two molecules lie in the orientation of the trinitromethyl groups relative to the ring system [e.g. torsional angles: C(4A)-C(4)-C(10)-N(3) 49.8(5)°, C(4A')-C(4')-C(10')-N(3') 56.2(6)°] and are presumably related to optimum packing in the crystal lattice and have no chemical significance. The spectroscopic data were in accord with the established structure.

Extension of the reaction time for the photolysis reaction at 20° to 2 h (Tables 3.1 and 8.3.1) resulted in a significant reduction in the yield of 1-methoxy-4-trinitromethylnaphthalene **309**, and the precipitation of some 4-methoxy-1-naphthoic acid **308**. This observation indicates clearly that the 4-methoxy-1-naphthoic acid **308** reported earlier⁴ is indeed derived from hydrolysis of the trinitromethyl aromatic **309** under the prevailing acidic reaction conditions (Scheme 3.4).



Scheme 3.4

Neither of the unstable adducts **314** and **315** could be isolated from the Chromatotron plate or by h.p.l.c. on a cyanopropyl column, and their identification is based on consideration of n.m.r. data derived from a product mixture for a reaction at -20°, below.

Photolysis of 1-methoxynaphthalene and tetranitromethane in dichloromethane at -20°.

Reaction of 1-methoxynaphthalene and tetranitromethane for 1 h, as above except at -20°, gave a product which was shown by ¹H n.m.r. spectra to be a mixture (Table 8.3.1) of 1-methoxy-2-nitronaphthalene **305** (3%), 1-

methoxy-4-nitronaphthalene **306** (47%), 1-methoxy-4-trinitromethylnaphthalene **309** (34%), and the two unstable adducts **314** (7%) and **315** (8%).

The two adducts were labile in solution, with the less stable adduct **315** having a half-life of ca. 4.5 h in (^2H)-chloroform at 23°. The structures of the two adducts were assigned tentatively on the basis of n.m.r. data. The more stable adduct was assigned the 4-methoxy-*r*-1-nitro-*t*-2-trinitromethyl-1,2-dihydro-naphthalene structure **314**. A nuclear Overhauser experiment allowed the location of H3 (δ 4.73) between the 4-OCH₃ (δ 3.79) and H2 (δ 5.50) substituents, leaving the signal at δ 5.79 to be assigned to H1 in the structure (Figure 3.2).

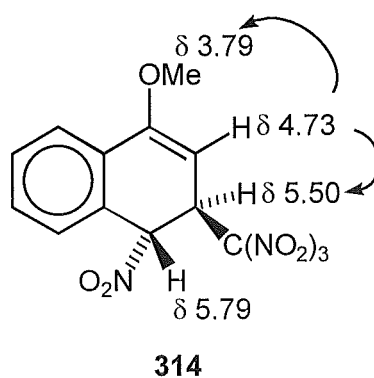


Figure 3.2 - Observed nuclear Overhauser enhancements in the ^1H n.m.r. of **314**

The ^{13}C n.m.r. resonances for adduct **314** were partially assigned on the basis of reverse detected heteronuclear correlation spectra (HMQC). The crucial signal at δ 41.7, a chemical shift consistent with the H-C-C(NO₂)₃ structural feature, was assigned to C2. The assignment of the signal at δ 81.8 is as expected for the H-C-NO₂ structural feature at C1. Although no stereochemical information could be obtained from the spectroscopic data, the *r*-1-nitro-*t*-2-trinitromethyl stereochemistry can be assigned by comparison with the similar structure **316**, for which an X-ray crystal structure was obtained. A comparison of the relevant ^1H n.m.r. chemical shifts and coupling constants for **314** and **316** is shown in Figure 3.3, overleaf.

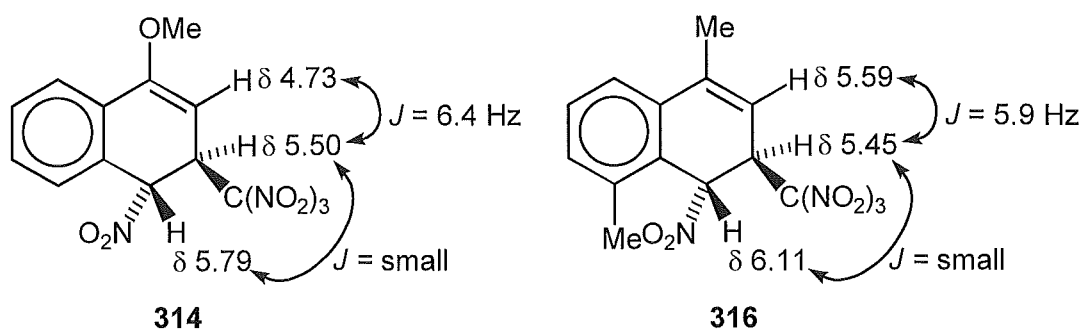


Figure 3.3 - Comparison of ^1H n.m.r. data for **314** and **316**

For the less stable adduct, tentatively identified as 4-methoxy-*r*-2-nitro-*t*-1-trinitromethyl-1,2-dihydronaphthalene **315**, nuclear Overhauser experiments allowed the assignment of the signals arising from the methoxy protons (δ 3.75), H1 (δ 5.42), H2 (δ 5.22) and H3 (δ 4.48) (Figure 3.4).

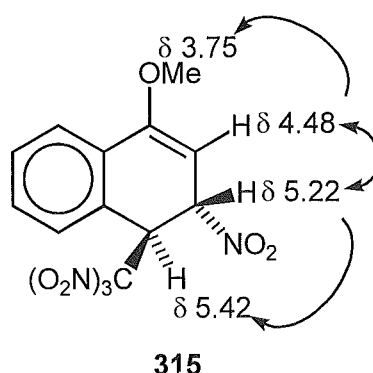
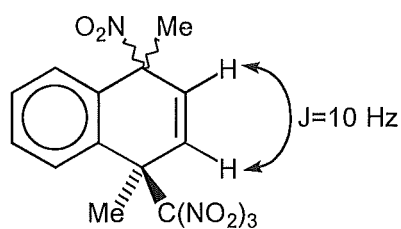


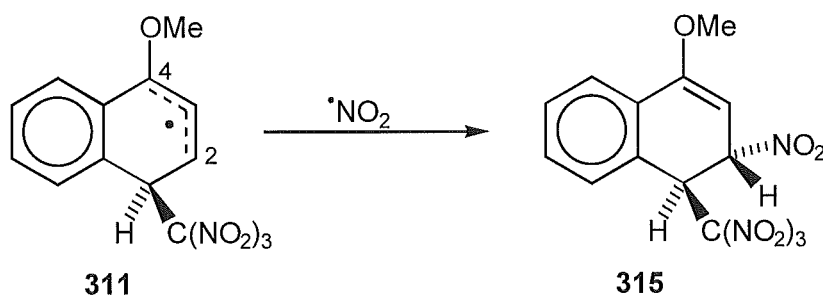
Figure 3.4 - Observed nuclear Overhauser enhancements in the ^1H n.m.r. spectra of **315**.

Using reverse detected heteronuclear correlation spectra (HMQC) only the signal due to C1 (δ 44.9) could be assigned with certainty, but this chemical shift allows the location of the trinitromethyl group at C1. The attachment of the nitro function at C2 is implied by the coupling constant $J_{\text{H2,H3}} = 6.8$ Hz which would be much higher (*ca.* 10 Hz) if the adduct possessed a C4 nitro substituent as in compound **317** below, formed in photolysis reactions of 1,4-dimethylnaphthalene and tetranitromethane.



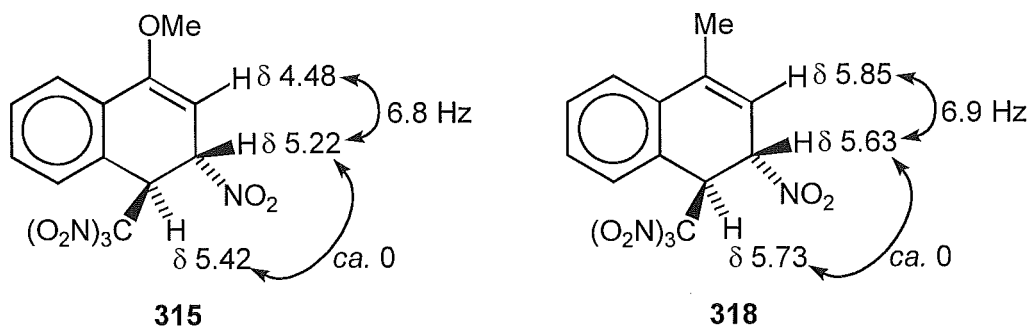
317

The stereochemistry of **315** was assigned by comparison with structures possessing similar regiochemistry and which are all formed by nitrogen dioxide addition to C2 of phenyl allylic radicals similar to **311**, *trans* to the bulky trinitromethyl group (Scheme 3.5).^{2(i), (l)-(n)}



Scheme 3.5

Figure 3.5 displays a comparison of the relevant ¹H n.m.r. chemical shift and coupling data for **315** and the analogous adduct **318**, for which the X-ray crystal structure has been determined, from the photolysis of 1-methylnaphthalene with tetranitromethane.^{2(m)} The similarity of the coupling patterns of adducts **315** and **318** supports the stereochemical assignment.

Figure 3.5 - Comparison of ¹H n.m.r. data for **315** and **318**

Photolysis of 1-methoxynaphthalene and tetranitromethane in dichloromethane in the presence of trifluoroacetic acid at 20°.

A solution of 1-methoxynaphthalene (0.4 mol l⁻¹) and tetranitromethane (0.8 mol l⁻¹) in dichloromethane containing trifluoroacetic acid (0.8 mol l⁻¹) was irradiated at 20°. The composition of the reaction mixture was monitored by withdrawing samples for ¹H n.m.r. spectral analysis (Table 3.2).

Table 3.2 - Overview of yields of products from the photolysis of 1-methoxynaphthalene (0.4 mol l⁻¹) and tetranitromethane (0.8 mol l⁻¹) in dichloromethane with added trifluoroacetic acid (0.8 mol l⁻¹).

Reaction		Yield (%)			
Conditions	t/h	Conversion (%)	306	319	Nitrodimers
20°	0.08	14.9	Trace	~100	-
	0.25	26.8	Trace	~100	Trace
	0.50	59.2	14.5	85.5	Trace
-50°	0.08	38.3	Trace	~100	Trace
	0.25	60.3	Trace	95	5
	0.50	100	Trace	88.1	11.9

The solution after 15 minutes (conversion ca. 27%), after work-up, contained essentially a mixture of 4,4'-dimethoxy-1,1'-binaphthyl **319** and unreacted 1-methoxynaphthalene. The dimer **319** was isolated by crystallisation from dichloromethane and its structure determined by single crystal X-ray analysis. A perspective drawing of 4,4'-dimethoxy-1,1'-binaphthyl **319**, C₂₂H₁₈O₂, m.p. 264-266°, is presented in Figure 3.6, and the corresponding atomic coordinates are given in Table 8.3.5.

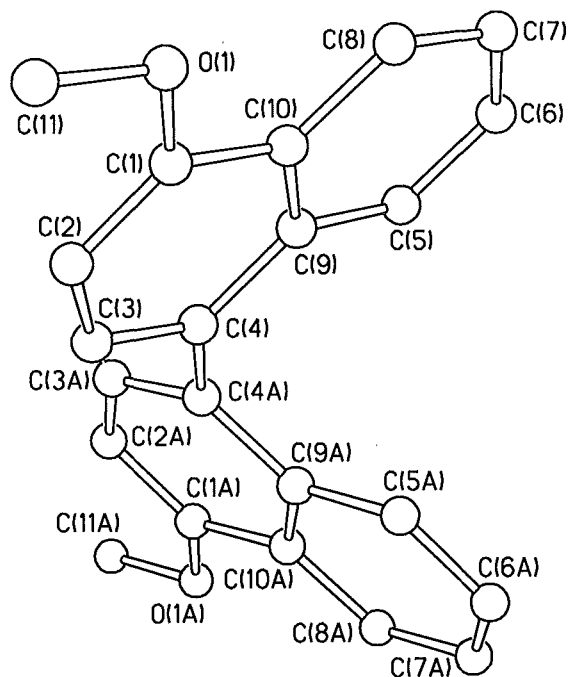
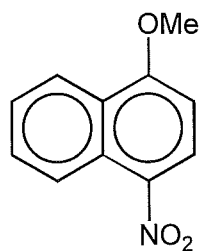


Figure 3.6 - Perspective drawing of **319**

In this structure **319** the O(1)-C(11) and C(1)-C(2) bonds are eclipsed and the displacement of the two naphthalene ring systems from coplanarity is indicated by the torsional angle: C(3)-C(4)-C(4a)-C(3a) $61.5(7)^\circ$. The spectral data were all in accord with the established structure.

At longer reaction times in these reactions, significant amounts of 1-methoxy-4-nitronaphthalene **306** (15%) were formed in addition to the dimer **319**.



306

For the corresponding reaction at -50°C , the formation of 1-methoxy-4-nitronaphthalene was substantially suppressed and the products were the dimer **319** and what appeared to be a mixture of nitrodimers which were not investigated further (Table 3.2).

Photolysis of 1-methoxynaphthalene and tetranitromethane in dichloromethane at -78° .

A solution of 1-methoxynaphthalene (0.4 mol l^{-1}) and tetranitromethane (0.8 mol l^{-1}) in dichloromethane was irradiated at -78° , as above, and the composition of the reaction mixture was monitored by withdrawing samples for ^1H n.m.r. spectral analysis (Table 8.3.1). The notable feature of this reaction was the formation of 4,4'-dimethoxy-1,1'-binaphthyl **319** (11% relative yield) among the products at relatively low conversion (39%) of starting material into products.

Photolysis of 1-methoxynaphthalene and tetranitromethane in acetonitrile

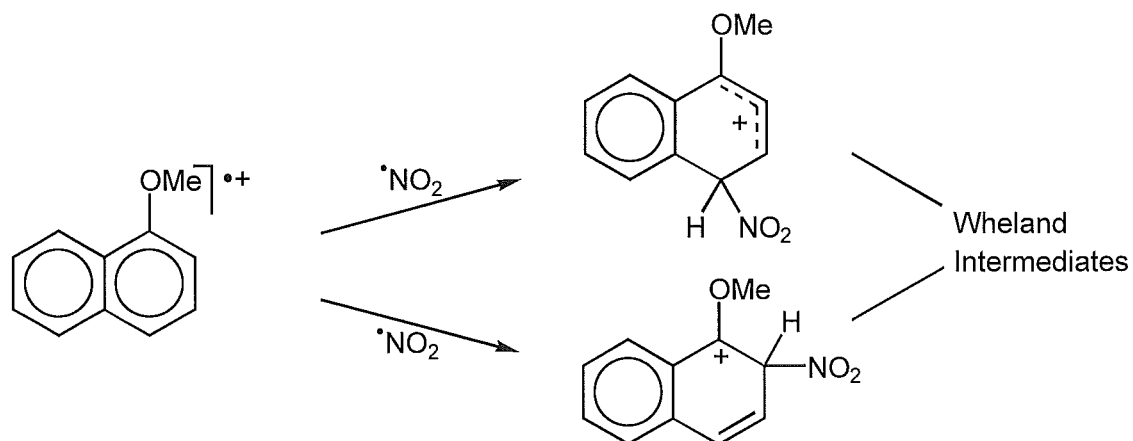
The charge-transfer complex of 1-methoxynaphthalene and tetranitromethane in acetonitrile was photolysed at 20° and -20° and the composition of the reaction mixture was monitored by withdrawing samples for ^1H n.m.r. spectral analysis (Table 8.3.2). The product compositions were similar to those obtained for dichloromethane solutions at the appropriate reaction temperatures, except that for the reaction in acetonitrile at -20° adducts **314** and **315** were not detected among the products, and the formation of 1-methoxy-2-nitronaphthalene **305** became more significant.

Discussion

*The mode of formation of the nitro-1-methoxynaphthalenes **305** and **306**, 1-methoxy-4-trinitromethylnaphthalene **309**, the adducts **314** and **315**, and 4,4'-dimethoxy-1,1'-binaphthyl **319** in the photolysis of the 1-methoxynaphthalene–tetranitromethane charge transfer complex.*

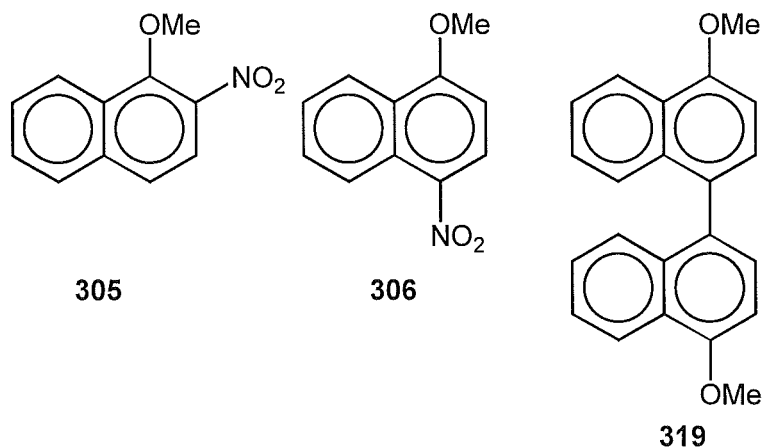
As discussed earlier, the first chemical reaction step in the recombination of the components of the triad $[\text{ArH}^{*\cdot}, \text{C}(\text{NO}_2)_3^{\cdot-}, \cdot\text{NO}_2]$ involves the attack of

the trinitromethanide ion on the aromatic radical cation.¹ Addition of trifluoroacetic acid to these photolysis reactions leads to the protonation of the trinitromethanide ion to give nitroform which is weakly nucleophilic. Under such reaction conditions it might be expected that radical addition of nitrogen dioxide to the aromatic radical cation would then occur to give the Wheland intermediates of conventional electrophilic nitration (Scheme 3.6).

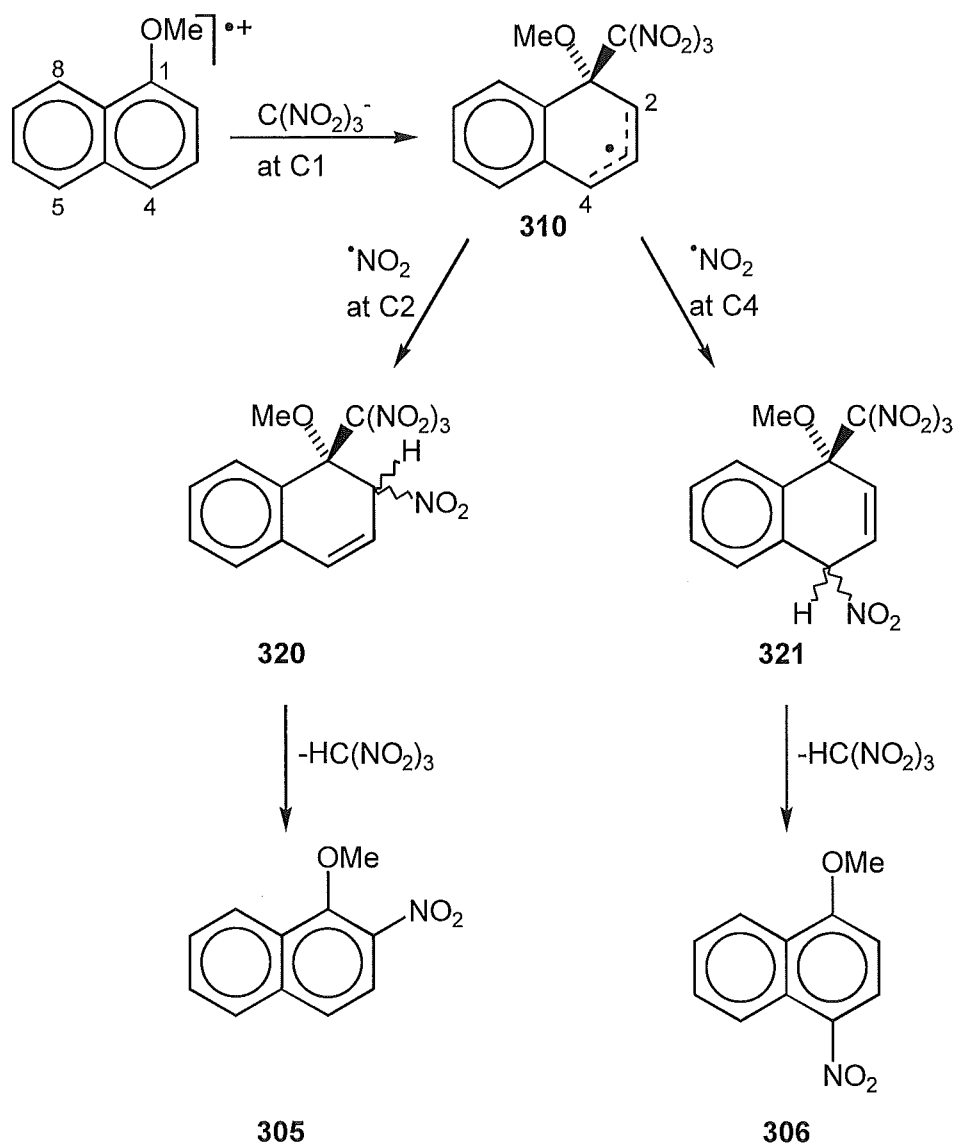


Scheme 3.6

In this context it is notable that photolysis reactions of the charge transfer complex of 1-methoxynaphthalene with tetranitromethane in dichloromethane with added trifluoroacetic acid led not to 1-methoxy-2-nitronaphthalene **305** or 1-methoxy-4-nitronaphthalene **306**, but to dimerisation and the formation of 4,4'-dimethoxy-1,1'-binaphthyl **319** exclusively at low conversions of 1-methoxynaphthalene (Table 3.2).

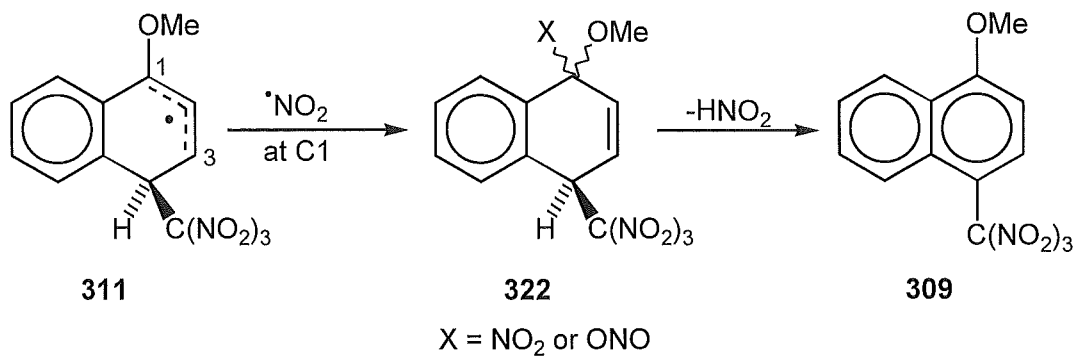


The implication of this observation is that, at least at 20° and -50° in dichloromethane solution, the nitro-substitution products **305** and **306** do not arise directly *via* radical coupling of the radical cation of 1-methoxynaphthalene and nitrogen dioxide. The mode of formation of these nitro compounds **305** and **306** at low photolytic conversions under standard reaction conditions must be by an alternative mechanism. The decomposition of the 1-methoxy-4-trinitromethyl-naphthalene **309** is certainly one source of nitro compound **306** at longer reaction times, as demonstrated by the decrease in relative yield of **309** and concomitant increase in **306** over the course of photolysis reactions in both acetonitrile and dichloromethane (Tables 3.1 and 8.3.1). This process was examined by Eberson *et al.*,⁵ who also observed some decay of the trinitromethyl compound **309** in solution to give 1-methoxy-2-nitro-naphthalene **305** under certain conditions. However, this decomposition pathway will clearly not account for the extent of the formation of either nitro compound at short reaction times. A simple rationalisation is the formation of highly labile adducts **320** and **321** as intermediates, which decompose rapidly with loss of nitroform to give 1-methoxy-2-nitronaphthalene **305** and 1-methoxy-4-nitronaphthalene **306**, respectively (Scheme 3.7, overleaf). The formation of adducts **320** and **321** would occur *via* attack of trinitromethanide ion *ipso* to the methoxy substituent in the radical cation of 1-methoxynaphthalene **304** to give the delocalised carbon radical **310**. In the subsequent radical coupling reaction between the delocalised carbon radical **310** and nitrogen dioxide it appears likely, for steric reasons, that the 1-methoxy-4-nitro-1-trinitromethyl adducts **321** would be formed in higher yield than the alternative 1-methoxy-2-nitro-1-trinitromethyl adducts **320**; this argument is consistent with the observed 2-nitro-/4-nitro- product ratio.



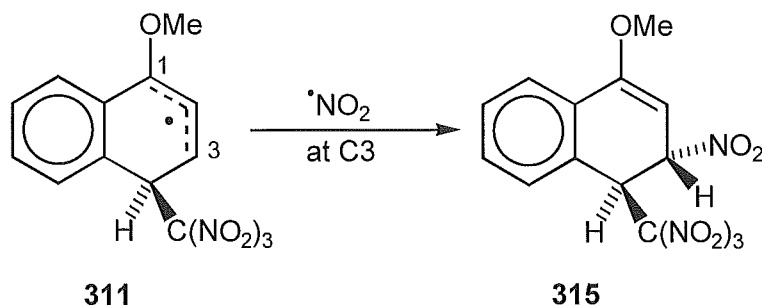
Scheme 3.7

The precise mode of formation of the 1-methoxy-4-trinitromethyl-naphthalene **309** is somewhat uncertain, but it is clear that it arises by further reaction of intermediate 1-methoxy-4-trinitromethyl-1-X-adduct(s) **322** (Scheme 3.8, overleaf), where X may be either NO_2 or ONO . In either case, loss of nitrous acid from the 1,4-positions would give the observed trinitromethyl substitution product **309**.



Scheme 3.8

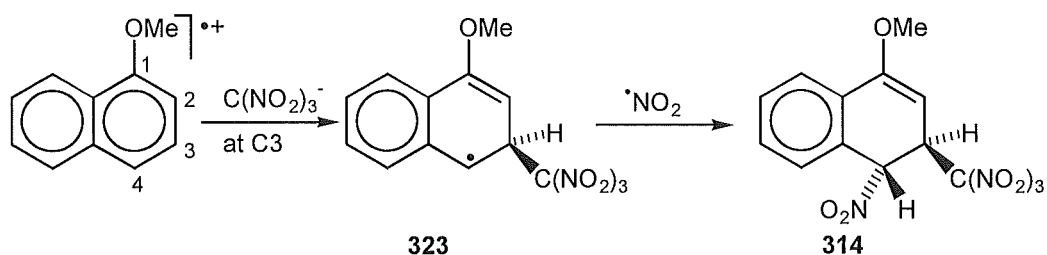
It should be noted that the alternative radical reaction of nitrogen dioxide with the delocalised carbon radical **311** as above but at C3 would lead to the 1-methoxy-*r*-2-nitro- -1-trinitromethyl-1,2-dihydronaphthalene **315** (Scheme 3.9) which has been identified as a labile reaction product.



Scheme 3.9

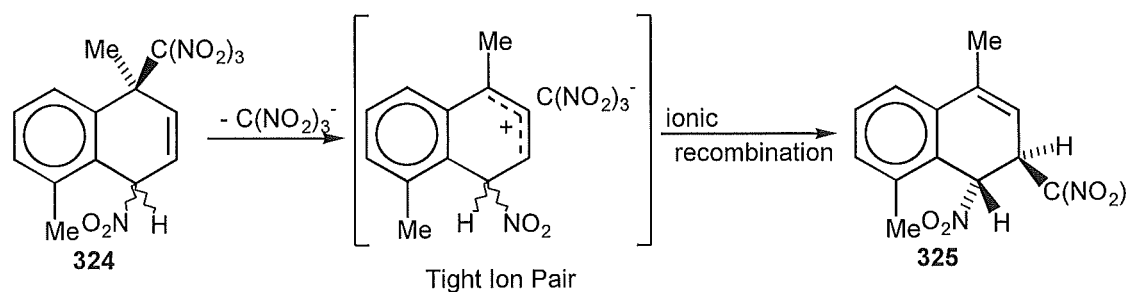
Unfortunately this adduct **315** could not be isolated, and the mixture in which it was obtained was too complex for meaningful decomposition experiments to be conducted.

The origin of the more stable, but still labile, adduct **314** is similarly uncertain. It is possible that it is formed directly by trinitromethanide ion attack at C3 of the 1-methoxynaphthalene radical cation and subsequent $\cdot\text{NO}_2$ coupling to the carbon radical **323** (Scheme 3.10, overleaf).



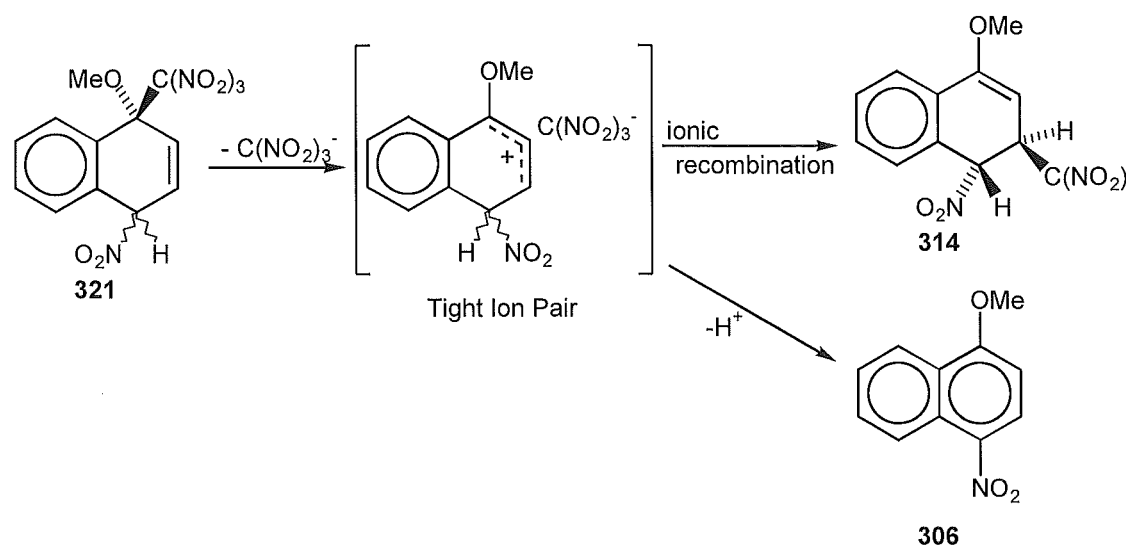
Scheme 3.10

However, given the observed 1,3-allylic rearrangement of 1,4-nitro-trinitromethyl adduct **324** into the 1-nitro-2-trinitromethyl adduct **325** (Scheme 3.11) discussed in the previous chapter,



Scheme 3.11

and the proposed intermediacy of the related species **321** in the formation of 4-nitro-1-methoxynaphthalene, it seems likely that the analogous rearrangement of adduct **321** leads to the formation of the 1-*r*-nitro-2-*t*-trinitromethyl adduct **314** (Scheme 3.12).



Scheme 3.12

The regiochemistry of the attack of trinitromethanide ion on the radical cation of 1-methoxynaphthalene.

On the basis of the product yields at low conversion of reactants (Tables 8.3.1 and 8.3.2), and the analysis above of the regiochemistry of trinitromethanide ion attack on the radical cation of 1-methoxynaphthalene giving rise to those products, the overall pattern of the regiochemistry of trinitromethanide ion attack can be determined; these data are presented in Table 3.3.

Table 3.3 - The regiochemistry of trinitromethanide ion attack on the radical cation of 1-methoxynaphthalene in dichloromethane solutions.

Reaction Conditions	Products arising from attack of $C(NO_2)_3^-$ (%)	
	Attack at C1	Attack at C4
20°	47	52
-20°	50	49
-50°	51	52
-78°	33	52

Although the high incidence of trinitromethanide ion attack at C1 of the radical cation might be considered unsurprising given the calculated (AM1) atomic charge at that ring carbon atom (Figure 3.7), it is not possible to account for the observed relative levels of attack of trinitromethanide ion at C4 and yet none at C5, on this basis.

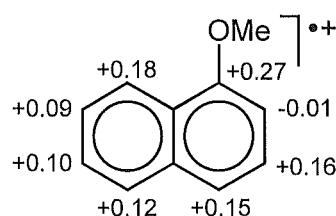
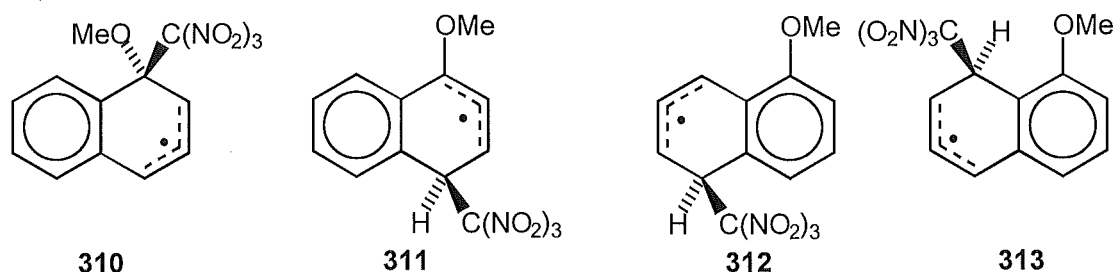


Figure 3.7 - Calculated (AM1) charge distribution on the 1-methoxynaphthalene radical cation

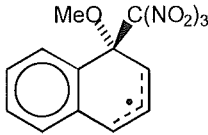
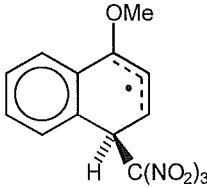
For the reaction of trinitromethanide ion with the radical cation of 1-methoxynaphthalene it is clear that once again the relative energies of the products of ionic coupling of the trinitromethanide ion and the radical cation, *i.e.* the carbon radicals **310-313**, influence the reaction pathway.



Structure **313** is a phenyl allylic radical species with inherent steric compression between the *peri* trinitromethyl and methoxy groups. Similarly, species **311** and **312** are both phenyl allylic radicals but contain no significant steric compression. Additionally, structure **311** possesses the stabilising 1-methoxy function which lowers its energy further.

The relatively even distribution of trinitromethanide addition at both C1 and C4 of the 1-methoxynaphthalene radical cation (Table 3.3), to give structures **310** and **311** respectively, seems unusual given that intermediate **310** possesses an unsubstituted phenyl allylic radical in addition to suffering from steric compression between the methoxy and trinitromethyl groups. The alternative structure **311** is a 1-methoxy-phenyl allylic radical species and suffers no significant steric compression. To explain the unusually high level of intermediacy of **311** it is necessary to examine closely the influences on the energies of the two competing intermediate species. These influences are summarised in Table 3.4, overleaf.

Table 3.4 - Summary of influences on the energies of the intermediate radical species **310** and **311**.

 310	 311
Steric compression between OMe and C(NO ₂) ₃	No significant steric compression
Unsubstituted radical system	Methoxy stabilisation of radical system
ΔH of substituted C1 carbon (-18.2 kJ/mol)	ΔH of substituted C4 carbon (-9.3 kJ/mol)

As discussed above the first two effects listed in Table 3.4, steric compression and the energy of the delocalised carbon radical, favour structure **311**. The third influence invoked in Table 3.4 is the inherent stability of the substituted carbon C1 or C4 in each case. From the study of bond energies of various molecules⁶ it has been found that a C-C-O bonding structure as at C1 of **310** is more stable by ca. 9 kJ/mol than an analogous C-C-H bonding as at C4 of **311**. It is therefore suggested that this enthalpy difference is sufficient to enable structure **310** to be a viable competitor for **311** as the active intermediate species in the reaction of trinitromethanide ion with the 1-methoxynaphthalene radical cation

Summary

The formation of a stable intermediate species is the dominant factor on the regiochemistry of trinitromethanide addition to the radical cations of naphthalene derivatives. The formation of highly labile adduct intermediates with either nitro or trinitromethyl substituents *ipso* to the methoxy group are seen as the source of the trinitromethyl and nitro aromatic compounds respectively. Subsequent chapters will discuss the implications of these findings to the products observed in the photolysis reactions of tetranitromethane with various anisole substrates.

References

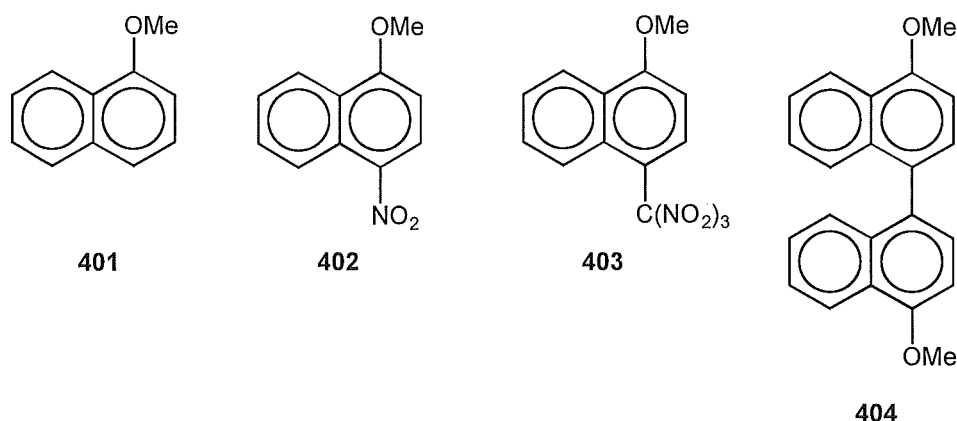
- ¹ Ebersson, L., Hartshorn, M. P., Radner, F., and Svensson, J. O., *J. Chem. Soc. Perkin Trans. 2*, 1994, 1719.
- ² (a) Ebersson, L., Hartshorn, M. P., Radner, F., Merchán, M., and Roos, B. O., *Acta Chem. Scand.*, 1993, **47**, 176; (b) Ebersson, L., Hartshorn, M. P., Radner, F., and Robinson, W.T., *J. Chem. Soc. Chem. Commun.*, 1992, **7**, 566; (c) Ebersson, L., Hartshorn, M. P., and Radner F., *J. Chem. Soc. Perkin Trans. 2.*, 1992, 1793; (d) Ebersson, L., and Hartshorn, M. P., *J. Chem. Soc. Chem. Commun.*, 1992, 1563. (e) Ebersson, L., Hartshorn, M. P., Radner, F., and Robinson, W. T., *Acta Chem. Scand.*, 1993, **47**, 410; (f) Ebersson, L., Hartshorn, M. P., and Svensson, J. O., *Acta Chem. Scand.*, 1993, **47**, 925; (g) Ebersson, L., Calvert, J. L., Hartshorn, M. P., and Robinson W.T., *Acta Chem. Scand.*, 1993, **47**, 1025; (h) Butts, C. P., Calvert, J. L., Ebersson, L., Hartshorn, M. P., and Robinson, W.T., *J. Chem. Soc. Chem. Commun.*, 1993, **19**, 1513; (i) Ebersson, L., Hartshorn, M. P., and Svensson, J. O., *J. Chem. Soc. Chem. Commun.*, 1993, **21**, 1614; (j) Butts, C. P., Calvert, J. L., Ebersson, L., Hartshorn, M. P. Maclagan, R. G. A. R., and Robinson, W. T., *Aust. J. Chem.*, 1994, **47**, 1087; (k) Ebersson, L., Calvert, J. L., Hartshorn, M. P., and Robinson, W. T., *Acta Chem. Scand.*, 1994, **48**, 347; (l) Calvert, J. L., Ebersson, L., Hartshorn, M. P., Maclagan, R. G. A. R., and Robinson, W. T., *Aust. J. Chem.*, 1994, **47**, 1211; (m) Calvert, J. L., Ebersson, L., Hartshorn, M. P., Maclagan, R. G. A. R., and Robinson, W. T., *Aust. J. Chem.*, 1994, **47**, 1591; (n) Butts, C. P., Calvert, J. L., Ebersson, L., Hartshorn, M. P., Radner, F., and Robinson, W. T., *J. Chem. Soc. Perkin Trans. 2*, 1994, 1485; (o) Calvert, J. L., Ebersson, L., Hartshorn, M. P., Robinson, W. T., and Timmerman-Vaughan, David, J., *Acta Chem. Scand.*, 1994, **47**, 1087; (p) Ebersson, L., Hartshorn, M. P., Persson, O., Robinson, W. T., and Timmerman-Vaughan, D. J., *Acta Chem. Scand.*, 1995, **49**, 482; (q) Ebersson, L., Hartshorn, M. P., Robinson, W. T., and Timmerman-Vaughan, D. J., *Acta Chem. Scand.*, 1995, **49**, 571;
- ³ Sankararaman, S., and Kochi, J. K., *Recl Trav Chim. Pays-Bas*, 1986, **105**, 278.
- ⁴ Ebersson, L., and Radner, F., *J. Am. Chem. Soc.*, 1991, **113**, 5825.

- ⁵ Ebersson, L., Hartshorn, M. P., Radner, F., Svensson, J., O., *Acta Chem. Scand.*, *in press*.
- ⁶ See Berkowitz, J., Ellison, G. B., and Gutman, D., *J. Phys. Chem.*, 1994, **98**, 2744 and references therein.

Chapter 4

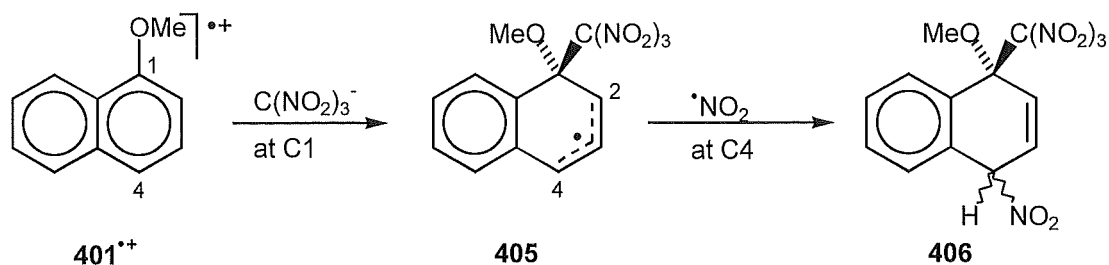
Introduction

The photolysis of aromatic compounds with tetranitromethane proceeds *via* the recombination of the three solvent caged components termed the “triad”; the aromatic radical cation, trinitromethanide anion $[\text{C}(\text{NO}_2)_3]^-$, and nitrogen dioxide. The initiating step is the addition of trinitromethanide ion to the radical cation.¹ In earlier chapters it has been shown for methylnaphthalenes that the formation of the most stable trinitromethyl substituted radical species is the dominant factor controlling the regiochemistry of trinitromethanide ion attack on these aromatic radical cations. Methoxy substitution of the aromatic system, discussed for the case of 1-methoxynaphthalene **401** in Chapter 3, does not appear to alter this criterion, but the formation of highly unstable adducts with one substituent *ipso* to the methoxy group makes the interpretation of observed product distributions more difficult.



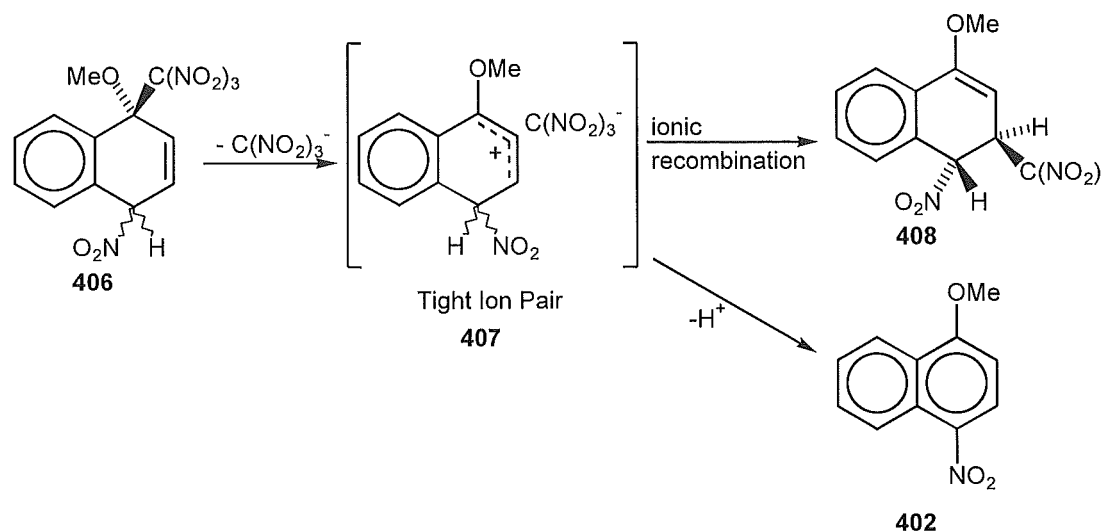
The formation of large quantities of 1-methoxy-4-nitronaphthalene **402** and 1-methoxy-4-trinitromethylnaphthalene **403** in the photolysis reactions of 1-methoxynaphthalene with tetranitromethane appears to indicate direct nitration or trinitromethylation of the 1-methoxynaphthalene radical cation. However, addition of acid to the photolysis mixtures, which is known¹ to reduce trinitromethanide ion reactivity in the triad by protonation, results in dimerisation of the radical cation to 4,4'-dimethoxy-1,1'-binaphthyl **404**. This dimerisation is not observed under standard reaction conditions and implies that nitrogen

dioxide will not react directly with the aromatic radical cation. Thus the mode of formation of 1-methoxy-4-nitronaphthalene **402** must proceed via initial trinitromethanide ion attack on the radical cation.



Scheme 4.1

Trinitromethanide ion addition to the radical cation at C1 to give the allylic radical species **405** and subsequent nitrogen dioxide coupling at C4 would yield the unstable adducts **406** (Scheme 4.1). Heterolytic cleavage of the trinitromethanide ion from adducts **406** would give the tight ion pair **407** (Scheme 4.2).

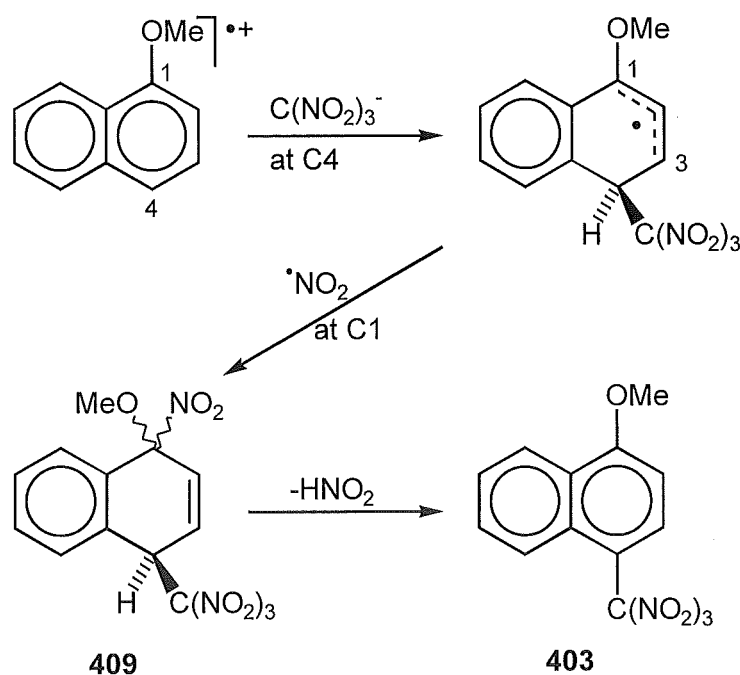


Scheme 4.2

Elimination of nitroform $[\text{HC}(\text{NO}_2)_3]$ from the ion pair **407** would give the nitro aromatic compound **402** while ionic recombination with attachment of the trinitromethyl group at C3 would give the 4-methoxy-1-nitro-2-trinitromethyl-

dihydronaphthalene adduct **408**, a product observed at low levels in these photolysis mixtures.

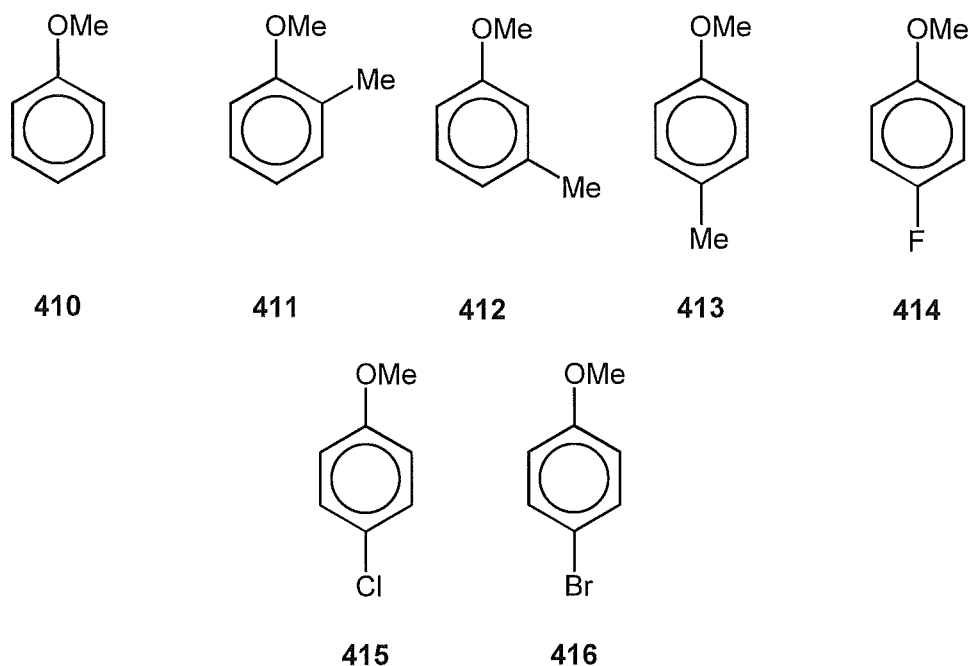
A similar addition-elimination mechanism is proposed for the generation of 1-methoxy-4-trinitromethylnaphthalene **403**. Trinitromethanide ion attack at C4 of the radical cation and subsequent NO_2 coupling at C1 would yield an analogous adduct **409** which, on 1,4-elimination of nitrous acid, would yield 1-methoxy-4-trinitromethylnaphthalene **403** (Scheme 4.3).



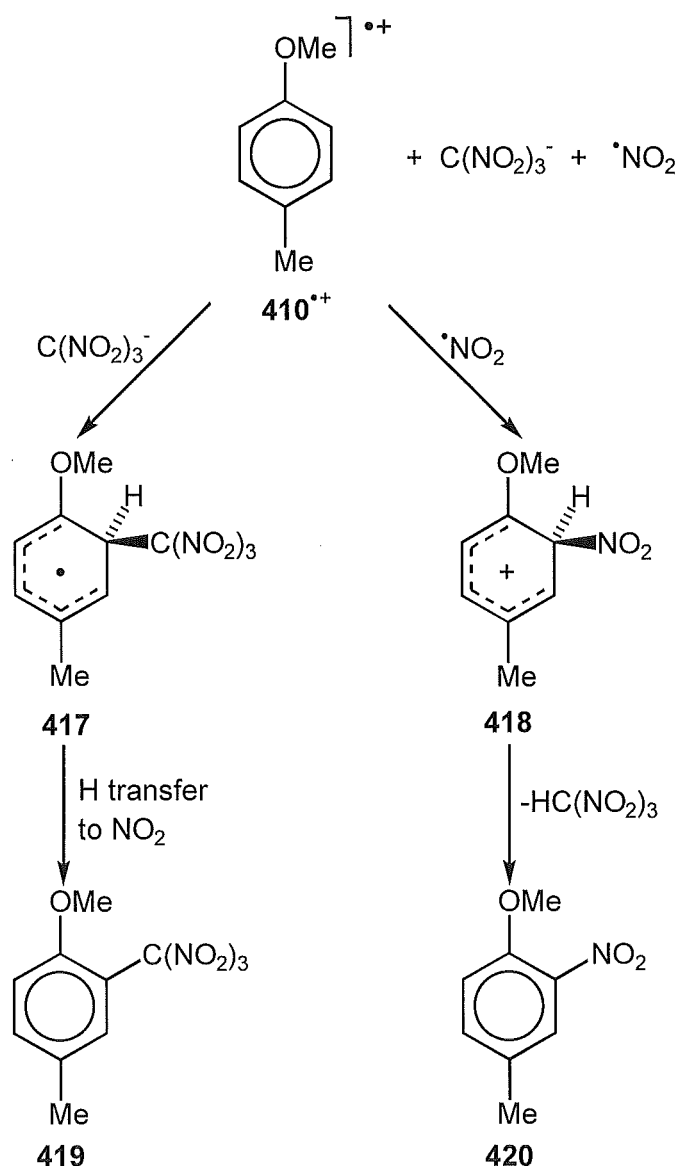
Scheme 4.3

Given these observations for 1-methoxynaphthalene, it would seem reasonable to propose the intermediacy of adducts analogous to adducts **406** and **409** in the formation of the observed aromatic products in photolysis reactions of other methoxy substituted aromatic substrates.

Kochi *et al.* reported² the apparent nitration and trinitromethylation of anisole **410** and a number of its derivatives, **411-416** below, on photolysis with tetranitromethane in various solvents.



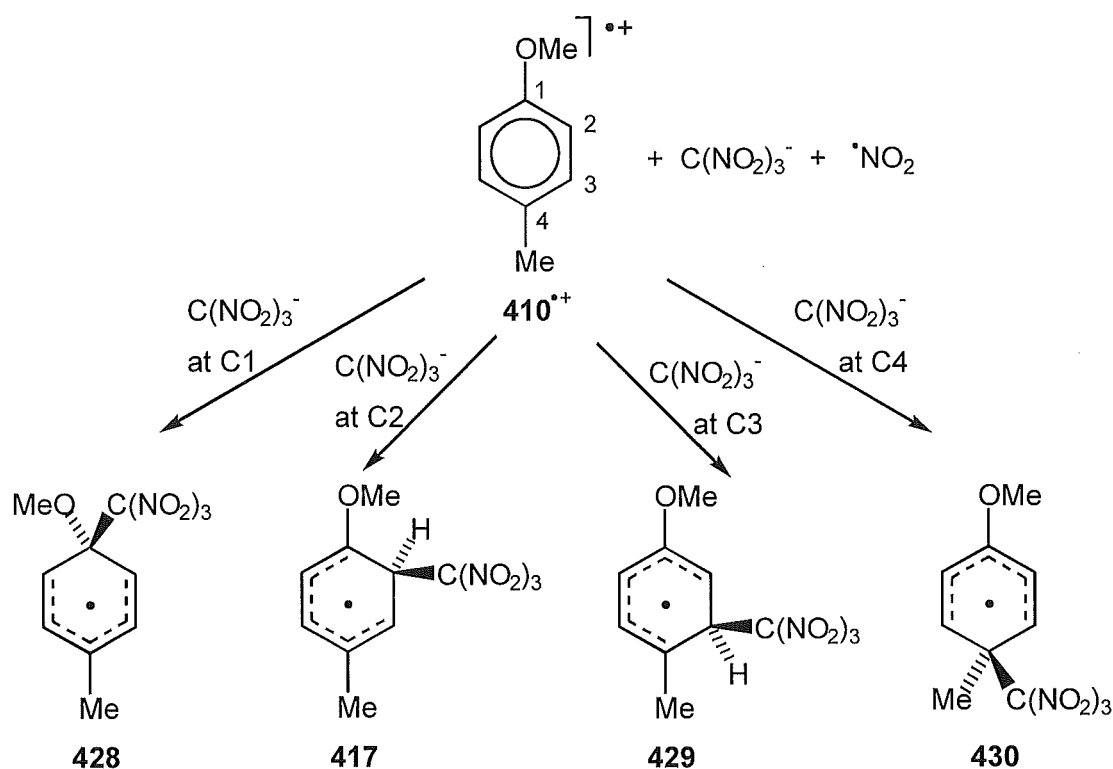
In general, photolysis reactions of the aromatic substrates with tetranitromethane in dichloromethane and non-polar solvents such as *n*-hexane gave high yields of trinitromethyl aromatic compounds while nitro aromatic products predominated in acetonitrile solutions. In addition, an increase in nitro aromatic product yields was observed in dichloromethane solutions with the addition of an “innocuous” salt, tetrabutylammonium perchlorate ($\text{Bu}_4\text{N}^+\text{ClO}_4^-$, TBAP); this was described as a “special salt” effect. Alternatively, the addition of low concentrations (0.01 mol l^{-1}) of the “common ion” salt tetrabutylammonium trinitromethanide [$\text{Bu}_4\text{N}^+\text{C}(\text{NO}_2)_3^-$] gave ambiguous results, marginally increasing the yield of trinitromethyl aromatic products in benzene solutions while decreasing their yield in dichloromethane solutions. Kochi *et al.*² supported these results with kinetic data which assumed the reaction mechanisms to be the two-step substitution reactions shown in Scheme 4.4, overleaf.



Scheme 4.4

At the outset of the present work it was considered that this mechanistic interpretation was not correct, given the results discussed above for 1-methoxynaphthalene.

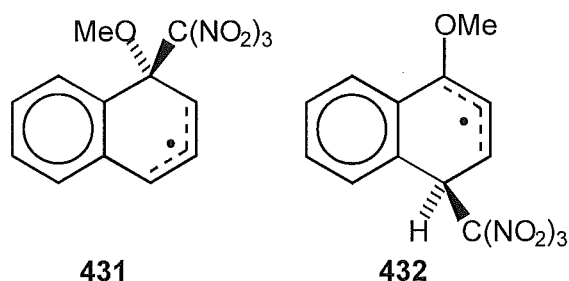
Assuming that trinitromethanide ion attack on the 4-methylanisole radical cation is the first step in the triad recombination, the radical species that could be formed are shown in Scheme 4.5, overleaf.



Scheme 4.5

Trinitromethanide addition to C1 of the radical cation would give the delocalised carbon radical **428** which is stabilised by the position of the methyl substituent on the ring. Attack of the trinitromethanide ion at C2 would give structure **417** for which the delocalised carbon radical is stabilised by the position of the methoxy substituent. The delocalised carbon radical intermediate **429** formed by trinitromethanide ion attack at C3 of the 4-methylanisole radical cation would be destabilised by the steric compression between the vicinal trinitromethyl and methyl substituents, and the delocalised radical stabilised by the methyl function. Finally, trinitromethanide ion attack at C4 of the 4-methylanisole radical cation would give structure **430** which is destabilised by the steric compression between the geminal methyl and trinitromethyl substituents, but is stabilised by the position of the methoxy function on the delocalised carbon radical system. In addition to these effects, the inherent stability of the C-C-O bonding pattern at C1 of structure **428** stabilises this intermediate by ca. 9 kJ/mol relative to structures **417** and **429** which possess a C-C-H bonding pattern at C2 and C3 respectively.³ The C-C-C bonding structure at C4 of **430** destabilises this radical species by a further 8 kJ/mol relative to **417** and **429**.

The photolysis of 1-methoxynaphthalene and tetranitromethane in dichloromethane yielded almost equal quantities of products derived from the two radical species **431** and **432**.



This implies that the stabilisation of trinitromethyl substitution *ipso* to a methoxy function in structure **431** is sufficient to counter the stabilisation of the carbon radical by the methoxy substituent in structure **432**. A similar observation could be expected for products derived from the delocalised carbon radical species **428** and **417** in the photolysis of 4-methylanisole with tetranitromethane.

This chapter reports the results of an investigation of the photolysis reactions of 4-methylanisole with tetranitromethane using low temperature work-up and separation techniques in an attempt to isolate and ascertain the mechanistic origins of any intermediate adducts formed. In the event, compounds of this nature were isolated and a simple explanation is presented for the solvent and “added salt” effects reported by Kochi *et al.*²

Results

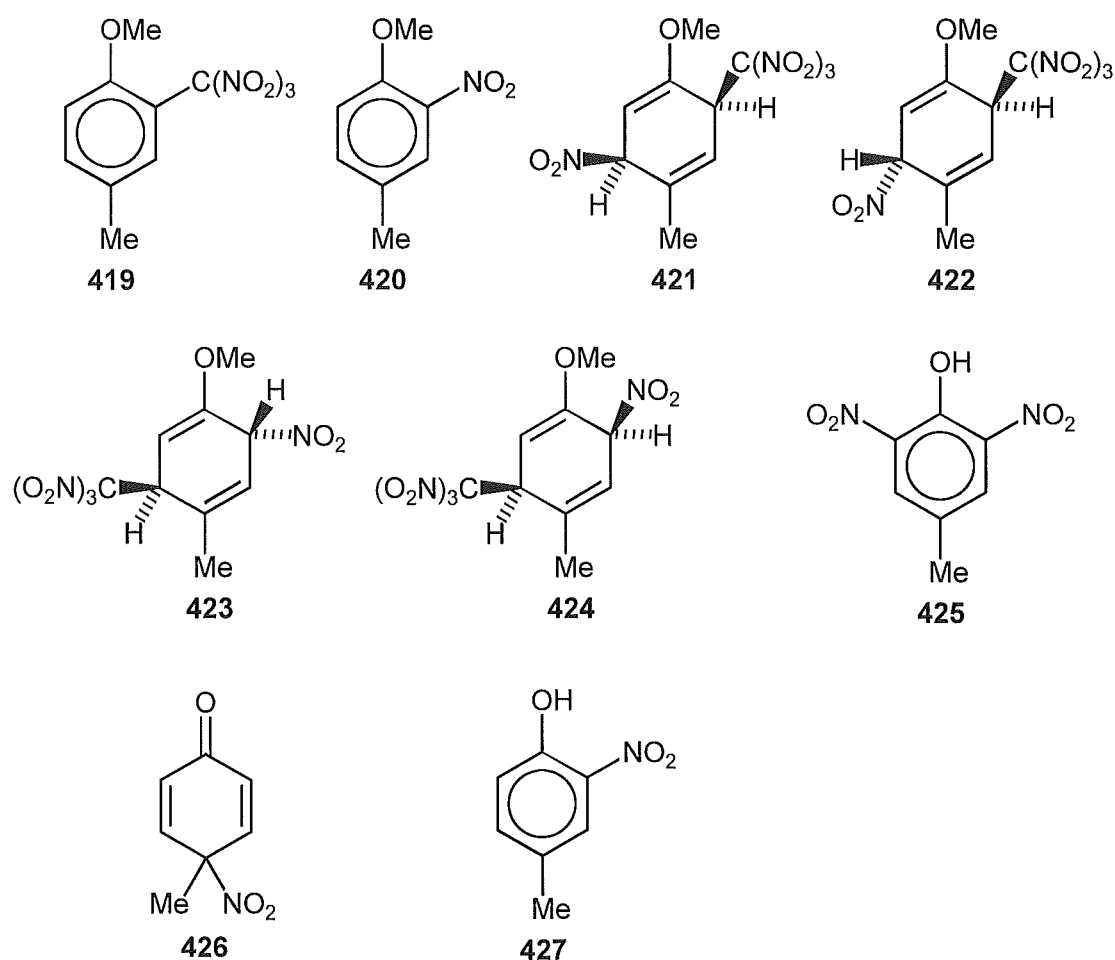
*General procedure for the photolysis of 4-methylanisole **413** with tetranitromethane.*

A solution of 4-methylanisole (0.51 mol l⁻¹) and tetranitromethane (1.02 mol l⁻¹) was irradiated with filtered light (λ cut-off 435 nm; see Experimental section for details) in solution and small samples were withdrawn for analysis at suitable intervals. The work-up procedure, involving evaporation of solvent and excess tetranitromethane, was conducted at a temperature $\leq 0^\circ$. The crude product mixtures were stored at -78° and were analysed by ¹H n.m.r.

spectroscopy (Experimental section; Tables 8.4.1 and 8.4.2) as soon as possible.

Photolysis in dichloromethane at 20° and identification of adducts.

A solution of 4-methylanisole (0.51 mol l⁻¹) and tetranitromethane (1.02 mol l⁻¹) in dichloromethane was irradiated at 20°. The composition of the mixture was monitored by withdrawing samples for ¹H n.m.r. spectral analysis (Experimental Section; Table 8.4.1). The solution after 1 h, on work-up, contained the adducts **421** (11 %), **422** (3 %), **423** (2 %), and **424** (2 %), 4-methyl-2-trinitromethylanisole **419** (47 %), 4-methyl-2-nitroanisole **420** (10 %), 4-methyl-2,6-dinitrophenol **425** (10 %), 4-methyl-4-nitrocyclohexa-2,5-dienone **426** (3 %), 4-methyl-2-nitrophenol **427** (1 %), and other unidentified materials (total 11 %).



The products were separated partially by h.p.l.c. on a cyanopropyl column using hexane-dichloromethane mixtures as the eluting solvents. The order of

elution of materials from the h.p.l.c. column are given in the Experimental section, but here for simplicity the evidence for structural assignments will be presented for groups of compounds.

1-Methoxy-4-methyl-3-nitro-6-trinitromethylcyclohexa-1,4-dienes **421** and **422**.

The structure of the nitro-trinitromethyl adduct **421** was determined by single crystal X-ray analysis. A perspective drawing for 1-methoxy-4-methyl-*r*-3-nitro-*c*-6-trinitromethyl-cyclohexa-1,4-diene, C₉H₁₀N₄O₉, m.p. 58-60° (decomp.) is presented in Figure 1, and corresponding atomic coordinates are given in Table 8.4.3.

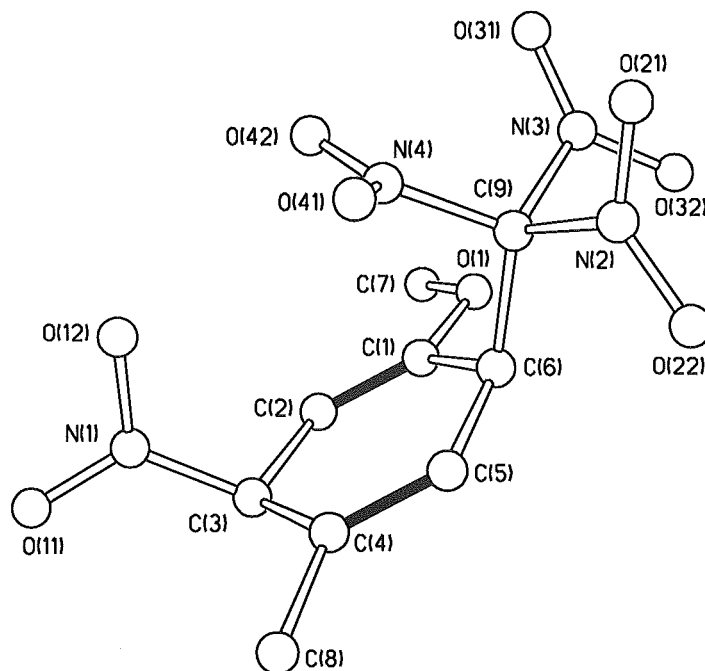
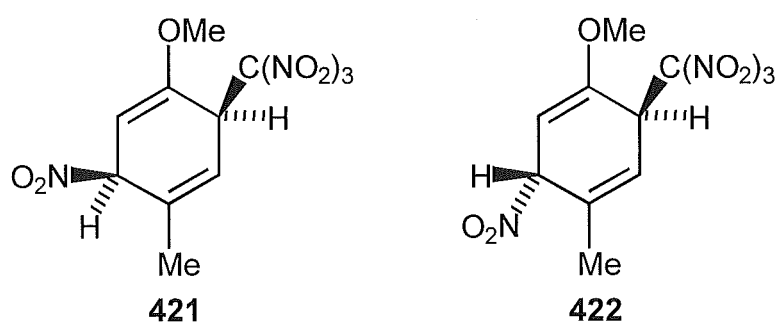


Figure 1 - Perspective drawing of **421**

In the solid state the cyclohexa-1,4-diene ring system is close to planar [torsional angles: C(2)-C(1)-C(6)-C(5) 9.1(3)°; C(1)-C(2)-C(3)-C(4) -5.4(3)°], but with both the C(3)-NO₂ and C(6)-C(NO₂)₃ bonds tending towards the flagpole orientation in a boat conformation [torsional angles: O(1)-C(1)-C(6)-C(9) 65.5(2)°; N(1)-C(3)-C(4)-C(8) 64.9(2)°], presumably a compromise in terms of steric interactions between vicinal groups -OMe/-C(NO₂)₃ and -NO₂/ -Me, and

the two near-flagpole groups NO_2 and $\text{C}(\text{NO}_2)_3$. In the structure the methoxy group is close to coplanar with the $\text{C}(1)\text{-C}(2)$ bond [torsional angle: $\text{C}(2)\text{-C}(1)\text{-O}(1)\text{-C}(7)$ $-4.4(3)^\circ$], and the plane of the 3- NO_2 group is eclipsed with the $\text{C}(3)\text{-H}(3)$ bond [torsional angle: $\text{O}(11)\text{-N}(1)\text{-C}(3)\text{-H}(3)$ $1.1(2)^\circ$]. The spectroscopic data for the nitro-trinitromethyl adduct **421** were in accord with the established structure. In particular the coupling constants $J_{\text{H}_2,\text{H}_3} = 4.8$ Hz and $J_{\text{H}_5,\text{H}_6} = 3.9$ Hz were in accord with the solid state torsional angles $\text{H}(2)\text{-C}(2)\text{-C}(3)\text{-H}(3) = 53.8(1)^\circ$ and $\text{H}(5)\text{-C}(5)\text{-C}(6)\text{-H}(6) = 53.3(1)^\circ$ respectively. The ^1H n.m.r. spectrum of nitro-trinitromethyl adduct **421** was assigned on the basis of the multiplicity of the various signals confirmed in many cases by double irradiation experiments. Vicinal protons on the structure were highlighted by the results of nuclear Overhauser experiments. Finally, the ^{13}C n.m.r. spectrum was assigned on the basis of the results of long range reverse detected heteronuclear correlation spectra (HMQC), in particular the carbon resonances at δ 84.8 (C3), indicative of the $\text{CH}\text{-NO}_2$ function, and δ 44.6, indicative of the $\text{CH}\text{-C}(\text{NO}_2)_3$ function, were identified. An interesting feature of the ^{13}C n.m.r. spectra was the identification of the C2 carbon resonance at δ 95.5. This chemical shift is significantly upfield of a normal vinyl carbon resonance (typically around δ 120-130) and is presumably the result of the enolic nature of the $\text{C}1\text{-C}2$ bond.

Although 1-methoxy-4-methyl-*r*-3-nitro-*t*-6-trinitromethylcyclohexa-1,4-diene **422** could not be obtained in a pure state, the structure of this adduct appears certain from its spectroscopic data and their comparison with those for the *r*-3-nitro-*c*-6-trinitromethyl adduct **421**, the structure of which is determined above.



The connectivity in the *r*-3-nitro-*t*-6-trinitromethyl adduct **422** was established by a combination of nuclear Overhauser experiments (Figure 4.1) and long range reverse detected heteronuclear correlation spectra (HMQC).

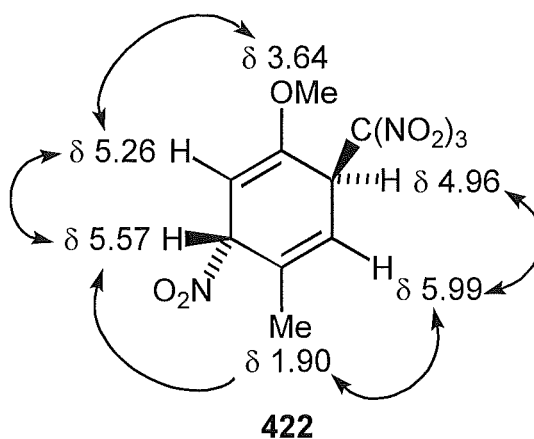


Figure 4.1 - Relevant nuclear Overhauser enhancements observed in the ¹H n.m.r. spectrum of **422**

To the extent that the ¹³C n.m.r. spectrum of adduct **422** could be assigned from the spectrum of a mixture with adduct **423** below, the chemical shifts for adduct **422** mirror closely those for the *r*-3-nitro-*c*-6-trinitromethyl adduct **421** (Table 4.1).

Table 4.1 - Comparison of ¹³C n.m.r. chemical shift data for adducts **421** and **422**.

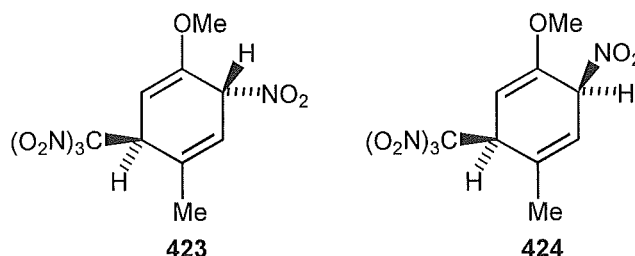
421		422	
Resonance	δ	Resonance	δ
C2	44.6	C2	44.2
C3	119.0	C3	119.2
C5	84.8	C5	85.9
C6	95.5	C6	95.1
-OCH ₃	56.2	-OCH ₃	55.9

The multiplicities of signals in the ^1H n.m.r. spectrum of the *r*-3-nitro-*t*-6-trinitromethyl adduct **422** were confirmed whenever possible by suitable double irradiation experiments.

The ^1H n.m.r. spectra of adducts **421** and **422** were notable for the coupling constant, $J_{\text{H}_3,\text{H}_6}$ 4.9 Hz, for both adducts. These homoallylic coupling constants are comparable with those reported by Appel *et al.*⁴ (5 Hz), but significantly less than those reported by Durham *et al.*⁵ (7.4 - 11 Hz) for the coupling between the 1- and 4-protons of unsymmetrically substituted 1,4-dihydrobenzenes.

Finally, it should be noted that the *r*-3-nitro-*t*-6-trinitromethyl adduct **422** is eluted from the cyanopropyl h.p.l.c. column significantly earlier than the *r*-3-nitro-*c*-6-trinitromethyl adduct **421**. As was the case for methylated naphthalenes^{6,8} the *trans* adduct elutes from h.p.l.c. before its *cis* epimer. This feature will be invoked below to enable the assignment of the stereochemistry of the epimeric 3-trinitromethyl-6-nitro adducts **423** and **424**.

1-Methoxy-4-methyl-3-trinitromethyl-6-nitrocyclohexa-1,4-dienes **423** and **424**.



Neither of these 3-trinitromethyl-6-nitro adducts **423** and **424** could be obtained in a pure state and the assignment of their structures is dependent on a consideration of their spectroscopic data. The connectivity in adducts **423** and **424** was established, as for adduct **422** above, by a combination of nuclear Overhauser experiments (Figure 4.2) and long range reverse detected heteronuclear correlation spectra (HMQC).

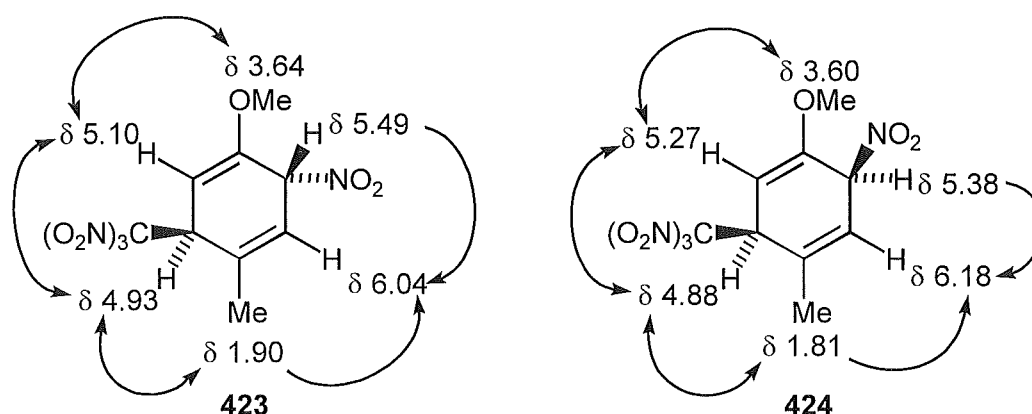


Figure 4.2 - Observed nuclear Overhauser enhancements in the ^1H n.m.r. spectra of **423** and **424**

The pattern of ^{13}C n.m.r. resonance assignments which emerged from the above techniques clearly placed the trinitromethyl group at C3, and the nitro group at C6 on a 1-methoxycyclohexa-1,4-diene system for both compounds (Table 4.2).

Table 4.2 - Comparison of ^{13}C n.m.r. data for adducts **423** and **424**

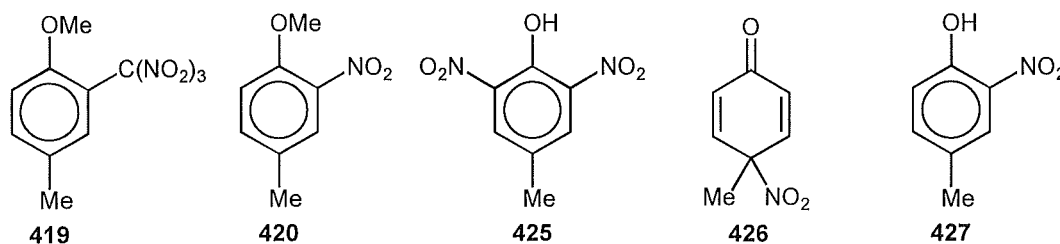
423		424	
Resonance	δ	Resonance	δ
C2	91.3	C2	93.0
C3	47.1	C3	46.8
C5	126.1	C5	124.7
C6	81.9	C6	80.6
-OCH₃	55.8	-OCH₃	55.9

These data demonstrate the similar connectivity in the structures and the only remaining feature to be assigned is the stereochemistry of each compound. This was assigned from the established order of elution of such stereoisomers from a cyanopropyl h.p.l.c. column, the *r*-3-trinitromethyl-*t*-6-nitro adduct **423** being eluted significantly earlier than its *r*-3-trinitromethyl-*c*-6-nitro isomer **424**.

It is notable that for adducts **423** and **424** the homoallylic coupling constant, $J_{\text{H3,H6}}$ was smaller than for the regioisomers **421** and **422**; for adduct

423 this coupling constant was J_{H_3,H_6} 3.9 Hz and for adduct **424** it was 2.9 Hz (cf. 4.9 Hz for both **421** and **422**).

Aromatic products **419**, **420**, **425** and **427**, and 4-methyl-4-nitrocyclohexa-2,5-dienone **426**.



The 4-methyl-2,6-dinitrophenol **425** and the nitrodienone **426** were isolated by h.p.l.c. separation of the reaction mixture which yielded the adducts **421-424** above, and they were identified by comparison of their ¹H n.m.r. spectra with those of authentic samples. 4-Methyl-2-trinitromethylanisole **419** was obtained by crystallisation of the crude reaction product from a photolysis reaction in dichloromethane at 20°. The crystalline material gave essentially identical physical and spectroscopic data to that reported earlier by Kochi *et al.*² The remaining products, 4-methyl-2-nitroanisole **420** and 4-methyl-2-nitrophenol **427**, were isolated by chromatography on a silica gel Chromatotron plate of the crude reaction mixture from a photolysis reaction in dichloromethane at -50°, and were identical with authentic samples.

Photolysis in dichloromethane at -20° and -50°.

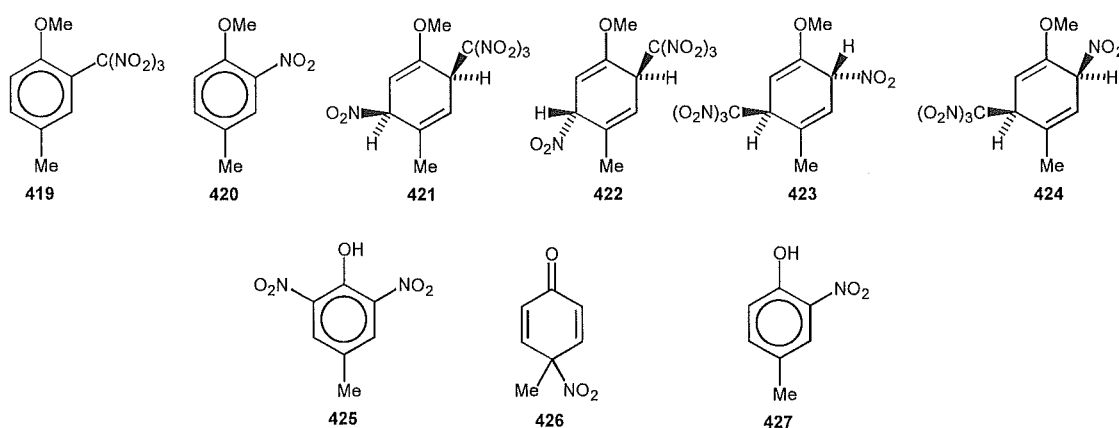
The same products were observed when the temperature of the photolysis reaction was lowered to -20° and -50°, but the yields of each were significantly altered (Table 4.3 {overleaf} and Experimental Section; Table 8.4.1). This was particularly evident in the first (0.5h) point where significantly lower yields of trinitromethyl aromatic **419** (44% at 20°, 11% at -50°) and adducts **421** and **422** (total 22% at 20°, 0% at -50°) were observed. Concomitant increases in the nitro aromatic compound **420** and nitrocyclodienone **426** were observed.

Table 4.3 - Overview of product yields from the photolysis of 4-methylanisole **413** (0.51 mol l^{-1}) with tetranitromethane (1.02 mol l^{-1}) in dichloromethane^A

t/h	Yields (%)										
	421	422	423	424	Unknown Adducts	419	420	425	426	427	Unknown Aromatics
20°											
.5	12.6	9.8	2.4	1.6	3.1	44.3	7.1	6.3	3.1	1.0	8.7
1	10.9	3.2	1.9	2.2	2.3	47.1	9.7	10.0	2.8	1.1	8.8
2	6.4	-	2.1	2.0	2.1	51.8	12.1	13.3	2.1	0.8	7.2
-20°											
0.5	2.5	2.5	2.5	3.4	1.1	19.6	29.6	-	29.1	2.5	5.0
1	2.5	1.9	2.0	^B	10.6	14.0	36.7	-	24.8	2.3	3.8
2	2.9	1.6	2.1	^B	15.7	13.3	32.5	-	26.0	2.4	3.3
-50°											
0.5	-	-	3.4	3.5	12.8	10.5	34.9	-	29.3	1.7	3.8
1	-	-	2.2	3.1	15.4	9.7	35.5	-	27.8	1.6	4.6
2	-	-	3.3	3.8	12.3	8.4	41.0	-	22.6	1.8	6.7

^A Conversions not quoted due to substrate volatility during work-up

^B Unreliable integral due to overlapping ¹H n.m.r. resonances



Photolysis in acetonitrile at 20°, -20°, and -50°.

In acetonitrile none of the adducts **421-424** were detectable at 20° and only adducts **423** and **424** were detected at low levels at -20° and -50°. There is an apparent increase in the yield of 4-methyl-2-trinitromethylanisole **419** with

lower reaction temperatures but this may simply reflect a lower rate of decomposition of the 4-methyl-2-trinitromethylanisole **419** to give 4-methyl-2-nitroanisole **420** (Table 4.4).

Table 4.4 - Overview of yields of products from the photolysis of 4-methylanisole **413** (0.51 mol l^{-1}) with tetranitromethane (1.02 mol l^{-1}) in acetonitrile^A

t/h	Yields (%)										
	421	422	423	424	Unknown Adducts	419	420	425	426	427	Unknown Aromatics
20°											
.5	-	-	-	-	6.8	5.4	50.8	2.2	19.0	6.1	8.6
1	-	-	-	-	0.8	4.7	49.5	4.1	23.6	9.3	7.2
2	-	-	-	-	0.4	4.3	45.1	11.3	16.2	16.2	4.8
-20°											
0.5	-	-	0.8	1.1	8.7	8.7	34.8	-	34.3	4.3	6.7
1	-	-	0.8	0.8	7.6	9.0	42.5	-	29.7	3.6	3.7
2	-	-	1.7	^B	7.6	7.1	47.2	-	28.9	2.2	3.7
-50°											
0.5	-	-	1.4	1.5	2.1	14.5	29.5	-	38.7	1.9	10.4
1	-	-	1.5	1.3	4.6	13.0	35.5	-	39.1	2.0	2.8
2	-	-	1.4	1.7	4.0	10.9	36.6	-	37.7	2.2	6.4

^A Conversions not quoted due to substrate volatility during work-up

^B Unreliable integral due to overlapping ¹H n.m.r. resonances

Photolysis in dichloromethane at 20° with added trifluoroacetic acid.

Photolysis of 4-methylanisole (0.51 mol l^{-1}), tetranitromethane (1.02 mol l^{-1}), and trifluoroacetic acid (0.7 mol l^{-1}) in dichloromethane at 20° after short reaction time (0.5h) gave 4-methyl-4-nitrodienone **426** and its decomposition product 4-methyl-2-nitrophenol **427** in a combined yield of 30%, 4-methyl-2-nitroanisole **420** in 52% yield and a 17% yield of unknown aromatic compounds. No adducts were observed in the photolysis mixture.

Discussion

Overview of photolysis reaction products in dichloromethane at 20°, -20° and -50°.

In dichloromethane at 20° all four adducts **421-424** are formed, but with adducts **421** and **422** predominant at short reaction times (0.5 h); at longer reaction times (2 h) adducts **423** and **424** remain at their earlier levels, but adducts **421** and **422** clearly undergo further reaction to give apparently 4-methyl-2-trinitromethylanisole **419** (Table 4.3). The increase in the yield of 4-methyl-2-nitroanisole **420** is attributed to the known thermal and photochemical decomposition of trinitromethyl arene compounds to nitro aromatic species.⁷ For photolysis reactions in dichloromethane at lower temperatures there is a progressive reduction in the yields of adducts **421** and **422**, and also in 4-methyl-2-trinitromethylanisole **419**, the yield of which drops (for 0.5 h reaction times) progressively from 44 % at 20°, through 20 % at -20°, to 11 % at -50°. At lower reaction temperatures the initial yield of the 4-methyl-2-nitroanisole **420** increases steadily, and this increase is accompanied by increased yields of 4-methyl-4-nitrocyclohexa-2,5-dienone **426**, and some marginal increase in the yields of adducts **423** and **424**. These changes in product yields with reaction temperature are interpreted below in terms of changes in the balance of the regiochemistry of reaction of trinitromethanide ion with the radical cation of 4-methylanisole with reaction temperature.

The calculated atomic charges on the ring carbon atoms of the radical cation of 4-methylanisole are given in Figure 4.3.

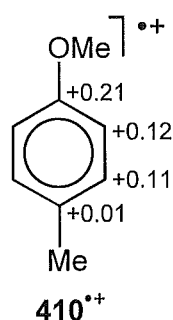
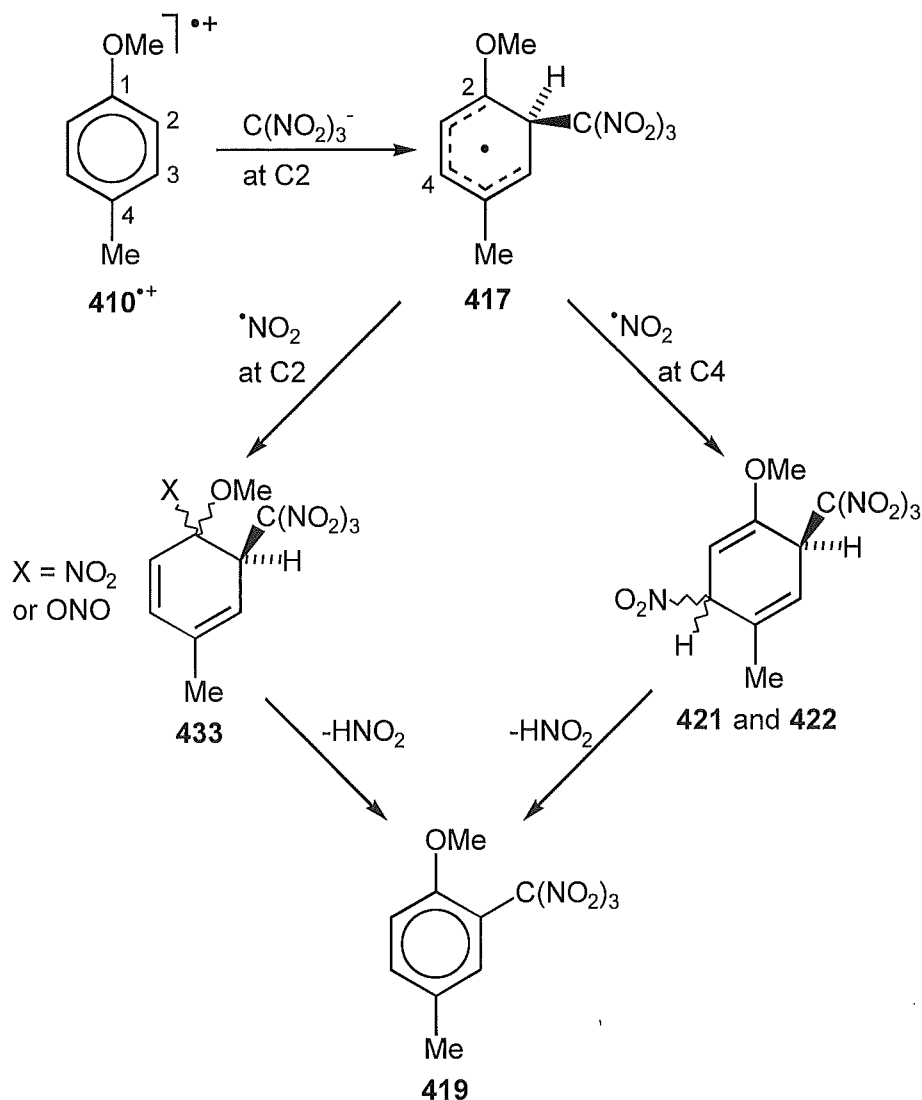


Figure 4.3 - Calculated atomic charges on the radical cation of 4-methylanisole. On the basis of charge distribution it appears likely that trinitromethanide ion would attack the radical cation of 4-methylanisole either *ipso* to the methoxy

group or at the vicinal 2-position, the third possibility at the 3-position being disfavoured by the known reluctance of trinitromethanide ion to attack a radical cation vicinal to a methyl group.⁸

Attack of trinitromethanide ion at the 2-position of 4-methylanisole radical cation would give the delocalised carbon radical **417** (Scheme 4.6), the stability of which would be enhanced by the position of the methoxy group.

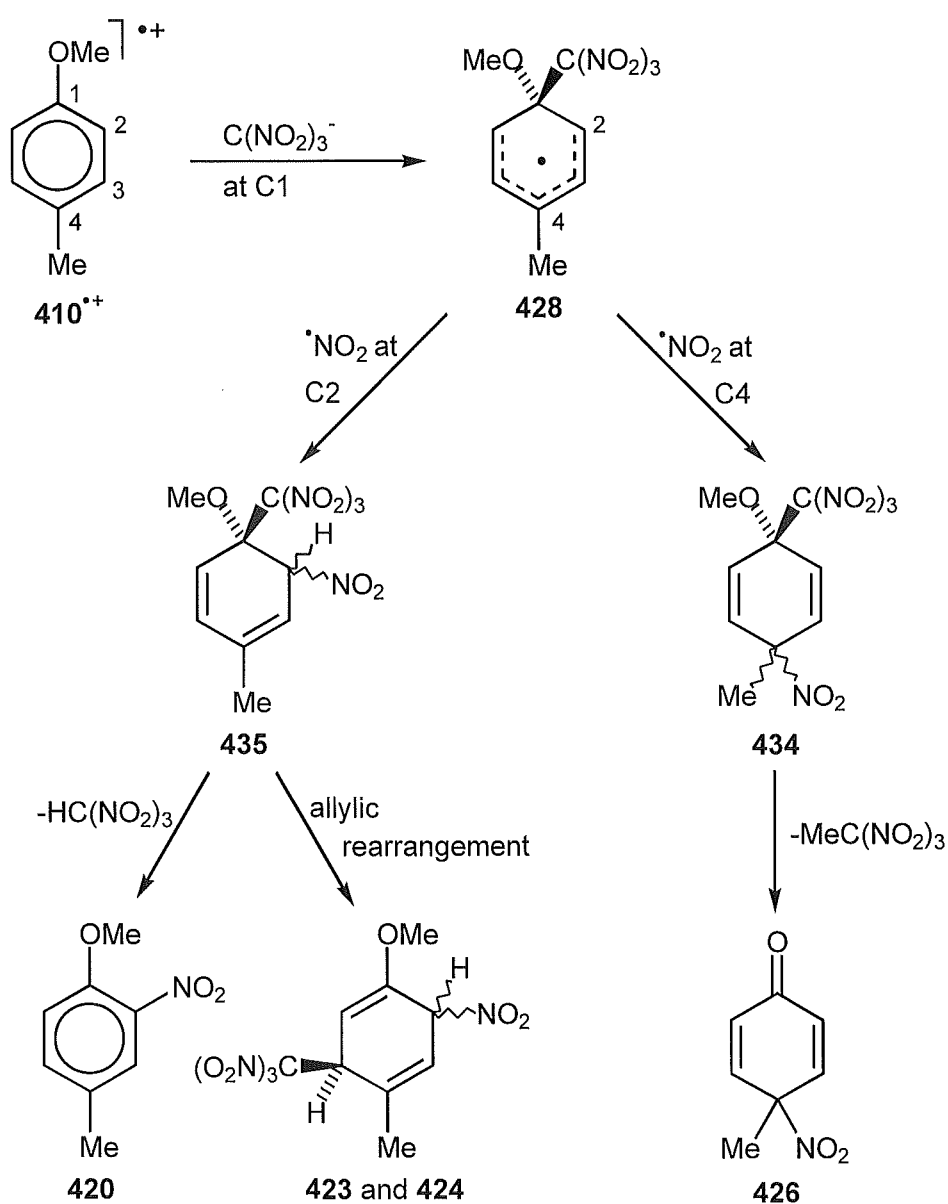


Scheme 4.6

Attack of nitrogen dioxide at C4 in the delocalised carbon radical **417** would yield adducts **421** and **422**. Alternatively, nitrogen dioxide could attack *ipso* to the methoxy group to give the diene **433** (where X = NO_2 or ONO); loss of nitrous acid from this sterically compressed diene **433** would provide a mechanistic pathway to 4-methyl-2-trinitromethylanisole **419** which does not

require the intermediacy of adducts **421** and **422**; it appears likely therefore, that 4-methyl-2-trinitromethylanisole **419** is formed *via* decomposition of adducts **421** and **422** (evident in the photolysis reaction at 20°) and by decomposition of diene **433** (Scheme 4.6 above).

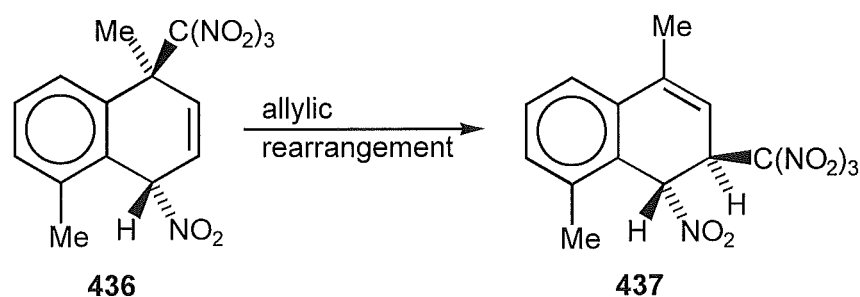
Alternatively, attack of trinitromethanide ion *ipso* to the methoxy group would give the delocalised carbon radical **428** (Scheme 4.7), the stability of which would be enhanced by the position of the methyl group, and the C-C-O bonding pattern at C1.³



Scheme 4.7

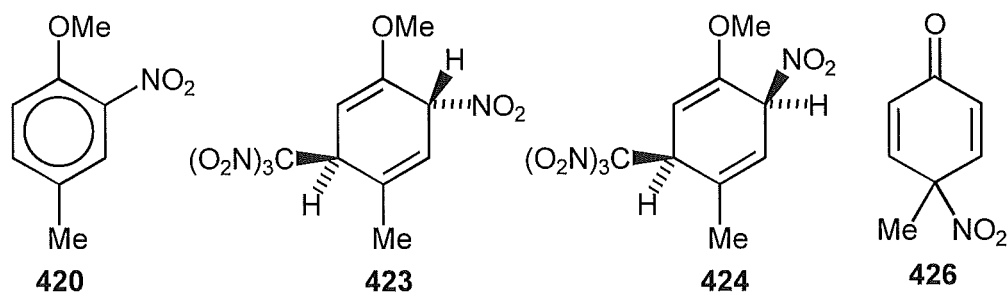
Attack of nitrogen dioxide *ipso* to the methyl group at C4 in the delocalised carbon radical **428** would give the diene **434**, which could lose the elements of

Me/C(NO₂)₃ to give 4-methyl-4-nitrocyclohexa-2,5-dienone **426**. The alternative coupling of nitrogen dioxide at C2 in the carbon radical **428** would give the diene **435**, for which an easy decomposition pathway would involve the elimination of nitroform [HC(NO₂)₃] and yield 4-methyl-2-nitroanisole **420**. A possible alternative reaction pathway for diene **435** would involve allylic rearrangement, with migration of the trinitromethyl group, to form the 3-trinitromethyl-6-nitro adducts **423** and **424**; This rearrangement is analogous with that demonstrated in Chapter 2 for the conversion of 1,5-dimethylnaphthalene adduct **436** into adduct **437** (Scheme 4.8).

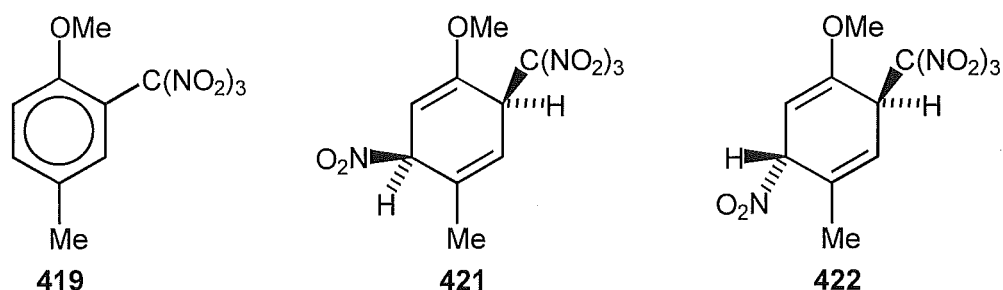


Scheme 4.8

The observed effects of reaction temperature on product yields can be rationalised if the assumption is made that at lower temperatures reaction of trinitromethanide ion *ipso* to the methoxy group in the radical cation of 4-methylanisole becomes more favoured relative to attack vicinal to the methoxy group. Thus the products from Scheme 4.7, *i.e.* 4-methyl-2-nitroanisole **420**, 4-methyl-4-nitrocyclohexa-2,5-dienone **426**, and 3-trinitromethyl-6-nitro adducts **423** and **424**,



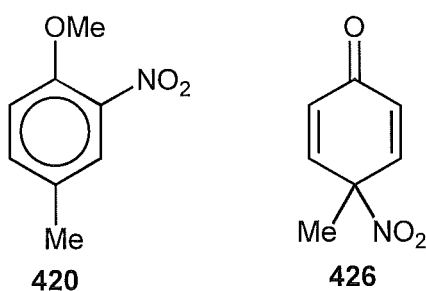
would become more dominant at lower temperatures (Table 4.3), at the expense of the products formed *via* Scheme 4.6, *i.e.* 4-methyl-2-trinitromethylanisole **419**, and 3-nitro-6-trinitromethyl adducts **421** and **422**.



This change in regiochemistry of trinitromethanide ion attack on the 4-methylanisole radical cation can be rationalised in terms of the higher charge distribution at C1 of the radical cation. It appears likely that at lower temperatures the inherent reactivity of trinitromethanide ion is lower and the magnitude of the charge at the reacting carbon of the radical cation becomes more important relative to the stability of the resulting radical species formed, leading therefore to more reaction *ipso* to the methoxy group.

Overview of photolysis reaction products in acetonitrile at 20°, -20° and -50°.

The change in the pattern of product yields from dichloromethane to acetonitrile relative to photolysis reaction temperature (Tables 4.3 and 4.4) again demonstrates the substantially increased operation of the reaction pathways illustrated in Scheme 4.7 earlier *i.e.* increased yields of the 2-nitroanisole **420** and the cyclodienone **426**.

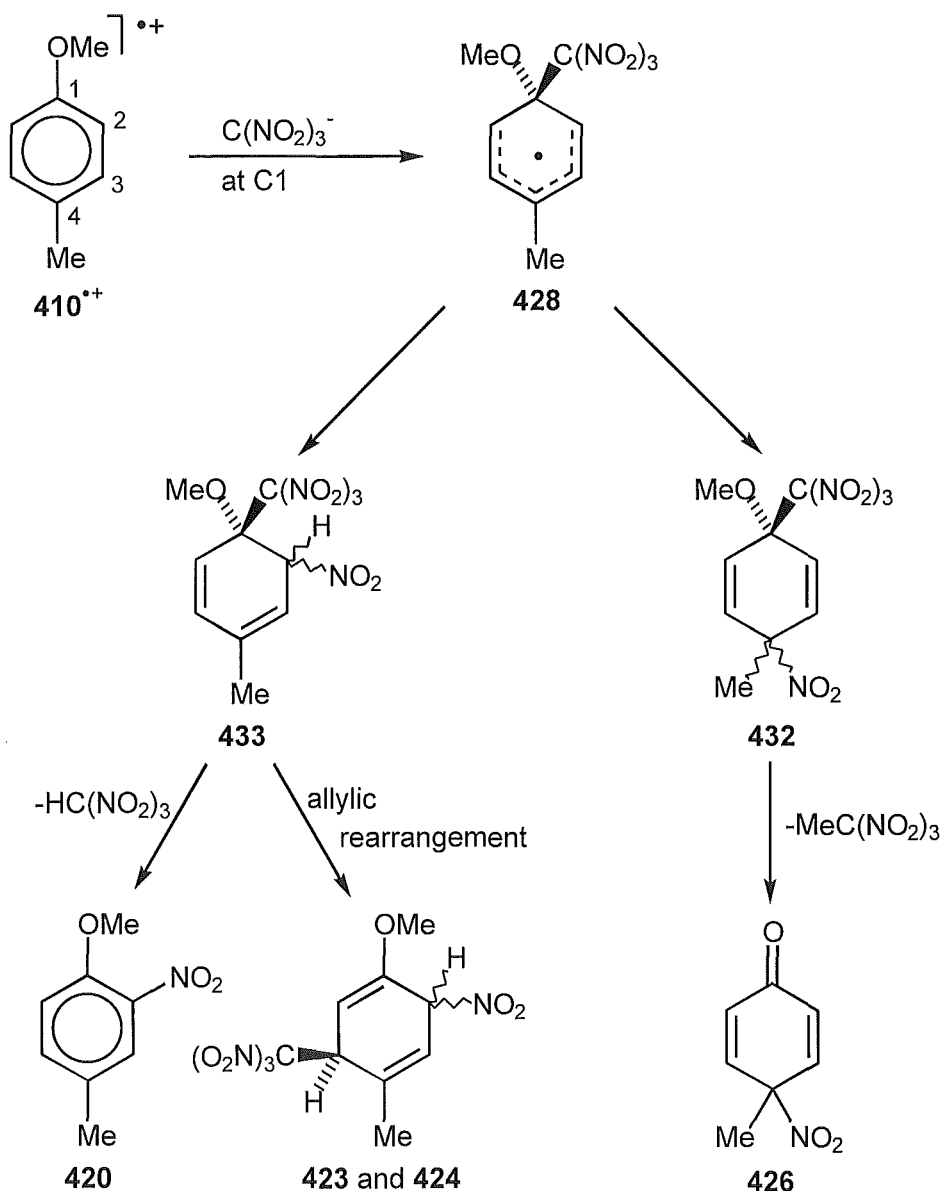


The change in regiochemistry of trinitromethanide ion attack is again interpreted in terms of the lower reactivity of trinitromethanide ion in the more polar

acetonitrile even at 20°. This leads to an increased influence of the charge distribution of the radical cation on the position of trinitromethanide ion attack and consequently higher yields of products derived from trinitromethanide ion attack at C1 of the 4-methylanisole radical cation.

Kochi *et al.* described a "solvent effect" in the photolysis of the charge transfer complex between 4-methylanisole and tetranitromethane² whereby "trinitromethylation" is observed in dichloromethane and "nitration" in acetonitrile. As discussed above, the change in products is merely the consequence of the lower reactivity of trinitromethanide ion towards the radical cation of 4-methylanisole in acetonitrile. This affects the regiochemistry of attack of trinitromethanide ion on that radical cation in a similar way to the decrease in temperature.

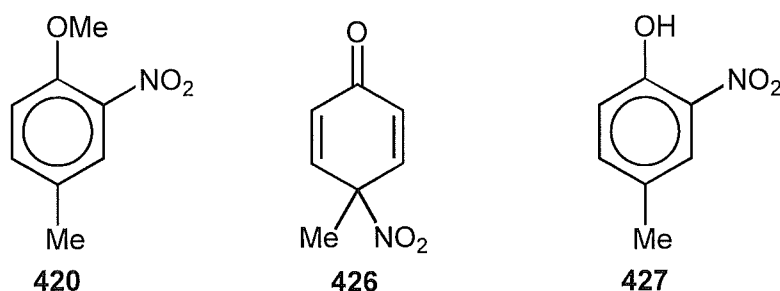
The other notable feature of the reactions in acetonitrile is the steady increase in yield of 4-methyl-4-nitrocyclohexa-2,5-dienone **426** as the reaction temperature is lowered at the expense of the nitro aromatic compound **420**. This presumably results from some change in the balance of nitrogen dioxide coupling to the radical species **428** (Scheme 4.9; overleaf).



Scheme 4.9

The effects of added salts $\text{Bu}_4\text{N}^+\text{ClO}_4^-$ (TBAP) or $\text{Bu}_4\text{N}^+\text{C}(\text{NO}_2)_3^-$ (TBAT) on the photolysis products in dichloromethane.

Earlier Kochi *et al.*² reported the effect of the added salt, $\text{Bu}_4\text{N}^+\text{ClO}_4^-$ (0.2 mol l^{-1}), on the photolysis reaction in dichloromethane, which resulted in the formation of 4-methyl-2-nitroanisole **420** (65 %) and the rearrangement product of 4-methyl-4-nitrodienone **426**, 4-methyl-2-nitrophenol **427** (35 %).



In the context of the study reported here, this result can be re-interpreted. It is clear that the effect is *not* a matter of competition between ion-pair and radical-pair collapse as Kochi and co-workers claimed, but rather a consequence of the increased polarity of the solvent system due to the added salt. This gives a more stabilising solvent environment, analogous to that of acetonitrile, for the attack of trinitromethanide ion on the radical cation of 4-methylanisole. Interpretation of the effect of the added "common ion" salt $\text{Bu}_4\text{N}^+\text{C}(\text{NO}_2)_3^-$ (TBAT) is difficult as the results reported by Kochi *et al.* were ambiguous and only reactions with very low concentrations (0.01 mol l^{-1}) of the added salt were reported.²

Summary

The photolysis reactions of 4-methylanisole with tetranitromethane appear follow a similar reaction pathway to those observed for naphthalene and its derivatives *i.e.* by recombination of the triad fragments with initial trinitromethanide addition to the radical cation and subsequent nitrogen dioxide coupling to the delocalised radical species formed. The adducts thus formed are prone to facile elimination or rearrangement to the observed reaction products. The following chapters aim to further demonstrate the intermediacy of these types of adducts in photolysis reactions of tetranitromethane with anisole derivatives.

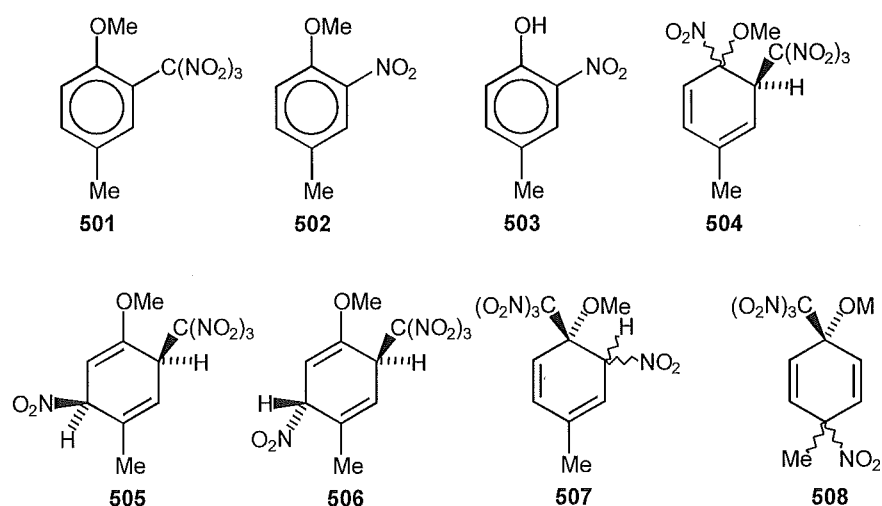
References

- ¹ Eberson, L., Hartshorn, M. P., Radner, F., and Svensson, J. O., *J. Chem. Soc. Perkin Trans. 2*, 1994, 1719.
- ² Sankararaman, S., Haney, W. A., and Kochi, J. K., *J. Am. Chem. Soc.*, 1987, **109**, 7824.
- ³ See Berkowitz, J., Ellison, G. B., and Gutman, D., *J. Phys. Chem.*, 1994, **98**, 2744 and references therein.
- ⁴ Appel, H. H., Bond, R. P. M., and Overton, K. H., *Tetrahedron*, 1963, **19**, 635.
- ⁵ Durham, L. J., Studebaker, J., and Perkins, M. J., *Chem. Commun.*, 1965, 456.
- ⁶ Butts, C. P., Calvert, J. L., Eberson, L., Hartshorn, M. P., Maclagan, R. G. A. R., and Robinson, W. T., *Aust. J. Chem.*, 1994, **47**, 1087.
- ⁷ Eberson, L., Hartshorn, M. P., Radner, F., Svensson, J., O., *Acta Chem. Scand.*, 1996, **50**, *in press*.
- ⁸ Calvert, J. L., Eberson, L., Hartshorn, M. P., Maclagan, R. G. A. R., and Robinson, W. T., *Aust. J. Chem.*, 1994, **47**, 1591.

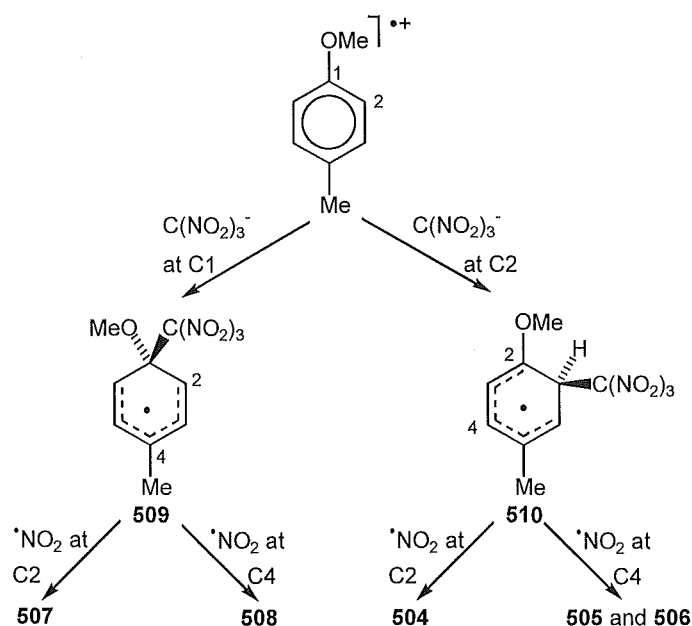
Chapter 5

Introduction

In Chapter 4 the formation of the observed aromatic products **501-503** in the photolysis reactions of 4-methylanisole and tetranitromethane was attributed to the decomposition of the initially formed adducts **504-508**.

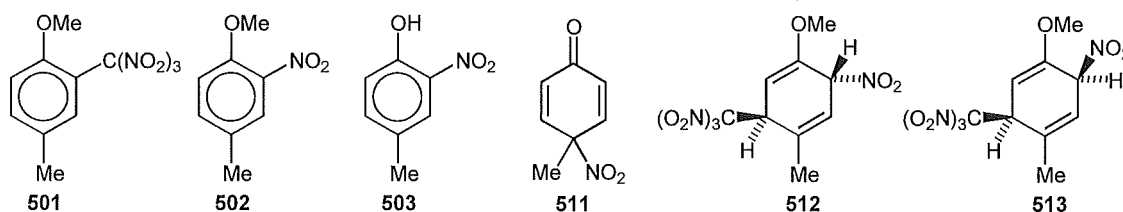


These adducts are formed by trinitromethanide anion attack at either C1 or C2 of the radical cation of 4-methylanisole to give the delocalised radical intermediates **509** and **510** (Scheme 5.1) and subsequent nitrogen dioxide coupling at either C2 or C4 of these species gives adduct **504-508**.

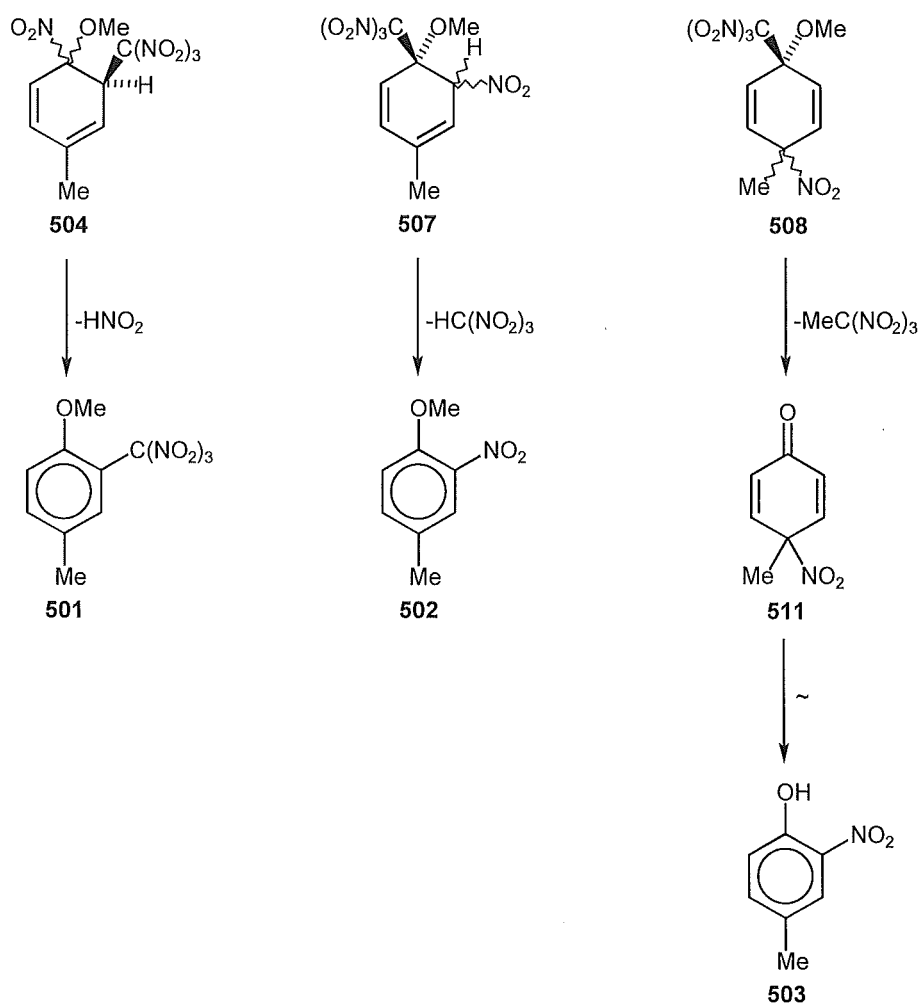


Scheme 5.1

Adducts **505** and **506** were observed in the reaction mixtures. They were observed to decompose to the trinitromethyl aromatic compound **501** during the photolysis reaction. The nature of the other adducts **504**, **507**, and **508** was implied by the formation of products **501-503**, and **511-513**.

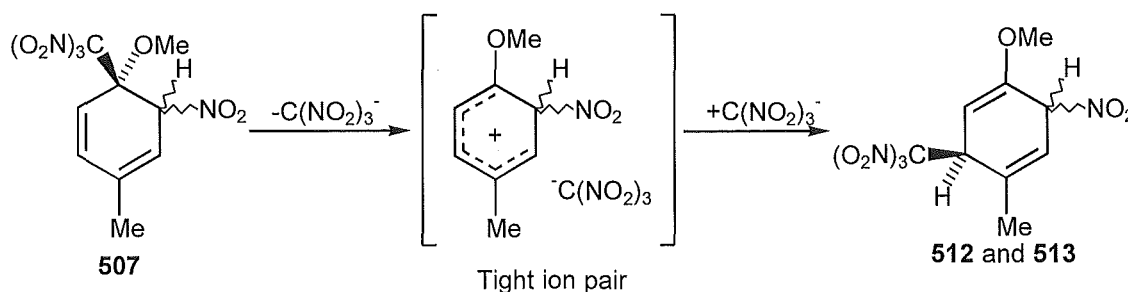


The mode of formation of some of these products involves either elimination of the substituent *ipso* to the methoxy function to give the aromatic species observed (Scheme 5.2).



Scheme 5.2

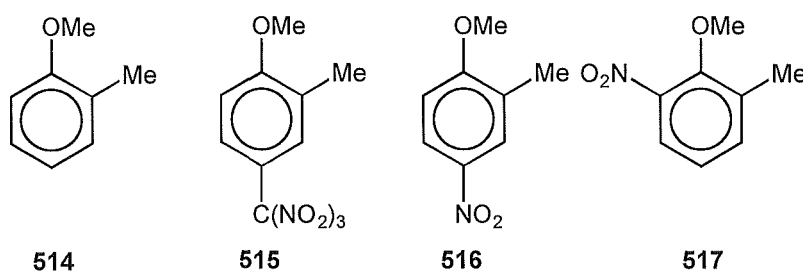
Alternatively, allylic rearrangement of the trinitromethyl function *via* a tight ion pair yields the adducts **512** and **513** (Scheme 5.3).



Scheme 5.3

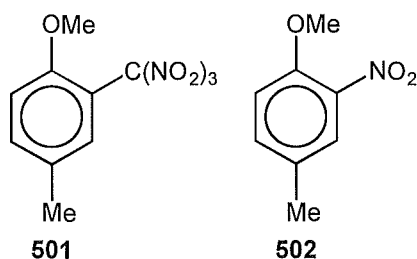
The adducts **504**, **507**, and **508** which possess substituents *ipso* to the methoxy function are highly labile species which were not observed in any reaction mixtures and their existence can only be implied from the observed reaction products. It was considered that the study of the photolysis reactions of tetranitromethane with other related anisole substrates would allow further insight into the operative mechanism in these systems and might enable the isolation of one or more *ipso* substituted adduct.

Kochi *et al.*¹ examined the products formed in the photolysis reactions of 2-methylanisole **514** with tetranitromethane in various solvents.



They found that in dichloromethane solutions the major photolysis product was the 4-trinitromethyl aromatic compound **515** (60% yield), with lesser quantities of the two nitro aromatic compounds **516** and **517** (10% and 6% yields respectively). In acetonitrile they found that the trinitromethyl arene compound **515** was not formed and the 4-nitro aromatic species **516** was now the major

component of the reaction mixtures (68% yield). The remainder of the photolysis product mixture consisted of the 2-nitro aromatic compound **517**. This solvent induced change in products was similar to that observed in photolysis reactions of 4-methylanisole and tetranitromethane¹ where 4-methyl-2-trinitromethylanisole **501** predominated in dichloromethane solutions but the yield of 4-methyl-2-nitroanisole **502** was significantly increased in acetonitrile photolysis solutions.



As discussed above, these compounds **501** and **502** are derived from unstable adduct species and thus it seems likely that a similar mechanism would account for the formation of the analogous aromatic species **515-7** in the photolysis reactions of 2-methylanisole and tetranitromethane.

To test this postulate, studies of the photolysis reactions of tetranitromethane with 2-methylanisole and 2,4-dimethylanisole were conducted using low temperature work-up and careful separation techniques.

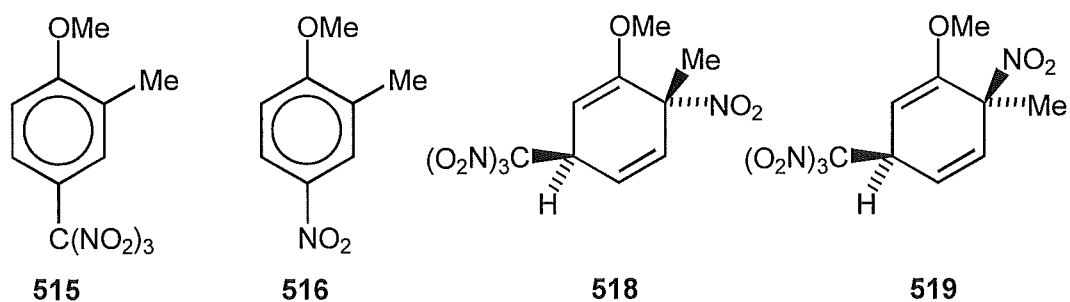
Results

*General procedure for the photolysis of 2-methylanisole **514** with tetranitromethane.*

The photochemical experiments were performed with filtered light (cut-off < 435 nm, 5 cm water IR-filter, from a 300 W lamp; See Experimental section for details) and small samples were withdrawn for analysis at suitable intervals. The work-up procedure, involving evaporation of solvent and excess tetranitromethane, was conducted at a temperature $\leq 0^\circ$. The crude product mixtures were stored at -78° and were analysed (¹H n.m.r. spectroscopy, see Experimental section; Tables 8.5.1 and 8.5.2) as soon as possible.

Photolysis of 2-methylanisole **514** in dichloromethane at 20° and the identification of products **515**, **516**, **518** and **519**.

A solution of 2-methylanisole **514** (0.51 mol l⁻¹) and tetranitromethane (1.02 mol l⁻¹) in dichloromethane was irradiated at 20°. The composition of the mixture was monitored by withdrawing samples for ¹H n.m.r. spectral analysis (Tables 5.2 and 8.5.1). The final solution (after 4 h, conversion ca. 50 %) after work-up contained the 4-trinitromethyl compound **515** (65 %), 2-methyl-4-nitroanisole **516** (25 %), unidentified aromatic compounds (total 4 %), and the nitro-trinitromethyl adducts **518** (4 %) and **519** (2 %).



The aromatic products **515** and **516** were separated by chromatography on a silica gel Chromatotron plate and identified from literature data.^{2,3} The two nitro-trinitromethyl adducts **518** and **519** were separated partially by h.p.l.c. on a cyanopropyl column using hexane-dichloromethane mixtures as eluting solvents. The structure of the minor nitro-trinitromethyl adduct **519** was determined by single crystal X-ray analysis. A perspective drawing of 1-methoxy-6-methyl-*c*-6-nitro-*r*-3-trinitromethyl-cyclohexa-1,4-diene **519**, C₉H₁₀N₄O₉, m.p. 75-77° (decomp.), is presented in Figure 5.1, overleaf and the corresponding atomic coordinates are given in Table 8.5.3.

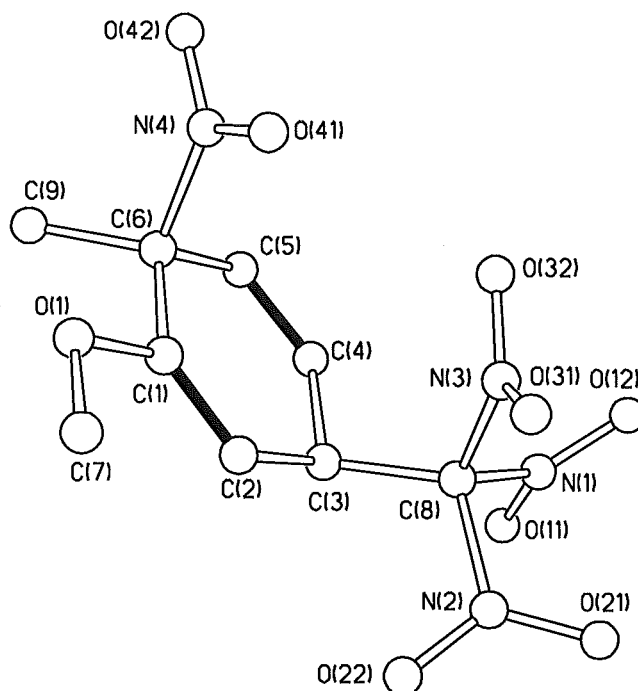


Figure 5.1 - Perspective drawing of **519**.

In the solid state the alicyclic ring is close to planar (torsional angles C(2)-C(3)-C(4)-C(5) $1.4(4)^\circ$ and C(2)-C(1)-C(6)-C(5) $0.1(3)^\circ$) with the methoxy group slightly displaced from that plane (torsional angle C(7)-O(1)-C(1)-C(2) $12.3(4)^\circ$), as shown in Figure 5.2.

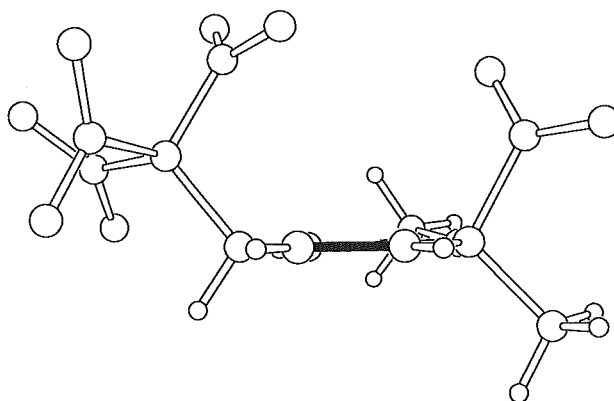
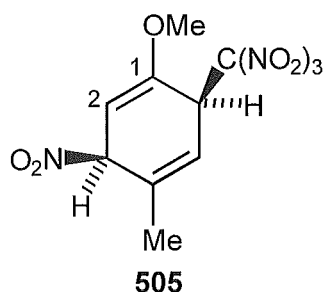
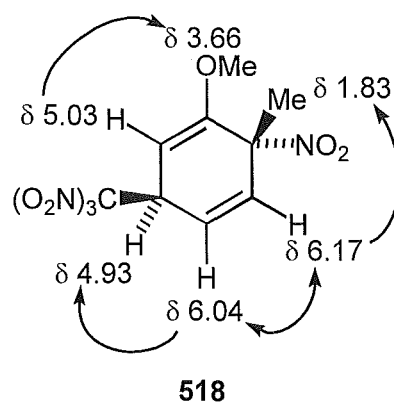


Figure 5.2 - Side view of **519**

The methyl and nitro substituents at C(6) are close to being perfectly staggered with respect to the adjacent methoxy group, and the orientations of the C-NO₂ bonds in the trinitromethyl group relative to the alicyclic ring are such as to minimise steric interactions. The spectroscopic data for adduct **519** were consistent with the established structure. In particular the observed ¹H n.m.r. coupling constant $J_{H3,H4}$ 3.5 Hz is consistent with the solid state torsional angle H(4)-C(4)-C(3)-H(3) -60.4(1)°. The ¹H n.m.r. spectra was assigned by examination of nuclear Overhauser experiments and subsequent heteronuclear correlation spectra (HMQC/HMBC) allowed unequivocal assignment of the ¹³C n.m.r. resonances. The critical ¹³C resonances at δ 42.6 (C-C(NO₂)₃) and δ 85.5 (C-NO₂) were assigned to C3 and C6 respectively. The C2 carbon resonance (δ 89.5) was at much higher field than expected for a vinyl carbon. This effect was also observed for C2 (δ 95.5) of the analogous adduct **505** from the photolysis of 4-methylanisole with tetranitromethane for which the structure was also established by single crystal X-ray analysis.



The structure of the epimeric adduct **518**, which could not be induced to crystallise, was established from a consideration of its n.m.r. spectra and comparison with corresponding data for adduct **519**. The results of nuclear Overhauser experiments (Figure 5.3, overleaf) allowed the assignment of the ¹H n.m.r. spectra.

Figure 5.3 - Observed nuclear Overhauser enhancements for adduct **518**

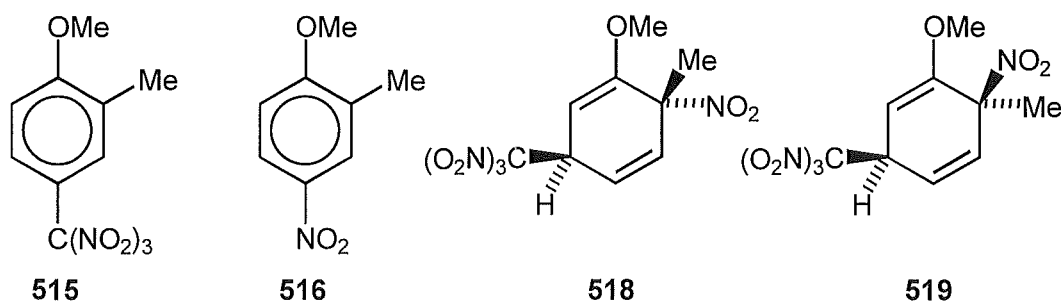
Subsequent interpretation of heteronuclear correlation spectra (HMQC/HMBC) allowed the connectivity of adduct **518** to be established. The ^1H and ^{13}C n.m.r. spectra for adducts **518** and **519** were very similar (Table 5.1) as would be expected given their epimeric relationship.

Table 5.1 - Comparison of ^1H and ^{13}C n.m.r. resonances of **518** and **519**.

Resonance	518		519	
	^{13}C	^1H	^{13}C	^1H
-OMe	δ 55.7	δ 3.66	δ 55.8	δ 3.71
-Me	δ 23.5	δ 1.83	δ 23.6	δ 1.85
1-C	δ 157.5	-	δ 157.1	-
2-CH	δ 89.3	δ 5.03	δ 89.6	δ 5.03
3-CH	δ 43.7	δ 4.95	δ 42.6	δ 4.86
4-C	δ 121.8	δ 6.04	δ 121.8	δ 5.99
5-CH	δ 133.9	δ 6.17	δ 133.6	δ 6.22
6-CH	δ 85.7	-	δ 85.5	-

Photolysis of 2-methylanisole **514** in dichloromethane at -20° , -50° and -78° and in acetonitrile at 20° , -20° and -45° .

Similar reactions to the above were performed in dichloromethane at -20° , -50° and -78° and acetonitrile at 20° , -20° and -45° . In each case the composition of the mixture was monitored by withdrawing samples for ^1H n.m.r. spectral analysis and the results are summarised in Table 5.2, overleaf. The most notable feature of these reactions is the lower yields of the 4-trinitromethyl aromatic compound **515** in acetonitrile and the concomitant increase in the yields of the nitro aromatic compound **516**, and adducts **518** and **519**.



Photolysis of 2-methylanisole **514** in 1,1,1,3,3,3-hexafluoropropan-2-ol (HFP) at 20° .

Photolysis of the CT-complex of 2-methylanisole **514** and tetranitromethane in HFP at 20° resulted in a low conversion into products (*ca.* 8 % at 2 h; *cf.* *ca.* 21 % in dichloromethane under comparable conditions) and, after 2 h, the formation of compounds **515** (35 %), **516** (30 %), unidentified aromatic compounds (total 15 %), adducts **518** (8 %) and **519** (4 %), and unidentified adducts (total 8 %). See Table 8.5.2 (Experimental section) for details.

Table 5.2 - Overview of product yields from the photolysis of 2-methylanisole **514** (0.51 mol l⁻¹) with tetranitromethane (1.02 mol l⁻¹) in dichloromethane and acetonitrile.^A

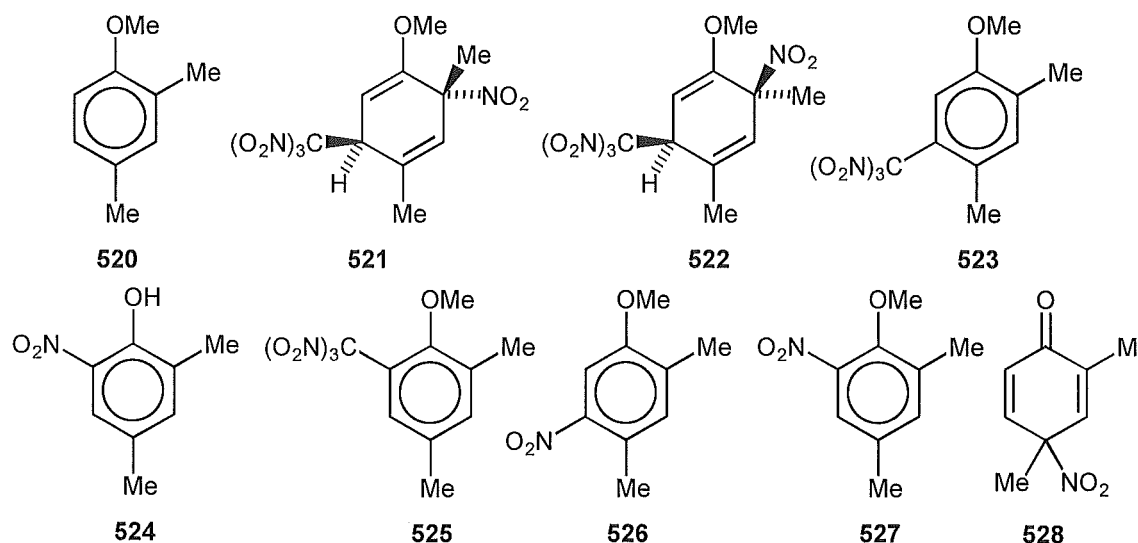
Conditions	t/h	Yields (%)					Unknown Adducts
		515	516	Unknown ArX	518	519	
DCM/20°	0.5	78.2	9.8	5.5	4.6	1.9	0.0
	1	75.4	11.7	5.8	4.7	2.4	0.0
	2	70.7	17.4	5.2	4.5	2.2	0.0
	4	65.2	35.0	3.9	4.1	1.7	0.0
DCM/-20°	0.5	78.8	10.3	2.7	5.9	1.3	0.9
	1	77.6	9.7	4.0	5.8	2.1	0.9
	2	72.6	12.0	3.8	8.0	2.9	0.7
	4	68.4	15.5	7.0	6.3	1.8	1.1
DCM/-50°	0.5	75.6	11.9	4.0	6.0	2.0	0.5
	1	74.2	11.3	4.0	7.4	2.7	0.4
	2	72.6	11.8	6.5	6.4	2.3	0.4
	4	70.3	12.5	7.3	7.0	2.3	0.5
DCM/-78°	0.5	71.4	12.7	4.5	8.0	2.9	0.6
	1	72.6	11.8	4.5	7.2	3.6	0.4
	2	70.5	12.6	6.4	7.1	2.9	0.6
	4	70.3	11.8	6.9	7.4	3.0	0.6
AN/20°	0.5	35.2	37.9	3.8	16.1	4.3	2.7
	1	30.7	40.8	4.7	17.5	4.2	2.0
	2	26.0	43.3	5.7	18.3	4.3	2.4
	4	23.9	44.8	4.5	19.5	4.1	3.2
AN/-20°	1	39.1	34.6	3.8	15.9	4.4	2.2
	2	33.7	37.6	5.5	17.7	4.6	0.9
	4	29.9	39.2	7.9	17.7	4.2	1.1
AN/-45°	1	41.4	28.5	4.8	19.2	5.8	0.4
	2	39.2	30.8	6.8	18.7	3.9	0.6
	4	38.7	31.9	8.2	16.4	4.1	0.7

^A Conversions not quoted due to substrate volatility during work-up

Photolysis of 2,4-Dimethylanisole with Tetranitromethane

Photochemistry of 2,4-dimethylanisole 520 in dichloromethane at 20° and the identification of adducts 521 and 522.

A solution of 2,4-dimethylanisole **520** (0.46 mol l⁻¹) and tetranitromethane (0.92 mol l⁻¹) in dichloromethane was irradiated at 20°. The composition of the mixture was monitored by withdrawing samples for n.m.r. spectral analysis (Table 5.4 and 8.5.4). The final solution (after 3 h, conversion ca. 81 %) after work-up contained the nitro-trinitromethyl adducts **521** (15 %) and **522** (2 %), unidentified adducts (total 8 %), 4,6-dimethyl-3-trinitromethylanisole **523** (30 %), 4,6-dimethyl-2-nitrophenol **524** (9 %), 4,6-dimethyl-2-trinitromethylanisole **525** (5 %), 4,6-dimethyl-3-nitroanisole **526** (1.5 %), 4,6-dimethyl-2-nitroanisole **527** (11 %), 2,4-dimethyl-4-nitrocyclohexa-2,5-dienone **528** (14 %), and unidentified aromatic compounds (total 5 %).



The nitro-trinitromethyl adducts **521** and **522** were separated partially by h.p.l.c. and gave, in elution order, a mixture of aromatic compounds **523-527**, and the two adducts **521** and **522**. The mixture of aromatic compounds **523-527** was separated subsequently by radial chromatography on a silica gel Chromatotron plate.

Although the epimeric nitro-trinitromethyl adducts **521** and **522** could be isolated by h.p.l.c., they were too unstable for complete purification and neither could be induced to crystallise. The connectivity in each epimer was established from the results of nuclear Overhauser experiments (Figure 5.4) and reverse detected heteronuclear correlation spectra (HMQC/HMBC).

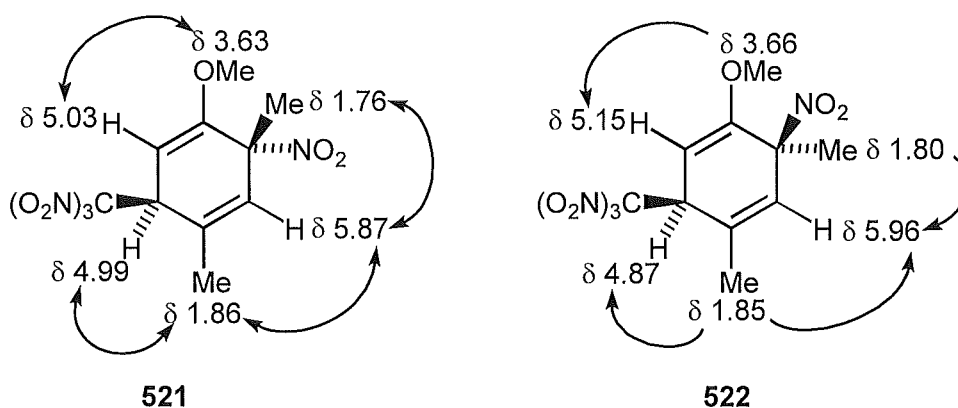


Figure 5.4 - Observed nuclear Overhauser enhancements for adducts **521** and **522**.

The two ^{13}C n.m.r. spectra were closely similar, and the ^1H n.m.r. spectra were as might be expected for such epimers. These data are given in Table 5.3, overleaf, together with n.m.r. data for the analogous adduct **519**, the structure of which had been established by single crystal X-ray analysis (p. 125-126).

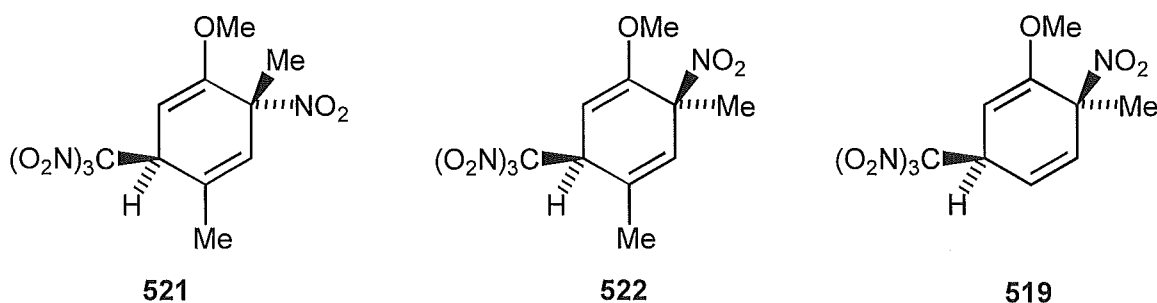
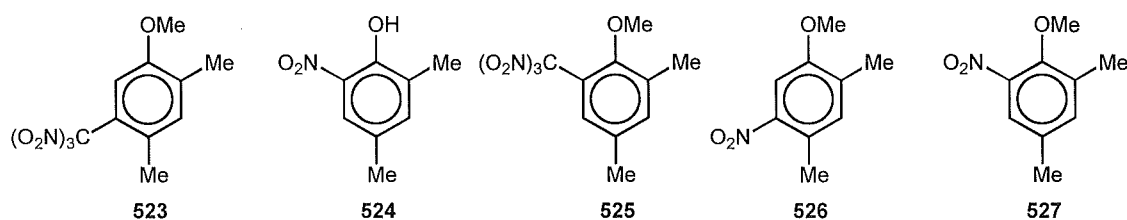


Table 5.3 - Comparison of ^1H and ^{13}C n.m.r. resonances of **519**, **521**, and **522**.

Resonance	521		522		519	
	^{13}C	^1H	^{13}C	^1H	^{13}C	^1H
-OMe	δ 55.2	δ 3.63	δ 55.7	δ 3.66	δ 55.8	δ 3.71
4-Me	δ 20.9	δ 1.86	δ 21.3	δ 1.85	-	-
6-Me	δ 23.2	δ 1.76	δ 23.8	δ 1.80	δ 23.6	δ 1.85
1-C	δ 157.3	-	δ 157.0	-	δ 157.1	-
2-CH	δ 89.5	δ 5.03	δ 91.0	δ 5.15	δ 89.6	δ 5.03
3-CH	δ 46.6	δ 4.99	δ 46.9	δ 4.87	δ 42.6	δ 4.86
4-C	δ 128.7	-	δ 130.3	-	δ 121.8	N/A
5-CH	δ 131.3	δ 5.87	δ 131.5	δ 5.96	δ 133.6	δ 6.22
6-C	δ 86.2	-	δ 84.8	-	δ 85.5	-

The assignment of stereochemistry was made on the basis of the elution order of the two epimers from the h.p.l.c. column,^{4,5} the *t*-6-nitro-*r*-3-trinitromethylmethyl compound **521** being eluted before the *c*-6-nitro-*r*-3-trinitromethyl adduct **522**.

The aromatic compounds **523-527** were separated by radial chromatography on a silica gel Chromatotron plate.



The structures of the regioisomeric trinitromethyl aromatic compounds **523** and **525** were determined from their spectroscopic data. For the major isomer **523** crystalline material was obtained but of an inadequate quality for single crystal X-ray analysis. However, the ^1H n.m.r. spectra showed two singlet resonances in the aromatic region (δ 7.18, δ 6.66) indicating either a 5- or 6- substitution of the 2,4-dimethylanisole parent compound. Given the molecular formula

($C_{10}H_{11}N_3O_7$, mass spectrum), its structure was securely established from the observed enhancement of the signal due to H2 (δ 6.66, singlet) on irradiation at the OMe resonance (δ 3.79) in a nuclear Overhauser experiment.

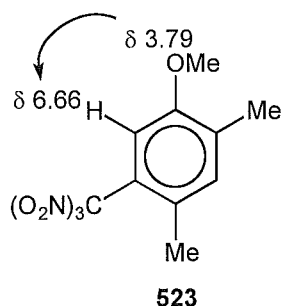


Figure 5.5 - Observed nuclear Overhauser enhancement in the 1H n.m.r. of **523**

The structure of the minor isomer **525** then followed by exclusion, the 1H n.m.r. signals due to H3 (δ 6.81) and H5 (δ 7.00) again appearing as singlets. The structures of the 3-nitro- and 2-nitro- 4,6-dimethylanisoles **526** and **527** were established in a similar manner from their spectroscopic data (Experimental section).

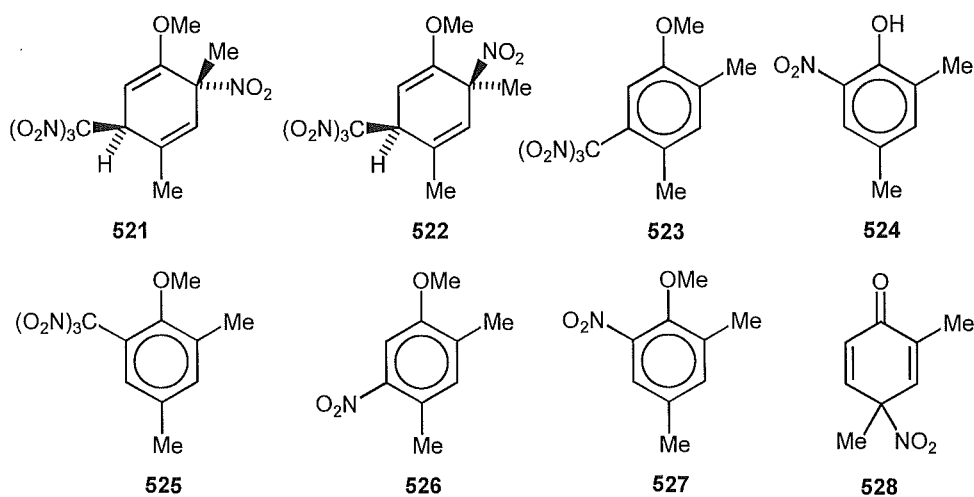
The structures of the nitro phenol **524** and its precursor, 2,4-dimethyl-4-nitrocyclohexa-2,5-dienone **528**, were assigned by comparison with literature data.⁶ The nitro dienone **528** was not isolated from chromatography on the silica gel Chromatotron plate, and under those conditions it would be expected to undergo isomerisation to give the nitro phenol **524**.

Photochemistry of 2,4-dimethylanisole 520 in dichloromethane at -20°, -50° and -78° and in acetonitrile at 20° and -20°.

Similar reactions to the above were performed in dichloromethane at -20°, -50°, and -78°, and in acetonitrile solution at 20°, and -20°. In each case the composition of the mixture was monitored by withdrawing samples for 1H n.m.r. spectral analysis and the results are summarised in Table 5.4, overleaf.

Table 5.4 - Overview of product yields from the photolysis of 2,4-dimethylanisole **520** (0.46 mol l^{-1}) with tetranitromethane (0.92 mol l^{-1}) in dichloromethane and acetonitrile.^A

Conditions	t/h	Yields (%)									
		Unknown							Unknown		
		521	522	Adducts	523	524	525	526	527	528	ArX
DCM/20°	1	11.4	1.8	15.8	14.2	5.3	6.5	1.3	13.6	18.1	7.5
	2	14.9	1.8	9.1	24.9	4.9	6.0	1.0	9.4	14.0	11.0
	3	15.2	2.1	4.7	29.7	9.0	4.6	1.5	11.0	13.8	6.2
DCM/-20°	1	11.5	1.8	11.8	1.9	1.9	2.4	1.9	12.7	27.9	23.2
	2	16.9	2.7	8.6	2.0	2.9	3.5	3.9	15.9	29.3	8.9
	3	21.3	3.2	12.8	2.4	2.0	1.9	5.0	16.8	24.8	5.9
DCM/-50°	1	32.8	4.1	11.5	0.4	1.3	1.1	5.6	13.5	21.5	6.0
	2	36.5	4.3	6.6	1.8	0.7	1.1	7.3	14.5	17.5	4.1
	3	38.0	4.4	7.6	1.7	0.9	0.8	8.5	15.2	14.8	3.9
DCM/-78°	1	30.8	3.2	6.3	6.8	2.6	3.8	0.8	3.2	28.4	11.2
	2	34.7	4.0	8.5	1.5	1.4	1.5	2.8	6.6	25.0	9.6
	3	39.0	3.8	7.3	1.9	2.2	1.2	4.4	8.1	21.7	6.5
AN/20°	2	47.0	13.4	0.0	0.9	3.0	1.1	6.4	9.6	9.6	8.1
	3	44.4	16.1	0.0	1.3	3.7	0.9	7.3	11.0	7.3	6.5
AN/-20°	2	49.2	7.2	0.0	0.6	1.4	1.1	2.9	1.6	23.4	8.6
	3	49.0	7.2	0.0	1.2	1.3	0.9	3.0	1.5	21.5	7.2



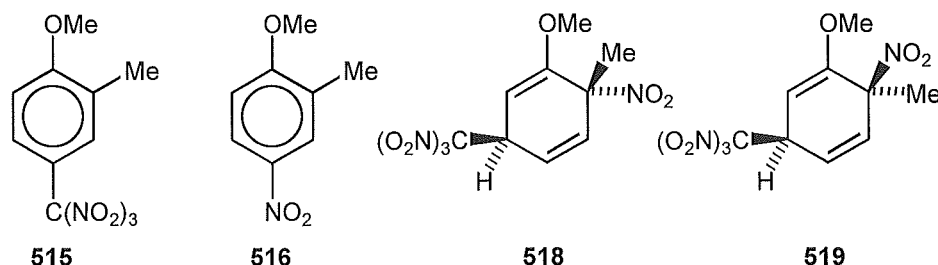
Photochemistry of 2,4-dimethylanisole **520** in 1,1,1,3,3,3-hexafluoropropan-2-ol (HFP) at 20°.

Photolysis of the CT-complex of 2,4-dimethylanisole **520** and tetranitromethane in HFP at 20° for 3 h resulted in a conversion (ca. 46 %; *c.f.* 81 % in dichloromethane under similar conditions) into nitro-trinitromethyl adducts **521** (1 %) and **522** (2 %), aromatic compounds **523** (21 %), **524** (6 %), **525** (2 %), **526** (16 %), **527** (38 %), and unidentified aromatic compounds (total 14 %). For details see Experimental section and Table 8.5.5.

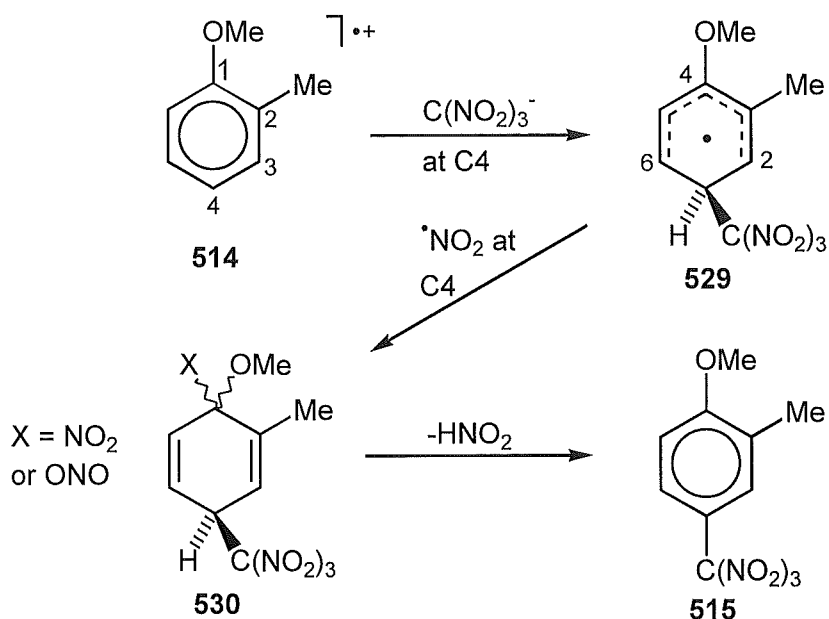
Discussion

*The photolysis of the charge transfer complex of 2-methylanisole **514** with tetranitromethane.*

At all reaction temperatures in dichloromethane (from 20° to -78°) and in acetonitrile (from 20 to -45°) the trinitromethyl compound **515**, nitro compound **516**, and the two epimeric 1-methoxy-6-methyl-6-nitro-3-trinitromethyl-cyclohexa-1,4-dienes **518** and **519** were formed (Table 5.2).



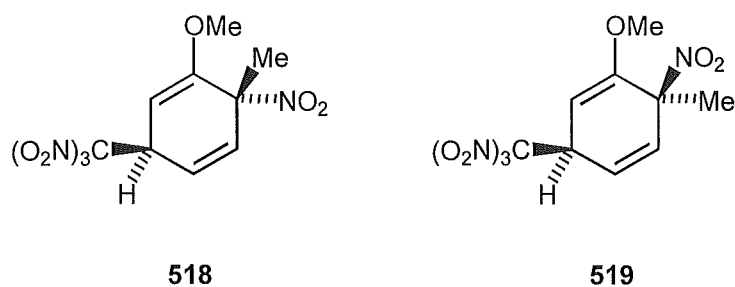
In dichloromethane at 20°, and in acetonitrile at 20° and -20°, some decomposition of the trinitromethyl compound **515** occurred yielding, in part, the nitro compound **516**. The formation of the trinitromethyl compound **515** is envisaged as occurring *via* initial attack of trinitromethanide ion at C4 in the radical cation of 2-methylanisole to give the delocalised carbon radical **529** (Scheme 5.4, overleaf).



Scheme 5.4

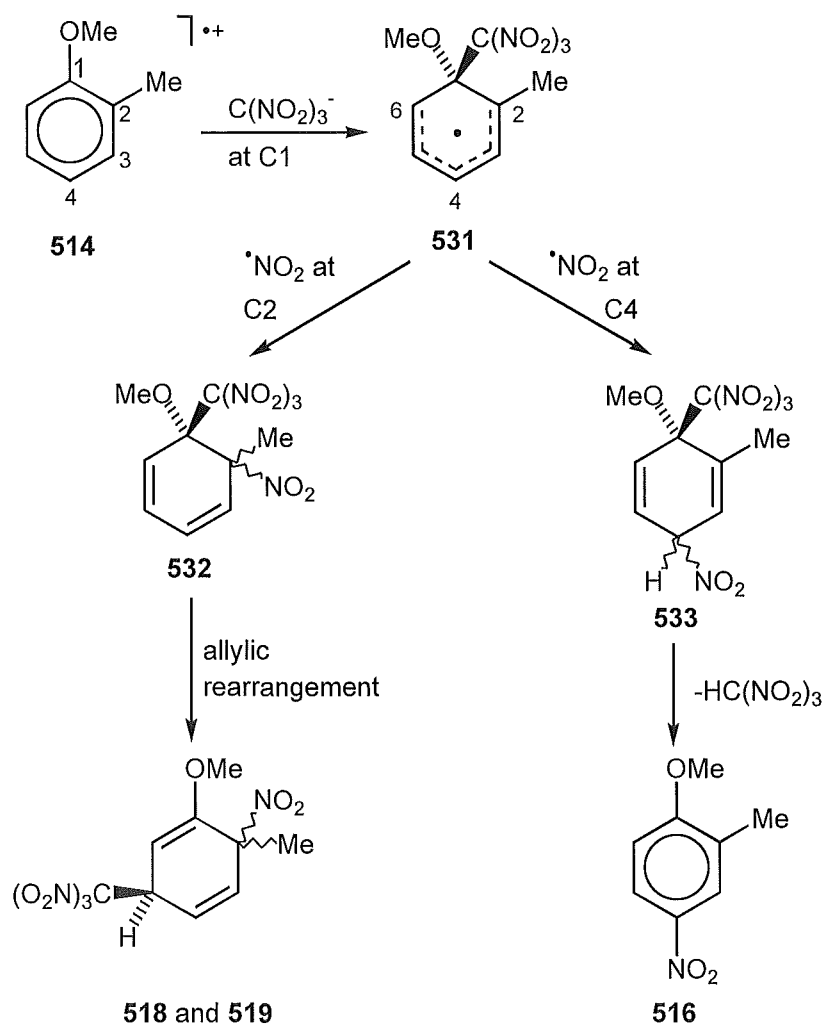
Radical coupling at C4 of this delocalised carbon radical **529** with nitrogen dioxide and subsequent loss of nitrous acid from the adduct **530** would give the trinitromethyl compound **515**.

Notably the change of solvent from the less polar dichloromethane to the more polar acetonitrile results in increased yields of the nitro compound **516** and the epimeric adducts **518** and **519**.



These observations are similar to those made in the photolysis reactions of 4-methylanisole with tetranitromethane where increased yields of 4-methyl-2-nitro-anisole were observed in acetonitrile at the expense of 4-methyl-2-trinitromethylanisole. The change in product yields seen in acetonitrile may be rationalised in terms of some shift in the regiochemistry of attack of trinitromethanide ion on the radical cation of 2-methylanisole towards attack *ipso* to the methoxy group when the trinitromethanide ion is rendered less

nucleophilic by the more polar solvent. This mode of attack would give the delocalised carbon radical **531** (Scheme 5.5).

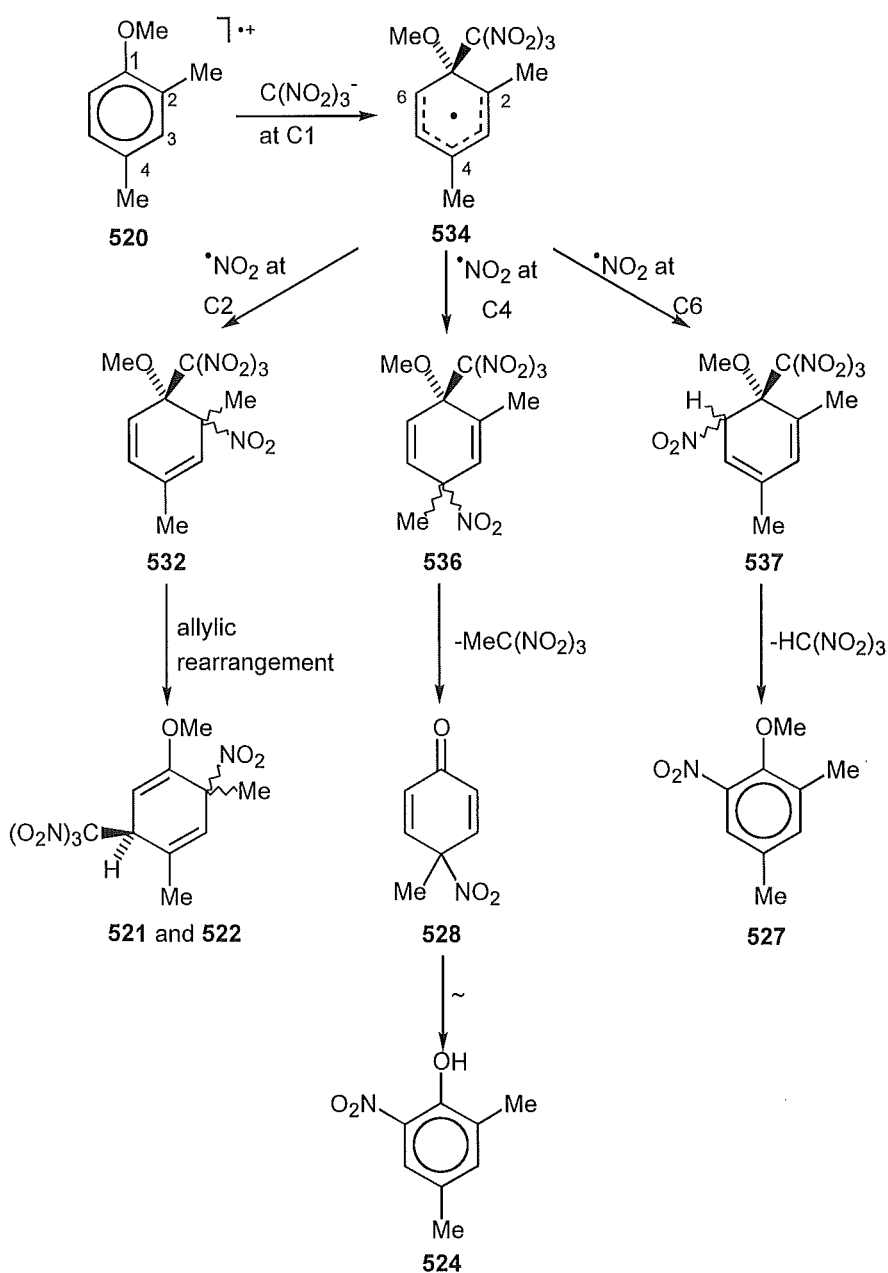


Scheme 5.5

Radical coupling with nitrogen dioxide at C2 would give adducts **532**, which might be expected to undergo heterolytic allylic rearrangement to give the epimeric 6-methyl-6-nitro-3-trinitromethyl adducts **518** and **519**. In the radical coupling to form the postulated intermediate adducts **532**, the preferred orientation of bond formation would be *anti* to the adjacent bulky trinitromethyl group. If the heterolytic allylic rearrangement proceeds *via* a "tight" ion pair as discussed in previous chapters, the observed higher yield of the *t*-6-nitro-*r*-3-trinitromethyl adduct **518** may be rationalised. The alternative radical coupling of nitrogen dioxide with the delocalised carbon radical **531** at C4 would give adducts **533**, from which nitro compound **516** could arise by loss of nitroform.

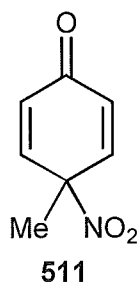
The photolysis of the charge transfer complex of 2,4-dimethylanisole **520** with trinitromethane.

At low temperatures in both dichloromethane and acetonitrile solution the major products formed were 1-methoxy-4,6-dimethyl-6-nitro-3-trinitromethylcyclohexa-1,4-diene **521**, and the 2,4-dimethyl-4-nitro-cyclohexa-2,5-dienone **528**. These products are envisaged as being formed *via* initial attack of trinitromethanide ion *ipso* to the methoxy group in the radical cation of 2,4-dimethylanisole to give the delocalised carbon radical **534** (Scheme 5.6).



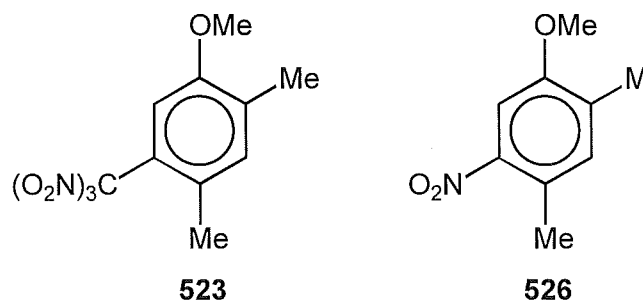
Scheme 5.6

As with the reaction sequence for 2-methylanisole (Scheme 5.5), radical coupling at C2 of this carbon radical **534** with nitrogen dioxide followed by allylic rearrangement of adducts **532** would yield the epimeric 1-methoxy-4,6-dimethyl-6-nitro-3-trinitromethylcyclohexa-1,4-dienes **521** and **522**, with the *t*-6-nitro-*r*-3-trinitromethyl epimer predominant (Table 5.6). Alternatively, radical coupling of nitrogen dioxide at C4 of the delocalised carbon radical **534** would give the adducts **536**, which on the loss of the elements of Me/C(NO₂)₃ would form the nitro dienone **528**. An analogous process was postulated to account for formation of the nitrodienone **511** in the photolysis of the charge transfer complex of 4-methylanisole with tetranitromethane.



Nitrogen dioxide coupling at C6 of the delocalised carbon radical **534** would give the adduct **537** which would lead to the formation of nitro aromatic compound **527** on elimination of nitroform.

The modes of formation of 4,6-dimethyl-3-trinitromethylanisole **523** and 4,6-dimethyl-3-nitroanisole **526** are unclear.

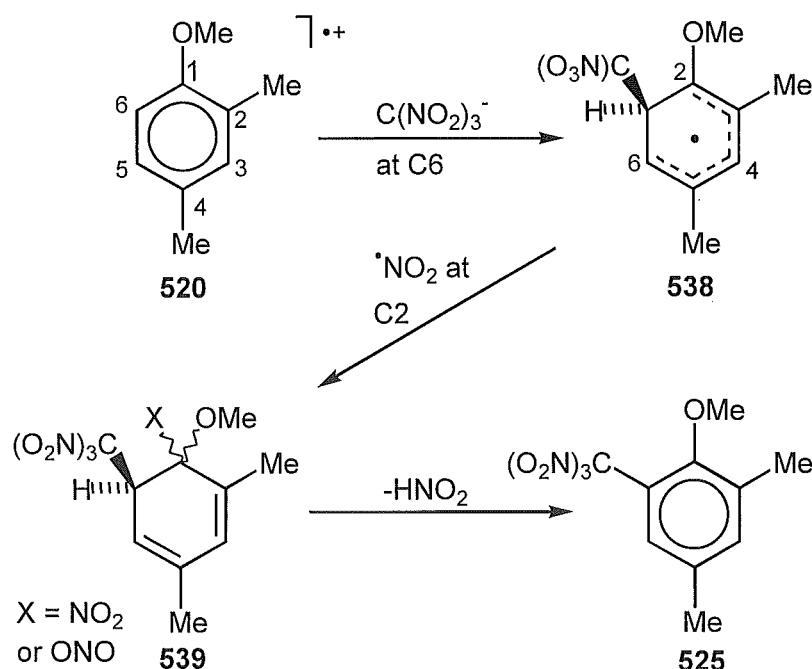


The 4,6-dimethyl-3-trinitromethylanisole **523** was formed in dichloromethane at 20° in a yield which increases over the course of the reaction (14 % at 1 h, 25 % at 2 h, 30 % at 3h). This is presumably the result of the decomposition of

unidentified adducts, the yield of which decreases during the course of the reaction (16 % at 1 h, 9 % at 2 h, 5 % at 3 h).

The nitro aromatic compound **526** was not observed in yields greater than 9% under any reaction conditions, and its origin remains uncertain.

The final compound, 4,6-dimethyl-2-trinitromethylanisole **525**, is envisaged to result from initial attack of trinitromethanide ion at C6 of the radical cation of 2,4-dimethylanisole **520**, with nitrogen dioxide coupling at C2 of the resultant delocalised carbon radical species **538** to give the adduct **539** (Scheme 5.7). Subsequent elimination of nitrous acid from the adduct **539** would give the 4,6-dimethyl-2-trinitromethylanisole **524**.



Scheme 5.7

*Photolysis reactions of 2-methylanisole **514**, and 2,4-dimethylanisole **520** in 1,1,1,3,3,3-hexafluoropropan-2-ol (HFP).*

HFP has been found to strongly stabilise radical cations, presumably by rendering any nucleophilic species present exceedingly unreactive.⁷ It was therefore anticipated that reaction of both radical cations with trinitromethanide ion would be slow and allow competition from the $\text{ArH}^{\bullet+} / ^{\bullet}\text{NO}_2$ coupling process. For both substrates **514** and **520**, the conversion into products was

somewhat slowed but product formation involving attack by trinitromethanide ion remained a significant reaction pathway.

Summary

It appears that the photolysis reactions of both 2-methyl- and 2,4-dimethyl- anisoles with tetranitromethane follow similar mechanistic pathways described for previous substrates *i.e.* recombination of the triad fragments by the initial attack of trinitromethanide ion on the aromatic radical cation, followed by nitrogen dioxide coupling to the resulting delocalised radical species. The nitro-trinitromethyl adducts thus formed may then undergo further reactions, whether by elimination or rearrangement to give the observed reaction products.

Chapter 6 discusses the results of the photolysis reactions of tetranitromethane with 4-fluoroanisole and 4-fluoro-3-methylanisole where the effects of halogen substituents on the aromatic system are examined.

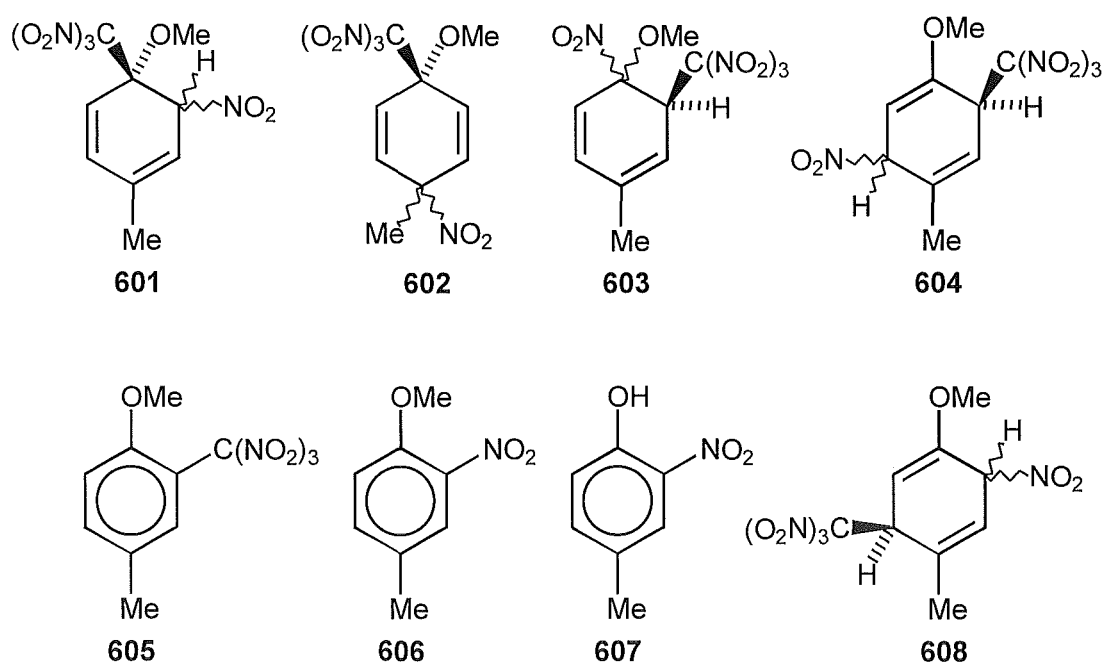
References

- ¹ Sankararaman, S. Haney, W. A., and Kochi, J. K., *J. Am. Chem. Soc.*, 1987, **109**, 7824.
- ² Sankararaman, S., and Kochi, J. K., *Rec. Trav. chim.*, 1986, **105**, 278.
- ³ Gibson, G. P., *J. Chem. Soc.*, 1925, **1527**, 42.
- ⁴ Butts, C. P., Ebersson, L., Hartshorn, M. P., and Robinson, W. T., *Aust. J. Chem.*, 1995, **48**, 1989.
- ⁵ Butts, C. P., Calvert, J. L., Ebersson, L., Hartshorn, M. P., Radner, F., and Robinson, W. T., *J. Chem. Soc. Perkin Trans. 2*, 1994, 1485; and references cited therein.
- ⁶ Cross, G. G., Fischer, A., Henderson, G. N., and Smyth, T. A., *Can. J. Chem.*, 1984, **62**, 1446.
- ⁷ Ebersson, L. Hartshorn, M. P., and Persson, O., *Angew Chem. Int. Ed. Engl.*, 1995, **34**, 2268; Ebersson, L., Hartshorn, M. P., and Persson, O., *J. Chem. Soc. Chem. Commun.*, 1995, 1131; Ebersson, L., Hartshorn, M. P., and Persson, O., *J. Chem. Soc. Perkin Trans. 2*, 1995, 1735; Ebersson, L. Hartshorn, M. P., and Persson, O., *Acta Chem. Scand.*, 1995, **49**, 640; Ebersson, L. Hartshorn, M. P., and Persson, O., *J. Chem. Soc. Perkin Trans. 2*, 1996, 141; Ebersson, L. Hartshorn, M. P., and Persson, O., *J. Chem. Soc. Perkin Trans. 2*, 1996, 151.

Chapter 6

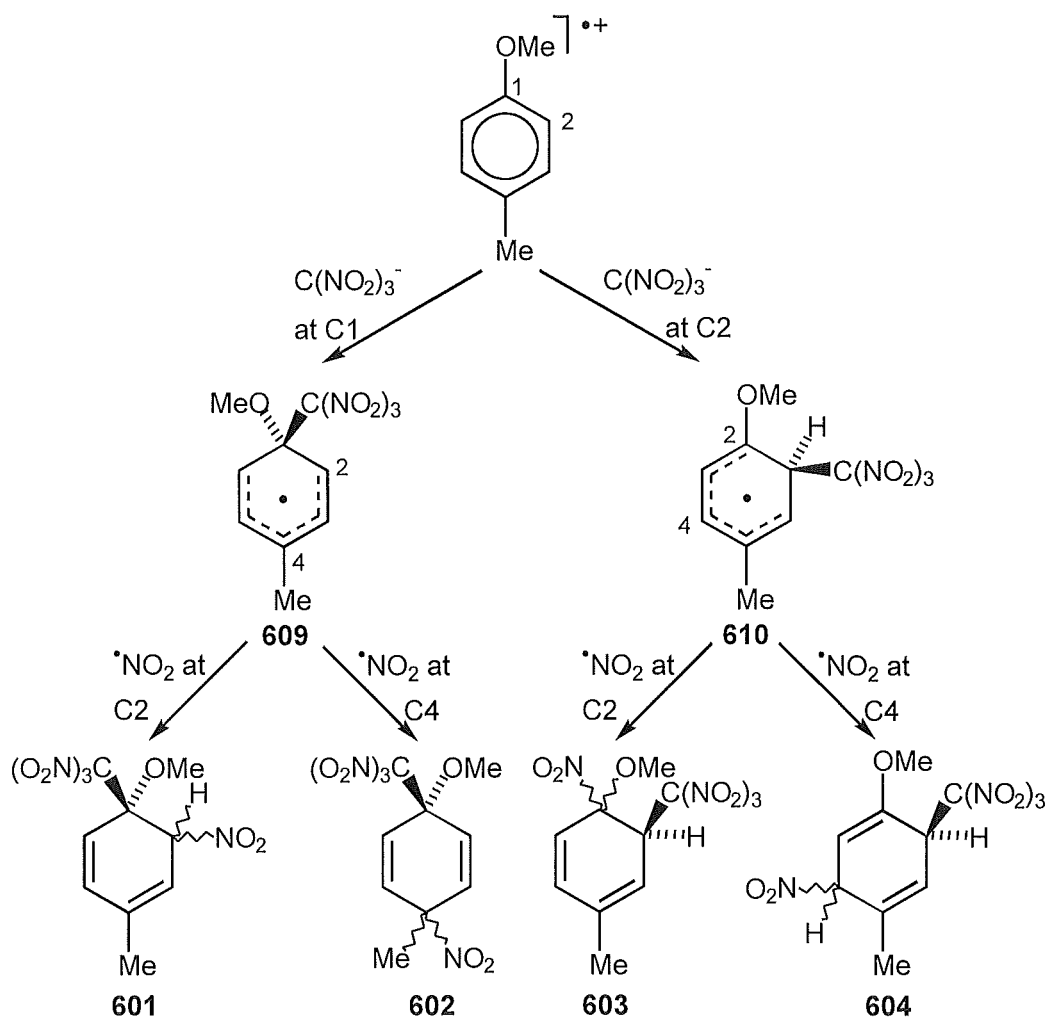
Introduction

In Chapters 4 and 5 it has been demonstrated that the photolysis reactions of methyl substituted anisoles with tetranitromethane proceed *via* intermediate adduct species, e.g. **601-604** from 4-methylanisole.



Adducts **604** were isolated from the reaction mixture and fully characterised by X-ray crystallography or n.m.r. spectroscopy as discussed in Chapter 4. The intermediacy of adducts **601-603** was implied by the observation of their elimination and rearrangement products **605-608**.

The adducts **601-604** are formed by attack of trinitromethanide ion on the 4-methylanisole radical cation at either C1 or C2 (Scheme 6.1, overleaf).

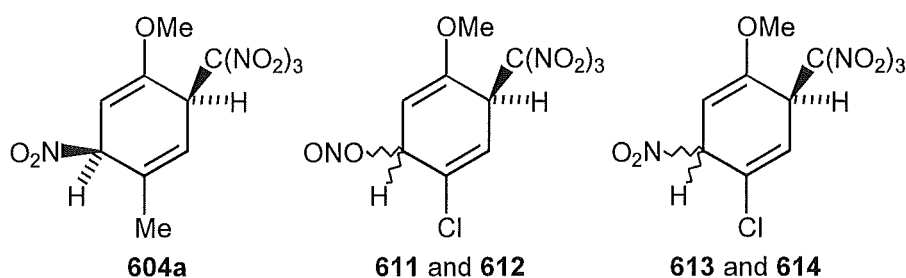


Scheme 6.1

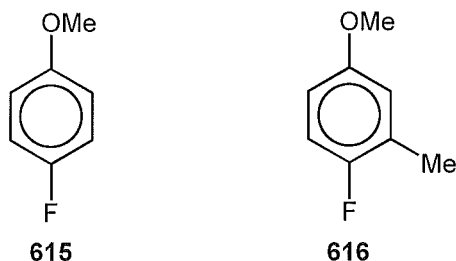
Subsequent nitrogen dioxide coupling at either C2 or C4 of the delocalised carbon radicals **609** and **610** would form adducts **601-604**. The observation of solvent induced changes in product distribution can be rationalised in terms of a change in regiochemistry of trinitromethanide ion attack in Scheme 6.1. More polar solvents such as acetonitrile will lower the reactivity of the trinitromethanide ion in the triad allowing the high positive charge at C1 of the aromatic radical cation to become a more significant driving force for trinitromethanide ion addition. This effect was also observed in the photolysis reactions of tetranitromethane with 4-methylanisole (Chapter 4) and the 2-methyl- and 2,4-dimethyl- anisoles (Chapter 5).

The effect of the methyl substituents appears to be mainly steric in nature, and it was considered of interest to observe the changes induced by halogen functions on the aromatic substrate. Ebersson *et al.* performed a study

of the photolysis reactions of tetranitromethane with 4-chloroanisole¹ and identified a pair of adducts in the reaction mixtures which were assigned as the nitrito species **611** and **612**. These adducts were later reassigned² as the nitro adducts **613** and **614** by comparison with the X-ray structure and the full n.m.r. spectral characterisation of adduct **604a** from 4-methylanisole.



Kochi *et al.* studied the photolysis reactions of 4-fluoroanisole **615** with tetranitromethane.³ Only aromatic products were isolated and identified from the reaction mixtures but some resonances in the olefinic region of the ¹H n.m.r. spectra of reaction mixtures were also observed. The compounds from which these signals originated were not isolated or identified.



It was considered of interest to re-examine more closely the photolysis reactions of 4-fluoroanisole with tetranitromethane using low temperature work-up and careful separation techniques to isolate the unidentified compounds observed by Kochi *et al.* In addition, a study of the photolysis reactions of tetranitromethane with the asymmetric substrate 3-methyl-4-fluoroanisole **616** was performed to help further understand the influences of the halogen substituent. In the event six nitro-trinitromethyl adducts **617-620** and a hydroxy-trinitromethyl adduct **621** were identified from reactions of 4-fluoroanisole **615** and three labile nitro-trinitromethyl adducts were identified in the photolysis mixtures of 4-fluoro-3-methylanisole **616**.

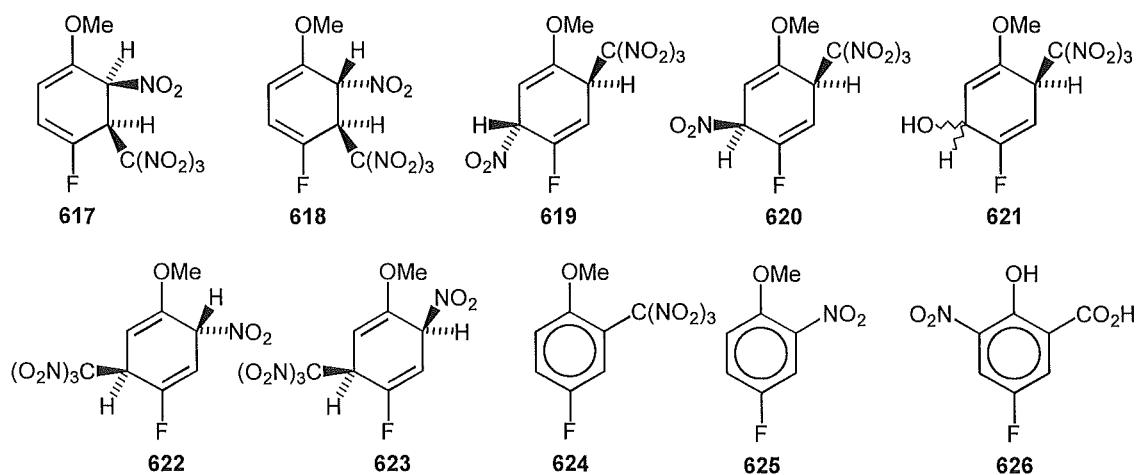
Results

General procedure for the photolysis of 4-fluoroanisole or 4-fluoro-3-methylanisole with tetranitromethane.

The photochemical experiments were performed with filtered light (cut-off < 435 nm, 5 cm water IR-filter, from a 300 W lamp) see the Experimental section for details, and small samples were withdrawn for analysis at suitable intervals. The work-up procedure, involving evaporation of solvent and excess tetranitromethane, was conducted at a temperature $\leq 0^\circ$. The crude product mixtures were stored at -78° and were analysed (^1H n.m.r. spectroscopy, see Experimental section; Tables 8.6.1 - 8.6.4) as soon as possible.

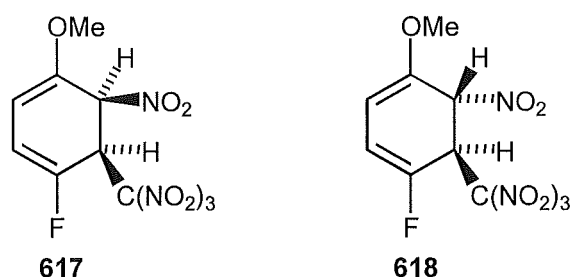
Photolysis of 4-fluoroanisole 615 in dichloromethane at -20° and the identification of adducts 617-621 and aromatic compounds 624, 625 and 626.

A solution of 4-fluoroanisole **615** (0.5 mol l^{-1}) and tetranitromethane (1.0 mol l^{-1}) in dichloromethane was irradiated at -20° . The composition of the mixture was monitored by withdrawing samples for ^1H n.m.r. spectral analysis (Tables 6.3 and 8.6.1). The final solution (after 3 h) after work-up contained the nitro-trinitromethyl adducts **617** (1 %), **618** (trace), **622** (6 %), **619** (19 %), **623** (1 %), and **620** (19 %), hydroxy-trinitromethyl adduct **621** (8 %), unidentified adducts (total 19 %), aromatic compounds **624** (17 %), **625** (2 %), and **626** (1.5 %) and unidentified aromatic compounds (total 6 %).



These products were separated partially by h.p.l.c. on a cyanopropyl column using hexane-dichloromethane mixtures as the eluting solvents. The order of elution of materials from the h.p.l.c. column are given in the Experimental section, but here for simplicity the evidence for structural assignments will be presented for groups of products.

The epimeric 1-fluoro-4-methoxy-5-nitro-6-trinitromethylcyclohexa-1,3-dienes **617** and **618**.



These adducts **617** and **618** were isolated only in low yield and always in admixture with other minor compounds, and their structures were assigned on the basis of their n.m.r. spectra. The connectivity in adduct **617** was established from a consideration of the results of nuclear Overhauser experiments coupled with reverse detected heteronuclear correlation spectra (HMQC).

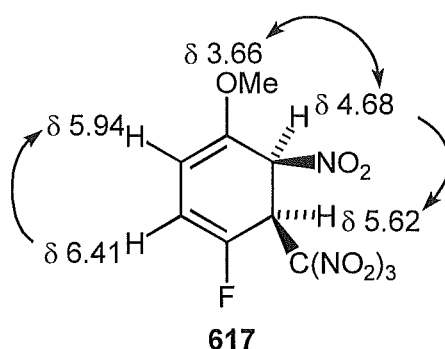


Figure 6.1 - Observed nuclear Overhauser enhancements in the ^1H n.m.r. of adduct **617**

The pattern of nuclear Overhauser enhancements shown does not allow the positive assignment of the H2 and H3 protons (δ 6.41 and δ 5.94). However, for adduct **617** a satisfactory partial ^{13}C n.m.r. spectrum could be obtained and the

carbon resonances at C2 and C3 were assigned by their relative C-F coupling constants ($J_{C2,F} = 22.9$ Hz and $J_{C3,F} = 11.4$ Hz). Subsequent interpretation of the HMQC spectra allowed H2 and H3 to be assigned.

For the epimer **618** only one n.O.e. was observed between the 4-OMe protons (δ 3.72) and the H3 proton (δ 5.17).

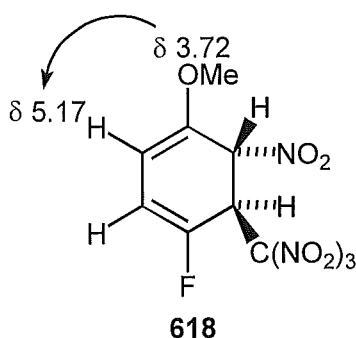


Figure 6.2 - Observed nuclear Overhauser enhancement in the ^1H n.m.r. of adduct **618**.

The ^{13}C n.m.r. resonances of the protonated carbon atoms C3, C5 and C6 were determined indirectly *via* the HMQC heteronuclear correlation spectrum. The identification of the C3 resonance at δ 131.0 is unusual as the carbon shift for a carbon of a double bond with a β -methoxy function is around 90 ppm as discussed in earlier chapters. This allowed the 1,3-cyclohexadiene structure to be assigned by analogy with the similarly high field C3 carbon (δ 132.7) observed in adduct **617**. The regiochemistry at C5 and C6 was assigned by comparison of the observed ^{13}C n.m.r. chemical shifts with the epimeric adduct **617** assigned earlier.

Table 6.1 - Comparison of the carbon shifts of **617** and **618**

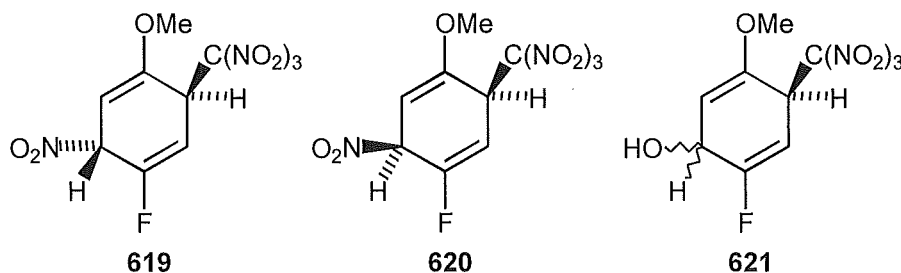
Resonance	617	618
C3	132.7	131.0
C5	84.1	82.5
C6	44.1	41.9

The relative stereochemistry of adducts **617** and **618** were assigned on the basis of the coupling constants, J_{H_5,H_6} . For the *cis*- isomer **617** this coupling constant was 5.4 Hz consistent with a H-C-C-H torsional angle of ca. 50°, while the *trans*- isomer **618** exhibited a small coupling constant (probably 0-1 Hz) corresponding to a torsional angle approaching 80°. These torsional angles are consistent with the results of an inspection of appropriate Dreiding models for the two adducts.

A notable feature of the results of nuclear Overhauser experiments on adducts **617** and **618** was the marked difference in the signal enhancements observed. For the *r*-5-nitro-*c*-trinitromethyl adduct **617** irradiation of the -OMe signal (δ 3.66) resulted in an enhancement (9.3 %) of the signal due to the CH-NO₂ proton (δ 4.68), while similar irradiation of the -OMe signal (δ 3.72) for the *r*-5-nitro-*t*-6-trinitromethyl adduct **618** resulted in an enhancement (10.4 %) of the signal due to the C(OMe)=CH proton (δ 5.17).

On brief storage in (²H)-chloroform the *cis*- isomer **617** was partially converted into a mixture of its epimer **618** and 4-fluoro-2-nitroanisole **625**, the latter arising by loss of nitroform. The isomerisation mechanism is not known, but in principle it could involve a radical C-NO₂ bond cleavage/reformation or a heterolytic C-C(NO₂)₃ bond cleavage/re-formation - if the latter possibility is operative it would point to the elimination of nitroform occurring *via* an E1-mechanism.

The epimeric 1-fluoro-4-methoxy-6-nitro-3-trinitromethylcyclohexa-1,4-dienes **619** and **620**, and the 6-hydroxy-3-trinitromethylcyclohexa-1,4-diene **621**.



The nitro-trinitromethyl adducts **619** and **620** were the major adducts formed in the photolysis reaction in dichloromethane at -20° but proved to be

too labile in solution for their crystallisation or complete purification by h.p.l.c.. The connectivity in each adduct was established from a consideration of the results of nuclear Overhauser experiments coupled with reverse detected heteronuclear correlation spectra (HMQC) and the observed $J_{C,F}$ coupling constants.

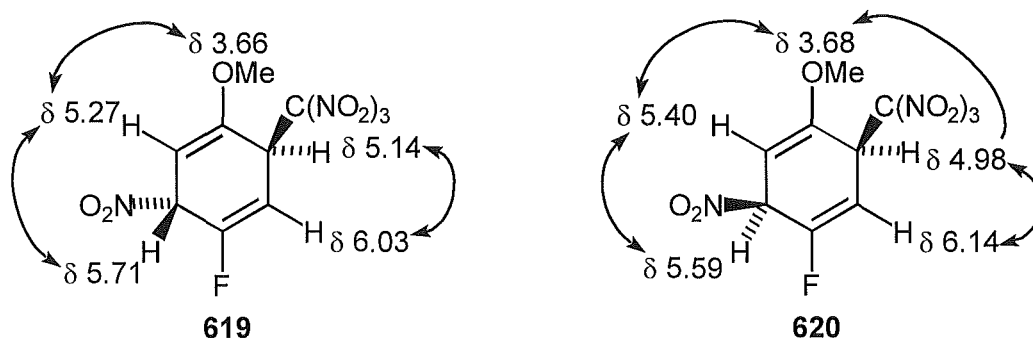


Figure 6.3 - Observed nuclear Overhauser enhancements in the ^1H n.m.r. of adducts **619** and **620**

The assignment of the ^1H resonances at H2 and H3, and subsequently the connectivities at C2 and C3 of **619**, are the only factors which are not entirely clear from the results of the nuclear Overhauser experiments however examination of the C-F coupling constants at these two positions allows unequivocal assignment of the ^{13}C resonances. The signal assigned to C2 (δ 102.5, HC=CF) has a large C-F coupling constant ($J_{C_2,F} = 26.1$ Hz) while the C3 resonance (δ 44.5, HC-C(NO₂)₃) has a much smaller C-F coupling ($J_{C_3,F} = 8.4$ Hz).

It was not possible to define the relative stereochemistry of the two adducts **619** and **620** by spectroscopic means, but this assignment was made on the basis of the known order of elution from a cyanopropyl h.p.l.c. column using hexane-dichloromethane mixtures, *i.e.* that *r*-6-nitro-*t*-3-trinitromethylcyclohexa-1,4-diene **619** is eluted before *r*-6-nitro-*c*-3-trinitromethylcyclohexa-1,4-diene **620**.^{2,4}

The connectivity of the 6-hydroxy-3-trinitromethyl adduct **621** was also established from a consideration of nuclear Overhauser experiments (Figure 6.4, overleaf) and reverse detected heteronuclear correlation spectra (HMQC).

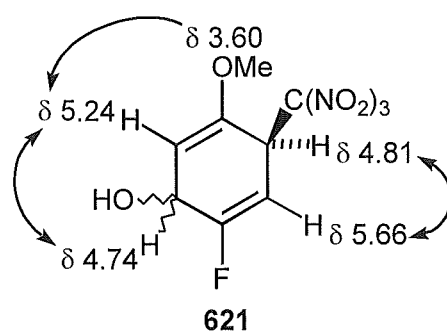


Figure 6.4 - Observed nuclear Overhauser enhancements in the ^1H n.m.r. of adduct **621**.

Again the nuclear Overhauser data alone was insufficient to assign the regiochemistry at C2 and C3 but consideration of the C-F couplings ($J_{\text{C2,F}} = 27.1$ Hz, $J_{\text{C3,F}} = 8.4$ Hz) allowed the positive identification of C2 and C3 and thus, from the heteronuclear correlation spectra (HMQC), the assignment of the ^1H n.m.r. spectra. The critical ^{13}C resonances at δ 44.4 (indicative of the HC-C(NO₂)₃ connectivity) and δ 61.4 (HC-OH) were assigned to the C3 and C6 positions respectively. Adduct **621** also proved to be too labile to allow crystallisation to be effective, and consequently the stereochemistry of this adduct could be neither determined nor otherwise assigned.

*The epimeric 1-fluoro-4-methoxy-3-nitro-6-trinitromethylcyclohexa-1,4-dienes **622** and **623**.*

The epimeric 3-nitro-6-trinitromethyl adducts **622** and **623** were insufficiently stable to allow complete purification and impure adduct **622** could be obtained only in low yield. Consequently the obtainable spectroscopic data for adduct **623** were more complete and the connectivity in that compound was established from the results of nuclear Overhauser experiments (Figure 6.5, overleaf) and reverse detected heteronuclear correlation spectra (HMQC).

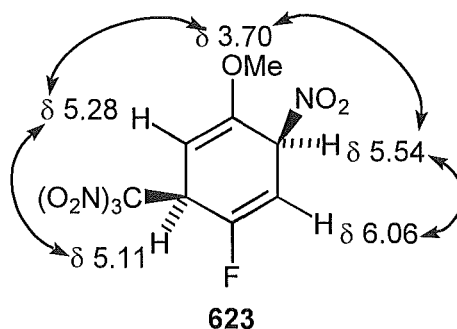


Figure 6.5 - Observed nuclear Overhauser enhancements in the ^1H n.m.r. of adduct **623**

The critical carbon resonances at δ 43.7 [$\text{HC-C}(\text{NO}_2)_3$] and δ 81.3 (HC-NO_2) were assigned to C6 and C3 respectively.

For the epimeric adduct **622** only ^1H n.m.r. spectra and the results of limited nuclear Overhauser experiments could be obtained.

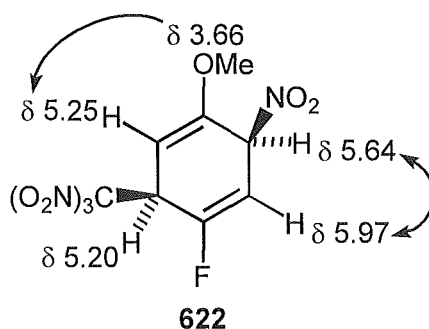


Figure 6.6 - Observed nuclear Overhauser enhancements in the ^1H n.m.r. of adduct **622**

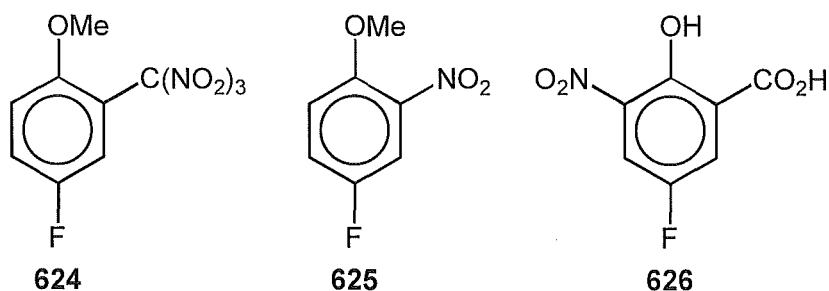
The assignment of the ^1H n.m.r. resonance at δ 5.97 to H2 was made on the basis of the observed H-F coupling constant $J_{\text{H}_2,\text{F}} = 15.6$ Hz which is consistent with the $\text{HC}=\text{CF}$ couplings observed in earlier structures of this type (see Experimental section for details). The data appear sufficient to assign adducts **622** and **623** as epimers. The ^1H n.m.r. chemical shift and coupling data for both is shown in Table 6.2, overleaf.

Table 6.2 - Comparison of the ^1H n.m.r. chemical shift data for adducts **622** and **623**

Resonance	622	623
-OMe	δ 3.66	δ 3.70
H2	δ 5.97 ($J_{\text{H}_2,\text{F}}$ 15.6 Hz)	δ 6.06 ($J_{\text{H}_2,\text{F}}$ 13.7 Hz)
H3	δ 5.64 ($J_{\text{H}_3,\text{F}}$ 8.8 Hz)	δ 5.54 ($J_{\text{H}_3,\text{F}}$ 10.6 Hz)
H5	δ 5.25	δ 5.28 ($J_{\text{H}_5,\text{F}}$ 5.8 Hz)
H6	δ 5.20	δ 5.11

The assignment of stereochemistry to these two adducts **622** and **623** was made, as for the regioisomeric pair of adducts **619** and **620** above, on the basis of the elution order, *i.e.* that *r*-3-nitro-*t*-6-trinitromethylcyclohexa-1,4-diene **622** is eluted before *r*-3-nitro-*c*-6-trinitromethyl-cyclohexa-1,4-diene **623**.^{2,4}

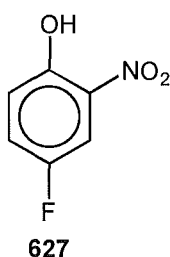
Aromatic compounds **624**, **625** and **626**.



The 2-trinitromethylanisole **624**³ and the 2-nitroanisole **625**⁵ were identified by comparison of their ^1H n.m.r. spectra with literature data. The assignment of structure to 3-fluoro-6-hydroxy-5-nitrobenzoic acid **626**, recovered only in low yield, was based on its mass spectrum ($M^{++} = 201.00735$, $\text{C}_7\text{H}_4\text{NO}_5$) and its ^1H n.m.r. spectrum. The large H-F coupling constants for both aromatic ^1H resonances ($J_{\text{H-F}} = 7.8$ and 7.3 Hz) pointed to a tetra-substituted benzene structure with the unsubstituted ring positions flanking the fluorine substituent.

Photolysis of 4-fluoroanisole 615 in acetonitrile at 20 °C and the identification of nitro phenol 627.

A solution of 4-fluoroanisole **615** (0.5 mol l^{-1}) and tetranitromethane (1.0 mol l^{-1}) in acetonitrile was irradiated at 20° . The composition of the mixture was monitored by withdrawing samples for n.m.r. spectral analysis (Tables 6.4 and 8.6.2). The final solution (after 2 h) after work-up contained 4-fluoro-2-trinitromethylanisole **624** (4 %), 4-fluoro-2-nitroanisole **625** (62 %), 4-fluoro-2-nitrophenol **627** (23 %), and unidentified aromatic compounds (total 10 %).



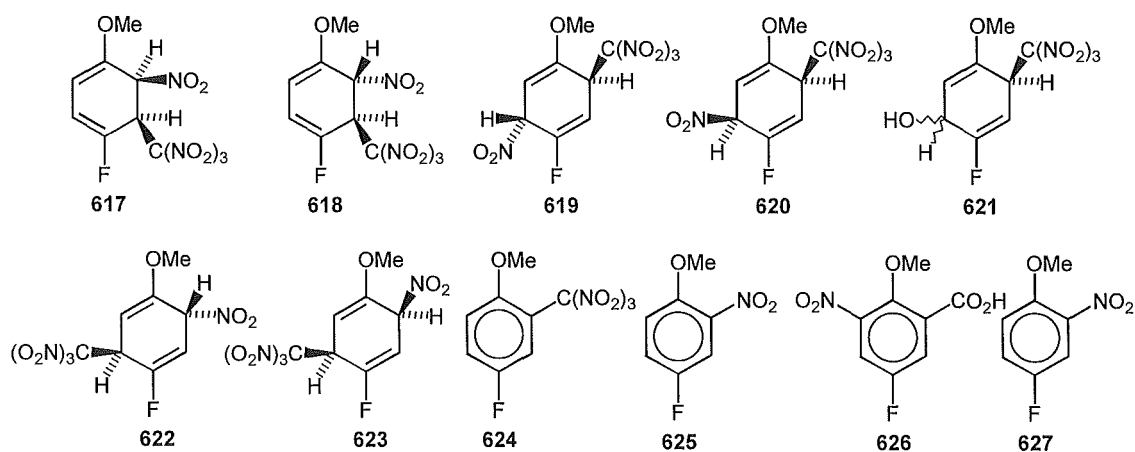
The 4-fluoro-2-nitrophenol **627** was separated by radial chromatography on a silica gel Chromatotron plate and identified by comparison of its ^1H n.m.r. spectrum with literature data.⁶

Photolysis of 4-fluoroanisole 615 in dichloromethane at 20° or -78° .

Photolysis of the charge-transfer complex of 4-fluoroanisole-tetranitromethane in dichloromethane at 20° (3 h) or at -78° (4 h), as above, gave mixtures of products, the composition of which were determined by ^1H n.m.r. spectral analysis and are summarised in Table 6.3 (overleaf).

Table 6.3 - Overview of product yields from the photolysis of 4-fluoroanisole **615** (0.46 mol l^{-1}) with tetranitromethane (0.92 mol l^{-1}) in dichloromethane.

t/h	Yields												
	617	618	619	620	621	622	623	Unknown Adducts	624	625	626	627	Unknown ArX
at 20°													
1	1.3	-	20.0	17.2	10.0	5.9	1.5	11.8	22.6	1.6	3.3	-	4.6
2	1.3	-	17.5	15.8	9.0	4.7	1.3	13.4	26.0	1.8	3.5	-	6.0
3	0.6	-	17.7	15.3	6.8	6.4	2.0	7.7	33.8	2.0	2.9	-	4.8
at -20°													
1	1.4	-	17.4	19.1	9.2	5.8	1.9	16.9	18.6	2.6	1.8	-	5.4
2	1.5	trace	16.6	20.3	8.7	6.0	1.5	19.5	17.0	2.3	1.5	-	4.9
3	1.2	trace	19.0	19.0	7.6	6.1	1.2	19.2	16.5	2.3	1.5	-	6.4
at -78°													
1	4.3	-	17.4	17.9	8.7	2.7	2.9	9.6	25.1	5.8	-	-	5.6
2	4.5	trace	16.7	19.2	8.6	4.2	3.1	7.9	24.7	4.2	1.1	-	5.8
3	5.7	trace	15.9	20.2	6.9	4.2	3.2	7.4	24.8	3.2	1.3	-	7.2

*Photolysis of 4-fluoroanisole **615** in acetonitrile at -20°.*

Photolysis of the charge-transfer complex of 4-fluoroanisole-tetranitromethane in acetonitrile for 2 h at -20°, as above, gave mixtures of products, the

composition of which were determined by ^1H n.m.r. spectral analysis and are summarised in Table 6.4.

Table 6.4 - Overview of product yields from the photolysis of 4-fluoroanisole **615** (0.46 mol l^{-1}) with tetranitromethane (0.92 mol l^{-1}) in acetonitrile.

t/h	Yields												
	617	618	619	620	621	622	623	Unknown Adducts	624	625	626	627	Unknown ArX
at 20°													
1	-	-	-	1.1	-	-	-	3.1	8.1	61.3	-	14.5	11.9
2	-	-	-	-	-	-	-	-	4.3	62.2	-	23.0	10.4
at -20°													
1	-	-	-	4.4	3.1	-	-	12.3	16.2	33.9	-	24.0	6.1
2	-	-	-	3.5	2.2	-	-	8.7	16.8	39.9	-	20.2	9.7

*Photolysis of 4-fluoroanisole **615** in 1,1,1,3,3,3-hexafluoropropan-2-ol (HFP) at 20°.*

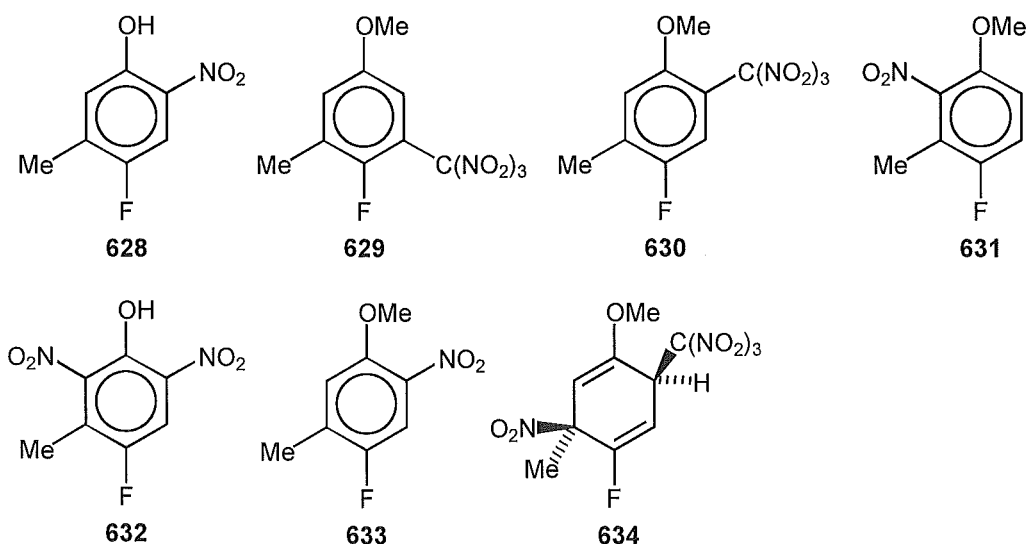
Photolysis of the charge-transfer complex of 4-fluoroanisole-tetranitromethane in HFP for 5 h at 20°, as above, resulted in a 18 % conversion exclusively into 4-fluoro-2-nitroanisole **625**.

*Photolysis of 4-fluoroanisole **615** at 20° in dichloromethane containing trifluoroacetic acid (0.7 mol l^{-1}).*

Photolysis of the charge-transfer complex of 4-fluoroanisole-tetranitromethane in dichloromethane containing trifluoroacetic acid (0.7 mol l^{-1}) for 2 h at 20°, as above, resulted in a 29 % conversion into predominantly 4-fluoro-2-trinitromethylanisole **624** (25 %) and 4-fluoro-2-nitroanisole **625** (48 %), together with lesser amounts of adducts **617** (5 %), **622** (2 %), **619** (2 %), **623** (1 %) and **620** (8 %), aromatic compounds **626** (trace), **627** (2 %), and unidentified aromatic compounds (total 7 %).

Photochemistry of 4-fluoro-3-methylanisole 616 in dichloromethane at 20° and the identification of aromatic compounds 628-633.

Photolysis of the charge-transfer complex of 4-fluoro-3-methylanisole-tetranitromethane in dichloromethane at 20°, as above, for 6 h resulted in a partial conversion (ca. 75 %, See Tables 6.6 and 8.6.3) into a mixture of 4-fluoro-5-methyl-2-nitrophenol **628** (3 %), 4-fluoro-5-methyl-3-trinitromethyl-anisole **629** (1 %), 4-fluoro-5-methyl-2-trinitromethylanisole **630** (64 %), 4-fluoro-3-methyl-2-nitroanisole **631** (5 %), 4-fluoro-3-methyl-2,6-dinitrophenol **632** (6 %), 4-fluoro-5-methyl-2-nitroanisole **633** (12 %), nitro-trinitromethyl adduct **634** (4 %) and unidentified adducts (total 2 %).



The aromatic compounds were separated by radial chromatography on a silica gel Chromatotron plate. Compounds **628**, **629**, **631** and **632** were isolated only in low yield and characterised from their mass spectra and ^1H n.m.r. spectra. The structures of compounds **630** and **633** were determined by single crystal X-ray analysis. A perspective drawing of 4-fluoro-5-methyl-2-trinitromethyl-anisole **630**, $\text{C}_9\text{H}_8\text{FN}_3\text{O}_7$, m.p. 55-59°, is presented in Figure 6.7, overleaf, and the corresponding atomic coordinates are given in Table 8.6.5.

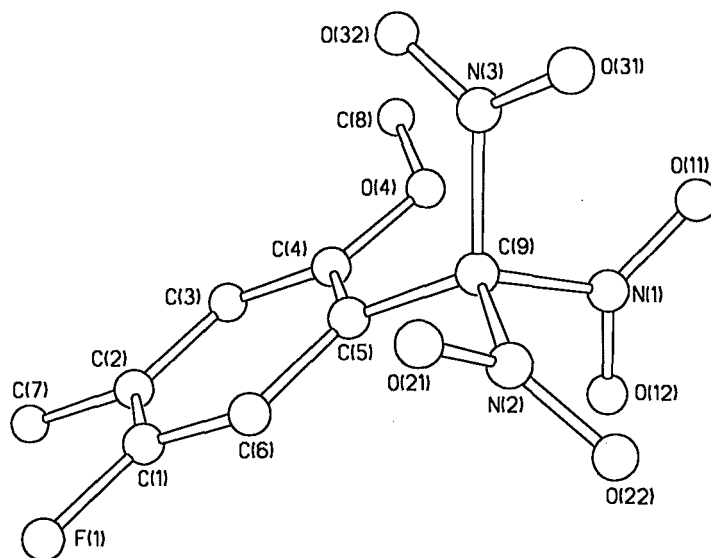


Figure 6.7 - Perspective drawing of 4-fluoro-5-methyl-2-trinitromethylanisole

630

In the solid state the conformations of the methoxy group and trinitromethyl group for trinitromethyl compound **630** are defined by the torsional angles, C(3)-C(4)-O(4)-C(8) $18.8(3)^\circ$ and C(6)-C(5)-C(9)-N(2) $-169.6(2)^\circ$. The conformation of the trinitromethyl group is presumably largely determined by steric interactions with the adjacent methoxy group. The spectroscopic data were in accord with the established structure.

A perspective drawing of 4-fluoro-5-methyl-2-nitroanisole **633**, $C_8H_8FNO_3$, m.p. $84-85^\circ$, is presented in Figure 6.8 (for molecule 1), overleaf, and the corresponding atomic coordinates in Table 8.6.6.

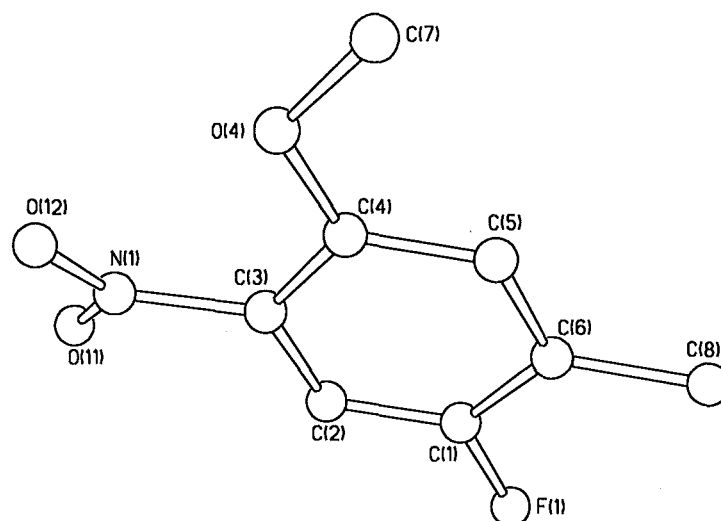
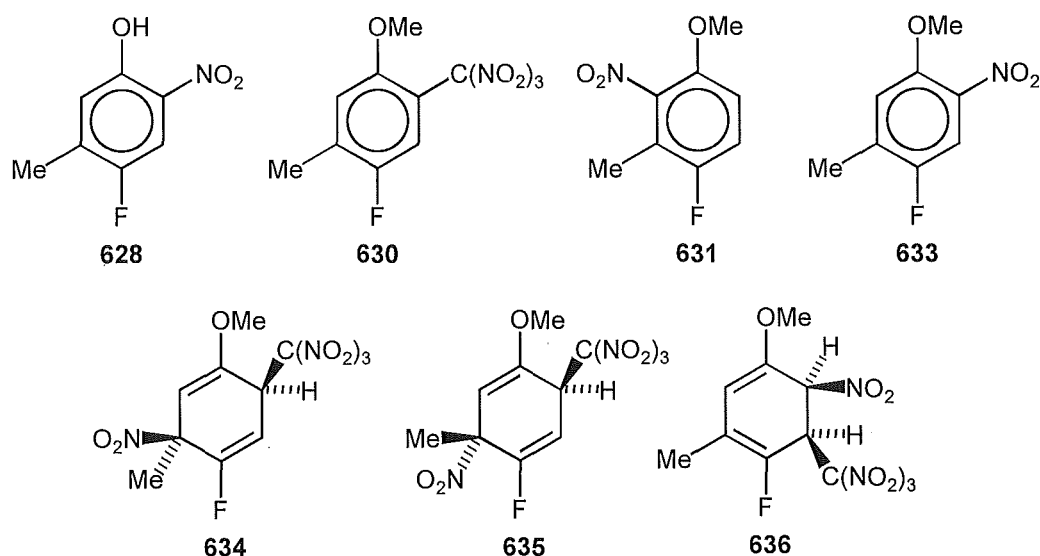


Figure 6.8 - Perspective drawing of 4-fluoro-5-methyl-2-nitroanisole **633**

For 4-fluoro-5-methyl-2-nitroanisole **633** the structure consists of two crystallographically independent molecules. The differences between the two molecules lie in the conformations of the nitro and methoxy functions [molecule 1: C(4)-C(3)-N(1)-O(12) $-21.8(6)^\circ$, C(5)-C(4)-O(4)-C(7) $-2.1(6)^\circ$; corresponding data for molecule 2: $-38.6(6)^\circ$ and $2.5(6)^\circ$]. These differences are not chemically significant. The spectroscopic data for compound **633** were in accord with the established structure.

*Photochemistry of 4-fluoro-3-methylanisole **616** in dichloromethane at -20° and the identification of nitro-trinitromethyl adducts **634** and **635**.*

Photolysis of the charge-transfer complex of 4-fluoro-3-methylanisole and tetranitromethane in dichloromethane at -20° , as above, for 6 h resulted in a partial conversion (ca. 73 %, See Tables 6.6 and 8.6.3) into a mixture of 4-fluoro-5-methyl-2-nitrophenol **628** (2 %), 4-fluoro-5-methyl-2-trinitromethyl-anisole **630** (62 %), 4-fluoro-3-methyl-2-nitroanisole **631** (3 %), 4-fluoro-5-methyl-2-nitroanisole **633** (7 %), and nitro-trinitromethyl adducts **634** (15 %), **635** (5 %) and **636** (2 %).



None of the adducts could be isolated by h.p.l.c. on a cyanopropyl column even at -20° and consequently the nitro-trinitromethyl adducts **634-636** were identified by spectroscopic studies on mixtures of products. The spectroscopic data for the major nitro-trinitromethyl adduct, 1-fluoro-4-methoxy-6-methyl-*c*-6-nitro-*r*-3-trinitromethylcyclohexa-1,4-diene **634**, are more complete. The connectivity of adduct **634** was established by consideration of the results of nuclear Overhauser experiments (Figure 6.9) and reverse detected ^1H - ^{13}C heteronuclear correlation spectroscopy (HMQC/HMBC).

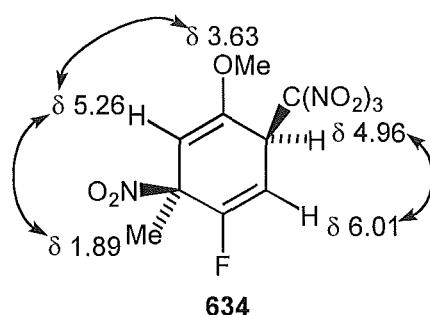


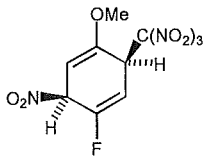
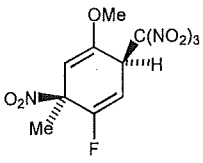
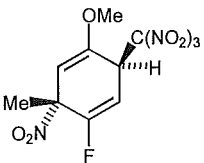
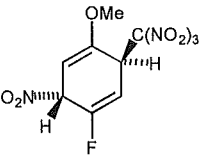
Figure 6.9 - Observed nuclear Overhauser enhancements in the ^1H n.m.r. spectra of adduct **634**

The assignment of the H2 and H3 n.m.r. resonances (δ 6.01 and δ 4.96) is not possible from the n.o.e. data alone. However, the observed coupling constant $J_{\text{H},\text{F}} = 13.6$ Hz for the ^1H resonance at δ 6.01 unequivocally assigns this

resonance to H2. The critical ^{13}C resonances at δ 44.7 [$\text{HC-C}(\text{NO}_2)_3$] and δ 85.0 (Me-C-NO_2) were assigned to C3 and C6 respectively.

The connectivity in the epimeric nitro-trinitromethyl adduct **635**, and the stereochemistry of the pair of adducts **634** and **635**, were established by comparison of the ^1H n.m.r. spectra for the epimeric nitro-trinitromethyl adducts **619** and **620** and the data for adducts **634** and **635** (Table 6.5).

Table 6.5 - Comparison of the ^1H n.m.r. chemical shift for **619-620** and **634-635**

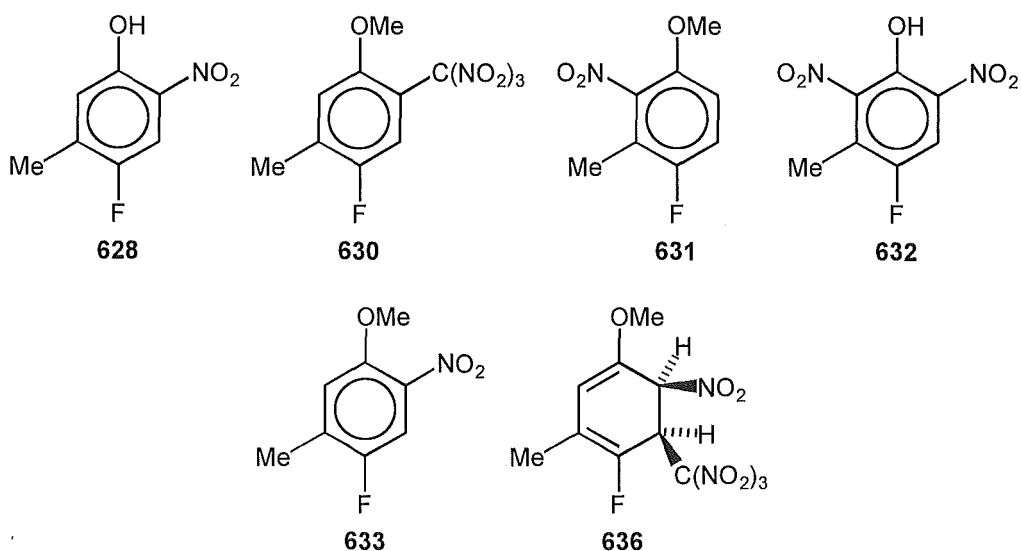
Resonance				
H2	δ 6.14	δ 6.09	δ 5.92	δ 6.03
H3	δ 4.98	δ 4.96	δ 5.10	δ 5.14
H5	δ 5.40	δ 5.26	δ 5.15	δ 5.27

In such structures, the steric requirements of the trinitromethyl group will be dominant,⁷ and it is therefore a reasonable expectation that the introduction of the methyl substituent in adducts **634** and **635** will have only a limited effect on the conformations of these molecules. This underlying assumption is apparently validated by the systematic ^1H n.m.r. chemical shift differences between the methylated and non-methylated pairs of compounds. In particular, for the *c*-6-nitro-*r*-3-trinitromethyl adducts **620** and **634** the signal due to H2 appears downfield ($\Delta\delta$ 0.11-0.17), the signal due to H3 appears upfield ($\Delta\delta$ 0.14-0.16), and the signal due to H5 appears downfield ($\Delta\delta$ 0.11-0.13) of the corresponding signals for the *t*-6-nitro-*r*-3-trinitromethyl adducts **619** and **635**. If the stereochemical assignments of the non-methylated adducts **619** and **620** (above) are accepted, it appears that the stereochemical assignments of the epimeric 6-methyl derivatives **634** and **635** follow.

Photochemistry of 4-fluoro-3-methylanisole 616 in acetonitrile at -20° and the identification of nitro-trinitromethyl adduct 636.

Photolysis of the charge-transfer complex of 4-fluoro-3-methylanisole

and tetranitromethane in acetonitrile at -20° , as above, for 6 h resulted in a partial conversion (ca. 72 %, See Tables 6.7 and 8.6.4) into a mixture of 4-fluoro-5-methyl-2-nitrophenol **628** (13 %), 4-fluoro-5-methyl-2-trinitromethyl-anisole **630** (17 %), 4-fluoro-3-methyl-2-nitroanisole **631** (14 %), 4-fluoro-3-methyl-2,6-dinitrophenol **632** (3 %), 4-fluoro-5-methyl-2-nitroanisole **633** (32 %), unidentified aromatic compounds (total 9 %), nitro-trinitromethyl adduct **636** (9 %), and unidentified adducts (total 2 %).



The connectivity in the nitro-trinitromethyl adduct **636** was established by a consideration of the results of nuclear Overhauser experiments (Figure 6.10) and reverse detected heteronuclear correlation spectra (HMQC), the latter of which allowed the identification of the ^{13}C n.m.r. resonances to the protonated-carbons, C3, C5 and C6.

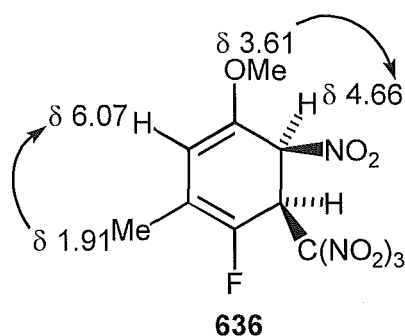


Figure 6.10 - Observed nuclear Overhauser enhancements in the ^1H n.m.r. spectra of adduct **636**.

The critical carbon resonances, δ 44.4 [HC-C(NO₂)₃] and δ 83.4 (HC-NO₂) were assigned to C6 and C5 respectively. The *r*-5-nitro-*c*-6-trinitromethyl stereochemistry was assigned to adduct **636** on the basis of the result of the nuclear Overhauser experiment involving the irradiation of the methoxy ¹H n.m.r. signal. For adduct **636** irradiation at δ 3.61 (OMe signal) resulted in an enhancement (12.0 %) of the signal due to H5 (δ 4.66), as for the non-methylated *r*-5-nitro-*c*-6-trinitromethyl adduct **617** earlier.

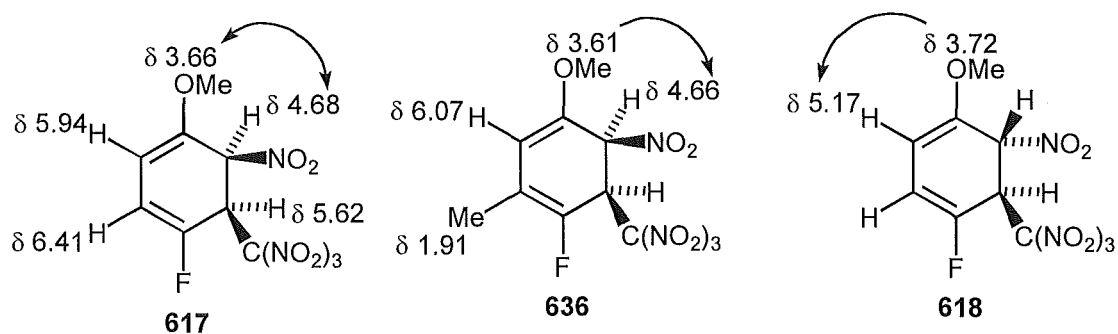


Figure 6.11 - Comparison of nuclear Overhauser experiment results for **617**, **618**, and **636**.

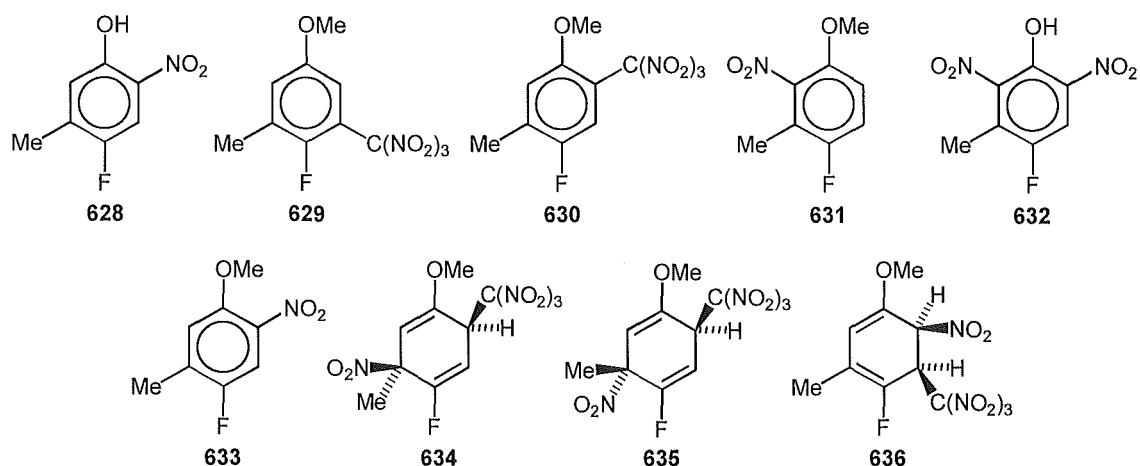
In contrast, the non-methylated *r*-5-nitro-*t*-6-trinitromethyl adduct **618** gave an enhancement of the signal due to H3 [δ 5.17 (10.4 %)] on irradiation at the frequency of the OMe signal (δ 3.72).

Photochemistry of 4-fluoro-3-methylanisole 616 in dichloromethane at -78°.

Photolysis of the charge-transfer complex of 4-fluoro-3-methylanisole-tetranitromethane in dichloromethane for 6 h at -78°, as above, gave mixtures of products, the composition of which were determined by ¹H n.m.r. spectral analysis and are summarised in Table 6.6 (overleaf).

Table 6.6 - Overview of product yields from the photolysis of 4-fluoro-3-methylanisole **616** (0.45 mol l^{-1}) with tetranitromethane (0.90 mol l^{-1}) in dichloromethane.

t/h	Yield (%)										
	Known							Unknown			
	628	629	630	631	632	633	Ar X	634	635	636	Adducts
20°											
2	2.5	-	61.8	-	0.3	7.6	5.0	13.9	1.3	2.0	5.6
4	2.8	0.5	64.9	3.4	3.4	11.3	2.0	9.1	-	0.2	2.3
6	2.6	1.4	64.0	5.2	5.9	12.3	2.0	4.2	-	-	2.5
-20°											
2	0.1	-	45.3	0.1	0.1	5.4	5.1	18.2	11.8	6.8	7.3
4	0.8	-	53.8	1.0	0.1	5.4	5.4	18.6	8.6	6.2	-
6	1.6	-	61.5	3.0	0.1	6.9	5.2	15.0	1.6	4.8	-
-78°											
2	6.7	-	36.8	5.9	1.9	22.6	2.4	6.1	3.5	11.7	2.4
4	6.5	-	24.3	10.0	1.9	35.3	0.8	4.2	1.2	14.9	0.8
6	6.1	-	23.1	9.8	3.1	39.3	-	3.3	-	12.9	2.3



*Photochemistry of 4-fluoro-3-methylanisole **616** in acetonitrile at 20° or -50°.*

Photolysis of the charge-transfer complex of 4-fluoro-3-methylanisole-tetranitromethane in acetonitrile for 6 h at 20 or at -50 °C, as above, gave

mixtures of products, the composition of which were determined by ^1H n.m.r. spectral analysis and are summarised in Table 6.7.

Table 6.7 - Overview of product yields from the photolysis of 4-fluoro-3-methylanisole **616** (0.45 mol l^{-1}) with tetranitromethane (0.90 mol l^{-1}) in acetonitrile.

t/h	Yield (%)										
	628	629	630	631	632	633	Unknown Ar X	634	635	636	Unknown Adducts
20°											
4	9.5	4.0	7.3	19.1	10.9	45.5	-	-	-	3.6	0.2
6	8.3	4.8	6.8	19.7	13.3	44.2	-	-	-	2.0	0.8
-20°											
4	11.6	-	18.4	15.2	5.1	32.4	9.5	-	-	6.2	1.7
6	12.7	-	17.0	13.9	3.0	32.0	9.5	-	-	9.1	1.7
-78°											
4	6.0	0.1	13.3	14.0	3.2	37.6	2.2	-	-	23.7	-
6	7.7	0.1	11.2	13.5	2.9	36.7	1.9	-	-	26.1	-

*Photochemistry of 4-fluoro-3-methylanisole **616** in 1,1,1,3,3,3-hexafluoropropan-2-ol (HFP) at 20°.*

Photolysis of the charge-transfer complex of 4-fluoro-3-methylanisole-tetranitromethane in HFP for 4 h at 20°, as above, resulted in a low conversion (ca. 18 %) exclusively into 4-fluoro-3-methyl-2-nitroanisole **631** (26 %) and 4-fluoro-5-methyl-2-nitroanisole **633** (74 %).

*Photochemistry of 4-fluoro-3-methylanisole **616** at 20° in dichloromethane containing trifluoroacetic acid (0.7 mol l^{-1}).*

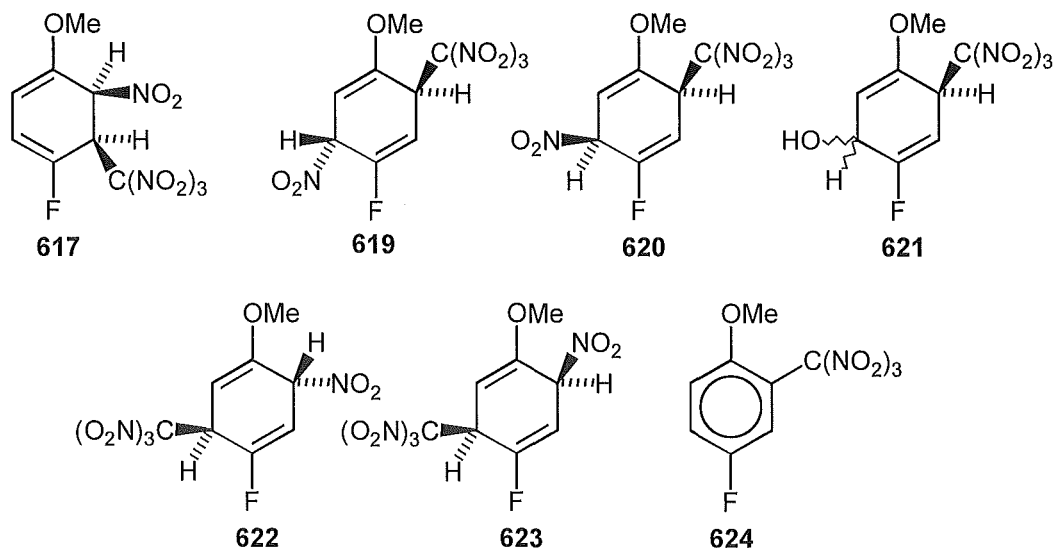
Photolysis of the charge-transfer complex of 4-fluoro-3-methylanisole-tetranitromethane in dichloromethane containing trifluoroacetic acid (0.7 mol l^{-1}) for 4 h at 20°, as above, resulted in a 47 % conversion into predominantly 4-

fluoro-3-methyl-2-nitroanisole **631** (18 %) and 4-fluoro-5-methyl-2-nitroanisole **633** (60 %), together with lesser amounts of aromatic compounds **628** (9 %), **630** (6 %), **632** (3 %), and unidentified aromatic compounds (total 3 %).

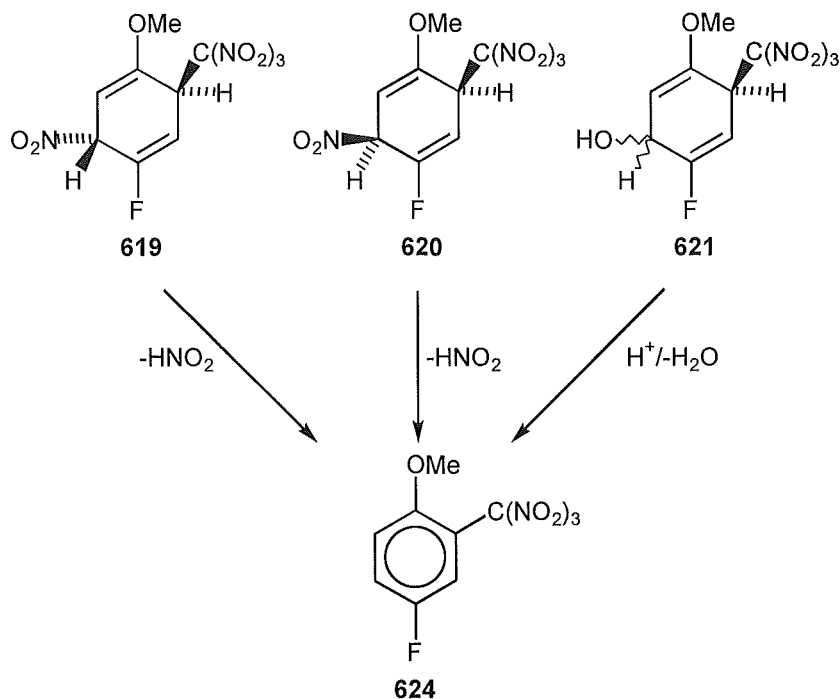
Discussion

Overview of the photolysis products from 4-fluoroanisole 615 in dichloromethane at 20°, -20° and -78°.

In dichloromethane at 20° six adducts, **617** and **619-623** were identified as products in addition to significant quantities of 4-fluoro-2-trinitromethylanisole **624** (Table 6.6).

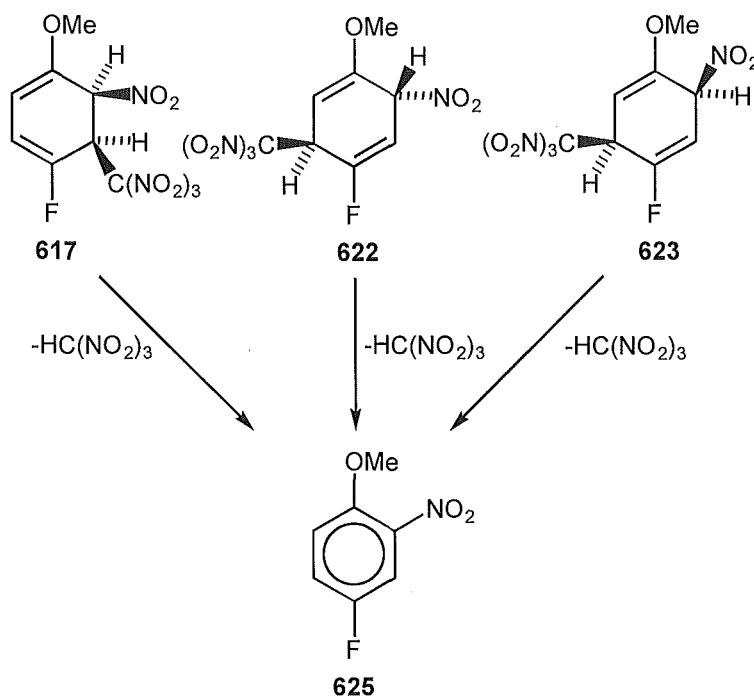


Of the six adducts **617** and **619-623**, three adducts **619**, **620** and **621** contain a 2-trinitromethyl structural feature and their decomposition would be expected to augment the yield of 4-fluoro-2-trinitromethylanisole **624** (Scheme 6.2, overleaf).



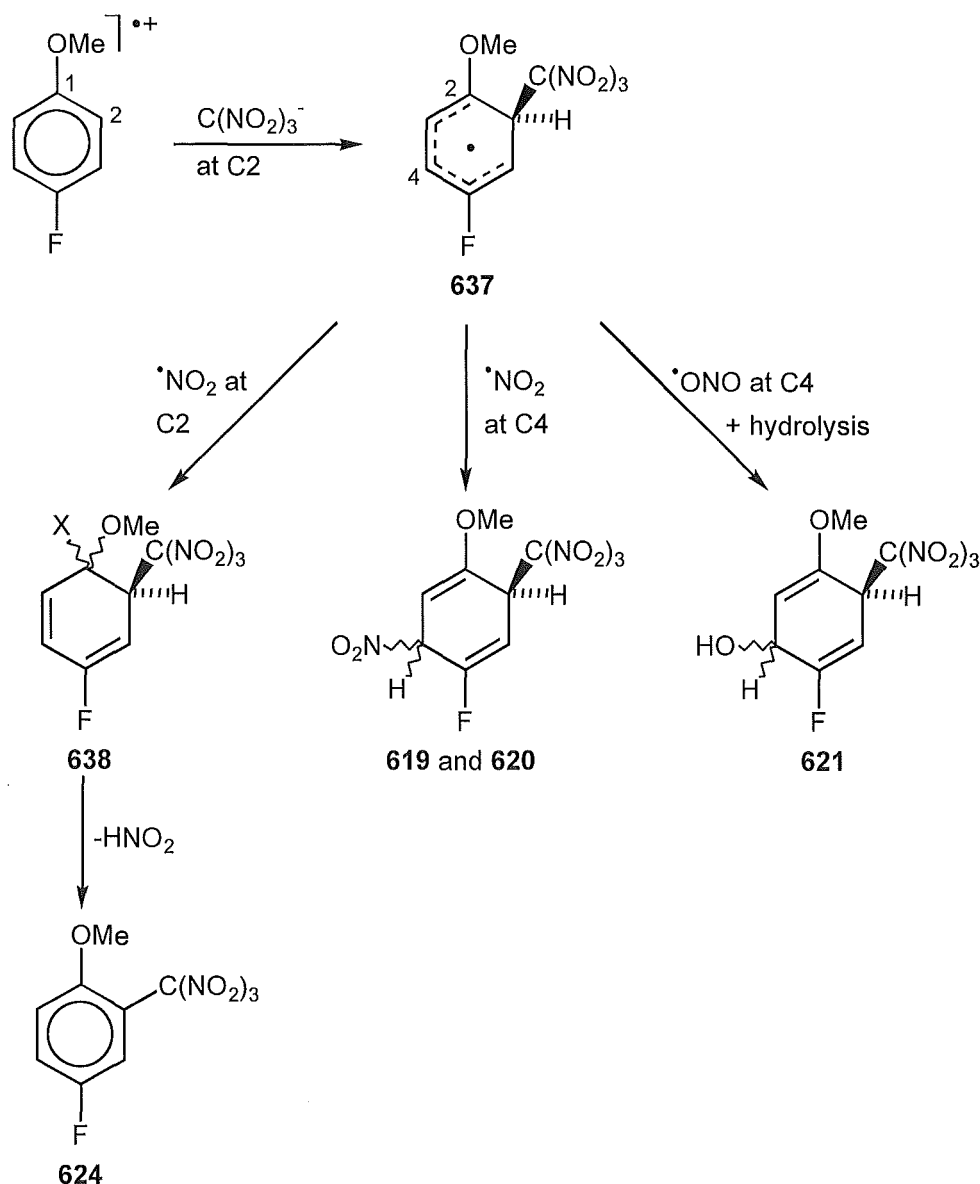
Scheme 6.2

In this study the total yields of adducts **619**, **620** and **621**, together with the amount of the 2-trinitromethyl compound **624** isolated, would account for the yield (73 %) of compound **624** reported earlier by Kochi *et al.*³ In addition, the loss of nitroform by decomposition from the three 3-trinitromethyl adducts **617**, **622** and **623** would augment the yield of 4-fluoro-2-nitroanisole **625**, thus accounting for the yield of that compound reported earlier (Scheme 6.3).



Scheme 6.3

The mode of formation of the observed products appears to be analogous to that discussed earlier in this thesis for anisole derivatives. Attack of trinitromethanide ion at C2 of the 4-fluoroanisole radical cation would give the delocalised carbon radical **637**, the stability of which would be enhanced by the position of the methoxy group (Scheme 6.4).

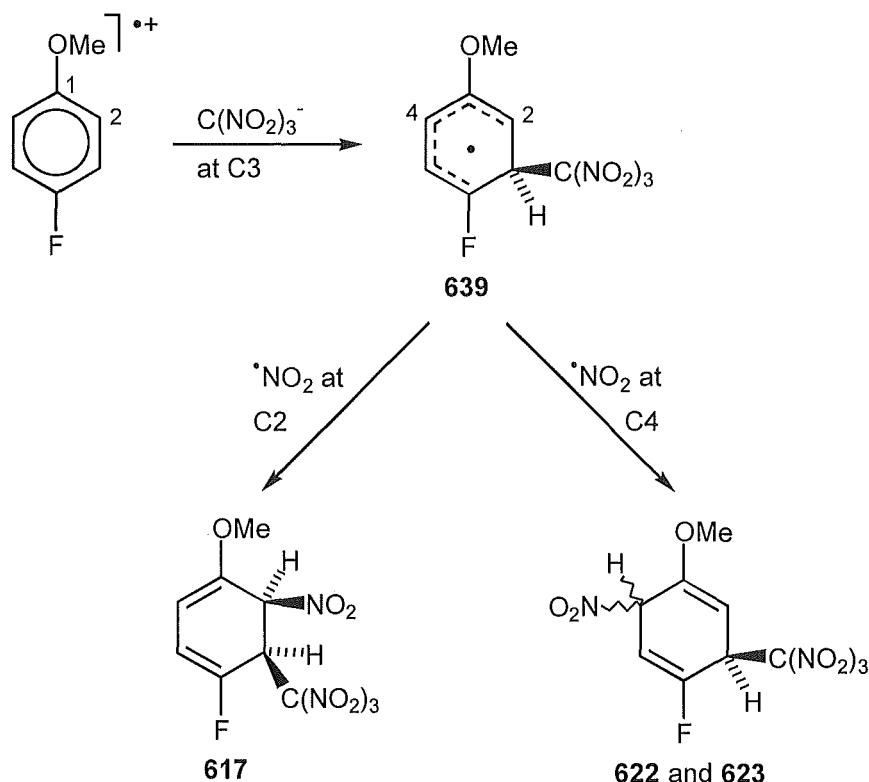


Scheme 6.4

Attack of nitrogen dioxide at C4 of this delocalised carbon radical species with C-N bond formation would yield adducts **619** and **620**; the alternative C-O mode of bond formation by nitrogen dioxide followed by hydrolysis, either on work-up or in the prevailing reaction conditions, would give the hydroxy-trinitromethyl adduct **621**. Although the possibility of the formation of some 4-fluoro-2-

trinitromethylanisole **624** by decomposition of adducts **619**, **620** and **621** can not be excluded, it appears likely that much of the 4-fluoro-2-trinitromethylanisole **624** isolated in the present study from reactions in dichloromethane arises by decomposition during the photolysis reaction of the sterically compressed diene **638** (where X = NO₂ or ONO). This diene **638** would be formed by attack of nitrogen dioxide on the delocalised carbon radical at C6 *ipso* to the methoxy group (Scheme 6.4).

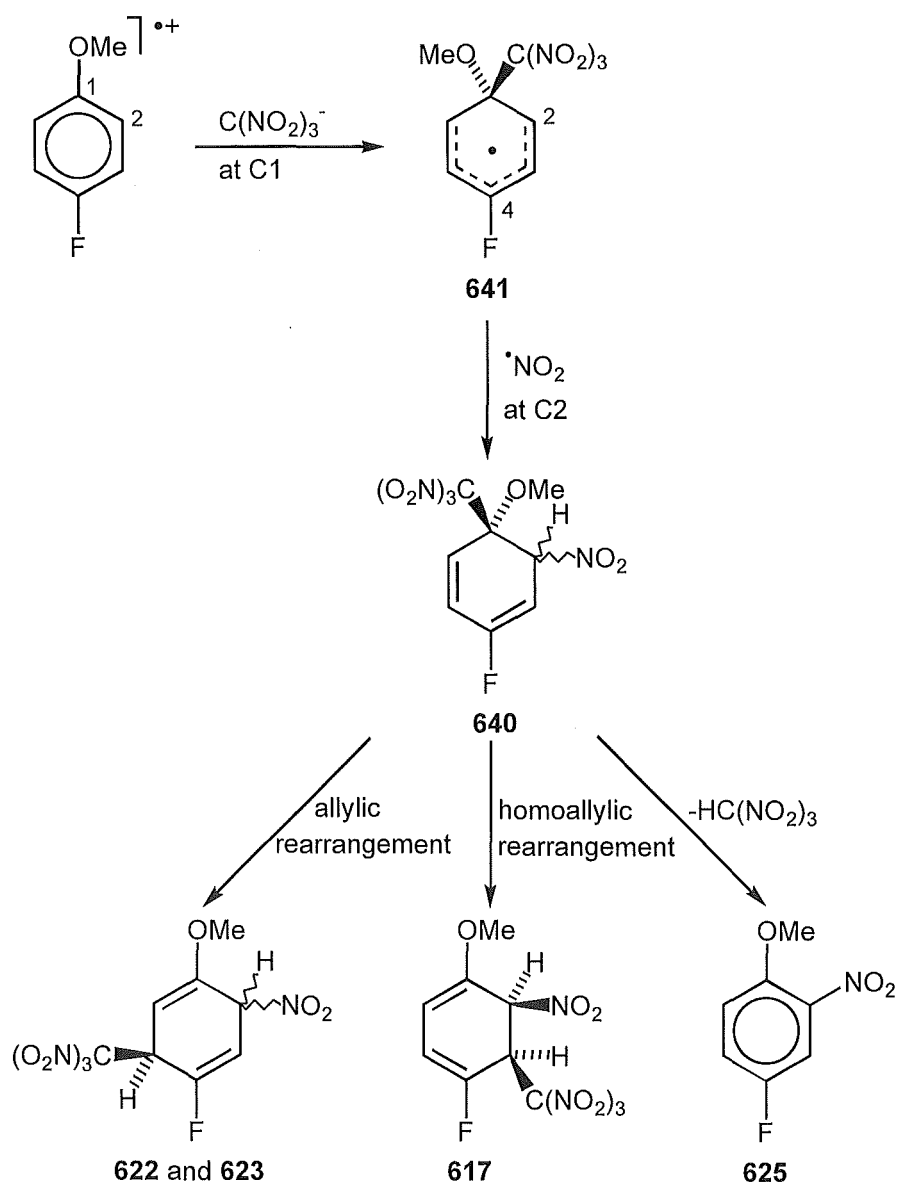
The modes of formation of the trinitromethyl adducts **617**, **622** and **623** are less certain. It is possible that these adducts are formed *via* initial attack of trinitromethanide ion at C3 in the 4-fluoroanisole radical cation to give the delocalised carbon radical **639** (Scheme 6.5).



Scheme 6.5

Subsequent radical coupling of nitrogen dioxide with this delocalised carbon radical at C2 would give the epimeric adducts **622** and **623**, while coupling at C6 would give adduct **617**. However, allylic rearrangement of the trinitromethyl group in the sterically compressed adduct **640** (Scheme 6.6, overleaf) would

also yield the 6-nitro-3-trinitromethyl adducts **622** and **623**, while an apparent homoallylic rearrangement would give adduct **617**.

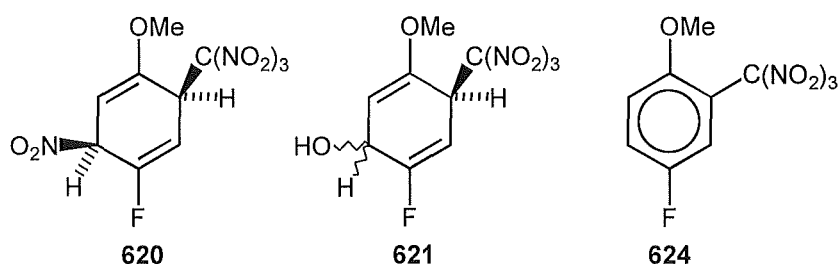


Scheme 6.6

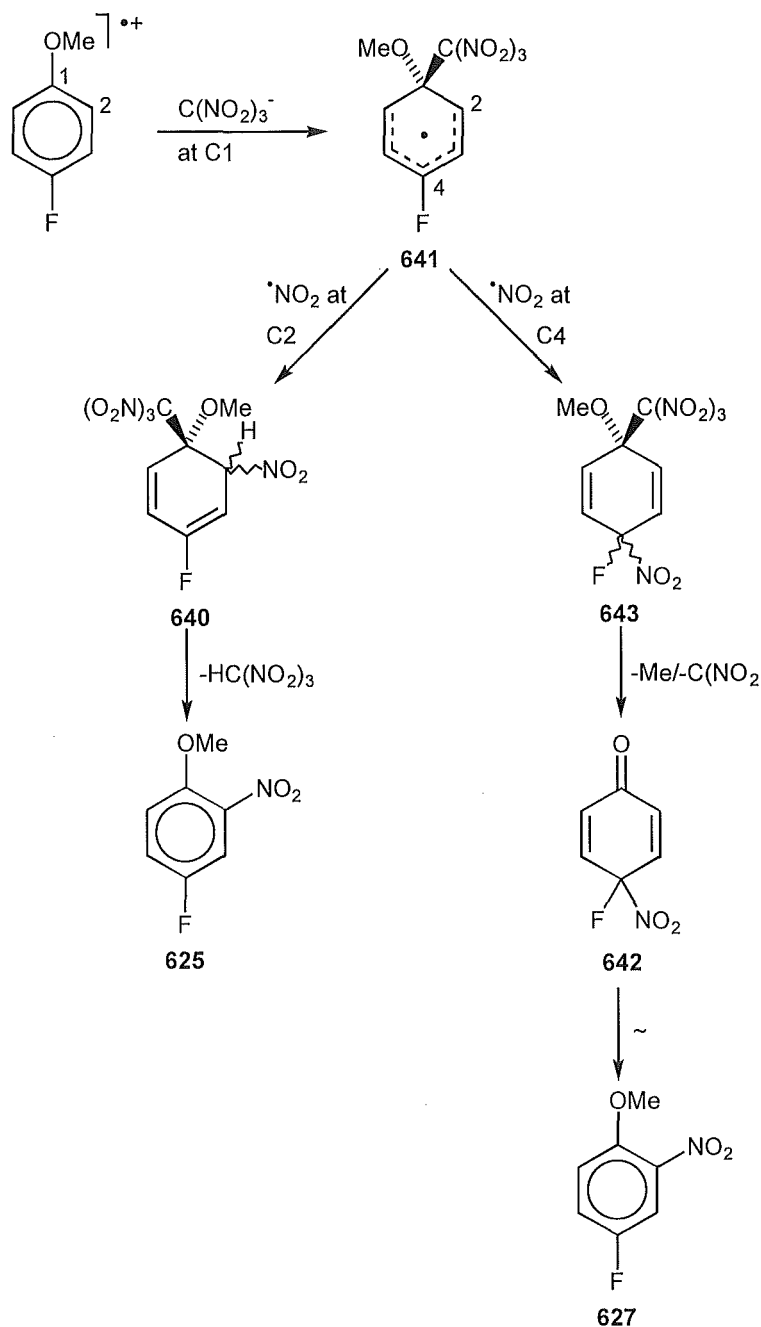
This same adduct **640** could give rise to the nitro aromatic compound **625** by loss of nitroform. The labile adduct **640** would be formed by initial attack of trinitromethanide ion *ipso* to the methoxy group in the 4-fluoroanisole radical cation, followed by radical coupling with nitrogen dioxide at C2 in the delocalised carbon radical **641** (Scheme 6.6).

Overview of the photolysis products from 4-fluoroanisole **615** in acetonitrile at 20° and -20°.

The trinitromethyl derivatives isolated from photolysis reactions of 4-fluoroanisole **615** in acetonitrile were limited to the trinitromethyl adducts **620** and **621**, and 4-fluoro-2-trinitromethylanisole **624**. The formation of these three compounds implies that trinitromethanide ion is still capable, in acetonitrile particularly at lower reaction temperatures, of attacking the radical cation of 4-fluoroanisole at C2 (see Scheme 6.4).



As discussed earlier in the analogous photolysis reactions of 4-methylanisole with tetranitromethane, the yields of the 2-nitro derivative **625** were considerably higher in acetonitrile than in the corresponding reactions in dichloromethane. Furthermore, the isolation of 4-fluoro-2-nitrophenol **627** supports the detection of 4-fluoro-4-nitrocyclohexa-2,5-dienone **642** in product mixtures. Although the reaction data are less compelling for the reactions in acetonitrile of 4-fluoroanisole **615**, compared with those of 4-methylanisole, it seems reasonable that the nitro dienone **642** (and thence the 4-fluoro-2-nitrophenol **627** by homolytic rearrangement⁸) and much of the 4-fluoro-2-nitroanisole **625** are formed *via* the delocalised carbon radical **641** (Scheme 6.7, overleaf).

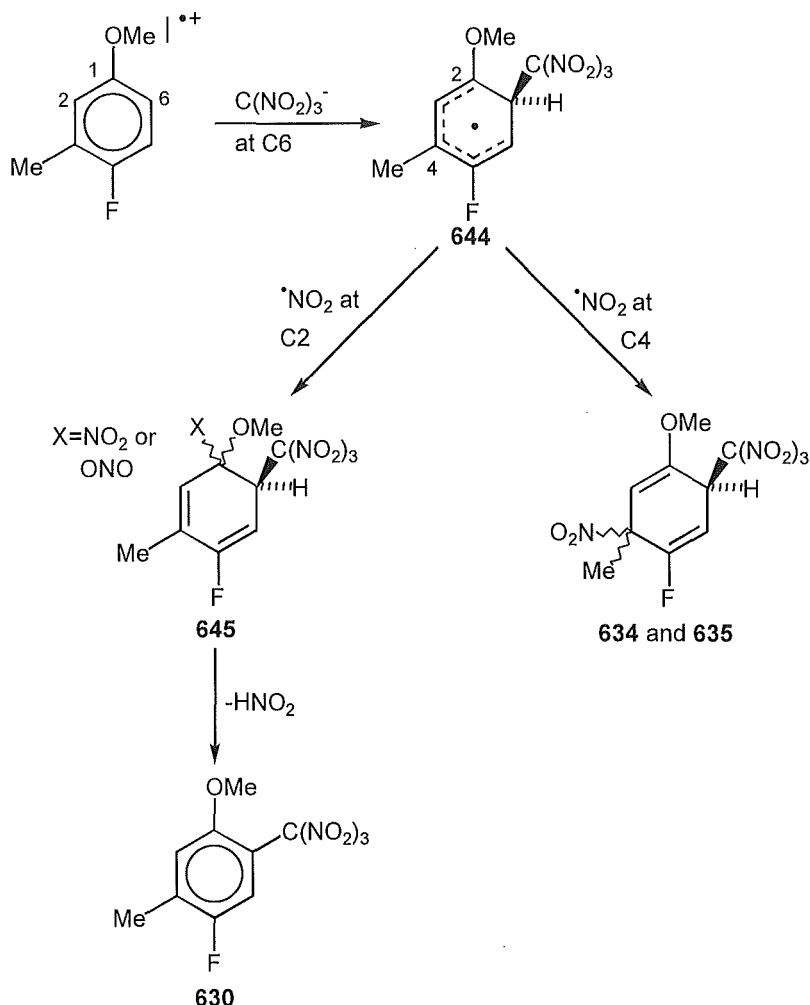


Scheme 6.7

Radical coupling of nitrogen dioxide at C4 of the delocalised carbon radical **641** would give the diene **643**, which on the loss of the elements of $\text{Me}-\text{C}(\text{NO}_2)_2$ would yield the nitro dienone **642**. Analogous radical coupling at C2 of the delocalised carbon radical **641** with nitrogen dioxide, followed by loss of nitroform from the labile adduct **640** in the polar acetonitrile solvent, would yield 4-fluoro-2-nitroanisole **625** as discussed earlier. However, the potential intermediacy of nitro-trinitromethyl adducts **617**, **622** and **623** in the transformation **640** \rightarrow **625** can not be excluded.

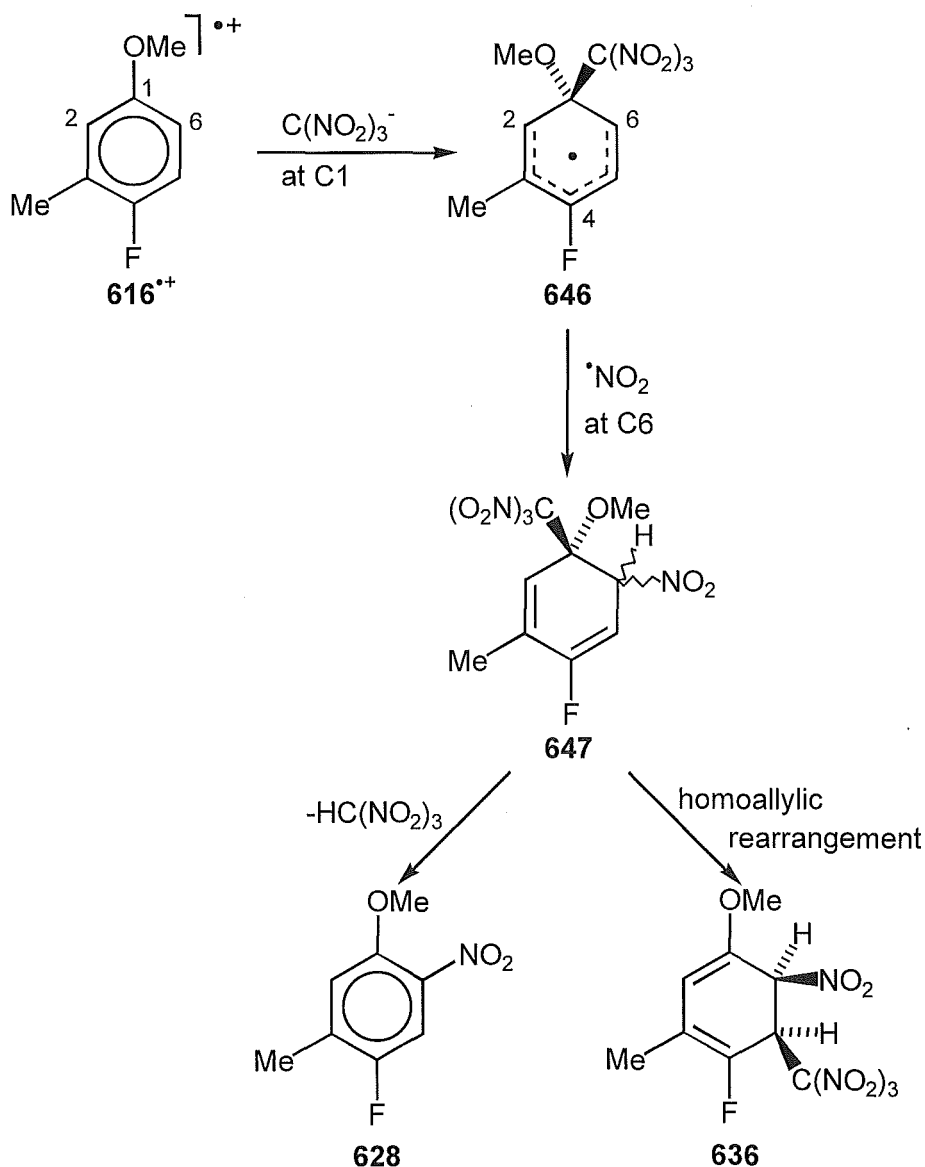
Overview of the photolysis products from 4-fluoro-3-methylanisole **616** in dichloromethane and acetonitrile.

Detailed comment on the photolysis products from these reactions is difficult because of the inherent lability of the nitro-trinitromethyl adducts **634-636**. However, some broad trends are evident in the product yield data which follow the pattern discussed earlier for 4-methylanisole and for 4-fluoroanisole **615**, above. At ambient temperatures in dichloromethane the photolysis of the charge transfer complex of 4-fluoro-3-methylanisole **616** involves the attack of trinitromethanide ion on the radical cation vicinal to the methoxy group at the less-hindered ring position *para* to the methyl substituent to give the delocalised radical species **644**. Nitrogen dioxide coupling at C2 and subsequent elimination of nitrous acid leads to 4-fluoro-5-methyl-2-trinitromethylanisole **630**. Analogous coupling at C4 gives the epimeric 2-trinitromethyl-5-nitro- adducts **634** and **635** (Scheme 6.8).



Scheme 6.8

At lower temperatures in dichloromethane and acetonitrile the yields of 2-nitro aromatic compound **628** and the 5-nitro-6-trinitromethyl adduct **636** increase, indicative of a change in the balance of the regiochemistry of attack of trinitromethanide ion on the radical cation of 4-fluoro-3-methylanisole **616** towards attack *ipso* to the methoxy function (Scheme 6.9).



Scheme 6.9

Nitrogen dioxide coupling at C6 of the delocalised radical species **646**, *para* to the methyl function gives the compressed diene **647**. Elimination of nitroform from diene **647** would give the 4-fluoro-5-methyl-2-nitroanisole **628**

while homoallylic rearrangement of this same diene would yield the 2-nitro-3-trinitromethyl adduct **636**.

*Overview of the photolysis products from 4-fluoroanisole **615** and 4-fluoro-3-methylanisole **616** in 1,1,1,3,3,3-hexafluoropropan-2-ol (HFP).*

HFP has been found to strongly stabilise radical cations, presumably by rendering any nucleophilic species present exceedingly unreactive.⁹ We therefore anticipated that in the present work HFP would inhibit the attack of trinitromethanide ion on the radical cation and by default favour the occurrence of the $\text{ArH}^{+\bullet} / \cdot\text{NO}_2$ coupling process. In the event, the conversion of each substrate into products was slow, 4-fluoroanisole **615** (18 % after 5 h) and 4-fluoro-3-methylanisole **616** (18 % after 4 h); 4-fluoroanisole **615** was converted exclusively into 4-fluoro-2-nitroanisole **625**, while 4-fluoro-3-methylanisole **616** gave the two nitro anisoles **631** (26 %) and **633** (74 %) as the exclusive products.

*Overview of the photolysis products from 4-fluoroanisole **615** and 4-fluoro-3-methylanisole **616** in dichloromethane containing trifluoroacetic acid (0.7 mol l⁻¹).*

In the presence of trifluoroacetic acid (0.7 mol l⁻¹) one component of the triad, trinitromethanide ion, formed on photolysis of a ArH-TNM charge transfer complex will be converted into the less nucleophilic nitroform $[\text{HC}(\text{NO}_2)_3]$ by protonation. For 4-fluoroanisole **615** the addition of trifluoroacetic acid (0.7 M) only partially suppressed adduct formation (total 18 %), and some 4-fluoro-2-trinitromethylanisole **624** (25 %) was also formed in addition to 4-fluoro-2-nitroanisole **625** (48 %). In contrast, the corresponding reaction of 4-fluoro-3-methylanisole **616** resulted in the formation of mainly the nitro anisoles **631** (18 %) and **633** (60 %), together with minor amounts of other aromatic products.

Summary

The halogen substituent does not appear to have a significant effect on the mechanistic pathway followed in the photolysis reactions of anisole

derivatives with tetranitromethane. The initial step in the recombination of the triad is trinitromethanide ion attack on the aromatic radical cation (amply demonstrated by the 60-70% yield of adducts observed in the photolysis reactions of 4-fluoroanisole in dichloromethane at 20°, -20° and -78°), followed by nitrogen dioxide coupling to the resultant delocalised carbon radical species. Subsequent elimination or rearrangement of the resultant adducts is likely if one of the substituents is *geminal* to the methoxy function, to give the observed reaction products.

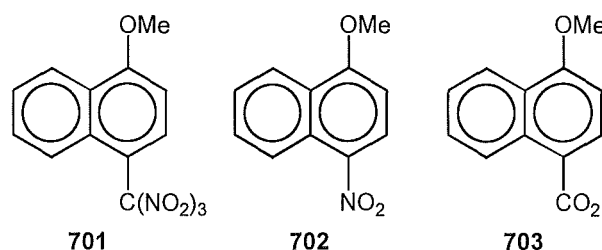
References

- ¹ Ebersson, L., Hartshorn, M. P., and Svensson, J. O., *Acta Chem. Scand.*, 1993, **47**, 925.
- ² Butts, C. P., Ebersson, L., Hartshorn, M. P., and Robinson, W. T., *Acta Chem. Scand.*, 1996, **50**, 122.
- ³ Sankararaman, S., Haney, W. A., and Kochi, J. K., *J. Am. Chem. Soc.*, 1987, **109**, 7824.
- ⁴ Butts, C. P., Ebersson, L., Hartshorn, M. P., and Robinson, W. T., *Aust. J. Chem.*, 1995, **48**, 1989.
- ⁵ Clewley, R. G., Fischer, A., and Henderson, G. N., *Can. J. Chem.*, 1989, 1472.
- ⁶ Clewley, R. G., Cross, G. G., Fischer, A., and Henderson, G. A., *Tetrahedron*, 1989, 1299.
- ⁷ Butts, C. P., Calvert, J. L., Ebersson, L., Hartshorn, M. P., Radner, F., and Robinson, W. T., *J. Chem. Soc. Perkin Trans. 2*, 1994, 1485; and references cited therein.
- ⁸ Barnes, C. E., and Myhre, P. C., *J. Am. Chem. Soc.*, 1978, **100**, 973.
- ⁹ Ebersson, L., Hartshorn, M. P., and Persson, O., *Angew Chem. Int. Ed. Engl.*, 1995, **34**, 2268; Ebersson, L., Hartshorn, M. P., and Persson, O., *J. Chem. Soc. Chem. Commun.*, 1995, 1131; Ebersson, L., Hartshorn, M. P., and Persson, O., *J. Chem. Soc. Perkin Trans. 2*, 1995, 1735; Ebersson, L., Hartshorn, M. P., and Persson, O., *Acta Chem. Scand.*, 1995, **49**, 640; Ebersson, L., Hartshorn, M. P., and Persson, O., *J. Chem. Soc. Perkin Trans. 2*, 1996, 141; Ebersson, L., Hartshorn, M. P., and Persson, O., *J. Chem. Soc. Perkin Trans. 2*, 1996, 151.

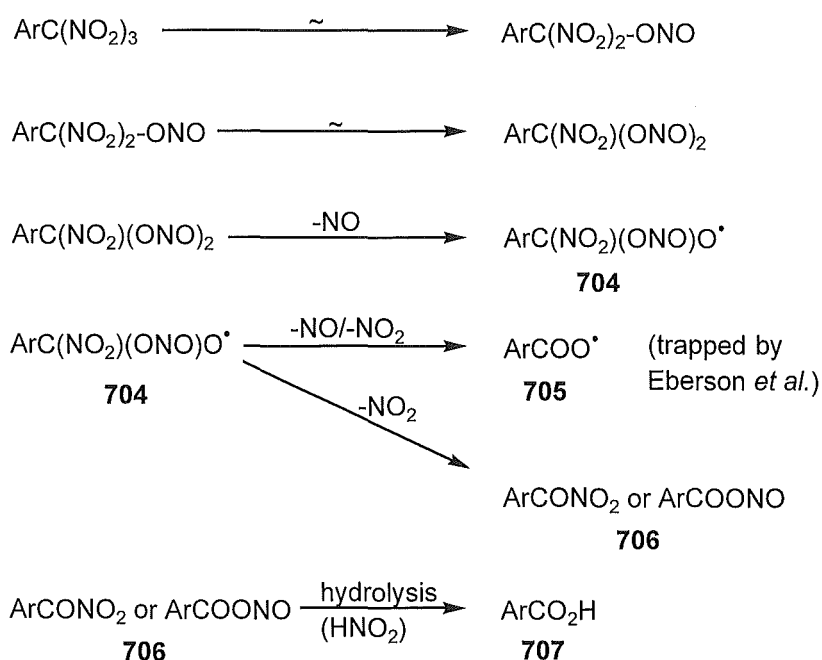
Chapter 7

Introduction

It was considered that one feature of the photochemical reactions of tetranitromethane with aromatic substrates which required closer examination was the conversion of trinitromethyl arene compounds such as **701** into the corresponding nitro species **702** or the carboxylic acid **703**.



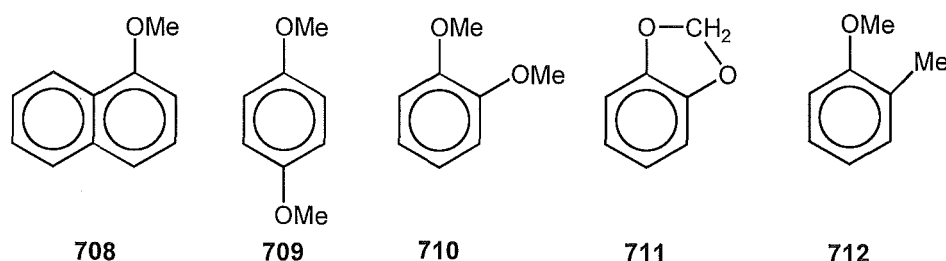
Earlier work by Ebersson *et al.* found¹ that the decomposition of trinitromethyl arene compounds could be promoted by a number of factors including added acid, the concentration of nitrogen dioxide, light, and the presence of the parent aromatic compound. A mechanism for the decomposition was suggested involving initial nitro-nitrito rearrangement within the trinitromethyl substituent (Scheme 7.1).



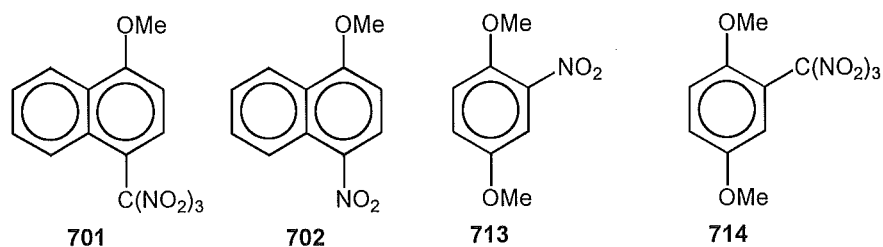
Scheme 7.1

A second nitro-nitrito rearrangement followed by cleavage of nitric oxide would yield the radical species **704**. Subsequent elimination of nitric oxide and nitrogen dioxide from this intermediate **704** would give a carboxyl radical species **705** which was trapped by Ebersson and co-workers.¹ Alternatively, elimination of nitrogen dioxide from **704** would give a nitro (or nitrito) ester **706** which could be hydrolysed to a carboxylic acid **707**. A nitro-decarboxylation reaction could then occur to give the corresponding nitro aromatic species; the reaction of nitrogen dioxide with carboxylic acid derivatives of 1-methoxynaphthalene and 4-chloroanisole confirmed the viability of this final step.

It was considered that addition of an alcohol to a photolysis system might trap one of the intermediate species in Scheme 7.1. Ethanol was deemed an appropriate alcohol and it was anticipated that its incorporation into a molecule could be monitored by the appearance of the characteristic CH₃ and CH₂ resonances in the ¹H n.m.r. spectra of photolysis product mixtures. The substrates employed in this study were 1-methoxynaphthalene **708**, 1,2-dimethoxybenzene **709**, 1,4-dimethoxybenzene **710**, 1,2-methylenedioxybenzene **711**, and 2-methylanisole **712**.



As discussed in Chapter 3, the photolysis reactions of tetranitromethane with 1-methoxynaphthalene in dichloromethane give relatively high yields of 1-methoxy-4-trinitromethylnaphthalene **701** (ca. 40%) in the product mixtures. Decomposition of trinitromethyl compound **701** to the corresponding 4-nitro species **702** was observed throughout the photolysis reaction. Addition of ethanol to the reaction mixture might therefore be expected to trap some of the intermediate species in this decomposition.



The photolysis reactions of 1,4-dimethoxybenzene with tetranitromethane were reported³ by Kochi *et al.* to give exclusively 1,4-dimethoxy-2-nitrobenzene **713** when the photolysis mixtures were examined by ¹H n.m.r. spectroscopy. It seemed likely that the observed nitro aromatic compound **713** was at least partially the product of a particularly facile conversion of the analogous 1,4-dimethoxy-2-trinitromethylbenzene **714** which was not observed in the product mixtures. It was anticipated that addition of ethanol to 1,4-dimethoxybenzene-tetranitromethane photolysis systems might support this theory by trapping an intermediate in this decomposition process. Similar results were expected in the cases of 1,2-dimethoxybenzene **710**, 1,2-methylenedioxybenzene **711**, and 2-methylanisole **712**. In the event, the anticipated trapping of intermediates in the trinitromethyl arene decomposition was not observed. The addition of ethanol to solutions of tetranitromethane and aromatic compounds appears to inhibit the decomposition of trinitromethyl aromatic products.

Results

General procedure for the photolysis of 1-methoxynaphthalene with tetranitromethane and ethanol.

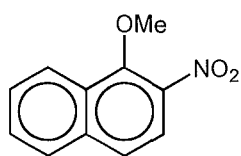
Solutions of 1-methoxynaphthalene **708**, (250mg, 0.4 mol l⁻¹), tetranitromethane (0.8 mol l⁻¹), and ethanol (8 % v/v), in dichloromethane or acetonitrile at 20° were irradiated with filtered light (λ cut-off at 435 nm). Aliquots were withdrawn from the reaction mixture at appropriate time intervals, the volatile material removed rapidly under reduced pressure at $\leq 0^\circ$, and the product composition determined by ¹H n.m.r. spectral analysis (for details see Experimental section; Table 8.7.1).

Photolysis of 1-methoxynaphthalene and tetranitromethane in dichloromethane with added ethanol (8 % v/v) at 20°.

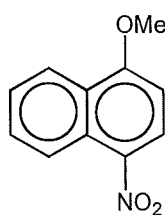
A solution of 1-methoxynaphthalene (0.4 mol l⁻¹) and tetranitromethane (0.8 mol l⁻¹) in dichloromethane with added ethanol (8 % v/v) was irradiated at 20°. The composition of the reaction mixture was monitored by withdrawing samples for ¹H n.m.r. spectral analysis (Table 7.1). All of the reaction products were identified by comparison of their ¹H n.m.r. spectral properties with authentic material.

Table 7.1 - Overview of yields from the photolysis of 1-methoxynaphthalene (0.4 mol l⁻¹) and tetranitromethane (0.8 mol l⁻¹) in dichloromethane at 20°, with added ethanol (8 % v/v).

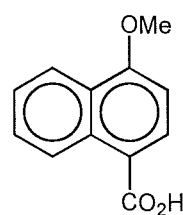
t/h	Conversion(%)	Yield (%)						
		715	702	703	701	716	717	718
DCM/20°/EtOH								
0.16	19.0	tce	9.1	-	68.2	7.7	tce	14.1
0.33	41.7	2.8	10.4	-	64.0	6.0	0.9	15.8
0.5	50.9	2.4	8.8	-	66.8	4.7	1.1	16.2
0.75	59.0	1.6	10.8	-	66.9	4.3	1.0	13.4
1	75.3	1.9	7.9	-	70.5	3.5	0.8	15.4



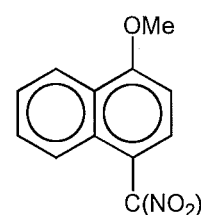
715



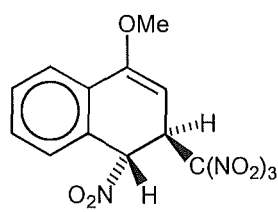
702



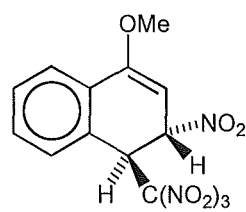
703



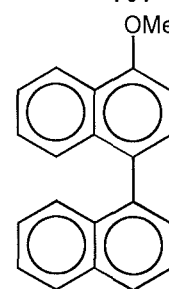
701



716



717



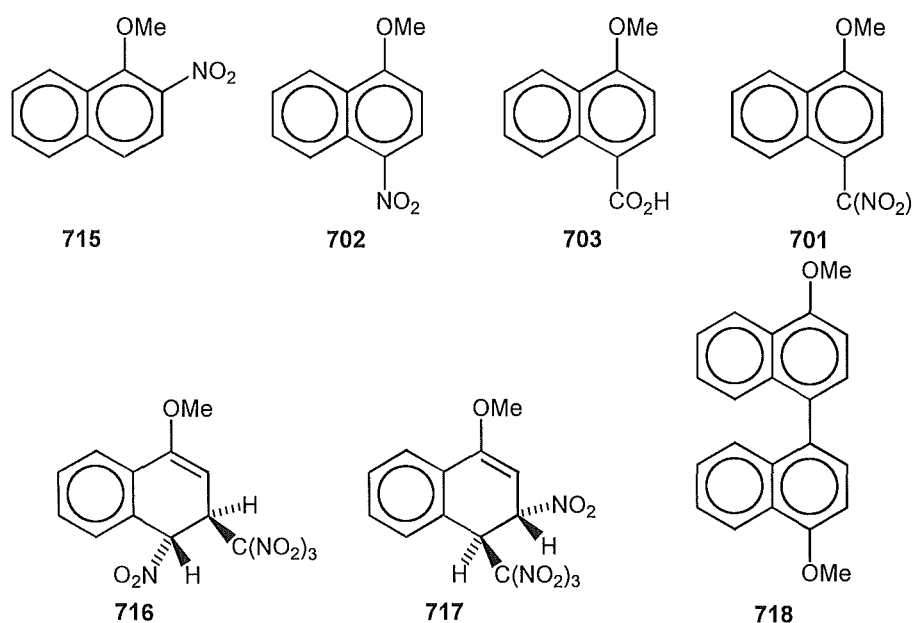
718

Photolysis of 1-methoxynaphthalene (0.4 mol l^{-1}) and tetranitromethane (0.8 mol l^{-1}) in acetonitrile with added ethanol (8 % v/v).

Reaction of 1-methoxynaphthalene and tetranitromethane for 1h as above except in acetonitrile, gave a product mixture which was monitored by withdrawing samples for ^1H n.m.r. spectral analysis (Table 7.2).

Table 7.2 - Overview of yields from the photolysis of 1-methoxynaphthalene (0.4 mol l^{-1}) and tetranitromethane (0.8 mol l^{-1}) in acetonitrile at 20° , with added ethanol (8 % v/v).

t/h	Conversion(%)	Yield (%)						
		715	702	703	701	716	717	718
AN/ 20° /EtOH								
0.33	20.7	0.9	31.1	-	56.9	-	-	11.1
0.5	25.2	1.6	34.1	-	53.1	-	-	11.2
0.75	36.4	1.4	30.6	-	56.0	-	-	12.0
1	41.3	1.6	30.1	-	53.8	-	-	14.5



General procedure for the photolysis of 1,2-dimethoxybenzene with tetranitromethane.

Solutions of 1,2-dimethoxybenzene **709**, (250mg, 0.45 mol l^{-1}), tetranitromethane (0.9 mol l^{-1}), in dichloromethane or acetonitrile, were

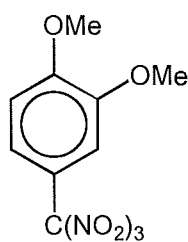
irradiated with filtered light (λ cut-off at 435 nm) at 20° and -20°. Aliquots were withdrawn from the reaction mixture at appropriate time intervals, the volatile material removed rapidly under reduced pressure at $\leq 0^\circ$, and the product composition determined by ^1H n.m.r. spectral analysis (for details see Experimental section; Tables 8.7.2 and 8.7.3).

Photolysis of 1,2-dimethoxybenzene and tetranitromethane in dichloromethane and the identification of 1,2-dimethoxy-4-trinitromethylbenzene 718 and 1,2-dimethoxy-4-nitrobenzene 719.

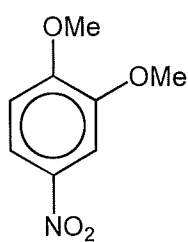
Solutions of 1,2-dimethoxybenzene (0.45 mol l^{-1}) and tetranitromethane (0.9 mol l^{-1}) in dichloromethane without added ethanol were photolysed, as above, at 20° and -20° for 3 h and the product compositions were monitored by ^1H n.m.r. spectral analysis (Table 7.3).

Table 7.3 - Overview of yields from the photolysis of 1,2-dimethoxybenzene (0.45 mol l^{-1}) and tetranitromethane (0.9 mol l^{-1}) in dichloromethane.

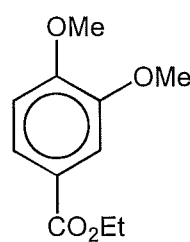
Reaction conditions	t/h	Conversion (%)	Yields (%)		
			718	719	720
DCM/20°	1	21.3	11.4	88.6	-
	2	47.0	11.8	88.2	-
	3	63.9	9.6	90.4	-
DCM/-20°	1	23.1	10.8	89.2	-
	2	47.5	6.9	93.1	-
	3	67.1	4.8	95.2	-



718



719



720

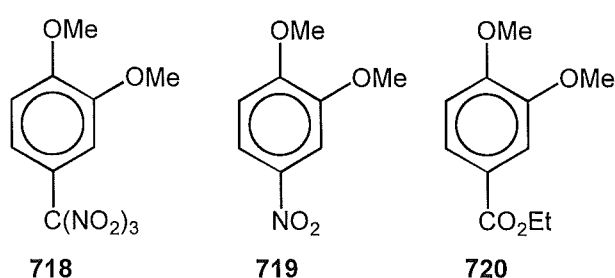
The trinitromethyl and nitro aromatic compounds **718** and **719** were isolated by radial chromatography of the -20° reaction product mixture on a silica gel Chromatotron plate using pentane-ether mixtures as the eluting solvent. The nitro aromatic compound **719** was identified by its ^1H n.m.r. spectral properties and known² mass spectrum. The assignment of the structure of the trinitromethyl compound **718** was based on its ^1H n.m.r. spectrum and its mass spectrum ($M^{*+} - \text{NO}_2$ 241.04606, $\text{C}_9\text{H}_9\text{N}_2\text{O}_6$) which suggested the presence of a trinitromethyl function. The doublet resonance at δ 7.04 in the ^1H n.m.r. spectrum of compound **718** allowed the assignment of the trinitromethyl substituent to C4 of the 1,2-dimethoxybenzene skeleton.

*Photolysis of 1,2-dimethoxybenzene and tetranitromethane in dichloromethane and ethanol (8 % v/v) at 20° and the identification of ethyl 1,2-dimethoxybenzoate **720**.*

A solution of 1,2-dimethoxybenzene (0.45 mol l^{-1}) and tetranitromethane (0.9 mol l^{-1}) in dichloromethane and ethanol (8 % v/v) was photolysed at 20° , and the composition of the reaction mixture was monitored by withdrawing samples for ^1H n.m.r. spectral analysis (Table 7.4). The ester **720** was identified by comparison of its ^1H n.m.r. spectral properties with authentic material.

Table 7.4 - Overview of yields from the photolysis of 1,2-dimethoxybenzene (0.45 mol l^{-1}) and tetranitromethane (0.9 mol l^{-1}) in dichloromethane with added ethanol.

Reaction conditions	t/h	Conversion (%)	Yields (%)		
			718	719	720
DCM/ 20° /EtOH (8% v/v)	1	35.0	82.0	17.0	1.0
	2	55.0	71.0	27.0	1.0
	3	72.0	62.0	36.0	2.0

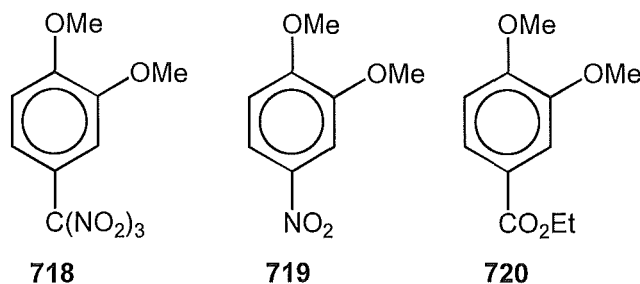


Photolysis of 1,2-dimethoxybenzene and tetranitromethane in dichloromethane and ethanol (4 % v/v) at 20°.

A reaction of 1,2-dimethoxybenzene and tetranitromethane performed in a manner similar to that described above, except that only 4 % ethanol by volume was added to the solution, and the product mixture monitored by ^1H n.m.r. spectral analysis (Table 7.4).

Table 7.4 - Overview of yields from the photolysis of 1,2-dimethoxybenzene (0.45 mol l^{-1}) and tetranitromethane (0.9 mol l^{-1}) in dichloromethane with added ethanol.

Reaction conditions	t/h	Conversion (%)	Yields (%)		
			718	719	720
DCM/20°/EtOH (4% v/v)	1	42.6	71.1	28.4	0.5
	2	64.7	50.6	48.9	0.6
	3	84.7	42.9	55.8	1.3



This reaction differed from the 8 % ethanol reaction only in a slightly higher initial yield of the 4-nitro aromatic compound **719** and a marginal increase in the rate of decomposition of the trinitromethyl aromatic compound **718**.

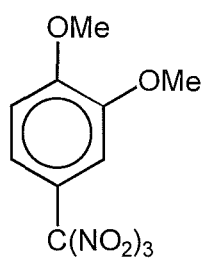
Photolysis of 1,2-dimethoxybenzene and tetranitromethane in acetonitrile.

Photolysis of solutions of 1,2-dimethoxybenzene (0.45 mol l^{-1}) and tetranitromethane (0.9 mol l^{-1}) in acetonitrile both with and without ethanol were performed. Reactions in the absence of ethanol were carried out at 20° and

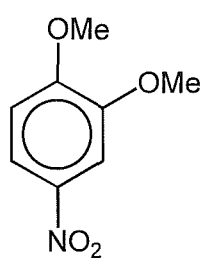
-20°, and the product compositions throughout all of the reactions were monitored by ^1H n.m.r. spectral analysis (Table 7.5).

Table 7.5 - Overview of yields from the photolysis of 1,2-dimethoxybenzene (0.45 mol l^{-1}) and tetranitromethane (0.9 mol l^{-1}) in acetonitrile.

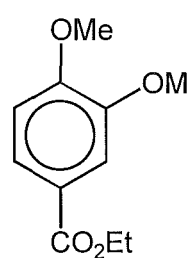
Reaction conditions	t/h	Conversion (%)	Yields (%)		
			718	719	720
AN/20°	1	22.9	3.8	96.2	-
	2	40.6	3.4	96.6	-
	3	58.7	3.4	96.6	-
AN/-20°	1	16.5	4.5	95.5	-
	2	34.5	3.0	97.0	-
	3	50.1	2.9	97.1	-
AN/20°/EtOH (8% v/v)	1	27.9	30.9	67.6	1.5
	2	49.1	30.6	66.9	2.5
	3	64.0	26.4	70.8	2.8



718



719



720

The products were the same as those seen in the corresponding dichloromethane reactions, but lesser quantities of the trinitromethyl aromatic compound **718** were observed in all cases. As seen in the corresponding dichloromethane reactions, greater yields of the trinitromethyl aromatic compound **718** were seen in reactions run with added ethanol.

General procedure for the photolysis of 1,4-dimethoxybenzene with tetranitromethane.

A solution of 1,4-dimethoxybenzene **710**, (250mg, 0.45 mol l⁻¹), tetranitromethane (0.9 mol l⁻¹), in dichloromethane or acetonitrile was irradiated with filtered light (λ cut-off at 435 nm) at 20°. Aliquots were withdrawn from the reaction mixture at appropriate time intervals, the volatile material removed rapidly under reduced pressure at $\leq 0^\circ$, and the product composition determined by ¹H n.m.r. spectral analysis (for details see Experimental section; Tables 8.7.5 and 8.7.6).

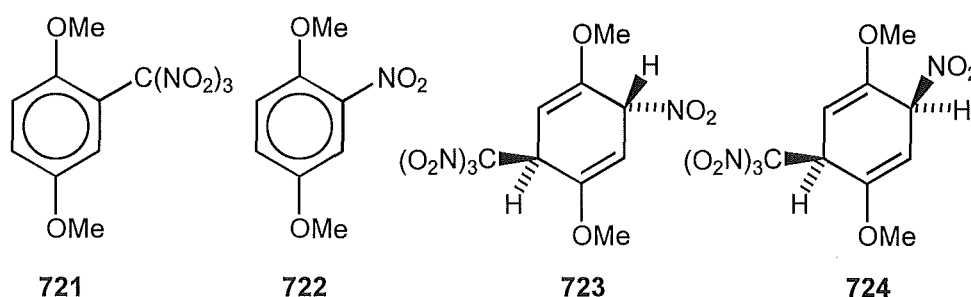
*Photolysis of 1,4-dimethoxybenzene and tetranitromethane in dichloromethane with added ethanol and the identification of aromatic compounds **721-2** and adducts **723-4**.*

Solutions of 1,4-dimethoxybenzene **710** (0.45 mol l⁻¹) and tetranitromethane (0.9 mol l⁻¹) in dichloromethane and ethanol (8 % v/v and 4 % v/v) were photolysed at 20°, and the composition of the reaction mixtures were monitored by withdrawing samples for ¹H n.m.r. spectral analysis (Table 7.6, overleaf).

The trinitromethyl aromatic compound **721** and nitro aromatic compound **722** were isolated by radial chromatography on a silica gel Chromatotron plate using pentane as the eluting solvent. The nitro aromatic compound **722** was identified by comparison of its ¹H n.m.r. spectral properties³ and melting point⁴ with literature values. The assignment of the structure of the trinitromethyl compound **721** was based on its ¹H n.m.r. (3 aromatic proton resonances observed) and mass spectra (M⁺⁺ 287.03896, C₉H₉N₃O₈).

Table 7.6 - Overview of yields from the photolysis of 1,4-dimethoxybenzene (0.45 mol l^{-1}) and tetranitromethane (0.9 mol l^{-1}) in dichloromethane with added ethanol.

Reaction conditions	t/h	Conversion	Yields (%)			
			721	722	723	724
20°/EtOH (8% v/v)	3	56.0	9.8	80.5	8.3	1.5
	5	84.0	9.7	82.5	6.3	1.5
20°/EtOH (4% v/v)	2	61.0	11.4	81.0	6.4	1.1
	3	88.0	9.7	83.1	5.7	1.5



The two nitro-trinitromethyl adducts **723** and **724** could not be isolated by h.p.l.c. even at -20° , and the structures of these adducts were assigned by consideration of the results of n.m.r. experiments performed on the crude photolysis product mixture. The *trans* adduct **723** was formed in higher yields and consequently the data for this compound is more complete. The structure of 1,4-dimethoxy-*r*-3-nitro-*t*-6-trinitromethylcyclohexa-1,4-diene **723** was assigned on the basis of the results of nuclear Overhauser experiments (Figure 7.1) and reverse detected heteronuclear correlation spectroscopy (HMQC)

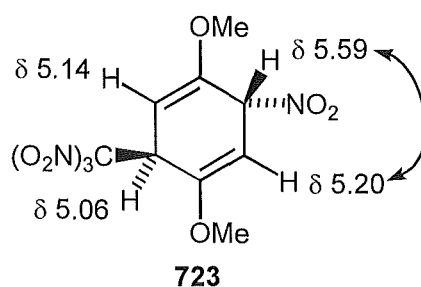


Figure 7.1 - Observed nuclear Overhauser enhancements in the ^1H n.m.r. spectrum of **723**.

The observed nuclear Overhauser enhancements between the ^1H resonances at δ 5.59 and δ 5.20 illustrates the vicinal relationship of these two protons. Subsequently, the assignment of the ^{13}C n.m.r. resonance at δ 83.1 (HC-NO_2) to C3, and the observed correlation between the carbon resonance at δ 44.6 [$\text{HC-C}(\text{NO}_2)_3$] and the proton resonance at δ 5.06 makes the assigned regiochemistry of adduct **723** the only reasonable possibility.

Due to the low yield of adduct **724** in the photolysis reaction mixture only ^1H n.m.r. data was able to be obtained and is presented together with that for its epimer **723** in Figure 7.2.

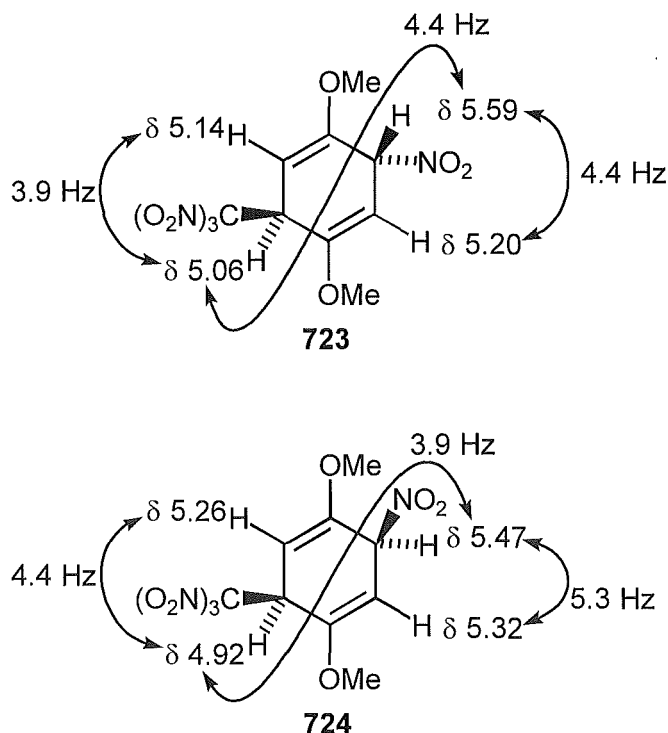
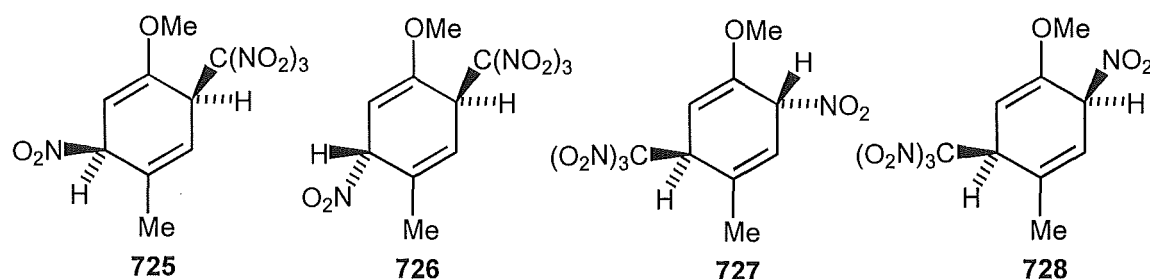


Figure 7.2 - ^1H n.m.r. chemical shift data and H,H-coupling constants for adducts **723** and **724**

An almost uniform downfield shift of 0.12 - 0.14 p.p.m. is observed from the proton signals in the olefinic region (δ 4.5 - 6.5) of the ^1H n.m.r. spectrum of adduct **723** to the corresponding proton resonances for adduct **724**

The stereochemistry of adducts **723** and **724** was assigned by comparison of their ^1H n.m.r. spectral data with those of adducts **725-728** from 4-methylanisole for which the stereochemistry was assigned in Chapter 4 from

the results of either single crystal X-ray analysis (p. 104) or relative h.p.l.c. elution orders.



By examining the trends in the n.m.r. chemical shift data for the protons vicinal to the methoxy functions within each epimeric pair of adducts **725-728** and comparing these to the corresponding resonances in the 1,4-dimethoxy adducts **723** and **724**, it is possible to assign the stereochemistry with reasonable certainty in each case. Figure 7.3 (overleaf) displays the appropriate data in this manner for each of the adducts **723-728**. The changes in chemical shift between the related ^1H n.m.r. resonances of protons vicinal to the methoxy function within each epimeric pair of adducts **725-728**, are consistent with those observed between adducts **723** and **724** if these adducts are assigned as 1,4-dimethoxy-*r*-3-nitro-*t*-6-trinitromethyl-cyclohexa-1,4-diene **723** and 1,4-dimethoxy-*r*-3-nitro-*c*-6-trinitromethyl-cyclohexa-1,4-diene **724** respectively.

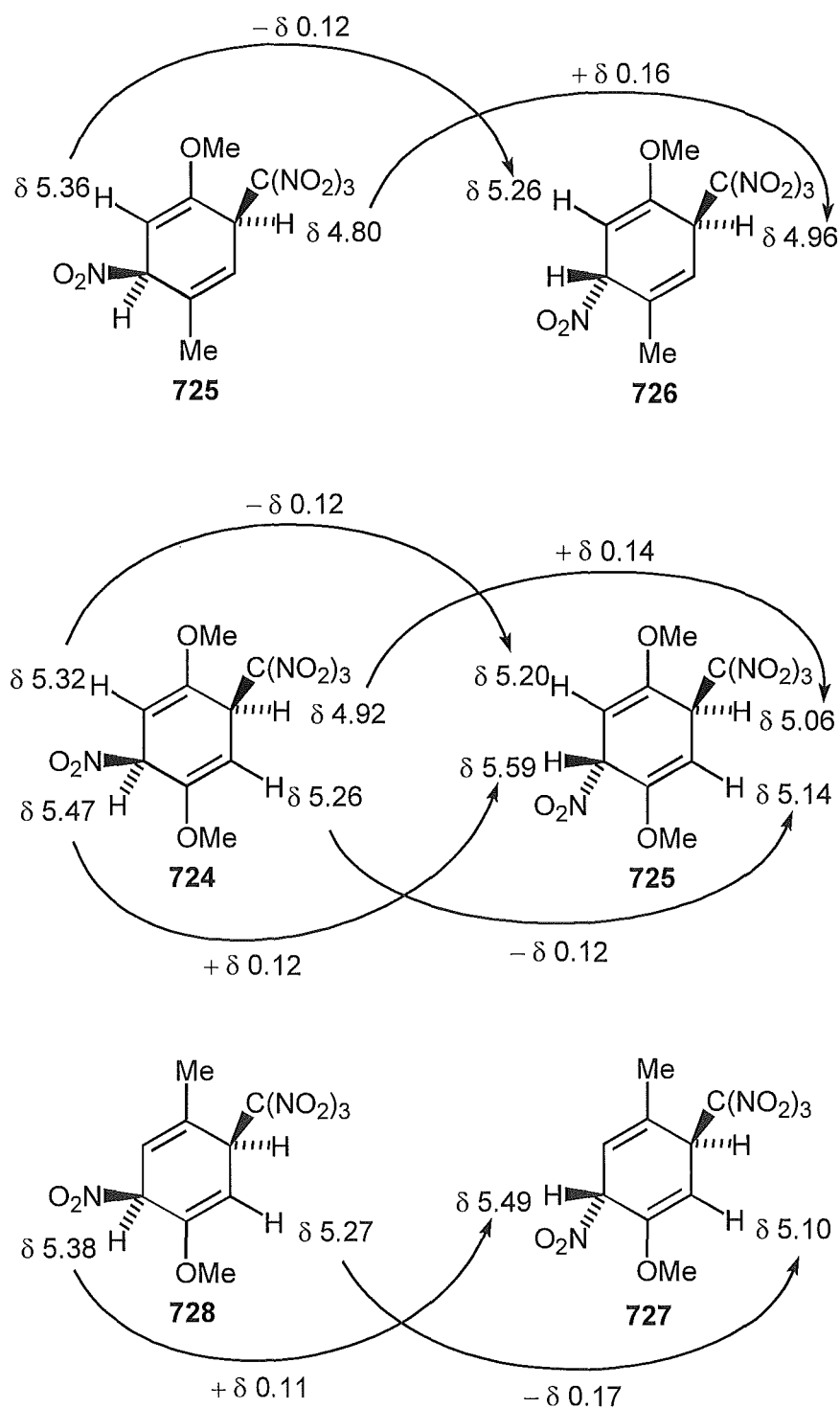


Figure 7.3 - ^1H n.m.r. chemical shift data used to assign the stereochemistry of adducts **723** and **724**.

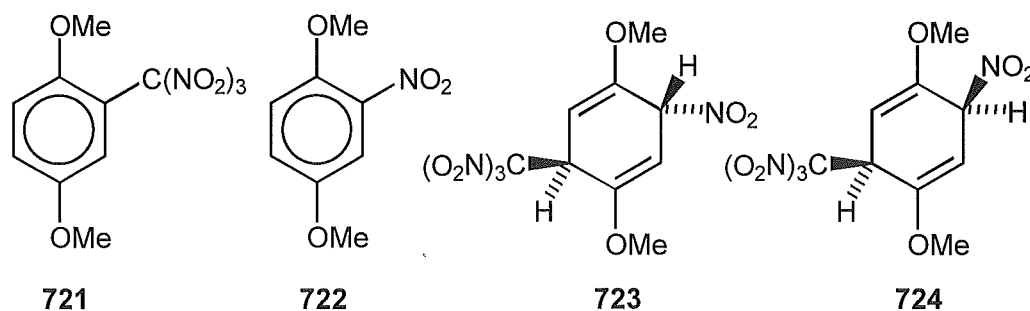
Photolysis of 1,4-dimethoxybenzene and tetranitromethane in dichloromethane at 20°.

A solution of 1,4-dimethoxybenzene **710** (0.45 mol l^{-1}) and tetranitromethane (0.9 mol l^{-1}) in dichloromethane was photolysed at 20°, and

the composition of the reaction mixture was monitored by withdrawing samples for ^1H n.m.r. spectral analysis (Table 7.7). The absence of the trinitromethyl aromatic compound **721** and the significantly lower yields of the two adducts **723** and **724** are notable in this reaction.

Table 7.7 - Overview of yields from the photolysis of 1,4-dimethoxybenzene (0.45 mol l^{-1}) and tetranitromethane (0.9 mol l^{-1}) in dichloromethane.

Reaction conditions	t/h	Conversion	Yields (%)			
			721	722	723	724
20°	1	36.6	-	96.4	3.6	tce
	2	74.0	-	96.5	3.1	0.4
	3	96.0	-	96.8	2.7	0.5

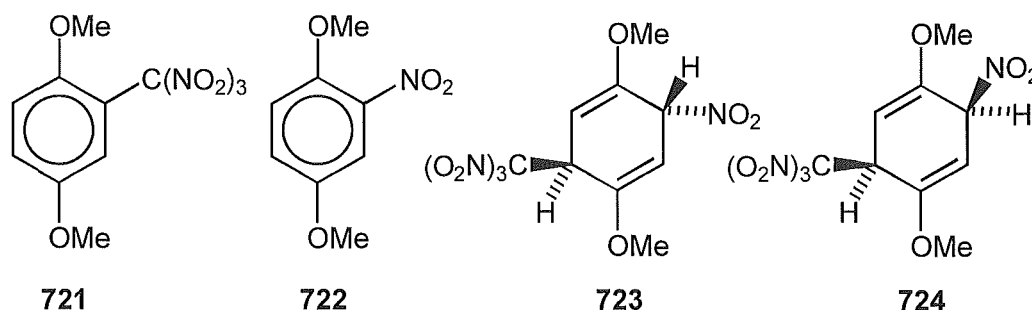


Photolysis of 1,4-dimethoxybenzene and tetranitromethane in acetonitrile at 20°.

Solutions of 1,4-dimethoxybenzene **710** (0.45 mol l^{-1}) and tetranitromethane (0.9 mol l^{-1}) in acetonitrile with and without added ethanol were photolysed at 20°, and the composition of the reaction mixtures were monitored by withdrawing samples for ^1H n.m.r. spectral analysis (Table 7.8, overleaf).

Table 7.8 - Overview of yields from the photolysis of 1,4-dimethoxybenzene (0.45 mol l^{-1}) and tetranitromethane (0.9 mol l^{-1}) in acetonitrile with and without added ethanol.

Reaction conditions	t/h	Conversion	Yields (%)			
			721	722	723	724
20°	1	42.7	-	100	tce	tce
	2	71.8	-	99.5	0.5	tce
	3	90.9	-	99.3	0.7	tce
	4	100	-	99.1	0.9	tce
20°/EtOH (8% v/v)	1	23.1	-	100	tce	tce
	2	52.5	-	100	tce	tce
	3	71.5	-	99.5	0.5	tce
	4	85.7	-	99.1	0.9	tce



Only trace quantities of the two adducts were observed in the ^1H n.m.r. spectra of the reaction mixtures, which otherwise consisted exclusively of 1,4-dimethoxy-2-nitrobenzene **722**.

General procedure for the photolysis of 1,2-methylenedioxybenzene with tetranitromethane.

A solution of 1,2-methylenedioxybenzene **711**, (250mg , 0.5 mol l^{-1}), tetranitromethane (1.0 mol l^{-1}), in dichloromethane or acetonitrile was irradiated with filtered light (λ cut-off at 435 nm). Aliquots were withdrawn from the reaction mixture at appropriate time intervals, the volatile material removed

rapidly under reduced pressure at $\leq 0^\circ$, and the product composition determined by ^1H n.m.r. spectral analysis (for details see Experimental section; Tables 8.7.7 and 8.7.8).

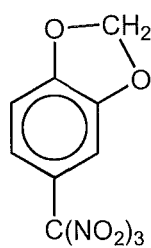
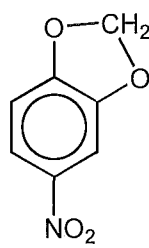
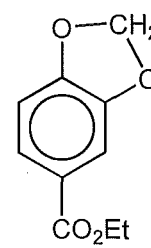
*Photolysis of 1,2-methylenedioxybenzene and tetranitromethane in dichloromethane and the identification of 1,2-methylenedioxy-4-trinitromethylbenzene **729** and 1,2-methylenedioxy-4-nitrobenzene **730**.*

Solutions of 1,2-methylenedioxybenzene **711** (0.5 mol l^{-1}) and tetranitromethane (1.0 mol l^{-1}) in dichloromethane were photolysed at 20° , -20° and -40° and the composition of the reaction mixtures were monitored by withdrawing samples for ^1H n.m.r. spectral analysis (Table 7.10, overleaf).

The trinitromethyl aromatic compound **729** and nitro aromatic compound **730** were isolated by radial chromatography of the 20° reaction mixture on a silica gel Chromatotron plate. The structure of compound **729** was assigned on the basis of its ^1H n.m.r. and mass spectral properties. The narrow doublet resonance at $\delta 7.66$ ($J_{\text{H,H}} 2.4 \text{ Hz}$) in the ^1H n.m.r. spectrum of **729** indicated C4 substitution of the 1,2-methylenedioxybenzene skeleton and the mass spectrum identified an ion at mass 225.01476 ($\text{M}^{++} - \text{NO}_2$, $\text{C}_8\text{H}_5\text{N}_2\text{O}_6$) which suggested the substituent was a trinitromethyl group. The nitro aromatic compound **730** was identified similarly by analysis of its ^1H n.m.r. and mass spectra ($\text{M}^{++} 167.02186$, $\text{C}_7\text{H}_5\text{NO}_4$).

Table 7.9 - Overview of yields from the photolysis of 1,2-methylenedioxybenzene (0.5 mol l^{-1}) and tetranitromethane (1.0 mol l^{-1}) in dichloromethane.

Reaction conditions	t/h	Conversion (%)	Yields (%)			
			729	730	731	Unknowns
20°	1	35.9	31.7	65.3	-	3.0
	1.5	58.7	25.0	70.9	-	4.1
	2	66.1	19.2	75.3	-	5.5
-20° ^A	1	29.6	18.6	76.4	-	5.0
	1.5	41.8	12.1	83.5	-	4.4
	2	50.6	9.1	89.0	-	1.9
-40° ^A	1	32.2	10.3	86.2	-	3.4
	1.5	41.9	7.4	91.6	-	1.0
	2	39.4	9.9	87.9	-	2.2

**729****730****731**

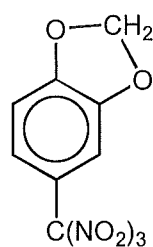
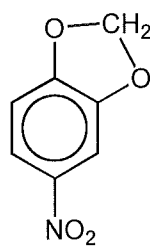
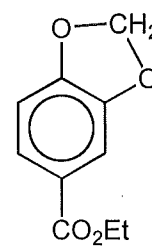
Photolysis of 1,2-methylenedioxybenzene in dichloromethane with added ethanol.

Reactions were run as above at 20° except with ethanol (8 % or 4 % v/v) added to the photolysis solutions. The rates of these reactions were significantly slower than the corresponding reaction in dichloromethane. After 10 h, after work-up, both reaction mixtures contained 1,2-methylenedioxy-4-trinitromethylbenzene **729** (ca. 60 % in the 8 % ethanol reaction and ca. 52 % in the 4 % ethanol reaction), 1,2-methylenedioxy-4-nitrobenzene **730** (19.2 %

and 33.1 %), the ethyl ester **731** (9 % and 5 %), and unknown aromatic compounds (12 % and 10 %) (Table 7.10).

Table 7.10 - Overview of yields from the photolysis of 1,2-methylenedioxybenzene (0.5 mol l^{-1}) and tetranitromethane (1.0 mol l^{-1}) in dichloromethane with added ethanol.

Reaction conditions	t/h	Conversion (%)	Yields (%)			
			729	730	731	Unknowns
20°/EtOH (8% v/v)	3	18.7	61.5	18.5	7.7	12.3
	6	29.3	56.3	19.4	9.7	14.6
	10	49.9	59.9	19.2	9.0	12.0
20°/EtOH (4% v/v)	3	32.4	74.5	11.8	3.9	9.8
	6	42.3	68.0	16.7	4.5	10.9
	10	58.8	51.7	33.1	5.1	10.1

**729****730****731**

The ester **731** was identified by comparison of its ^1H n.m.r. properties with authentic material. The most significant feature of these reactions is the large increase in the yield of the trinitromethyl aromatic compound **729** from the reactions without added ethanol, described above.

Photolysis of 1,2-methylenedioxybenzene in acetonitrile.

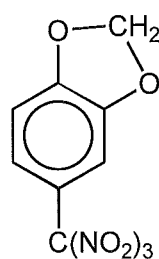
Photolysis of solutions of 1,2-methylenedioxybenzene and tetranitromethane as above except in acetonitrile, at 20° and -20° gave exclusively the 4-nitro aromatic compound **730**. However, a similar reaction with

added ethanol (8 % v/v) at 20° for 10 h gave a mixture of products including the trinitromethyl aromatic compound **729** and the ethyl ester **731** (Table 7.11).

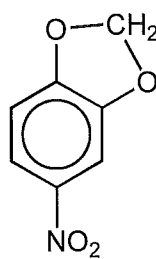
Table 7.11 - Overview of yields from the photolysis of 1,2-methylenedioxybenzene (0.5 mol l^{-1}) and tetranitromethane (1.0 mol l^{-1}) in acetonitrile with and without added ethanol (8 % v/v).

Reaction conditions	t/h	Conversion (%)	Yields (%)			
			729	730	731	Unknowns
20°	1	26.2	-	100	-	-
	1.5	43.0	-	100	-	-
	2	61.5	-	100	-	-
-20° ^A	1	29.1	-	100	-	-
	1.5	38.9	-	100	-	-
	2	32.9	-	100	-	-
20°/EtOH (8% v/v)	3	27.7	10.5	75.6	2.9	11.0
	6	34.8	12.3	72.1	4.9	10.7
	10	54.8	6.3	81.3	8.3	4.2

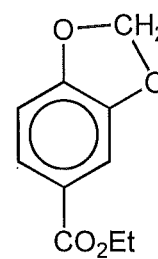
^A Solid precipitated in the reaction mixture after t = 1h



729



730



731

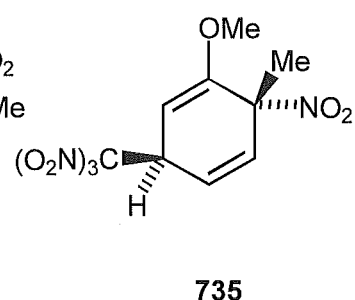
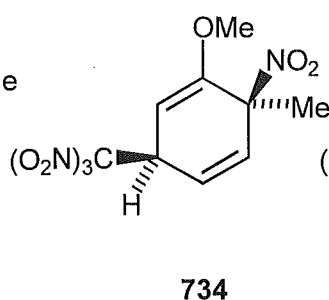
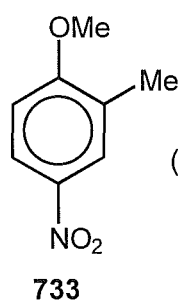
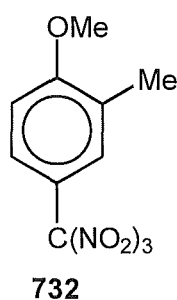
Photolysis of 2-methylanisole with tetranitromethane in the presence of ethanol.

Solutions of 2-methylanisole **712**, (250 mg , 0.46 mol l^{-1}), tetranitromethane (0.9 mol l^{-1}), in dichloromethane or acetonitrile, with added ethanol (8 % v/v) were irradiated with filtered light (λ cut-off at 435 nm). Aliquots were withdrawn from the reaction mixture at appropriate time intervals, the

volatile material removed rapidly under reduced pressure at $\leq 0^\circ$, and the product composition determined by ^1H n.m.r. spectral analysis (for details see Experimental section; Tables 8.7.9). The products were a mixture (Table 7.12) of the previously identified compounds **732-735** (Chapter 5).

Table 7.11 - Overview of yields from the photolysis of 2-methylanisole (0.46 mol l^{-1}) and tetranitromethane (0.92 mol l^{-1}) in dichloromethane or acetonitrile with added ethanol (8% v/v).

Reaction conditions	t/h	Conversion (%)	Yields (%)					
			Unknown			Unknown		
			732	733	Aromatics	734	735	Adducts
DCM/20°/EtOH	1	30.9	86.9	6.5	-	1.9	4.7	-
	2	60.0	87.6	7.0	-	1.2	4.1	-
	3	74.7	87.1	7.5	-	1.2	4.1	-
AN/20°/EtOH	1	16.6	81.2	12.6	-	1.1	5.0	-
	2	33.1	80.4	13.3	-	1.5	4.9	-
	3	49.2	73.7	21.2	-	1.5	3.6	-



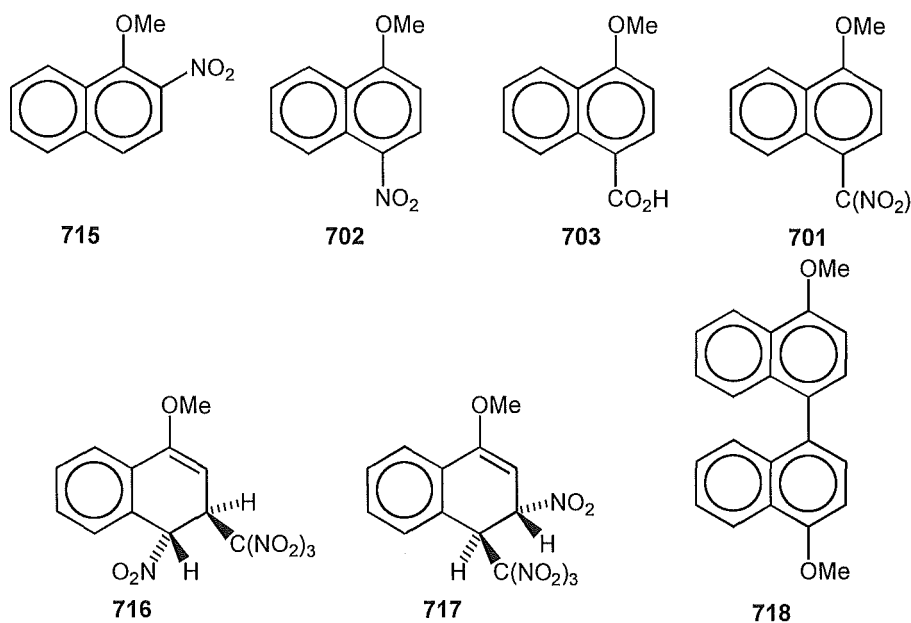
Discussion

Photochemistry of 1-methoxynaphthalene and tetranitromethane in the presence of ethanol.

A summary of the results of photolyses of 1-methoxynaphthalene and tetranitromethane in dichloromethane solutions is presented in Table 7.12.

Table 7.12 - Overview of yields from the photolysis of 1-methoxynaphthalene (0.4 mol l^{-1}) and tetranitromethane (0.8 mol l^{-1}) in dichloromethane at 20° , with or without added ethanol (8 % v/v).

t/h	Conversion(%)	Yield (%)						
		715	702	703	701	716	717	718
DCM/20°								
0.25	36.5	2.0	38.2	-	41.3	7.4	11.0	-
0.5	68.2	3.0	41.7	-	41.7	6.2	7.7	-
1	~100	5.2	50.4	-	34.6	6.3	3.3	-
2	100	7.3	57.4	4.8	24.1	6.5	-	-
DCM/20°/EtOH								
0.16	19.0	tce	9.1	-	68.2	7.7	tce	14.1
0.33	41.7	2.8	10.4	-	64.0	6.0	0.9	15.8
0.5	50.9	2.4	8.8	-	66.8	4.7	1.1	16.2
0.75	59.0	1.6	10.8	-	66.9	4.3	1.0	13.4
1	75.3	1.9	7.9	-	70.5	3.5	0.8	15.4



These data show a number of interesting features. First and foremost was the appearance of the dehydrodimer **718** among the reaction products when ethanol was added to the photolysis solution. The dehydrodimer is the

result of radical coupling of the aromatic radical cation species. This reaction is only competitive when the reactivity of the trinitromethanide anion has been significantly reduced. As discussed in Chapter 3, this was achieved previously by the addition of trifluoroacetic acid which protonates the trinitromethanide ion to form the less nucleophilic nitroform $[\text{C}(\text{NO}_2)_3]$. The formation of the dehydrodimer **718** implies that ethanol is reducing the reactivity of the trinitromethanide ion. It is suggested that hydrogen bonding between the hydroxy function of the ethanol solvent and the oxygen atoms of the nitro groups in the trinitromethanide ion is the origin of this stabilising effect.

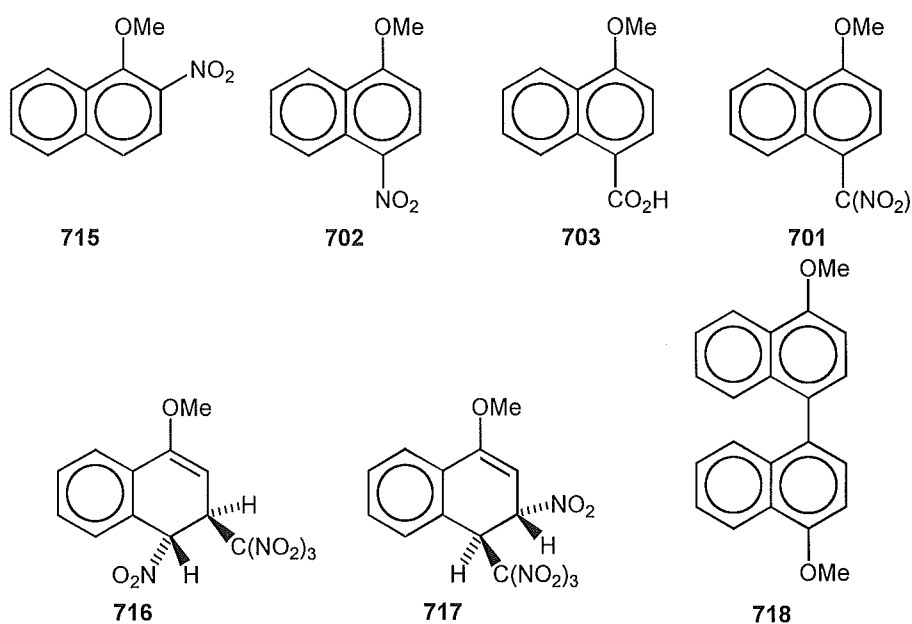
Further to this, it is apparent that the decomposition of the trinitromethyl aromatic compound **701** is negligible in the presence of ethanol and a similar explanation could be invoked for this effect *i.e.* hydrogen bonding of ethanol to the trinitromethyl substituent which would reduce the driving force for the postulated initial nitro-nitrito rearrangement.

A third feature of the photolysis reaction of 1-methoxynaphthalene and tetranitromethane in the presence of ethanol is the low yield of 1-methoxy-4-nitronaphthalene **702**. The relatively low yield of 1-methoxy-4-nitronaphthalene **702** is probably due to two effects. First, in the presence of ethanol in the photolysis medium the decomposition of the trinitromethyl aromatic compound **701** to give the nitro compound **702** is limited by the ethanol-induced stabilisation of the trinitromethyl compound **701**. Second, solvation by ethanol of trinitromethanide ion would be expected to reduce the reactivity and increase the steric demand of the solvated trinitromethanide ion. This second effect may reduce the extent therefore of attack of trinitromethanide ion *ipso* to the methoxy group, a form of attack implicated (See Chapter 3) in the formation of much of the 1-methoxy-4-nitronaphthalene **702**.

Similar features were observed in the acetonitrile photolysis solution of 1-methoxynaphthalene and tetranitromethane with added ethanol (8 % v/v). A summary of the product yield data from this reaction together with those discussed in Chapter 3 from the corresponding reaction in acetonitrile is given in Table 7.13, overleaf.

Table 7.13 - Overview of yields from the photolysis of 1-methoxynaphthalene (0.4 mol l⁻¹) and tetranitromethane (0.8 mol l⁻¹) in acetonitrile at 20°, with or without added ethanol (8 % v/v).

t/h	Conversion(%)	Yield (%)						
		715	702	703	701	716	717	718
AN/20°								
0.25	23.6	3.2	42.0	-	49.5	2.7	2.0	-
0.5	47.1	4.1	50.5	-	38.8	3.3	3.3	-
1	88.0	4.3	54.1	-	38.0	2.2	1.4	-
2	100	5.0	75.5	-	17.5	1.3	0.7	-
AN/20°/EtOH								
0.33	20.7	0.9	31.1	-	56.9	-	-	11.1
0.5	25.2	1.6	34.1	-	53.1	-	-	11.2
0.75	36.4	1.4	30.6	-	56.0	-	-	12.0
1	41.3	1.6	30.1	-	53.8	-	-	14.5



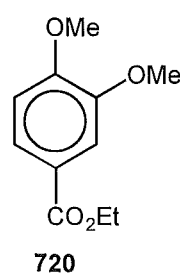
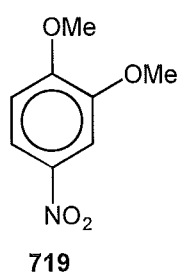
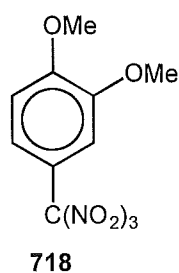
In the presence of ethanol, a marginally lower yield of 1-methoxy-4-nitronaphthalene **702** was seen in conjunction with a higher yield of 1-methoxy-4-trinitromethyl-naphthalene **701**. As in the corresponding dichloromethane-ethanol reaction, the trinitromethyl aromatic compound **701** appears to be stable within the time-scale of the photolysis.

Photochemistry of 1,2-dimethoxybenzene and tetranitromethane in dichloromethane.

The photolysis of 1,2-dimethoxybenzene and tetranitromethane in dichloromethane at 20° for 1 h, after work-up, gave a mixture of only two products, 1,2-dimethoxy-4-trinitromethylbenzene **718** (11 %) and 1,2-dimethoxy-4-nitrobenzene **719** (89 %) (Table 7.14).

Table 7.14 - Overview of yields from the photolysis of 1,2-dimethoxybenzene (0.45 mol l⁻¹) and tetranitromethane (0.9 mol l⁻¹) in dichloromethane with or without added ethanol.

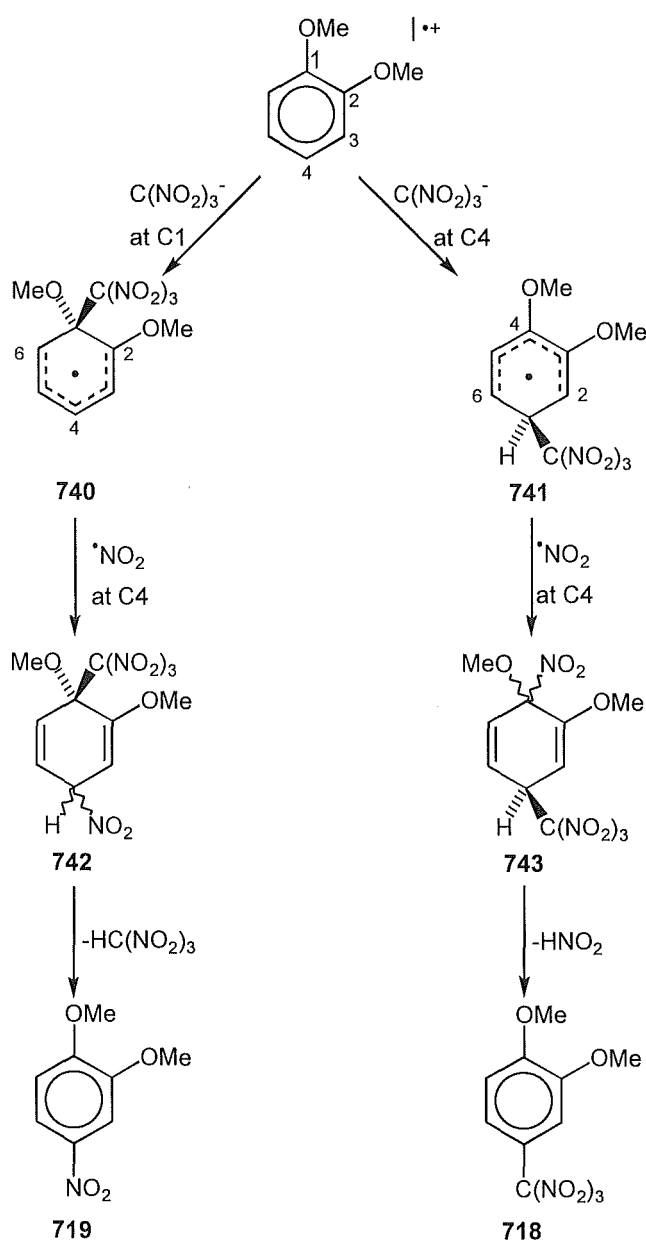
Reaction conditions	t/h	Conversion (%)	Yields (%)		
			718	719	720
DCM/20°	1	21.3	11.4	88.6	-
	2	47.0	11.8	88.2	-
	3	63.9	9.6	90.4	-
DCM/-20°	1	23.1	10.8	89.2	-
	2	47.5	6.9	93.1	-
	3	67.1	4.8	95.2	-
DCM/20°/EtOH (8% v/v)	1	35.0	82.0	17.0	1.0
	2	55.0	71.0	27.0	1.0
	3	72.0	62.0	36.0	2.0
DCM/20°/EtOH (4% v/v)	1	42.6	71.1	28.4	0.5
	2	64.7	50.6	48.9	0.6
	3	84.7	42.9	55.8	1.3



Lowering the photolysis reaction temperature to -20° appeared to have little effect on the initial products formed, the same two compounds **718** and **719**

were observed in essentially the same yields (11 % and 89 % respectively after 1 h).

The mode of formation of these products is believed to be similar to that discussed earlier for related methoxy substituted aromatic compounds *i.e.* initial trinitromethanide ion attack at either C1 or C4 of the 1,2-dimethoxybenzene radical cation (Scheme 7.4) followed by nitrogen dioxide coupling at C4 of the resultant delocalised radical species **740** or **741** to give the unstable intermediate species **742** or **743**.



Scheme 7.4

Elimination of nitroform from the intermediate **742** would give the observed 1,2-dimethoxy-4-nitrobenzene **719** while similar elimination of nitrous acid from **743** would result in the formation of 1,2-dimethoxy-4-trinitromethylbenzene **718**.

The addition of ethanol (8 % or 4 % v/v) to dichloromethane photolysis solutions of 1,2-dimethoxybenzene and tetranitromethane resulted in a dramatic change in the observed product yields. The trinitromethyl aromatic compound **718** was present in high yields at low conversion of starting material into products (82 % in the 8 % ethanol and 71 % in the 4 % ethanol reaction). Consequently the nitro aromatic compound **719** was observed in relatively low yields (17 % and 28 %) which increased throughout the reaction as a result of decomposition of the trinitromethyl aromatic compound **718**. In addition, a new product, the ethyl ester **720** was identified in minor quantities (≤ 2 %). The mode of formation of ester **720** is not clear, although it may involve trapping by ethanol of an intermediate in the decomposition process of the trinitromethyl aromatic compound **718**.

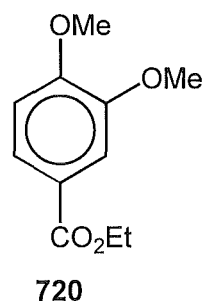
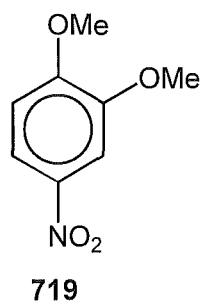
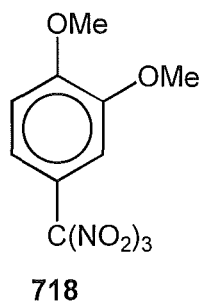
The extreme change in the observed product yields on the addition of ethanol to the photolysis solutions can be rationalised in terms of solvation of the trinitromethanide ion by ethanol increasing the steric demand of the nucleophile; consequently trinitromethanide ion attack at the sterically compressed C1 site of the 1,2-dimethoxybenzene radical cation is disfavoured. By the mechanisms described in Scheme 7.3 and 7.4 above, this would lead to a lower yield of the 4-nitro aromatic compound **719** and consequently more of the 4-trinitromethyl aromatic compound **718**.

Photochemistry of 1,2-dimethoxybenzene and tetranitromethane in acetonitrile.

The observation of lower yields of trinitromethyl aromatic compound **718** and greater quantities of the nitro aromatic compound **719** in acetonitrile photolysis solution product mixtures than in the corresponding dichloromethane solution product mixtures appears to be the main feature of these reactions (Table 7.15, overleaf)

Table 7.15 - Overview of yields from the photolysis of 1,2-dimethoxybenzene (0.45 mol l⁻¹) and tetranitromethane (0.9 mol l⁻¹) in acetonitrile with or without added ethanol.

Reaction conditions	t/h	Conversion (%)	Yields (%)		
			718	719	720
AN/20°	1	22.9	3.8	96.2	-
	2	40.6	3.4	96.6	-
	3	58.7	3.4	96.6	-
AN/-20°	1	16.5	4.5	95.5	-
	2	34.5	3.0	97.0	-
	3	50.1	2.9	97.1	-
AN/20°/EtOH (8% v/v)	1	27.9	30.9	67.6	1.5
	2	49.1	30.6	66.9	2.5
	3	64.0	26.4	70.8	2.8



This appears reasonable given the similar observations for the anisole substrates discussed in Chapters 4-6. In the aprotic polar acetonitrile solvent the trinitromethanide ion will be less reactive, resulting in more ionic attack at C1 of the aromatic radical cation and consequently higher yields of the nitro aromatic compound **719**.

A significant increase in the yield of the trinitromethyl aromatic compound is observed when the photolysis reaction is performed in the presence of ethanol (8 % v/v). Solvation by ethanol of the attacking nucleophile, trinitromethanide ion, would lead to its attack at the less hindered C4-position

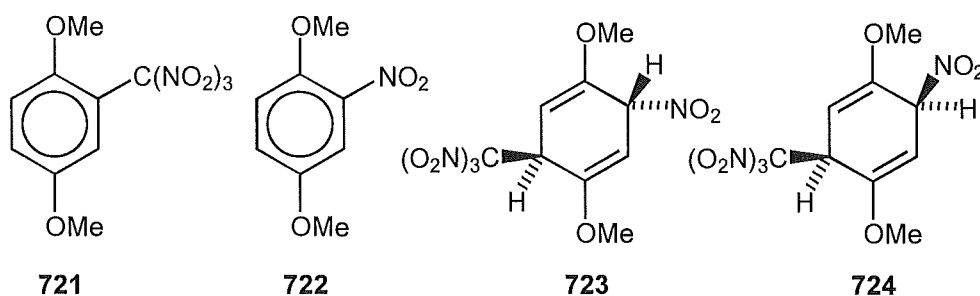
and the formation of the trinitromethyl compound **718**. Small quantities of the ethyl ester **720** were again observed in the ethanol reaction.

Photochemistry of 1,4-dimethoxybenzene and tetranitromethane in dichloromethane.

Photolysis of solutions of 1,4-dimethoxybenzene and tetranitromethane in dichloromethane gave mixtures consisting of 1,4-dimethoxy-2-nitrobenzene **722** and minor quantities of the epimeric adducts **723** and **724** (Table 7.16).

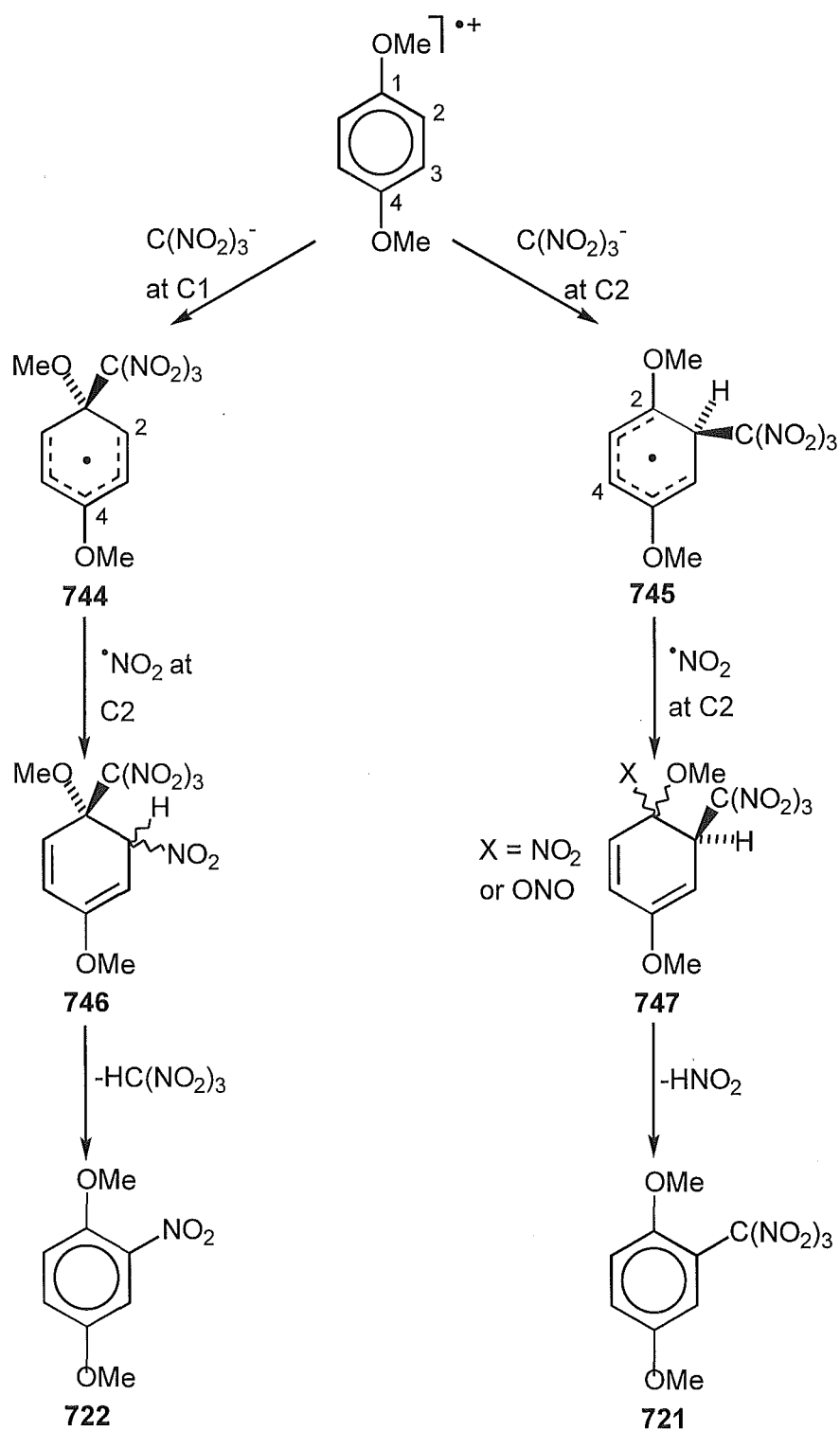
Table 7.16 - Overview of yields from the photolysis of 1,4-dimethoxybenzene (0.45 mol l^{-1}) and tetranitromethane (0.9 mol l^{-1}) in dichloromethane with or without added ethanol.

Reaction conditions	t/h	Conversion	Yields (%)			
			721	722	723	724
20°	1	36.6	-	96.4	3.6	tce
	2	74.0	-	96.5	3.1	0.4
	3	96.0	-	96.8	2.7	0.5
20°/EtOH (8% v/v)	3	56.0	9.8	80.5	8.3	1.5
	5	84.0	9.7	82.5	6.3	1.5
20°/EtOH (4% v/v)	2	61.0	11.4	81.0	6.4	1.1
	3	88.0	9.7	83.1	5.7	1.5



Similar reactions carried out in the presence of ethanol gave increased yields of the epimeric adduct pair **723** and **724** in addition to the appearance of the trinitromethyl aromatic compound **721**.

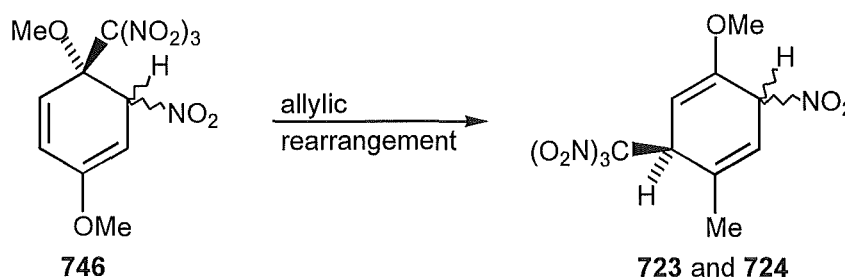
The mode of formation of the two aromatic compounds **721** and **722** is believed to be similar to that described above for the related compounds from 1,2-dimethoxybenzene *i.e.* by initial trinitromethanide ion attack at C1 or C2 of the 1,4-dimethoxybenzene radical cation to form the delocalised radical species **744** or **745** (Scheme 7.5).



Scheme 7.5

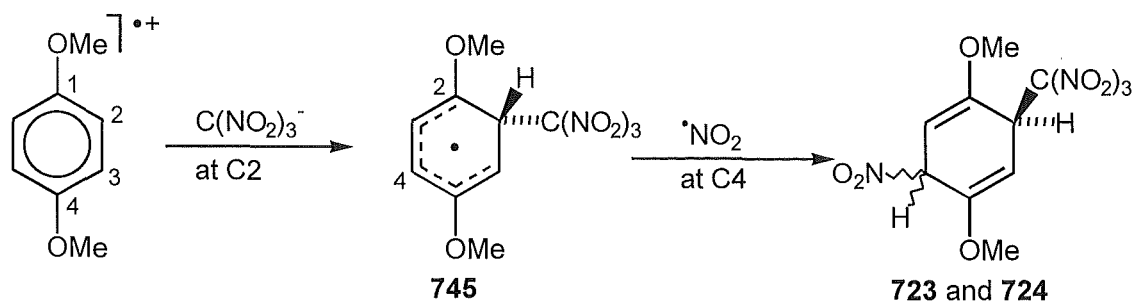
Subsequent nitrogen dioxide coupling at C2 of the allylic radical intermediates **744** and **745** would give the two unstable adducts **746** and **747**. Elimination of nitroform from adduct **746** would give the observed 1,4-dimethoxy-2-nitrobenzene **722** while elimination of nitrous acid from adduct **747** would give the observed 1,4-dimethoxy-2-trinitromethylbenzene **721**.

The precise mode of formation of the epimeric adduct pair **723** and **724** is unclear. However, given the modes of formation discussed in earlier chapters for similar adducts, two mechanisms could be proposed. The first involves the allylic rearrangement of the unstable intermediate **746** which was postulated in Scheme 7.5 (see Scheme 7.6).



Scheme 7.6

The second possible mode of formation of the adducts **723** and **724** is *via* nitrogen dioxide coupling at C4 of the delocalised radical **745**, in Scheme 7.5, which was formed by trinitromethanide ion addition to C2 of the 1,4-dimethoxybenzene aromatic radical cation (Scheme 7.7).



Scheme 7.7

The absence of the trinitromethyl aromatic compound **721** in the product mixtures of reactions performed without added ethanol can be rationalised in

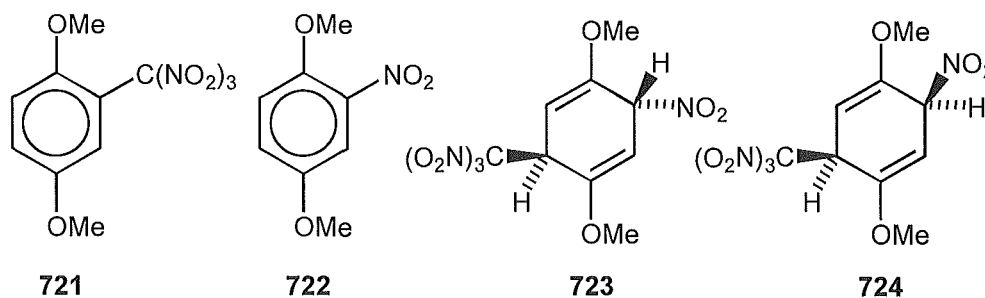
one of two manners. The first is the most simple and assumes that the highly unstable trinitromethyl compound **721** is formed in the dichloromethane photolysis reaction but undergoes a facile conversion into the nitro aromatic compound **722**. The presence of ethanol in the reaction medium serves to stabilise the trinitromethyl aromatic compound **721** allowing its observation under these conditions. The alternative explanation for the absence of the trinitromethyl compound **721** from the dichloromethane reaction mixture is a change in regiochemistry induced by the non-solvating dichloromethane solvent. This would allow more trinitromethanide ion attack at C1 of the 1,4-dimethoxybenzene radical cation and consequentially less (or no) formation of the trinitromethyl aromatic compound **721** in the photolysis reaction. The low yields of trinitromethyl compound **721** and adducts **723** and **724** under any photolysis conditions makes a clear distinction between these two mechanistic postulates difficult.

Photochemistry of 1,4-dimethoxybenzene and tetranitromethane in acetonitrile.

The photolysis of 1,4-dimethoxybenzene and tetranitromethane in acetonitrile solution at 20° gave almost exclusively 1,4-dimethoxy-2-nitrobenzene **722** with only trace quantities (<1 %) of the two adducts **723** and **724**. The addition of ethanol (8 % v/v) to the photolysis solutions did not appear to affect the observed product mixtures in any significant manner (Table 7.17, overleaf).

Table 7.17 - Overview of yields from the photolysis of 1,4-dimethoxybenzene (0.45 mol l⁻¹) and tetranitromethane (0.9 mol l⁻¹) in acetonitrile with and without added ethanol.

Reaction conditions	t/h	Conversion	Yields (%)			
			721	722	723	724
20°	1	42.7	-	100	tce	tce
	2	71.8	-	99.5	0.5	tce
	3	90.9	-	99.3	0.7	tce
	4	100	-	99.1	0.9	tce
20°/EtOH (8% v/v)	1	23.1	-	100	tce	tce
	2	52.5	-	100	tce	tce
	3	71.5	-	99.5	0.5	tce
	4	85.7	-	99.1	0.9	tce



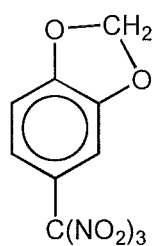
Photochemistry of 1,2-methylenedioxybenzene and tetranitromethane in dichloromethane.

Photolysis of dichloromethane solutions of 1,2-methylenedioxybenzene and tetranitromethane at 20°, -20°, and -40° gave mixtures of 1,2-methylenedioxy-4-nitrobenzene **730**, 1,2-methylenedioxy-4-trinitromethylbenzene **729**, and unknown aromatic compounds (Table 7.18, overleaf).

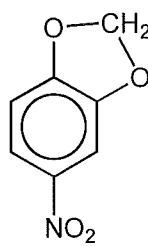
Table 7.18 - Overview of yields from the photolysis of 1,2-methylenedioxybenzene (0.5 mol l^{-1}) and tetranitromethane (1.0 mol l^{-1}) in dichloromethane.

Reaction conditions	t/h	Conversion (%)	Yields (%)			
			729	730	731	Unknowns
20°	1	35.9	31.7	65.3	-	3.0
	1.5	58.7	25.0	70.9	-	4.1
	2	66.1	19.2	75.3	-	5.5
-20° ^A	1	29.6	18.6	76.4	-	5.0
	1.5	41.8	12.1	83.5	-	4.4
	2	50.6	9.1	89.0	-	1.9
-40° ^A	1	32.2	10.3	86.2	-	3.4
	1.5	41.9	7.4	91.6	-	1.0
	2	39.4	9.9	87.9	-	2.2

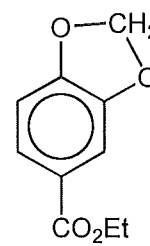
^A Solid precipitated in the reaction mixture after t = 1h



729

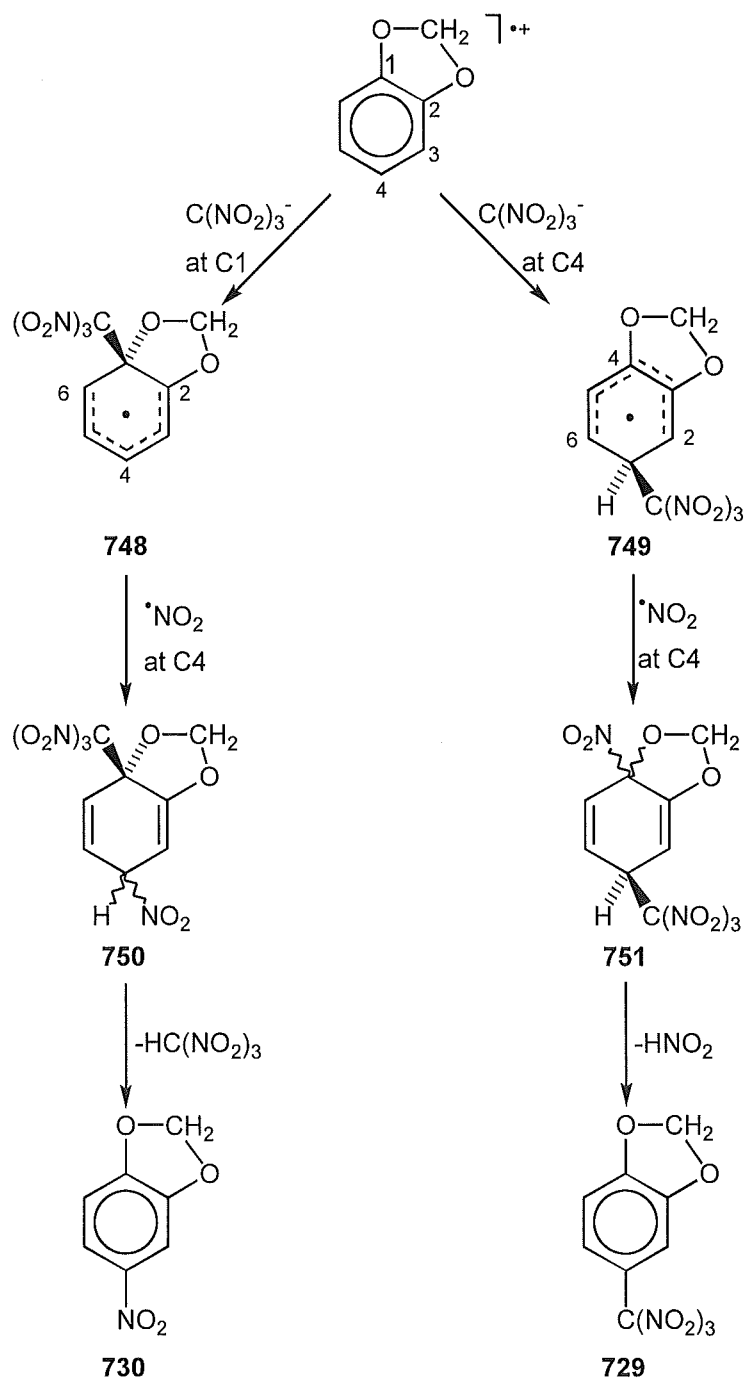


730



731

It appears likely that the aromatic compounds **729** and **730** are formed by mechanisms similar to those products discussed earlier for the related substrate 1,2-dimethoxybenzene (Scheme 7.4), *i.e.* by initial trinitromethanide ion attack at C1 or C4 of the aromatic radical cation to give the delocalised radical species **748** or **749** (Scheme 7.8, overleaf)



Scheme 7.8

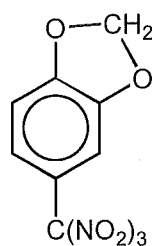
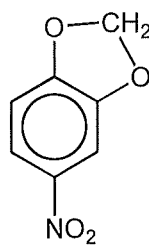
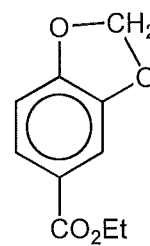
Subsequent nitrogen dioxide coupling at C4 of the delocalised radical species **748** would form the unstable adduct intermediates **750** and **751**. Loss of nitroform from intermediate **750** would give the observed 1,2-methylenedioxy-4-nitrobenzene **730**, while elimination of nitrous acid from diene **751** would give the observed 1,2-methylenedioxy-4-trinitromethylbenzene **729**.

However, it is clear that some decomposition of the trinitromethyl compound **729** to give the nitro aromatic compound **730** occurs during the

photolysis reaction. Addition of ethanol to the photolysis solution resulted in the apparent stabilisation of the trinitromethyl aromatic compound **729** and the formation of small amounts of ester **731**. The rate of the ethanol reactions was also markedly lower than the analogous reactions in dichloromethane (Table 7.19).

Table 7.19 - Overview of yields from the photolysis of 1,2-methylenedioxybenzene (0.5 mol l^{-1}) and tetranitromethane (1.0 mol l^{-1}) in dichloromethane with added ethanol.

Reaction conditions	t/h	Conversion (%)	Yields (%)			
			729	730	731	Unknowns
20°/EtOH (8% v/v)	3	18.7	61.5	18.5	7.7	12.3
	6	29.3	56.3	19.4	9.7	14.6
	10	49.9	59.9	19.2	9.0	12.0
20°/EtOH (4% v/v)	3	32.4	74.5	11.8	3.9	9.8
	6	42.3	68.0	16.7	4.5	10.9
	10	58.8	51.7	33.1	5.1	10.1

**729****730****731**

The lower rate of reaction in the presence of ethanol can be rationalised in terms of the solvation of the trinitromethanide ion by ethanol leading to slower addition of the trinitromethanide ion to the radical cation, thus affecting particularly attack at the sterically more hindered C1 site. The consequential increase in trinitromethanide ion attack at C4 is reflected in the increased yield of the trinitromethyl aromatic compound **729**.

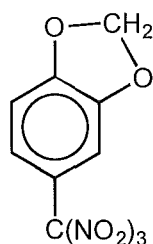
Photochemistry of 1,2-methylenedioxybenzene and tetranitromethane in acetonitrile.

Photolysis of 1,2-methylenedioxybenzene and tetranitromethane in acetonitrile solutions at 20° and -20° led to the exclusive formation of 1,2-methylenedioxy-4-nitrobenzene **730** (Table 7.20).

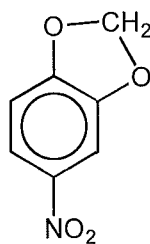
Table 7.20 - Overview of yields from the photolysis of 1,2-methylenedioxybenzene (0.5 mol l⁻¹) and tetranitromethane (1.0 mol l⁻¹) in acetonitrile with or without added ethanol (8 % v/v).

Reaction conditions	t/h	Conversion (%)	Yields (%)			
			729	730	731	Unknowns
20°	1	26.2	-	100	-	-
	1.5	43.0	-	100	-	-
	2	61.5	-	100	-	-
-20° ^A	1	29.1	-	100	-	-
	1.5	38.9	-	100	-	-
	2	32.9	-	100	-	-
20°/EtOH (8% v/v)	3	27.7	10.5	75.6	2.9	11.0
	6	34.8	12.3	72.1	4.9	10.7
	10	54.8	6.3	81.3	8.3	4.2

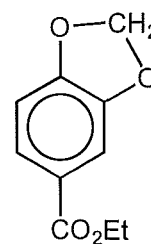
^A Solid precipitated in the reaction mixture after t = 1h



729



730



731

The addition of ethanol (8 % v/v) to the photolysis mixture results in the formation of small quantities of the trinitromethyl aromatic compound **729** and

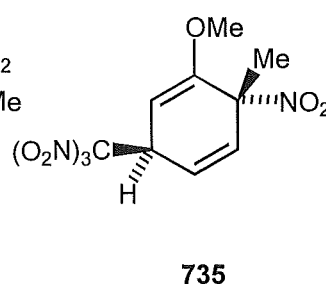
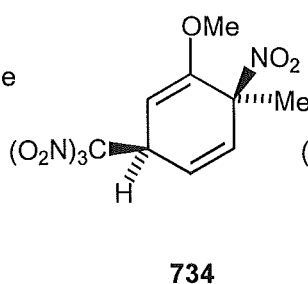
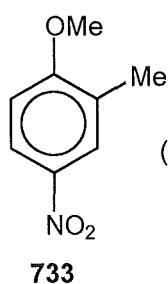
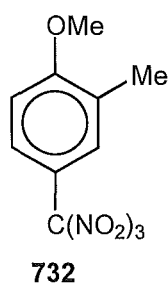
the ethyl ester **731**. As in the dichloromethane photolysis reactions, the added ethanol solvates the trinitromethanide ion, increasing the effective size of the nucleophile, resulting in less attack of the trinitromethanide ion at C1 of the radical cation. Consequentially the yield of the 4-nitro aromatic compound **730** is somewhat lower and concomitantly some of the 4-trinitromethyl aromatic compound **729** is formed.

Photochemistry of 2-methylanisole and tetranitromethane in dichloromethane with added ethanol.

The photolysis of 2-methylanisole and tetranitromethane in dichloromethane with added ethanol (8 % v/v) resulted in a mixture of products which differed only slightly from that observed for reaction in dichloromethane solutions (Table 7.21).

Table 7.21 - Overview of yields from the photolysis of 2-methylanisole (0.46 mol l⁻¹) and tetranitromethane (0.92 mol l⁻¹) in dichloromethane.

Reaction conditions	t/h	Conversion (%)	Yields (%)					
			Unknown			Unknown		
			732	733	Aromatics	734	735	Adducts
DCM/20°	0.5	N/A	78.2	9.8	5.5	1.9	4.6	-
	1	N/A	75.4	11.7	5.8	2.4	4.7	-
	2	21.4	70.7	17.4	5.2	2.2	4.5	-
	4	N/A	65.2	25.0	3.9	1.7	4.1	-
DCM/20°/EtOH	1	30.9	86.9	6.5	-	1.9	4.7	-
	2	60.0	87.6	7.0	-	1.2	4.1	-
	3	74.7	87.1	7.5	-	1.2	4.1	-



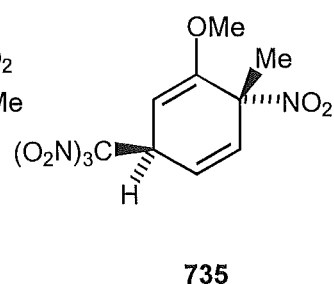
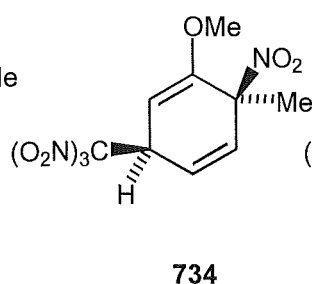
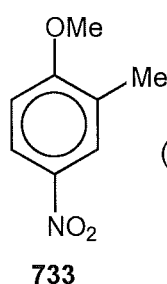
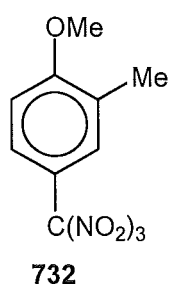
The major difference between the two product mixtures is the lack of conversion of the trinitromethyl aromatic compound **732** into the nitro aromatic compound **733** in the presence of ethanol. As with earlier examples of this effect, the lack of decomposition can be rationalised stabilisation of the trinitromethyl group by ethanol solvation reducing the driving force for the decay of the trinitromethyl function.

Photochemistry of 2-methylanisole and tetranitromethane in acetonitrile with added ethanol.

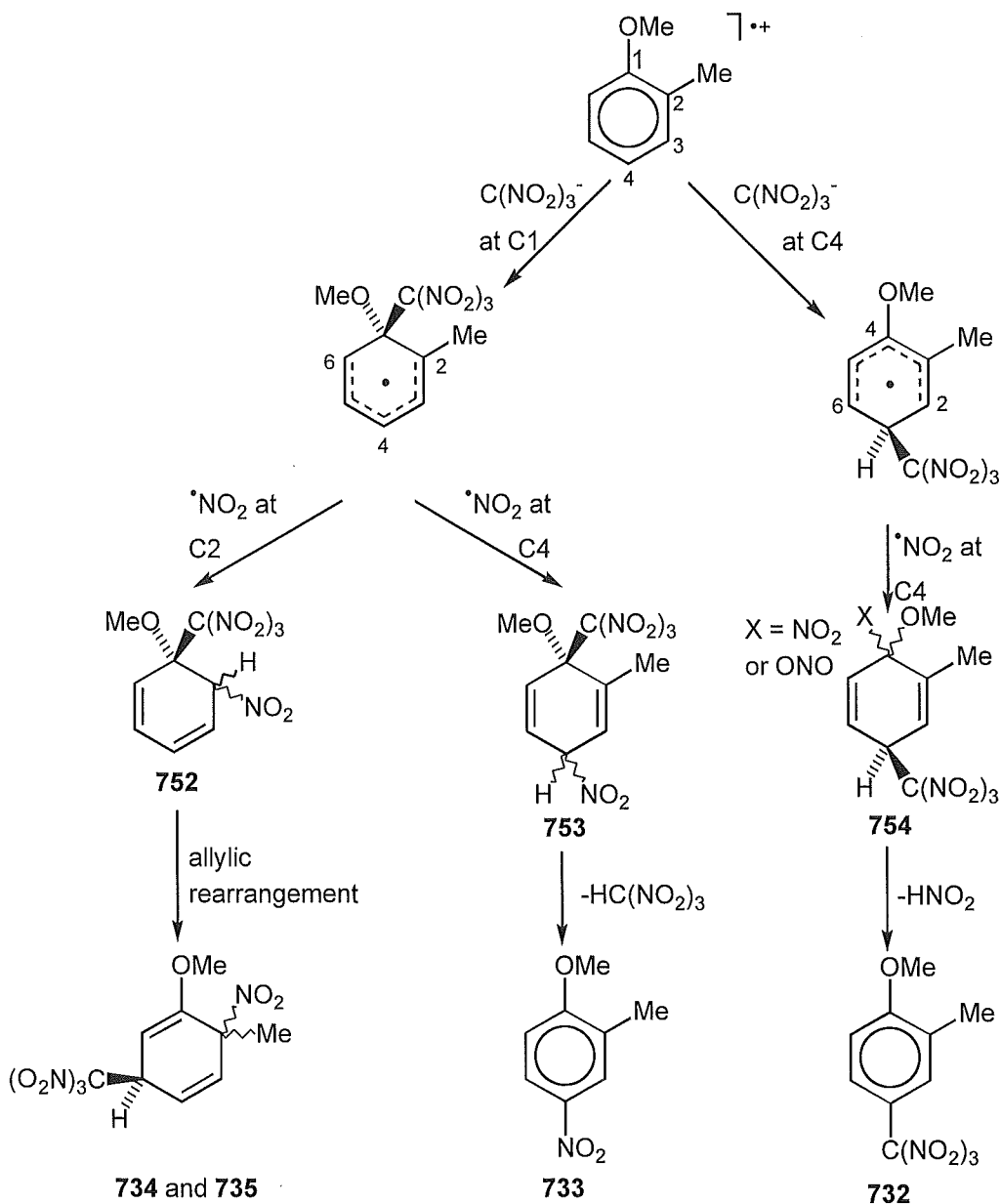
The photolysis of 2-methylanisole and tetranitromethane in acetonitrile with added ethanol (8 % v/v) resulted in a significantly different distribution of products from that observed in the photolysis reaction in acetonitrile solution (Table 7.22).

Table 7.22 - Overview of yields from the photolysis of 2-methylanisole (0.46 mol l⁻¹) and tetranitromethane (0.92 mol l⁻¹) in acetonitrile.

Reaction conditions	t/h	Conversion (%)	Yields (%)					
			Unknown Aromatics			Unknown Adducts		
			732	733		734	735	
AN/20°	0.5	N/A	35.2	37.9	3.8	4.3	16.1	2.7
	1	N/A	30.7	40.8	4.7	4.2	17.5	2.0
	2	N/A	26.0	43.3	5.7	4.3	18.3	2.4
	4	N/A	23.9	44.8	4.5	4.1	19.5	3.2
AN/20°/EtOH	1	16.6	81.2	12.6	-	1.1	5.0	-
	2	33.1	80.4	13.3	-	1.5	4.9	-
	3	49.2	73.7	21.2	-	1.5	3.6	-



A significant increase in the yield of the trinitromethyl aromatic compound **732** is accompanied by a decrease in the yields of both the nitro aromatic compound **733**, and the pair of epimeric adducts **734** and **735**. This observation is consistent with the proposed mode of formation of these products discussed in Chapter 5. The products **733**, **734**, and **735**, are all formed by initial attack of trinitromethanide ion at C1 in the radical cation of 2-methylanisole (Scheme 7.9). With the shift in the regiochemistry of initial trinitromethanide ion attack on the radical cation of 2-methylanisole toward C4, the formation of larger amounts of the trinitromethyl aromatic compound **732** would be expected.



Scheme 7.9

Summary

The addition of ethanol to solutions of tetranitromethane and methoxy substituted aromatic substrates did not achieve its intended purpose, namely the trapping of intermediate species in the decomposition processes of the trinitromethyl aromatic compounds formed in these reactions. Indeed in contrast, ethanol appears to slow the decomposition of the trinitromethyl aromatic compounds, presumably by hydrogen bonded solvation of the nitro groups on the trinitromethyl function. However, ethanol does influence the mechanistic pathway of the photolysis reaction by changing the regiochemistry of trinitromethanide ion attack on the aromatic radical cation presumably by solvation of the trinitromethanide ion. Solvation of the trinitromethanide ion would increase its effective size making ionic attack at the sterically hindered C1 position of methoxy radical cations unfavourable. Additionally this solvation has the effect of lowering the reactivity of the trinitromethanide ion, resulting in the observation of dehydrodimer among the reaction products of 1-methoxynaphthalene and tetranitromethane in the presence of ethanol and also a significant slowing of the overall reaction rate in some cases, e.g. the photolysis reactions of 1,2-methylenedioxybenzene and tetranitromethane.

References

- 1 Ebersson, L., Hartshorn, M. P., Radner, F., and Svensson, J. O., *Acta Chem. Scand.*, *in press*.
- 2 NIST/NBS Mass spectral library.
- 3 Sankararaman, S., and Kochi, J. K., *Recl. Trav. Chim. Pays-Bas.*, 1986, **105**, 278.
- 4 Ungnade, H. E., and Zilch, K. T., *J. Org. Chem.*, 1951, **16**, 68.

Experimental

General

Infrared spectra were recorded on a Shimadzu 8001PC FTIR spectrometer from liquid films, KBr disks or solution. ^1H , nOe, ^{13}C , and heteronuclear n.m.r. spectra were obtained in CDCl_3 using TMS as an internal standard on either a Varian XL-300 or Unity 300 spectrometer. All chemical shifts are expressed in part per million (ppm) downfield from TMS. Mass spectrometry was performed on a Kratos MS-80. Melting points were determined on a microscope slide and are uncorrected.

Preparative scale chromatography was carried out utilising a Chromatotron (a centrifugally accelerated, radial thin layer chromatograph. Model 7924, Harrison Research Inc.) equipped with rotors with Silica gel PF-254.

H.p.l.c. separation was achieved using a Varian 5000 liquid chromatograph equipped with an Alltech cyanopropyl column and Varian UV-50 detector.

The photonitration apparatus employed is shown in Figure 8.1

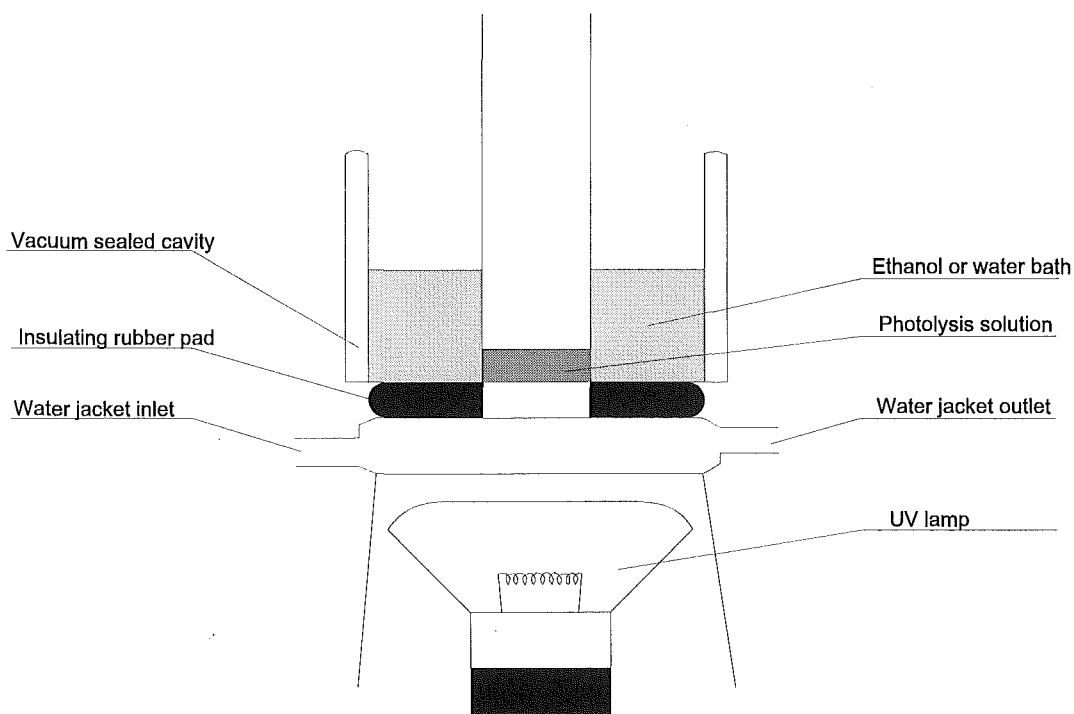


Figure 8.1

Tetranitromethane [C(NO₂)₄] was purchased from Aldrich.

WARNING while no incident was experienced in working with tetranitromethane, it should be noted that its mixtures with hydrocarbons are detonative within certain concentration limits and that due care should be taken in handling mixtures of tetranitromethane and organic compounds.

Experimental Data Relating to Chapter 2

1,5-Dimethylnaphthalene was purchased from Fluka A.G.

General procedure for the photonitration of 1,5-dimethylnaphthalene with tetranitromethane.

A solution of 1,5-dimethylnaphthalene (500 mg, equal to a 0.4 mol l⁻¹ solution) and tetranitromethane (0.8 mol l⁻¹) in dichloromethane (at 20°, -20°, -50°, or -78°) or acetonitrile (20° or -20°) was irradiated with filtered light (λ cut-off at 435 nm). Aliquots were withdrawn from the reaction mixture at appropriate time intervals, the volatile material removed rapidly under reduced pressure at $\leq 0^\circ$, and the product composition determined by n.m.r. spectral analysis (Table 8.2.1).

Reaction in dichloromethane at 20° and the identification of adducts 221-227 and 4,8-dimethyl-1-nitronaphthalene 220.

Reaction of 1,5-dimethylnaphthalene/tetranitromethane in dichloromethane at 20°, as above, for 1.5 h gave a product which was shown by ¹H n.m.r. spectra to be a mixture (Table 8.2.1) of adducts **221** (22 %), **222** (8 %), **223** (1.5 %), and **225** (14 %), cycloadducts **224** (9 %) and **226** (8 %), the nitronic ester **227** (1.5 %), adducts **228** and **229** (total 7 %), 4,8-dimethyl-1-nitronaphthalene **220** (20 %), and unidentified aromatic products (total 8 %). The adducts **221-227** and 4,8-dimethyl-1-nitronaphthalene **220** were partially separated by h.p.l.c. and gave in elution order:

1,5-Dimethyl-4-nitronaphthalene **220**. m.p. 90-92° (Literature m.p. 92-92.5°)¹ (Found: M⁺ 201.0793. C₁₂H₁₁NO₂ requires 201.0790). ¹H n.m.r. (CDCl₃) δ 2.55, s, 5-Me; 2.75, s, 1-Me; 7.32, br d, $J_{H5,H6}$ 8.3 Hz, H8; 7.47, br d, $J_{H7,H6}$ 6.8 Hz, H6; 7.51-7.59, m, H3, H7; 7.96, d, 8.3 Hz, H2. N.O.e. experiments gave the following results: irradiation at δ 2.55 gave an enhancement at δ 7.47 (2.9 %); irradiation at δ 2.75 gave enhancements at δ 7.32 (2.7 %) and at δ 7.96 (5.3 %).

4,8-Dimethyl-r-1-nitro-t-2-trinitromethyl-1,2-dihydronaphthalene 221, m.p. 68-70° (decomp.) (X-ray crystal structure determined below). ν_{\max} (KBr) 1616, 1576, 1560 cm^{-1} . ^1H n.m.r. (CDCl_3) δ 2.19, br s, 4-Me; 2.37, s, 8-Me; 5.45, d, $J_{\text{H}_2,\text{H}_3}$ 5.9 Hz, H2; 5.59, d, $J_{\text{H}_3,\text{H}_2}$ 5.9 Hz, 5.9 Hz, H3; 6.11, br s, H1; 7.29, m, H5, H7; 7.44, dd, $J_{\text{H}_6,\text{H}_5} \approx J_{\text{H}_6,\text{H}_7} \approx 7.6$ Hz, H6. Nuclear Overhauser enhancement experiments gave the following results: irradiation at δ 2.19 gave enhancements at δ 7.29 (5.1 %) and at δ 5.59 (6.1 %); irradiation at δ 2.37 gave enhancements at δ 6.11 (8.3 %) and at δ 7.29 (1.9 %); irradiation at δ 5.45 gave enhancements at δ 6.11 (4.6 %) and at δ 5.59 (6.4 %); irradiation at δ 5.59 gave enhancements at δ 5.45 (4.5 %) and at δ 2.19 (0.8 %); irradiation at δ 6.11 gave an enhancement at δ 2.37 (1.4 %); irradiation at δ 7.44 gave an enhancement at δ 7.29 (5.8 %). ^{13}C n.m.r. (CDCl_3) δ 18.9 (8-Me), 20.0 (4-Me), 40.8 (C2), 78.7 (C1), 110.4 (C3), 122.8, 131.6, 132.1 (C5, C6, C7), 121.9, 132.8, 139.7, 143.0, (C4, C4a, C8, C8a) resonance for $\text{C}(\text{NO}_2)_3$ not observed. The above assignments were confirmed by reverse detected heteronuclear correlation spectra (HMQC).

1,5-Dimethyl-r-1-nitro-t-4-trinitromethyl-1,4-dihydronaphthalene 222, m.p. 84-86° (decomp.) (X-ray crystal structure determined below). ν_{\max} (KBr) 1624, 1590, 1573, 1567 cm^{-1} . ^1H n.m.r. (CDCl_3) δ 2.03, s, 1-Me; 2.22, s, 5-Me; 5.78, d, $J_{\text{H}_4,\text{H}_3}$ 5.4 Hz, H4; 6.32, d, $J_{\text{H}_2,\text{H}_3}$ 10.3 Hz, H2; 6.40 (dd, $J_{\text{H}_3,\text{H}_2}$ 10.3 Hz, $J_{\text{H}_3,\text{H}_4}$ 5.4 Hz, H3; 7.21, m, H6; 7.34, m, H7, H8. Nuclear Overhauser enhancement experiments gave the following results: irradiation at δ 2.03 gave enhancements at δ 7.34 (7.3 %) and at δ 6.32 (6.1 %); irradiation at δ 2.22 gave enhancements at δ 5.78 (7.2 %) and at δ 7.21 (4.0 %); irradiation at δ 6.32 gave enhancements at δ 2.03 (0.9 %) and at δ 6.40 (7.1 %); irradiation at δ 6.40 gave enhancements at δ 5.78 (3.3 %) and at δ 6.32 (4.8 %). ^{13}C n.m.r. (CDCl_3) δ 19.9 (5-Me), 27.9 (1-Me), 42.5 (C4), 88.3 (C1), 122.4 (C3), 124.3, 130.1 (C7, C8); 132.3 (C6); 135.6 (C2); 123.3, 136.4, 138.3 (C4a, C5, C8a), resonance for $\text{C}(\text{NO}_2)_3$ not observed. The above assignments were confirmed by reverse detected heteronuclear correlation spectra (HMQC).

1,5-Dimethyl-*r*-1-nitro-*c*-4-trinitromethyl-1,4-dihydronaphthalene **223**, isolated only as an impure oil. ^1H n.m.r. (CDCl_3) δ 1.98, s, 1-Me; 2.28, s, 5-Me; 5.78, d, $J_{\text{H}_4,\text{H}_3}$ 4.4 Hz, H4; 6.52, m, H2, H3; 7.30-7.50, m, H6, H7; 7.80, d, $J_{\text{H}_8,\text{H}_7}$ 7.8 Hz, H8. ^{13}C n.m.r. (CDCl_3) δ 19.1 (5-Me), 31.1 (1-Me), 42.4 (C4), 86.6 (C1), 124.5, 135.5 (C2, C3), 126.5, 137.2 (C6, C7), 128.4 (C8), resonances for C4a, C8a, and $\text{C}(\text{NO}_2)_3$ not observed in poor quality spectrum. The above assignments were confirmed by reverse detected heteronuclear correlation spectra (HMBC, HMQC).

Nitro cycloadduct **224**, m.p. 168-170° (decomp.) (X-ray crystal structure determined below). ν_{max} (KBr) 1606, 1578, 1560 cm^{-1} . ^1H n.m.r. (CDCl_3) δ 2.03, s, 4-Me; 2.44, s, 8-Me; 5.45, dd, $J_{\text{H}_3,\text{H}_1}$ 2.0 Hz, $J_{\text{H}_3,\text{H}_2}$ 2.0 Hz, H3; 5.55, dd, $J_{\text{H}_1,\text{H}_2}$ 4.0 Hz, $J_{\text{H}_1,\text{H}_3}$ 2.0 Hz, H1; 5.68, dd, $J_{\text{H}_2,\text{H}_1}$ 4.0 Hz, $J_{\text{H}_2,\text{H}_3}$ 2.0 Hz, H2; 7.19-7.30, m, H5, H6, H7. Nuclear Overhauser enhancement experiments gave the following results: irradiation at δ 2.03 gave enhancements at δ 5.45 (6.9 %) and at δ 7.25 (4.9 %); irradiation at δ 2.44 gave enhancements at δ 5.55 (9.3 %) and at δ 7.25 (4.9 %); irradiation at δ 5.45 gave enhancements at δ 2.03 (0.8 %) and at δ 5.68 (2.6 %); irradiation at δ 5.55 gave enhancements at δ 2.44 (1.4 %) and at δ 5.68 (5.8 %); irradiation at δ 5.68 gave enhancements at δ 5.45 (1.9 %) and at δ 5.55 (4.6 %). ^{13}C n.m.r. (CDCl_3) δ 41.3 (C1), 79.4 (C2), 80.9 (C3), the remaining signals were not visible in a weak spectrum. The above assignments were confirmed by reverse detected heteronuclear correlation spectra (HMQC).

4,8-Dimethyl-*t*-2-trinitromethyl-1,2-dihydronaphthalen-*r*-1-ol **225**, isolated only as an impure oil. ^1H n.m.r. (CDCl_3) δ 2.20, br s, 4-Me; 2.40, s, 8-Me; 4.44, d, $J_{\text{H}_2,\text{H}_3}$ 5.3 Hz, H2; 5.24, br s, H1; 5.61, d, $J_{\text{H}_3,\text{H}_2}$ 5.3 Hz; the aromatic region was obscured by overlapping signals of impurities. Nuclear Overhauser enhancement experiments gave the following results: irradiation at δ 2.20 gave enhancements at δ 5.61 (6.5 %) and at δ 7.25 (4.6 %); irradiation at δ 2.40 gave enhancements at δ 5.24 (7.1 %) and at δ 7.20 (2.1 %); irradiation at δ 4.44 gave enhancements at δ 5.24 (2.2 %) and at δ 5.61 (3.9 %); irradiation at δ 5.24 gave enhancements at δ 2.40 (1.3 %) and at δ 4.44 (2.7 %); irradiation at δ 5.61 gave enhancements at δ 2.20 (0.6 %) and at δ 4.44 (3.4 %). ^{13}C n.m.r. (CDCl_3) δ 18.3

(4-Me), 20.3 (8-Me), 46.1 (C2), 63.4 (C1), 110.85 (C3), the remainder of the spectrum was obscured by signals due to impurities. The above assignments were confirmed by reverse detected heteronuclear correlation spectra (HMQC).

Hydroxy cycloadduct 226, m.p. 171-173° (decomp.) (X-ray crystal structure determined below). ν_{\max} (KBr) 3473, 1584 cm^{-1} . ^1H n.m.r. (CDCl_3) δ 1.93, s, 4-Me; 2.43, s, 8-Me; 4.65 (dd, $J_{\text{H}_3,\text{H}_2}$ 2.0 Hz, $J_{\text{H}_3,\text{H}_1}$ 2.0 Hz, H3), 4.90 (dd, $J_{\text{H}_2,\text{H}_1}$ 4.1 Hz, $J_{\text{H}_2,\text{H}_3}$ 2.0 Hz, H2), 5.08 (dd, $J_{\text{H}_1,\text{H}_2}$ 4.1 Hz, $J_{\text{H}_1,\text{H}_3}$ 2.0 Hz, H1), 7.25-7.35 (m, H5, H6, H7). Nuclear Overhauser enhancement experiments gave the following results: irradiation at δ 1.93 gave enhancements at δ 4.65 (1.7 %) and at δ 7.33 (2.0 %); irradiation at δ 2.43 gave an enhancement at δ 5.08 (4.5 %). ^{13}C n.m.r. (CDCl_3) δ 18.75 (8-Me), 21.45 (4-Me), 44.8 (C1), 67.0 (C2), 84.9 (C3), 122.5, 129.5 (C5,C6), 132.6 (C7), the remaining signals were not visible in a weak spectrum. The above assignments were confirmed by reverse detected heteronuclear correlation spectra (HMQC).

Nitronic ester 227, m.p. 157-159° (decomp.) (X-ray crystal structure determined²). ν_{\max} (KBr) 3490, 1612, 1560, 1283 cm^{-1} . ^1H n.m.r. (CDCl_3) δ 2.16 (s, 4-Me), 2.44 (s, 8-Me), 4.77 (br s, OH), 4.90 (dd, $J_{\text{H}_2,\text{H}_3}$ 3.9 Hz, $J_{\text{H}_2,\text{H}_1}$ 2.4 Hz, H2), 5.14 (d, $J_{\text{H}_3,\text{H}_2}$ 3.9 Hz, H3), 5.23 (br d, $J_{\text{H}_1,\text{H}_2}$ 2.4 Hz, H1), 7.37 (br d, $J_{\text{H}_7,\text{H}_6}$ 8.8 Hz, H7), 7.47 (dd, $J_{\text{H}_6,\text{H}_6}$ 8.3, $J_{\text{H}_6,\text{H}_7}$ 8.8 Hz, H6), 7.57 (br d, $J_{\text{H}_5,\text{H}_6}$ 8.3 Hz, H5). N.O.e. experiments gave the following results: irradiation at δ 2.16 gave enhancements at δ 5.14 (6.2 %) and at 7.57 (13.3 %); irradiation at δ 2.44 gave enhancements at δ 5.23 (7.0 %) and at 7.37 (3.9 %); irradiation at δ 4.90 gave enhancements at δ 5.14 (4.5 %) and at 5.23 (3.8 %). The ^{13}C n.m.r. spectrum could not be obtained because of the limited solubility of the nitronic ester **227**.

Reaction in Dichloromethane at -20° and the Identification of Adducts 228, 229 and 231, and 4,8-Dimethyl-2-trinitromethylnaphthalene 232.

Reaction of 1,5-dimethylnaphthalene/tetranitromethane in dichloromethane at -20°, as above, for 1.5 h gave a product which was shown by ^1H n.m.r. spectra to be a mixture (Table 8.2.1) of adducts **221** (14 %), **222** (6 %), **223** (2 %), and **225** (1 %), cycloadduct **226** (trace), the nitronic ester **227**

(trace), adduct **228** (20 %), adduct **229** (2 %), 4,8-dimethyl-1-nitronaphthalene **220** (46 %), and unidentified aromatic products (total 9 %). Adducts **228** and **229** were partially separated from this mixture by h.p.l.c.:

4,8-Dimethyl-*r*-1-nitro-*t*-4-trinitromethyl-1,4-dihydronaphthalene **228**, isolated only in admixture with adduct **221**. ^1H n.m.r. (CDCl_3) [by subtraction of the spectrum for adduct **221**] δ 2.25 (s, 4-Me), 2.29 (s, 8-Me), 6.26 (dd, $J_{\text{H1,H2}}$ 3.4 Hz, $J_{\text{H1,H3}}$ 2.0 Hz, H1), 6.48 (dd, $J_{\text{H2,H3}}$ 10.3 Hz, $J_{\text{H2,H1}}$ 3.4 Hz, H2), 6.70 (dd, $J_{\text{H3,H2}}$ 10.3 Hz, $J_{\text{H3,H1}}$ 2.0 Hz, H3), aromatic protons obscured. N.O.e. experiments gave the following results: irradiation at δ 6.26 gave an enhancement at δ 6.48 (1.0 %); irradiation at δ 6.48 gave enhancements at δ 6.26 (1.1 %) and at δ 6.70 (8.9 %); irradiation at δ 6.70 gave an enhancement at δ 6.48 (7.2 %).

4,8-Dimethyl-*r*-1-nitro-*c*-4-trinitromethyl-1,4-dihydronaphthalene **229**, isolated only in admixture with adduct **223**. ^1H n.m.r. (CDCl_3) [by subtraction of the spectrum for adduct **223**] δ 2.05 (s, 4-Me), 2.36 (s, 8-Me), 6.03 (br d, $J_{\text{H1,H2}}$ 5.4 Hz, H1), 6.70 (dd, $J_{\text{H3,H2}}$ 10.2 Hz, $J_{\text{H3,H1}}$ 1.0 Hz, H3), 6.79 (dd, $J_{\text{H2,H3}}$ 10.2 Hz, $J_{\text{H2,H1}}$ 5.4 Hz, H2), aromatic protons obscured. N.O.e. experiments gave the following results: irradiation at δ 6.03 gave an enhancement at δ 6.79 (3.8 %); irradiation at δ 6.70 gave an enhancement at δ 6.79 (9.5 %); irradiation at δ 6.79 gave enhancements at δ 6.70 (9.5 %) and at δ 6.03 (3.1 %). ^{13}C n.m.r. (CDCl_3) δ 19.9 (8-Me), 27.5 (4-Me), 49.1 (C4), 78.75 (C1), 126.5 (C3), 131.9 (C2), the remaining carbon resonances could not be identified with certainty for a mixture of adduct (9) with adduct (3). The above assignments were confirmed by reverse detected heteronuclear correlation spectra (HMQC).

A sample of the reaction mixture was also subjected to chromatography on a Chromatotron silica gel plate and allowed the separation of two further compounds, dinitro cycloadduct **231** and 4,8-dimethyl-2-trinitromethylnaphthalene **232** neither of which were present in the reaction mixture:

Dinitro cycloadduct 231, m.p. 120° (decomp.) (X-ray crystal structure determined below). ¹H n.m.r. (CDCl₃) δ 1.95 (s, 4-Me), 2.55 (s, 8-Me), 5.51 (dd, J_{H_3,H_2} 2.5 Hz, J_{H_3,H_1} 2.0 Hz, H3), 5.64 (dd, J_{H_1,H_2} 4.4 Hz, J_{H_1,H_3} 2.0 Hz, H1), 5.70 (dd, J_{H_2,H_1} 4.4 Hz, J_{H_2,H_3} 2.5 Hz, H2), 7.27 (d, J_{H_6,H_7} 8.3 Hz, H6), 7.35 (d, J_{H_7,H_6} 8.3 Hz, H7). N.O.e. experiments gave the following results: irradiation at δ 1.95 gave an enhancement at δ 5.51 (12.1 %); irradiation at δ 2.55 gave enhancements at δ 5.64 (8.1 %) and at δ 7.35 (4.8 %).

4,8-Dimethyl-2-trinitromethylnaphthalene **232**, isolated in low yield as a waxy solid (Found: M⁺, 305.06494. C₁₃H₁₁N₃O₆ requires 305.06478). ν_{\max} (liquid film) 1769, 1712, 1680, 1558 cm⁻¹. ¹H n.m.r. (CDCl₃) δ 2.72, 2.77 (s, 4-Me, 8-Me) 7.36 (br s, H1 or H3); 7.50 (d, $J_{H,H}$ 6.8 Hz, H5 or H7); 7.64 (dd, $J_{H,H}$ 8.3 Hz, $J_{H,H}$ 6.8 Hz, H6), 7.94 (d, $J_{H,H}$ 8.3 Hz, H7 or H5), 8.21 (d, $J_{H,H}$ 1.9 Hz, H3 or H1).

Reaction in Dichloromethane at -50° and Rearrangement Studies of the Epimeric 4,8-Dimethyl-1-nitro-4-trinitromethyl-1,4-dihydronaphthalenes 228 and 229.

Reaction of the 1,5-dimethylnaphthalene/tetranitromethane charge transfer complex in dichloromethane at -50°, as above, for 2 h gave a product which was shown by ¹H n.m.r. spectra to be a mixture (Table 8.2.1) of adducts **221** (12 %), **222** (11 %), adduct **228** (28 %), adduct **229** (4.5 %), unidentified adducts (12 %), 4,8-dimethyl-1-nitronaphthalene **220** (20 %), and unidentified aromatic products (total 10 %).

A solution of this reaction mixture in (D)-chloroform was stored at 22° in the dark and its ¹H n.m.r. spectrum monitored at appropriate time intervals. Under these conditions adducts **221**, **222**, and the unidentified adducts were stable, but adduct **228** was converted substantially into adduct **221**, with the formation of 4,8-dimethyl-1-nitronaphthalene **220** being probably a minor reaction pathway. The data are summarised in the plot of the significant product composition with time up to 25 h given in Figure 9.1 ; the rate constants were for the formation of adduct **221** 0.200(7) h⁻¹, and for the decay of adduct **228** 0.171(6) h⁻¹.

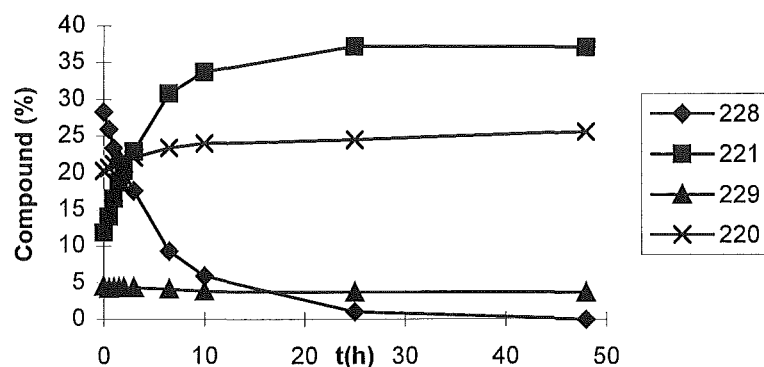


Figure 9.1 - Rearrangement study of adduct **228** in (D)-chloroform

A similar experiment, but in (D₂)-dichloromethane, resulted in the more rapid conversion of adduct **228** into adduct **221** (Figure 9.2, overleaf); the rate constants were for the formation of adduct **221** $0.67(2) \text{ h}^{-1}$, and for the decay of adduct **228** $0.77(2) \text{ h}^{-1}$.

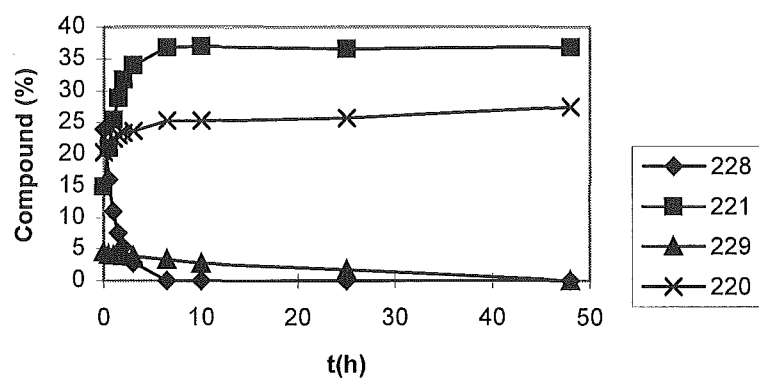


Figure 9.2 - Rearrangement study of adducts **228** and **229** in (D₂)-dichloromethane

In this latter experiment there was some indication that a minor reaction pathway for adduct **228** resulted in 4,8-dimethyl-1-nitronaphthalene **220** formation. At longer reaction times (48 h) adduct **229** was converted into 4,8-dimethyl-1-nitronaphthalene **220**.

Reaction in Dichloromethane at 20° in the Presence of Trifluoroacetic Acid (0.7 mol l⁻¹).

Reaction of the 1,5-dimethylnaphthalene/tetranitromethane charge transfer complex in dichloromethane at 20 °, as above except for the addition of trifluoroacetic acid (0.7 mol l⁻¹), for 3 h gave a product which was shown by ¹H n.m.r. spectra to be a mixture (Table 8.2.1) of adduct **228** (1 %), adduct **221** (3 %), unidentified adducts (1 %), 4,8-dimethyl-1-nitronaphthalene **220** (93 %), and unidentified aromatic products (total 1 %).

Reaction in 1,1,1,3,3,3-Hexafluoropropan-2-ol at 20°.

Reaction of the 1,5-dimethylnaphthalene/tetranitromethane charge transfer complex in 1,1,1,3,3,3-trifluoropropan-2-ol at 20°, as above, for 3 h gave a product which was shown by ¹H n.m.r. spectra to be a mixture (Table 8.2.1) of adduct **221** (20 %), unidentified adducts (4 %), 4,8-dimethyl-1-nitronaphthalene **220** (74 %), and unidentified aromatic products (total 3 %).

Product Yield Data

Table 8.2.1 - Overview of yields of products from the photolysis of 1,5-dimethylnaphthalene (0.4 mol l^{-1}) and tetranitromethane (0.8 mol l^{-1})

Reaction Conditions	t/h	Conver- sion (%)	Yields (%)											
			221	222	223	224	225	226	227	228	229	Adducts ^A	220	ArX ^A
DCM/+20°	1	62	23.3	9.2	2.3	9.1	16.2	7.7	2.3	2.7	1.5	74.3	20.2	25.7
	1.5	80	22.4	8.3	1.5	8.8	14.2	8.0	1.5	5.8	1.3	71.8	19.8	28.2
DCM/-20°	1	61	11.1	5.8	2.0	-	1.2	<.5	<.5	16.1	1.6	42.0	48.8	58.0
	1.5	85	13.6	6.1	1.7	-	0.9	<.5	<.5	19.8	1.8	44.9	46.2	54.8
DCM/-50°	1	65	12.1	10.5	-	-	-	-	-	30.5	4.5	69.9	24.4	30.1
	2	ca. 100	12.0	10.8	-	-	-	-	-	28.3	4.5	68.4	20.3	31.6
DCM/-78°	1	85	9.1	17.2	-	-	-	-	-	28.6	6.7	76.7	14.9	23.3
	2	97	9.2	16.3	-	-	-	-	-	26.7	4.3	73.6	15.7	26.4
AN/+20	1.5	82	16.3	14.3	4.6	-	-	-	-	-	-	35.8	53.4	64.1
	2.5	ca. 100	15.4	13.8	4.1	-	-	-	-	-	-	38.6	50.4	61.4
AN/-20	1.5	80	7.2	10.6	3.9	-	-	-	-	10.7	1.9	52.6	35.8	47.4
	2.5	ca. 100	9.5	10.6	5.0	-	-	-	-	10.6	1.8	48.3	37.7	51.7
DCM/TFA 20°	1	48	2.7	-	-	-	-	-	-	1.3	-	6.3	91.8	93.7
	1.5	58	2.7	-	-	-	-	-	-	1.0	-	5.7	92.5	94.3
	3	84	2.7	-	-	-	-	-	-	1.2	-	6.2	92.5	1.3
HFP/20°	1	32	14.6	-	-	-	-	-	-	-	-	17.4	76.8	82.6
	1.5	42	16.5	-	-	-	-	-	-	-	-	19.4	75.2	80.6
	3	69	19.7	-	-	-	-	-	-	-	-	23.6	73.7	76.3

^Atotal

Experimental Data Relating to Chapter 3

1-Methoxynaphthalene was purchased from Aldrich.

General procedure for the photonitration of 1-methoxynaphthalene with tetranitromethane.

A solution of 1-methoxynaphthalene (500 mg, 0.4 mol l⁻¹) and tetranitromethane (0.8 mol l⁻¹) in dichloromethane or acetonitrile was irradiated at +20°, -20°, -50° or -78° with filtered light ($\lambda_{\text{cut-off}} < 435$ nm). Aliquots were withdrawn from the reaction mixture at appropriate time intervals, the volatile material removed under reduced pressure at $\leq 0^\circ$, and the product composition determined by ¹H n.m.r. spectral analysis (Tables 8.3.1 and 8.3.2).

Reaction in dichloromethane at 20° and the identification of the aromatic products.

Reaction of 1-methoxynaphthalene-tetranitromethane in dichloromethane at 20°, as above, for 1 h gave a product which was shown by ¹H n.m.r. spectra to be a mixture (Table 8.3.1) of 1-methoxy-2-nitronaphthalene **305** (5 %), 1-methoxy-4-nitronaphthalene **306** (50 %), 1-methoxy-4-trinitromethylnaphthalene **309** (35 %), 4-methoxy-*r*-1-nitro-*t*-2-trinitromethyl-1,2-dihydronaphthalene **314** (6 %), and 4-methoxy-*r*-2-nitro-*t*-1-trinitromethyl-1,2-dihydronaphthalene **315** (3 %). The three aromatic compounds were separated by chromatography on a silica gel Chromatotron plate and gave in order of elution:

1-Methoxy-4-trinitromethylnaphthalene **309**, m.p. 192-194° (decomp.) (X-ray crystal structure determined, below). IR: $\nu(\text{max})$ (KBr) 1619, 1588, 1574 cm⁻¹. ¹H n.m.r. (CDCl₃) δ 4.11 (s, OMe), 6.87 (d, $J_{\text{H}_2, \text{H}_3}$ 8.8 Hz, H2), 7.28 (m, H5), 7.56 (d, $J_{\text{H}_3, \text{H}_2}$ 8.8 Hz, H3), 7.62 (m, H6, H7), 8.45 (m, H8). Nuclear Overhauser experiments gave the following results: irradiation at δ 6.87 gave enhancements at δ 4.11 (1.8 %) and at δ 7.56 (9.9 %); irradiation at δ 8.45 gave enhancements at δ 4.11 (1.7 %) and at δ 7.62 (1.3 %).

1-Methoxy-2-nitronaphthalene **305**, m.p. 78-80° (Literature³ m.p. 80°), identical with authentic material.

1-Methoxy-4-nitronaphthalene **306**, m.p. 83-84° (Literature³ 83-85°), identical with authentic material.

Neither of the adducts **314** and **315** could be isolated from the Chromatotron plate.

Extension of the reaction time for the reaction, above, to 2 h resulted in the precipitation of some 4-methoxy-1-naphthoic acid **308**, identified by comparison with an authentic sample.

*Reaction in dichloromethane at -20° and the identification of the nitro-trinitromethyl adducts **314** and **315**.*

Reaction of 1-methoxynaphthalene-tetranitromethane in dichloromethane at -20°, as above, for 1 h gave a product which was shown by ¹H n.m.r. spectra to be a mixture (Table 8.3.1) of 1-methoxy-2-nitronaphthalene **305** (3 %), 1-methoxy-4-nitronaphthalene **306** (47 %), 1-methoxy-4-trinitromethylnaphthalene **309** (34 %), 4-methoxy-*r*-1-nitro-*t*-2-trinitromethyl-1,2-dihydronaphthalene **314** (7 %), and 4-methoxy-*r*-2-nitro-*t*-1-trinitromethyl-1,2-dihydronaphthalene **315** (8 %). The two adducts **314** and **315** were labile in solution, the less stable adduct **315** having a half-life of ca. 4.5 h in (D)-chloroform at 23°. Although this lability precluded their isolation, the stability of the adducts was sufficient to allow their characterisation by n.m.r. techniques:

4-Methoxy-*r*-1-nitro-*t*-2-trinitromethyl-1,2-dihydronaphthalene **314**, ¹H n.m.r. (CDCl₃) δ 3.79 (s, OMe), 4.73 (dd, J_{H_3,H_2} 6.4 Hz, J_{H_3,H_1} 1.5 Hz, H3), 5.50 (d, J_{H_2,H_3} 6.4 Hz, H2), 5.79 (br s, H1), the remainder of the spectrum was obscured by signals of the other components of the mixture. Nuclear Overhauser experiments gave the following results: irradiation at δ 4.73 gave enhancements at δ 3.79 (2.1 %) and at δ 5.50 (3.9 %) ¹³C n.m.r. (CDCl₃) δ 41.67 (C2), 81.84 (C1), 82.36 (C3), the remainder of the spectrum was

obscured by signals of the other components of the mixture. The above assignments were confirmed by reverse detected heteronuclear correlation spectra (HMQC).

4-Methoxy-*r*-2-nitro-*t*-1-trinitromethyl-1,2-dihydronaphthalene **315**, ^1H n.m.r. (CDCl_3) δ 3.75 (s, OMe), 4.48 (dd, $J_{\text{H}_3,\text{H}_2}$ 6.8 Hz, $J_{\text{H}_3,\text{H}_1}$ 1.0 Hz, H3), 5.22 (d, $J_{\text{H}_2,\text{H}_3}$ 6.8 Hz, H2), 5.42 (br s, H1), the remainder of the spectrum was obscured by signals of the other components of the mixture. Nuclear Overhauser experiments gave the following results: irradiation at δ 4.48 gave enhancements at δ 3.75 (1.4 %) and at δ 5.22 (3.8 %); irradiation at δ 5.22 gave enhancements at δ 4.48 (5.0 %) and at δ 5.42 (3.2 %). ^{13}C n.m.r. (CDCl_3) δ 44.88 (C1), the remainder of the spectrum was obscured by signals of the other components of the mixture. The above assignment was confirmed by reverse detected heteronuclear correlation spectra (HMQC).

*Reaction in dichloromethane containing trifluoroacetic acid (0.8 mol l⁻¹) at 20° and the identification of 4,4'-dimethoxy-1,1'-binaphthyl **319**.*

Reaction of 1-methoxynaphthalene-tetranitromethane, as above, but in dichloromethane containing trifluoroacetic acid (0.8 mol l⁻¹) at 20° for 15 min. gave a product shown (^1H n.m.r.) to be essentially a mixture of 1-methoxynaphthalene (73 %) and 4,4'-dimethoxy-1,1'-binaphthyl **319** (27 %) (Table 8.3.3). The dimer **319** was isolated by crystallisation (dichloromethane) to give 4,4'-dimethoxy-1,1'-binaphthyl, m.p. 264-266° (Literature⁴ 252-254°) (X-ray crystal structure determined, below). IR: ν_{max} (KBr) 1264, 1239, 1084 cm⁻¹. ^1H n.m.r. (CDCl_3) δ 4.09 (s, OMe), 6.92 (d, $J_{\text{H}_3,\text{H}_2}$ 7.8 Hz, H3), 7.30 (dd, $J_{\text{H}_7,\text{H}_8}$ 7.4 Hz, $J_{\text{H}_7,\text{H}_6}$ 6.4 Hz, H7), 7.38 (d, $J_{\text{H}_2,\text{H}_3}$ 7.8 Hz, H2), 7.38 (d, $J_{\text{H}_8,\text{H}_7}$ 7.4 Hz, H8), 7.46 (dd, $J_{\text{H}_6,\text{H}_5}$ 8.3 Hz, $J_{\text{H}_6,\text{H}_7}$ 6.4 Hz, H6), 8.36 (d, $J_{\text{H}_5,\text{H}_6}$ 8.3 Hz, H5). Nuclear Overhauser experiments gave the following results: irradiation at δ 4.09 gave an enhancement at δ 6.92 (3.9 %); irradiation at δ 6.92 gave

enhancements at δ 4.09 (0.6 %) and at δ 7.38 (1.9 %); irradiation at δ 8.36 gave enhancements at δ 4.09 (0.15 %) and at δ 7.46 (0.5 %).

Product Yield Data

Table 8.3.1 - Overview of yields from the photolysis of 1-methoxynaphthalene (0.4 mol l⁻¹) and tetranitromethane (0.8 mol l⁻¹) in dichloromethane.

t/h	Conversion(%)	Yield (%)							Unknowns
		305	306	308	309	314	315	319	
DCM/20°									
0.25	36.5	2.0	38.2	-	41.3	7.4	11.0	-	-
0.5	68.2	3.0	41.7	-	41.7	6.2	7.7	-	-
1	~100	5.2	50.4	-	34.6	6.3	3.3	-	-
2	100	7.3	57.4	4.8	24.1	6.5	-	-	-
DCM/-20°									
0.5	53.8	2.0	42.2	-	40.7	6.3	8.6	-	-
1	92.6	3.1	47.4	-	34.3	7.2	8.0	-	-
2	100	5.1	61.4	-	21.4	10.2	2.0	-	-
DCM/-50°									
0.5	40	2.0	42.6	-	40.0	5.8	12.0	-	-
1	60	3.7	55.4	-	30.1	6.3	4.7	-	-
2	90.5	4.3	70.2	-	17.3	6.4	1.7	-	-
4	100	5.5	89.3	-	~0	5.3	~0	-	-
DCM/-78°									
0.25	38.9	5.0	24.3	-	42.7	4.2	9.7	11.3	2.7
0.5	77.5	4.7	37.0	-	36.5	2.9	6.8	7.8	4.2
1	85.0	4.7	37.0	-	11.5	2.9	2.4	~0	12.4

Table 8.3.2 - Overview of yields from the photolysis of 1-methoxynaphthalene (0.4 mol l^{-1}) and tetranitromethane (0.8 mol l^{-1}) in acetonitrile.

t/h	Conversion(%)	Yield (%)							
		305	306	308	309	314	315	319	Unknowns
DCM/20°									
0.25	23.6	3.2	42.0	-	49.5	2.7	2.0	-	-
0.5	47.1	4.1	50.5	-	38.8	3.3	3.3	-	-
1	88.0	4.3	54.1	-	38.0	2.2	1.4	-	-
2	100	5.0	75.5	-	17.5	1.3	0.7	-	-
DCM/-20°									
0.5	19.1	18.8	51.0	-	30.2	-	-	-	-
1	36.3	18.3	58.5	-	23.2	-	-	-	-
2	66.9	19.3	63.1	-	17.6	-	-	-	-

Table 8.3.3 - Overview of yields of products from the photolysis of 1-methoxynaphthalene (0.4 mol l^{-1}) and tetranitromethane (0.8 mol l^{-1}) in dichloromethane with added trifluoroacetic acid (0.8 mol l^{-1}).

Reaction		Yield (%)			
Conditions	t/h	Conversion (%)	306	319	Nitrodimers
20°	0.08	14.9	Trace	~100	-
	0.25	26.8	Trace	~100	Trace
	0.50	59.2	14.5	85.5	Trace
-50°	0.08	38.3	Trace	~100	Trace
	0.25	60.3	Trace	95	5
	0.50	100	Trace	88.1	11.9

Experimental Data relating to Chapter 4

4-Methylanisole was purchased from Aldrich.

General procedure for the photonitration of 4-methylanisole with tetranitromethane.

A solution of 4-methylanisole (500 mg, 0.51 mol l⁻¹) and tetranitromethane (1.02 mol l⁻¹) in dichloromethane (at 20°, -20° or -50°) or acetonitrile (20°, -20° or -50°) was irradiated with filtered light ($\lambda_{\text{cut-off}} < 435$ nm). Aliquots were withdrawn from the reaction mixture at appropriate time intervals, the volatile material removed rapidly under reduced pressure at $\leq 0^\circ$, and the product composition determined by n.m.r. spectral analysis (Tables 8.4.1 and 8.4.2).

Reaction in dichloromethane at 20° and the identification of adducts 421-424 aromatic products 419, 420, 425, and 427, and 4-methyl-4-nitro-cyclohexa-2,5-dienone 426.

Reaction of 4-methylanisole-tetranitromethane in dichloromethane at 20°, as above, for 1 h gave a product which was shown by ¹H n.m.r. spectra to be a mixture (Table 8.4.1) of adducts **421** (11 %), **422** (3 %), **423** (2 %), and **424** (2 %), 4-methyl-2-trinitromethylanisole **419** (47 %), 4-methyl-2-nitroanisole **420** (10 %), 4-methyl-2,6-dinitrophenol **425** (10 %), 4-methyl-4-nitrocyclohexa-2,5-dienone **426** (3 %), 4-methyl-2-nitrophenol **427** (1 %), and other unidentified materials (total 11 %). These products were partially separated by h.p.l.c. and gave the following in elution order:

1-methoxy-4-methyl-r-3-nitro-t-6-trinitromethylcyclohexa-1,4-diene 422, isolated only in admixture with 1-methoxy-4-methyl-t-6-nitro-r-3-trinitromethylcyclohexa-1,4-diene **423**, ¹H n.m.r. (CDCl₃) δ 1.90 (br s, 4-Me), 3.64 (s, OMe), 4.96 (dddq, $J_{\text{H}_6, \text{H}_2}$ 1.0 Hz, $J_{\text{H}_6, \text{H}_3}$ 4.9 Hz, $J_{\text{H}_6, 4\text{-Me}}$ 1.5 Hz, $J_{\text{H}_6, \text{H}_5}$ 2.9 Hz, H6), 5.26 (dd, $J_{\text{H}_2, \text{H}_3}$ 3.9 Hz, $J_{\text{H}_2, \text{H}_6}$ 1.0 Hz, H2), 5.57 (dd, $J_{\text{H}_3, \text{H}_2}$ 3.9 Hz, $J_{\text{H}_3, \text{H}_6}$ 4.9 Hz, H3), 5.99 (dq, $J_{\text{H}_5, 4\text{-Me}}$ 1.5 Hz, $J_{\text{H}_5, \text{H}_6}$ 2.9 Hz, H5). Nuclear Overhauser experiments gave the following results: irradiation at δ 1.90 gave enhancements at δ 5.57

(3.3 %) and at δ 5.99 (4.0 %); irradiation at δ 3.64 gave an enhancement at δ 5.26 (10.5 %); irradiation at δ 4.96 gave an enhancement at δ 5.99 (3.1 %); irradiation at δ 5.26 gave enhancements at δ 3.64 (0.6 %) and at δ 5.57 (4.3 %); irradiation at δ 5.57 gave an enhancement at δ 5.26 (2.0 %); irradiation at δ 5.99 gave enhancements at δ 1.90 (0.3 %) and at δ 4.96 (3.8 %). ^{13}C n.m.r. (CDCl_3) δ 44.1 (C6), 55.9 (OMe), 85.9 (C3), 95.1 (C2), 119.2 (C5), resonances for 4- CH_3 , C1 and C4 were not assigned in the spectrum of the mixture of adducts **422** and **423**. The above assignments were confirmed by reverse detected heteronuclear correlation spectra (HMQC).

1-methoxy-4-methyl-t-6-nitro-r-3-trinitromethylcyclohexa-1,4-diene **423**, isolated only in admixture with 1-methoxy-4-methyl-r-3-nitro-t-6-trinitromethylcyclohexa-1,4-diene **422**, ^1H n.m.r. (CDCl_3) δ 1.90 (br s, 4-Me), 3.64 (s, OMe), 4.93 (ddd, $J_{\text{H}_3,\text{H}_2}$ 4.4 Hz, $J_{\text{H}_3,\text{H}_5}$ 1.0 Hz, $J_{\text{H}_3,\text{H}_6}$ 4.9 Hz, H3), 5.10 (dd, $J_{\text{H}_2,\text{H}_3}$ 4.4 Hz, $J_{\text{H}_2,\text{H}_6}$ 1.0 Hz, H2), 5.49 (ddd, $J_{\text{H}_6,\text{H}_2}$ 1.0 Hz, $J_{\text{H}_6,\text{H}_3}$ 4.9 Hz, $J_{\text{H}_6,\text{H}_5}$ 2.9 Hz, H6), 6.04 (ddq, $J_{\text{H}_5,\text{H}_3}$ 1.0 Hz, $J_{\text{H}_5,\text{H}_6}$ 2.9 Hz, $J_{\text{H}_5,4\text{-Me}}$ 1.5 Hz, H5). Nuclear Overhauser experiments gave the following results: irradiation at δ 1.90 gave enhancements at δ 4.93 (4.0 %) and at δ 6.04 (6.3 %); irradiation at δ 3.64 gave an enhancement at δ 5.10 (11.5 %); irradiation at δ 4.93 gave an enhancement at δ 5.10 (3.2 %); irradiation at δ 5.10 gave an enhancement at δ 4.93 (3.5 %); irradiation at δ 5.49 gave an enhancement at δ 6.04 (1.0 %). ^{13}C n.m.r. (CDCl_3) δ 47.1 (C3), 55.8 (OMe), 81.9 (C6), 91.3 (C2), 126.1 (C5), resonances for 4- CH_3 , C1 and C4 were not assigned in the spectrum of the mixture of adducts **422** and **423**. The above assignments were confirmed by reverse detected heteronuclear correlation spectra (HMQC).

4-methyl-2,6-dinitrophenol **425**, isolated only in admixture with adducts **421**, **423**, and **424**, and identified by comparison of its ^1H n.m.r. spectrum with that of authentic material.

1-methoxy-4-methyl-c-6-nitro-r-3-trinitromethylcyclohexa-1,4-diene **424**, isolated only in admixture with 1-methoxy-4-methyl-r-3-nitro-c-6-trinitromethylcyclohexa-1,4-diene **421**, ^1H n.m.r. (CDCl_3) δ 1.81 (s, 4-Me), 3.60 (s, OMe),

4.88 (dd, J_{H_3,H_6} 2.9 Hz, J_{H_3,H_2} 4.4 Hz, H3), 5.27 (d, J_{H_2,H_3} 4.4 Hz, H2), 5.38 (dd, J_{H_6,H_5} 5.4 Hz, J_{H_6,H_3} 2.9 Hz, H6), 6.18 (dq, J_{H_5,H_6} 5.4 Hz, $J_{H_5,4-Me}$ 1.5 Hz, H5). Nuclear Overhauser experiments gave the following results: irradiation at δ 1.81 gave enhancements at δ 4.88 (6.5 %) and at δ 6.18 (8.5 %); irradiation at δ 3.60 gave an enhancement at δ 5.27 (18.6 %); irradiation at δ 4.88 gave enhancements at δ 5.27 (4.8 %) and at δ 1.81 (1.2 %); irradiation at δ 5.27 gave enhancements at δ 3.60 (1.5 %) and at δ 4.88 (4.7 %); irradiation at δ 5.38 gave an enhancement at δ 6.18 (2.6 %). ^{13}C n.m.r. (CDCl_3) δ 21.6 (4-Me), 46.8 (C3), 55.9 (OMe), 80.9 (C6), 93.0 (C2), 124.7 (C5), resonances for C1 and C4 were not assigned in the spectrum of the mixture of adducts **421** and **424**. The above assignments were confirmed by reverse detected heteronuclear correlation spectra (HMQC).

1-methoxy-4-methyl-r-3-nitro-c-6-trinitromethylcyclohexa-1,4-diene **421**, m.p. 58-60 °C (decomp.) (X-ray crystal structure determined, see below). IR: ν_{max} (KBr) 1664, 1622, 1600, 1561 cm^{-1} . ^1H n.m.r. (CDCl_3) δ 1.80 (d, J_{4-Me,H_5} 1.5 Hz, 4-Me), 3.57 (s, OMe), 4.80 (dddq, J_{H_6,H_2} 1.9 Hz, J_{H_6,H_3} 4.9 Hz, J_{H_6,H_5} 3.9 Hz, $J_{H_6,4-Me}$ 1.7 Hz, H6), 5.36 (dd, J_{H_2,H_3} 4.8 Hz, J_{H_2,H_6} 1.9 Hz, H2), 5.44 (dd, J_{H_3,H_2} 4.8 Hz, J_{H_3,H_6} 4.9 Hz, H3), 6.11 (dq, J_{H_5,H_6} 3.9 Hz, $J_{H_5,4-Me}$ 1.5 Hz, H5). Nuclear Overhauser experiments gave the following results: irradiation at δ 1.90 gave enhancements at δ 5.44 (4.4 %) and at δ 6.11 (5.7 %); irradiation at δ 3.57 gave an enhancement at δ 5.36 (10.0 %); irradiation at δ 4.80 gave an enhancement at δ 6.11 (2.1 %); irradiation at δ 5.36 gave enhancements at δ 3.57 (1.4 %) and at δ 5.44 (2.4 %); irradiation at δ 5.44 gave enhancements at δ 5.36 (1.2 %) and at δ 1.90 (0.5 %); irradiation at δ 6.11 gave enhancements at δ 1.90 (0.7 %) and at δ 4.80 (3.9 %). ^{13}C n.m.r. (CDCl_3) δ 21.0 (4-Me), 44.6 (C6), 56.2 (OMe), 84.8 (C3), 95.5 (C2), 119.0 (C5), 135.6 (C4), 152.0 (C1), resonance for $\text{C}(\text{NO}_2)_3$ not observed. The above assignments were confirmed by reverse detected heteronuclear correlation spectra (HMQC).

4-methyl-4-nitrocyclohexa-2,5-dienone **426**, obtained only in admixture with adduct **421**, and identified by comparison of its ^1H n.m.r. spectrum with that of authentic material.

From a separate photolysis reaction at 20° in dichloromethane the crude reaction product was crystallised from dichloromethane-hexane to give:-

4-methyl-2-trinitromethylanisole **419**, m.p. 105-107°; ¹H n.m.r. (CDCl₃) δ 2.35 (s, 4-Me), 3.80 (s, OMe), 7.00 (d, J_{H_6,H_5} 8.8 Hz, H6), 7.05 (s, H3), 7.49 (d, J_{H_5,H_6} 8.8 Hz, H5)].⁵

From a separate photolysis reaction at -50° in dichloromethane the crude reaction mixture was adsorbed onto a silica gel Chromatotron plate. Elution with pentane and pentane-ether mixtures gave:

4-methyl-2-nitrophenol **427**, ¹H n.m.r. (CDCl₃) δ 2.35 (s, Me), 7.06 (d, J_{H_6,H_5} 8.8 Hz, H6), 7.40 (dd, J_{H_5,H_3} 1.9 Hz, J_{H_5,H_6} 8.8 Hz, H5), 7.90 (d, J_{H_3,H_5} 1.9 Hz, H3), 10.45 (s, OH), identical with authentic material.

4-methyl-2-nitroanisole **420**, ¹H n.m.r. (CDCl₃) δ 2.34 (s, Me), 3.93 (s, OMe), 6.98 (d, J_{H_6,H_5} 9.3 Hz, H6), 7.35 (dd, J_{H_5,H_3} 1.9 Hz, J_{H_5,H_6} 9.3 Hz, H5), 7.65 (d, J_{H_3,H_5} 1.9 Hz, H3), identical with authentic material.

Product Yield Data

Table 8.4.1 - Overview of product yields from the photolysis of 4-methylanisole **413** (0.51 mol l^{-1}) with tetranitromethane (1.02 mol l^{-1}) in dichloromethane^A

t/h	Yields (%)											
	421	422	423	424	Unknown Adducts	419	420	425	426	427	Unknown Aromatics	
20°												
.5	12.6	9.8	2.4	1.6	3.1	44.3	7.1	6.3	3.1	1.0	8.7	
1	10.9	3.2	1.9	2.2	2.3	47.1	9.7	10.0	2.8	1.1	8.8	
2	6.4	-	2.1	2.0	2.1	51.8	12.1	13.3	2.1	0.8	7.2	
-20°												
0.5	2.5	2.5	2.5	3.4	1.1	19.6	29.6	-	29.1	2.5	5.0	
1	2.5	1.9	2.0	^B	10.6	14.0	36.7	-	24.8	2.3	3.8	
2	2.9	1.6	2.1	^B	15.7	13.3	32.5	-	26.0	2.4	3.3	
-50°												
0.5	-	-	3.4	3.5	12.8	10.5	34.9	-	29.3	1.7	3.8	
1	-	-	2.2	3.1	15.4	9.7	35.5	-	27.8	1.6	4.6	
2	-	-	3.3	3.8	12.3	8.4	41.0	-	22.6	1.8	6.7	

^A Conversions not quoted due to substrate volatility during work-up^B Unreliable integral due to overlapping ¹H n.m.r. resonances

Table 8.4.2 - Overview of yields of products from the photolysis of 4-methylanisole **413** (0.51 mol l⁻¹) with tetranitromethane (1.02 mol l⁻¹) in acetonitrile^A

t/h	Yields (%)										
	421	422	423	424	Unknown Adducts	419	420	425	426	427	Unknown Aromatics
20°											
.5	-	-	-	-	6.8	5.4	50.8	2.2	19.0	6.1	8.6
1	-	-	-	-	0.8	4.7	49.5	4.1	23.6	9.3	7.2
2	-	-	-	-	0.4	4.3	45.1	11.3	16.2	16.2	4.8
-20°											
0.5	-	-	0.8	1.1	8.7	8.7	34.8	-	34.3	4.3	6.7
1	-	-	0.8	0.8	7.6	9.0	42.5	-	29.7	3.6	3.7
2	-	-	1.7	^B	7.6	7.1	47.2	-	28.9	2.2	3.7
-50°											
0.5	-	-	1.4	1.5	2.1	14.5	29.5	-	38.7	1.9	10.4
1	-	-	1.5	1.3	4.6	13.0	35.5	-	39.1	2.0	2.8
2	-	-	1.4	1.7	4.0	10.9	36.6	-	37.7	2.2	6.4

^A Conversions not quoted due to substrate volatility during work-up

^B Unreliable integral due to overlapping ¹H n.m.r. resonances

Experimental Data Relating to Chapter 5

2-Methylanisole and 2,4-dimethylanisole were purchased from Aldrich.

General procedure for the photonitration of 2-methylanisole 514 with tetranitromethane.

A solution of 2-methylanisole **514** (500 mg, 0.51 mol l⁻¹) and tetranitromethane (1.02 mol l⁻¹) in dichloromethane (at 20°, -20°, -50° or -78°), acetonitrile (at 20°, -20° or -45°), or 1,1,1,3,3,3-hexafluoropropan-2-ol (20°) was irradiated with filtered light ($\lambda_{\text{cut-off}} < 435$ nm). Aliquots were withdrawn from the reaction mixture at appropriate time intervals, the volatile material removed under reduced pressure at $\leq 0^\circ$, and the product composition determined by n.m.r. spectral analysis (Table 8.5.1).

Photochemistry of 2-methylanisole 514 in dichloromethane at 20° and the identification of products 515, 516, 518 and 519.

Reaction of 2-methylanisole-tetranitromethane in dichloromethane at 20°, as above, for 4 h resulted in partial conversion (ca. 50 %) (¹H n.m.r. spectra) into 2-methyl-4-trinitromethylanisole **515** (65 %), 2-methyl-4-nitroanisole **516** (25 %), unidentified aromatic compounds (total 4 %), and nitro-trinitromethyl adducts **518** (4 %) and **519** (2 %) (Table 8.5.1). The aromatic compounds **515** and **516** were separated by chromatography on a silica gel Chromatotron plate and gave in elution order:

2-Methyl-4-trinitromethylanisole 515, ¹H n.m.r. (CDCl₃) δ 2.27 (s, 2-Me), 3.93 (s, OMe), 6.95 (d, *J* 8.8 Hz, H6), 7.36 (dq, *J* 2.9 Hz, *J*_{H3,2-Me} 1.0 Hz, H3), 7.45 (dd, *J* 8.8 Hz, *J* 2.9 Hz, H5); essentially identical with literature data.⁵

2-Methyl-4-nitroanisole 516, m.p. 62.5-63.5° (Literature⁶ m.p. 64°), ¹H n.m.r. (CDCl₃) δ 2.24 (s, 2-Me), 3.92 (s, OMe), 6.85 (d, *J* 8.8 Hz, H6), 7.97 (br s, H3), 8.05 (br d, *J* 8.8 Hz, H5).

The nitro-trinitromethyl adducts **518** and **519** were separated partially by h.p.l.c. and gave in elution order:

1-Methoxy-6-methyl-t-6-nitro-r-3-trinitromethylcyclohexa-1,4-diene **518**, isolated as an oil containing impurities (ca. 10 %). ^1H n.m.r. (CDCl_3) δ 1.83 (s, 6-Me), 3.66 (s, OMe), 4.95 (m, H3), 5.03 (m, H2), 6.04 (ddd, J 9.8 Hz, J 3.0 Hz, J 2.0 Hz, H4), 6.17 (dd, J 9.8 Hz, J 2.0 Hz, H5). Nuclear Overhauser experiments gave the following results: irradiation at δ 5.03 gave an enhancement at δ 3.66 (0.5 %); irradiation at δ 6.04 gave enhancements at δ 4.95 (0.1 %) and at δ 6.17 (3.3 %); irradiation at δ 6.17 gave enhancements at δ 1.83 (0.2 %) and at δ 6.04 (5.9 %). ^{13}C n.m.r. (CDCl_3) δ 23.5 (6-Me), 43.7 (C3), 55.7 (OCH_3), 85.7 (C6), 89.3 (C2), 121.8 (C4), 133.9 (C5), 157.5 (C1), resonance for $\text{C}(\text{NO}_2)_3$ not observed. The above correlations were confirmed by reverse detected heteronuclear correlation spectra (HMQC).

1-Methoxy-6-methyl-c-6-nitro-r-3-trinitromethylcyclohexa-1,4-diene **519**, m.p. 75-77° (decomp.) (X-ray crystal structure determined, see below). IR: ν_{max} (CDCl_3 solution) 1603, 1560, 1556 cm^{-1} . ^1H n.m.r. (CDCl_3) δ 1.85 (s, 6-Me), 3.71 (s, OMe), 4.86 (m, H3), 5.03 (m, H2), 5.99 (ddd, J 9.8 Hz, J 3.5 Hz, J 2.0 Hz, H4), 6.22 (dd, J 9.8 Hz, J 1.9 Hz, H5). Nuclear Overhauser experiments gave the following results: irradiation at δ 1.85 gave an enhancement at δ 6.22 (5.1 %); irradiation at δ 3.71 gave an enhancement at δ 5.03 (9.3 %); irradiation at δ 4.86 gave enhancements at δ 5.03 (2.0 %) and at δ 5.99 (1.6 %); irradiation at δ 5.03 gave enhancements at δ 3.71 (0.8 %) and at δ 4.86 (0.8 %); irradiation at δ 5.99 gave enhancements at δ 4.86 (1.3 %) and at δ 6.22 (5.5 %); irradiation at δ 6.22 gave an enhancement at δ 1.85 (0.5 %). ^{13}C n.m.r. (CDCl_3) δ 23.6 (6-Me), 42.6 (C3), 55.8 (OCH_3), 85.5 (C6), 89.5 (C2), 121.8 (C4), 133.6 (C5), 157.1 (C1), resonance for $\text{C}(\text{NO}_2)_3$ not observed. The above correlations were confirmed by reverse detected heteronuclear correlation spectra (HMQC).

Photochemistry of 2-methylanisole 514 in 1,1,1,3,3,3-hexafluoropropan-2-ol (HFP) at 20°.

Reaction of 2-methylanisole-tetranitromethane in HFP at 20°, as above, for 2 h resulted in a low conversion (ca. 8 %; to be compared with ca. 21 % in dichloromethane for 2 h at 20°) of 2-methylanisole **514** into 2-methyl-4-trinitromethylanisole **515** (35 %), 2-methyl-4-nitroanisole **516** (30 %), unidentified aromatic compounds (total 15 %), 1-methoxy-6-methyl-*t*-6-nitro-*r*-3-trinitromethylcyclohexa-1,4-diene **518** (8 %), 1-methoxy-6-methyl-*c*-6-nitro-*r*-3-trinitromethylcyclohexa-1,4-diene **519** (4 %), and unidentified adducts (total 8 %).

General procedure for the photonitration of 2,4-dimethylanisole 520 with tetranitromethane.

A solution of 2,4-dimethylanisole **520** (500 mg, 0.46 mol l⁻¹) and tetranitromethane (0.92 mol l⁻¹) in dichloromethane (at 20°, -20°, -50° or -78°), acetonitrile (at 20° or -20°), or 1,1,1,3,3,3-hexafluoropropan-2-ol (20°) was irradiated with filtered light ($\lambda_{\text{cut-off}} < 435 \text{ nm}$). Aliquots were withdrawn from the reaction mixture at appropriate time intervals, the volatile material removed under reduced pressure at $\leq 0^\circ$, and the product composition determined by n.m.r. spectral analysis (Table 8.5.2).

Photochemistry of 2,4-dimethylanisole 520 in dichloromethane at 20° and the identification of adducts 521 and 522.

Reaction of 2,4-dimethylanisole-tetranitromethane in dichloromethane at 20°, as above, for 3 h resulted in partial conversion (ca. 81 %) (¹H n.m.r. spectra) into nitro-trinitromethyl adducts **521** (15 %) and **522** (2 %), unidentified adducts (total 8 %), 4,6-dimethyl-3-trinitromethylanisole **523** (30 %), 4,6-dimethyl-2-nitrophenol **524** (9 %), 4,6-dimethyl-2-trinitromethylanisole **525** (5 %), 4,6-dimethyl-3-nitroanisole **526** (1.5 %), 4,6-dimethyl-2-nitroanisole **527** (11 %), 2,4-dimethyl-4-nitrocyclohexa-2,5-dienone **528** (14 %), and unidentified aromatic compounds (total 5 %) (Table 8.5.2). The nitro-trinitromethyl adducts **521** and **522** were partially separated by h.p.l.c. and gave in elution order:

1-Methoxy-4,6-dimethyl-t-6-nitro-r-3-trinitromethylcyclohexa-1,4-diene **521**, as a yellow oil containing impurities (ca. 10 %). ^1H n.m.r. (CDCl_3) δ 1.76 (s, 6-Me), 1.86 (d, $J_{\text{Me,H5}}$ 1.5 Hz, 4-Me), 3.63 (s, OMe), 4.99 (br d, J 3.9 Hz, H3), 5.03 (d, J 3.9 Hz, H2), 5.87 (q, $J_{\text{H5,Me}}$ 1.5 Hz, H5); assignments confirmed where possible by double irradiation experiments. Nuclear Overhauser experiments gave the following results: irradiation at δ 1.76 gave an enhancement at δ 5.87 (9.8 %); irradiation at δ 1.86 gave enhancements at δ 4.99 (5.2 %) and at δ 5.87 (13.3 %); irradiation at δ 3.63 gave an enhancement at δ 5.03 (15.3 %); irradiation at δ 5.87 gave enhancements at δ 1.76 (0.5 %) and at δ 1.86 (1.3 %). ^{13}C n.m.r. (CDCl_3) δ 20.9 (4-Me), 23.2 (6-Me), 46.6 (C3), 55.2 (OCH_3), 86.2 (C6), 89.5 (C2), 128.7 (C4), 131.3 (C5), 157.3 (C1); a resonance for $\text{C}(\text{NO}_2)_3$ was not observed. The above assignments were confirmed by reverse detected heteronuclear correlation spectra (HMBC, HMQC).

1-Methoxy-4,6-dimethyl-c-6-nitro-r-3-trinitromethylcyclohexa-1,4-diene **522**, as an oil containing impurities (ca. 10 %). ^1H n.m.r. (CDCl_3) δ 1.80 (s, 6-Me), 1.85 (app br s, 4-Me), 3.66 (s, OMe), 4.87 (d, J 3.9 Hz, H3), 5.15 (d, J 3.9 Hz, H2), 5.96 (q, $J_{\text{H5,Me}}$ 1.5 Hz, H5); assignments confirmed where possible by double irradiation experiments. Nuclear Overhauser experiments gave the following results: irradiation at δ 1.80 gave an enhancement at δ 5.96 (7.9 %); irradiation at δ 1.85 gave enhancements at δ 4.87 (5.7 %) and at δ 5.96 (7.4 %); irradiation at δ 3.66 gave an enhancement at δ 5.15 (12.1 %). ^{13}C n.m.r. (CDCl_3) δ 21.3 (4-Me), 23.8 (6-Me), 46.9 (C3), 55.7 (OCH_3), 84.8 (C6), 89.1 (C2), 130.3 (C4), 131.5 (C5), 157.0 (C1); a resonance for $\text{C}(\text{NO}_2)_3$ was not observed. The above assignments were confirmed by reverse detected heteronuclear correlation spectra (HMBC, HMQC).

Photochemistry of 2,4-dimethylanisole **520** in dichloromethane at -78° and the identification of aromatic compounds **523-528**.

Reaction of 2,4-dimethylanisole-tetranitromethane in dichloromethane at -78° , as above, for 3 h resulted in partial conversion (ca. 65 %) (^1H n.m.r. spectra) into nitro-trinitromethyl adducts **521** (39 %) and **522** (4 %), unidentified

adducts (total 7 %), aromatic compounds **523** (2 %), **524** (2 %), **525** (1 %), **526** (4 %), **527** (8 %), nitro dienone **528** (22 %), and unidentified aromatic compounds (total 10 %) (Table 8.5.2). Chromatography of this mixture on a silica gel Chromatotron plate gave in elution order:

4,6-Dimethyl-3-trinitromethylanisole **523**, m.p. 75-78° (decomp.) (Insufficient for elemental analysis, crystals inadequate for X-ray crystallography. Found: M^{++} 285.0596. $C_{10}H_{11}N_3O_7$ requires 285.0597). IR: ν_{\max} (KBr) 1618, 1591, 1560 cm^{-1} . 1H n.m.r. ($CDCl_3$) δ 2.10, 2.27 (both s, 4-Me, 6-Me), 3.79 (s, OMe), 6.66 (s, H2), 7.18 (s, H5). Nuclear Overhauser experiments gave the following results: irradiation at δ 2.10 gave an enhancement at δ 7.18 (5.5 %); irradiation at δ 2.27 gave an enhancement at δ 7.18 (4.4 %); irradiation at δ 3.79 gave an enhancement at δ 6.66 (13.5 %); irradiation at δ 6.66 gave an enhancement at δ 3.79 (1.1 %); irradiation at δ 7.18 gave enhancements at δ 2.10 (1.3 %) and at δ 2.27 (1.0 %).

4,6-Dimethyl-2-nitrophenol **524**, m.p. 68-69° (Literature⁷ 70-71°). IR: ν_{\max} (KBr) 1541 cm^{-1} . 1H n.m.r. ($CDCl_3$) δ 2.30 (s, 4-Me, 6-Me), 7.26 (d, J 1.0 Hz, H5), 7.74 (d, J 1.0 Hz, H3), 10.77 (s, OH).

4,6-Dimethyl-2-trinitromethylanisole **525**, as an oil (Insufficient for elemental analysis. Parent ion not visible. Found: $M^{+-}NO_2$ 239.06675. $C_{10}H_{11}N_2O_5$ requires 239.0668). 1H n.m.r. ($CDCl_3$) δ 2.17, 2.19 (both s, 4-Me, 6-Me), 3.91 (s, OMe), 6.81 (s, H3), 7.00 (s, H5).

4,6-Dimethyl-3-nitroanisole **526**, isolated in low yield as an oil (Insufficient for elemental analysis. Found: M^{+} 181.0738. $C_9H_{11}NO_3$ requires 181.0739). IR: ν_{\max} (liquid film) 1518 cm^{-1} . 1H n.m.r. ($CDCl_3$) δ 2.24 (s, 6-Me), 2.53 (s, 4-Me), 3.87 (s, OMe), 7.07 (s, H5), 7.50 (s, H2). Nuclear Overhauser experiments gave the following results: irradiation at δ 2.24 gave enhancements at δ 3.87 (0.2 %) and at δ 7.07 (2.6 %); irradiation at δ 2.53 gave an enhancement at δ 7.07 (3.6 %); irradiation at δ 3.87 gave enhancements at δ 2.24 (0.3 %) and at δ 7.50 (8.0 %); irradiation at δ 7.07 gave enhancements at δ

2.24 (0.8 %) and at δ 2.53 (0.8 %); irradiation at δ 7.50 gave an enhancement at δ 3.87 (0.8 %).

4,6-Dimethyl-2-nitroanisole **527**, isolated in low yield as an oil (Insufficient for elemental analysis. Found: M^{+} 181.0736. $C_9H_{11}NO_3$ requires 181.0739). IR: ν_{\max} (liquid film) 1531 cm^{-1} . ^1H n.m.r. (CDCl_3) δ 2.32 (s, 4-Me, 6-Me), 3.86 (s, OMe), 7.21 (s, H5), 7.44 (s, H3).

2,4-Dimethyl-4-nitrocyclohexa-2,5-dienone **528** was detected in the reaction product prior to chromatography by its partial ^1H n.m.r. spectrum (CDCl_3) δ 6.38 (d, J 10.3 Hz, H6), 6.88 (dq, J 2.9 Hz, $J_{\text{H3,Me}}$ 1.5 Hz, H3), 7.08 (dd, J 10.3 Hz, J 2.9 Hz, H5); Literature⁷ ^1H n.m.r. (Ac_2O) δ 6.37 (d, J 10 Hz, H6), 6.96 (dq, J 3.2 Hz, $J_{\text{H3,Me}}$ 1.4 Hz, H3), 7.18 (dd, J 10 Hz, J 3.2 Hz, H5). During chromatography the nitro dienone **528** rearranged to give 4,6-dimethyl-2-nitrophenol **524** additional to that present initially.

Photochemistry of 2,4-dimethylanisole **520** in 1,1,1,3,3,3-hexafluoropropan-2-ol (HFP) at 20° .

Reaction of 2,4-dimethylanisole-tetranitromethane in HFP at 20° , as above, for 3 h resulted in a lower conversion (ca. 46 %; to be compared with ca. 81 % in dichloromethane for 3 h at 20°) of 2,4-dimethylanisole **520** into nitro-trinitromethyl adducts **521** (1 %) and **522** (1 %), unidentified adducts (total 1 %), aromatic compounds **523** (21 %), **524** (6 %), **525** (2 %), **526** (16 %), **527** (38 %), and unidentified aromatic compounds (total 14 %).

Product Yield Data

Table 8.5.1 - Overview of product yields from the photolysis of 2-methylanisole **514** (0.51 mol l⁻¹) with tetranitromethane (1.02 mol l⁻¹) in dichloromethane and acetonitrile.^A

Conditions	t/h	Yields (%)					Unknown Adducts
		515	516	Unknown ArX	518	519	
DCM/20°	0.5	78.2	9.8	5.5	4.6	1.9	0.0
	1	75.4	11.7	5.8	4.7	2.4	0.0
	2	70.7	17.4	5.2	4.5	2.2	0.0
	4	65.2	35.0	3.9	4.1	1.7	0.0
DCM/-20°	0.5	78.8	10.3	2.7	5.9	1.3	0.9
	1	77.6	9.7	4.0	5.8	2.1	0.9
	2	72.6	12.0	3.8	8.0	2.9	0.7
	4	68.4	15.5	7.0	6.3	1.8	1.1
DCM/-50°	0.5	75.6	11.9	4.0	6.0	2.0	0.5
	1	74.2	11.3	4.0	7.4	2.7	0.4
	2	72.6	11.8	6.5	6.4	2.3	0.4
	4	70.3	12.5	7.3	7.0	2.3	0.5
DCM/-78°	0.5	71.4	12.7	4.5	8.0	2.9	0.6
	1	72.6	11.8	4.5	7.2	3.6	0.4
	2	70.5	12.6	6.4	7.1	2.9	0.6
	4	70.3	11.8	6.9	7.4	3.0	0.6
AN/20°	0.5	35.2	37.9	3.8	16.1	4.3	2.7
	1	30.7	40.8	4.7	17.5	4.2	2.0
	2	26.0	43.3	5.7	18.3	4.3	2.4
	4	23.9	44.8	4.5	19.5	4.1	3.2
AN/-20°	1	39.1	34.6	3.8	15.9	4.4	2.2
	2	33.7	37.6	5.5	17.7	4.6	0.9
	4	29.9	39.2	7.9	17.7	4.2	1.1
AN/-45°	1	41.4	28.5	4.8	19.2	5.8	0.4
	2	39.2	30.8	6.8	18.7	3.9	0.6
	4	38.7	31.9	8.2	16.4	4.1	0.7

^A Conversions not quoted due to substrate volatility during work-up

Table 8.5.2 - Overview of product yields from the photolysis of 2,4-dimethylanisole **520** (0.46 mol l⁻¹) with tetranitromethane (0.92 mol l⁻¹) in dichloromethane and acetonitrile.^A

Conditions	t/h	Yields (%)									
		Unknown							Unknown		
		521	522	Adducts	523	524	525	526	527	528	ArX
DCM/20°	1	11.4	1.8	15.8	14.2	5.3	6.5	1.3	13.6	18.1	7.5
	2	14.9	1.8	9.1	24.9	4.9	6.0	1.0	9.4	14.0	11.0
	3	15.2	2.1	4.7	29.7	9.0	4.6	1.5	11.0	13.8	6.2
DCM/-20°	1	11.5	1.8	11.8	1.9	1.9	2.4	1.9	12.7	27.9	23.2
	2	16.9	2.7	8.6	2.0	2.9	3.5	3.9	15.9	29.3	8.9
	3	21.3	3.2	12.8	2.4	2.0	1.9	5.0	16.8	24.8	5.9
DCM/-50°	1	32.8	4.1	11.5	0.4	1.3	1.1	5.6	13.5	21.5	6.0
	2	36.5	4.3	6.6	1.8	0.7	1.1	7.3	14.5	17.5	4.1
	3	38.0	4.4	7.6	1.7	0.9	0.8	8.5	15.2	14.8	3.9
DCM/-78°	1	30.8	3.2	6.3	6.8	2.6	3.8	0.8	3.2	28.4	11.2
	2	34.7	4.0	8.5	1.5	1.4	1.5	2.8	6.6	25.0	9.6
	3	39.0	3.8	7.3	1.9	2.2	1.2	4.4	8.1	21.7	6.5
AN/20°	2	47.0	13.4	0.0	0.9	3.0	1.1	6.4	9.6	9.6	8.1
	3	44.4	16.1	0.0	1.3	3.7	0.9	7.3	11.0	7.3	6.5
AN/-20°	2	49.2	7.2	0.0	0.6	1.4	1.1	2.9	1.6	23.4	8.6
	3	49.0	7.2	0.0	1.2	1.3	0.9	3.0	1.5	21.5	7.2

Experimental Data Relating to Chapter 6

4-Fluoroanisole and 4-fluoro-3-methylanisole were purchased from Aldrich.

General procedure for the photonitration of 4-fluoroanisole 615 with tetranitromethane.

A solution of 4-fluoroanisole **615** (500 mg, 0.5 mol l⁻¹) and tetranitromethane (1.0 mol l⁻¹) in dichloromethane (at 20°, -20° or -78°) or acetonitrile (20° or -20°) was irradiated with filtered light ($\lambda_{\text{cut-off}} < 435$ nm). Aliquots were withdrawn from the reaction mixture at appropriate time intervals, the volatile material removed under reduced pressure at $\leq 0^\circ$, and the product composition determined by n.m.r. spectral analysis (Tables 8.6.1 and 8.6.2). A similar reaction was carried out in 1,1,1,3,3,3-hexafluoropropan-2-ol.

Photochemistry of 4-fluoroanisole 615 in dichloromethane at -20° and the identification of adducts 617-623 and aromatic compounds 624, 625 and 626.

Reaction of 4-fluoroanisole-tetranitromethane in dichloromethane at -20°, as above, for 3 h resulted in partial conversion (ca. 50 %) into a product which was shown by ¹H n.m.r. spectra to be a mixture of the nitro-trinitromethyl adducts **617** (1 %), **618** (trace), **622** (6 %), **619** (18 %), **623** (2 %), **620** (19 %), hydroxy-trinitromethyl adduct **621** (8 %), unidentified adducts (total 19 %), aromatic compounds **624** (17 %), **625** (2 %), **626** (2 %), and unidentified aromatic compounds (total 6 %). The mixture was partially separated into its components by h.p.l.c. and gave the following in elution order:

4-Fluoro-2-trinitromethylanisole 624, ¹H n.m.r. (CDCl₃) δ 3.83 (s, OMe), 7.09 (m, H3 and H6), 7.44 (ddd, $J_{\text{H}_5, \text{H}_6}$ 9.5 Hz, $J_{\text{H}_5, \text{F}}$ 6.4 Hz, $J_{\text{H}_5, \text{H}_3}$ 2.5 Hz, H5); identical with literature⁵ values.

4-Fluoro-2-nitroanisole 625, m.p. 59-60 °C (Literature⁸ value 61.5-62 °C). ¹H n.m.r. (CDCl₃) δ 3.95 (s, OMe), 7.07 (dd, $J_{\text{H}_6, \text{H}_5}$ 9.8 Hz, $J_{\text{H}_6, \text{F}}$ 3.9 Hz, H6), 7.28 (ddd, $J_{\text{H}_5, \text{H}_6}$ 9.8 Hz, $J_{\text{H}_5, \text{F}}$ 7.3 Hz, $J_{\text{H}_5, \text{H}_3}$ 3.4 Hz, H5), 7.60 (dd, $J_{\text{H}_3, \text{F}}$ 7.8 Hz, $J_{\text{H}_3, \text{H}_5}$ 3.4 Hz, H3).

1-Fluoro-4-methoxy-r-5-nitro-c-6-trinitromethylcyclohexa-1,3-diene **617**, isolated only in admixture with aromatic compounds **624** and **625**, and its epimer **618** into which it isomerises in solution. ^1H n.m.r. (CDCl_3) δ 3.66 (s, OMe), 4.68 (ddd, $J_{\text{H}_5,\text{H}_6}$ 5.4 Hz, $J_{\text{H}_5,\text{F}}$ 2.5 Hz, $J_{\text{H}_5,\text{H}_3}$ 2.0 Hz, H5), 5.62 (dd, $J_{\text{H}_6,\text{F}}$ 5.8 Hz, $J_{\text{H}_6,\text{H}_5}$ 5.4 Hz, H6), 5.94 (dd, $J_{\text{H}_2,\text{F}}$ 11.8 Hz, $J_{\text{H}_2,\text{H}_3}$ 10.3 Hz, H2), 6.41 (dd, $J_{\text{H}_3,\text{H}_2}$ 10.3 Hz, $J_{\text{H}_3,\text{H}_5}$ 2.0 Hz, H3); assignments confirmed by double irradiation experiments. Nuclear Overhauser experiments gave the following results: irradiation at δ 3.66 gave an enhancement at δ 4.68 (9.3 %); irradiation at δ 4.68 gave enhancements at δ 3.66 (1.3 %) and at δ 5.62 (4.4 %); irradiation at δ 6.41 gave an enhancement at δ 5.94 (3.0 %). ^{13}C n.m.r. (CDCl_3) δ 44.1 (d, $J_{\text{C}_6,\text{F}}$ 13.6 Hz, C6), 55.3 (OMe), 84.05 (d, $J_{\text{C}_5,\text{F}}$ 2.9 Hz, C5), 121.2 (d, $J_{\text{C}_2,\text{F}}$ 22.9 Hz, C2), 132.7 (d, $J_{\text{C}_3,\text{F}}$ 11.4 Hz, C3), resonances for C1, C4, and $\text{C}(\text{NO}_2)_3$ were not observed; the above assignments were confirmed by reverse detected heteronuclear correlation spectra (HMQC).

1-Fluoro-4-methoxy-r-5-nitro-t-6-trinitromethylcyclohexa-1,3-diene **618**, isolated only in admixture with the nitro compound **625** and two minor aromatic compounds. ^1H n.m.r. (CDCl_3) δ 3.72 (s, OMe), 5.17 (dd, $J_{\text{H}_3,\text{H}_2}$ 7.3 Hz, $J_{\text{H}_3,\text{F}}$ 3.4 Hz, H3), 5.27 (br d, $J_{\text{H}_5,\text{F}}$ 4.9 Hz, $J_{\text{H}_5,\text{H}_6}$ small, H5), 5.43 (br d, $J_{\text{H}_6,\text{F}}$ 5.9 Hz, $J_{\text{H}_6,\text{H}_5}$ small, H6), 6.05 (dd, $J_{\text{H}_2,\text{F}}$ 10.7 Hz, $J_{\text{H}_2,\text{H}_3}$ 7.3 Hz, H2); assignments confirmed by double irradiation experiments. A nuclear Overhauser experiment gave the following result: irradiation at δ 3.72 gave an enhancement at δ 5.17 (10.4 %). ^{13}C n.m.r. (CDCl_3) δ 41.9 (C6), 82.5 (C5), 131.0 (C3), resonances for C1, C2, C4, and $\text{C}(\text{NO}_2)_3$ were not observed; the above ^{13}C n.m.r. assignments were made from reverse detected heteronuclear correlation spectra (HMQC).

3-Fluoro-6-hydroxy-5-nitrobenzoic acid **626**, a viscous oil (Insufficient for elemental analysis. Found: M^{++} 201.0073. $\text{C}_7\text{H}_4\text{FNO}_5$ requires 201.00735). ^1H n.m.r. (CDCl_3) δ 7.55 (dd, $J_{\text{H},\text{F}}$ 7.8 Hz, $J_{\text{H},\text{H}}$ 2.9 Hz), 8.26 (dd, $J_{\text{H},\text{F}}$ 7.3 Hz, $J_{\text{H},\text{H}}$ 2.9 Hz), 11.29 (br s, OH).

1-Fluoro-4-methoxy-r-3-nitro-t-6-trinitromethylcyclohexa-1,4-diene **622**, isolated in low yield in admixture with impurities (ca. 10 %). ^1H n.m.r. (CDCl_3) δ 3.66 (s, OMe), 5.20 (m, H6), 5.25 (m, H5), 5.64 (dd, $J_{\text{H}_3,\text{F}}$ 8.8 Hz, $J_{\text{H}_3,\text{H}_2}$ 3.9 Hz, H3), 5.97 (dd, $J_{\text{H}_2,\text{F}}$ 15.6 Hz, $J_{\text{H}_2,\text{H}_3}$ 3.9 Hz, H2). Nuclear Overhauser experiments gave the following results: irradiation at δ 3.66 gave an enhancement at δ 5.25 (9.0 %); irradiation at δ 5.64 gave an enhancement at δ 5.97 (2.9 %); irradiation at δ 5.97 gave an enhancement at δ 5.64 (2.2 %).

1-Fluoro-4-methoxy-t-6-nitro-r-3-trinitromethylcyclohexa-1,4-diene **619**, isolated only in admixture with impurities (ca. 10 %). ^1H n.m.r. (CDCl_3) δ 3.66 (s, OMe), 5.14 (br d, $J_{\text{H}_3,\text{H}_2}$ 3.9 Hz, $J_{\text{H}_3,\text{F}}$ and $J_{\text{H}_3,\text{H}_6}$ small, H3), 5.27 (dd, $J_{\text{H}_5,\text{F}}$ 5.4 Hz, $J_{\text{H}_5,\text{H}_6}$ 4.4 Hz, H5), 5.71 (m, $J_{\text{H}_6,\text{H}_5}$ 4.4 Hz, $J_{\text{H}_6,\text{F}}$ 2.9 Hz, $J_{\text{H}_6,\text{H}_5}$ small, H6), 6.03 (dd, $J_{\text{H}_2,\text{F}}$ 13.2 Hz, $J_{\text{H}_2,\text{H}_3}$ 3.9 Hz, H2); assignments confirmed by double irradiation experiments. Nuclear Overhauser experiments gave the following results: irradiation at δ 3.66 gave an enhancement at δ 5.27 (9.2 %); irradiation at δ 5.14 gave an enhancement at δ 6.03 (1.3 %); irradiation at δ 5.27 gave enhancements at δ 3.66 (1.0 %) and at δ 5.71 (2.4 %); irradiation at δ 5.71 gave an enhancement at δ 5.27 (1.4 %); irradiation at δ 6.03 gave an enhancement at δ 5.14 (2.5 %). ^{13}C n.m.r. (CDCl_3) δ 44.5 (d, $J_{\text{C}_3,\text{F}}$ 8.4 Hz, C3), 56.7 (OMe), 80.8 (d, $J_{\text{C}_6,\text{F}}$ 26.9 Hz, C6), 94.0 (d, $J_{\text{C}_5,\text{F}}$ 7.4 Hz, C5), 102.5 (d, $J_{\text{C}_2,\text{F}}$ 26.1 Hz, C2), 150.4 (C4), resonances for C1 and $\text{C}(\text{NO}_2)_3$ were not observed; the above assignments were confirmed by reverse detected heteronuclear correlation spectra (HMBC, HMQC).

1-Fluoro-4-methoxy-r-3-nitro-c-6-trinitromethylcyclohexa-1,4-diene **623**, isolated only in admixture with impurities (ca. 10 %). ^1H n.m.r. (CDCl_3) δ 3.70 (s, OMe), 5.11 (br m, H6), 5.28 (dd, $J_{\text{H}_5,\text{F}}$ 5.8 Hz, $J_{\text{H}_5,\text{H}_6}$ 3.9 Hz, H5), 5.54 (dd, $J_{\text{H}_3,\text{F}}$ 10.2 Hz, $J_{\text{H}_3,\text{H}_2}$ 4.9 Hz, H3), 6.06 (dd, $J_{\text{H}_2,\text{F}}$ 13.7 Hz, $J_{\text{H}_2,\text{H}_3}$ 4.9 Hz, H2); assignments confirmed by double irradiation experiments. Nuclear Overhauser experiments gave the following results: irradiation at δ 3.70 gave enhancements at δ 5.28 (6.1 %) and at δ 5.55 (0.5 %); irradiation at δ 5.11 gave an enhancement at δ 5.28 (1.5 %); irradiation at δ 5.28 gave enhancements at δ 3.70 (0.6 %) and at δ 5.11 (1.6 %); irradiation at δ 5.55 gave

enhancements at δ 3.70 (0.1 %) and at δ 6.06 (1.4 %); irradiation at δ 6.06 gave an enhancement at δ 5.55 (1.7 %). ^{13}C n.m.r. (CDCl_3) δ 43.7 (d, $J_{\text{C}_6,\text{F}}$ 22.1 Hz, C6), 56.5 (OMe), 81.3 (C3), 90.1 (C5), 105.1 (d, $J_{\text{C}_2,\text{F}}$ 25.2 Hz, C2), 157.0 (C4), resonances for C1 and $\text{C}(\text{NO}_2)_3$ were not observed; the above ^{13}C n.m.r. assignments were made from reverse detected heteronuclear correlation spectra (HMQC).

1-Fluoro-4-methoxy-c-6-nitro-r-3-trinitromethylcyclohexa-1,4-diene **620**, isolated only in admixture with impurities (total 5 %). ^1H n.m.r. (CDCl_3) δ 3.68 (s, OMe), 4.98 (ddd, $J_{\text{H}_3,\text{H}_6}$ 5.4 Hz, $J_{\text{H}_3,\text{F}}$ 4.4 Hz, $J_{\text{H}_3,\text{H}_2}$ 4.4 Hz, H3), 5.40 (dd, $J_{\text{H}_5,\text{F}}$ 5.4 Hz, $J_{\text{H}_5,\text{H}_6}$ 5.4 Hz, H5), 5.59 (ddd, $J_{\text{H}_6,\text{F}}$ 5.4 Hz, $J_{\text{H}_6,\text{H}_5}$ 5.4 Hz, $J_{\text{H}_6,\text{H}_3}$ 5.4 Hz, H6), 6.14 (br dd, $J_{\text{H}_2,\text{F}}$ 12.7 Hz, $J_{\text{H}_2,\text{H}_3}$ 4.4 Hz, H2); assignments confirmed by double irradiation experiments. Nuclear Overhauser experiments gave the following results: irradiation at δ 3.68 gave an enhancement at δ 5.40 (9.4 %); irradiation at δ 4.98 gave enhancements at δ 3.68 (0.1 %) and at δ 6.14 (2.4 %); irradiation at δ 5.40 gave enhancements at δ 3.68 (1.3 %) and at δ 5.59 (3.6 %); irradiation at δ 5.59 gave an enhancement at δ 5.40 (1.8 %); irradiation at δ 6.14 gave an enhancement at δ 4.98 (2.7 %). ^{13}C n.m.r. (CDCl_3) δ 44.8 (d, $J_{\text{C}_3,\text{F}}$ 8.3 Hz, C3), 56.9 (s, OMe), 79.7 (d, $J_{\text{C}_6,\text{F}}$ 28.2 Hz, C6), 94.3 (d, $J_{\text{C}_5,\text{F}}$ 7.3 Hz, C5), 102.4 (d, $J_{\text{C}_2,\text{F}}$ 25.9 Hz, C2), resonances for C1 and $\text{C}(\text{NO}_2)_3$ were not observed; the above assignments were confirmed by reverse detected heteronuclear correlation spectra (HMBC, HMQC).

1-Fluoro-6-hydroxy-4-methoxy-3-trinitromethylcyclohexa-1,4-diene **621**, isolated in admixture with impurities (total 10 %). ^1H n.m.r. (CDCl_3) δ 3.60 (s, OMe), 4.74 (m, H6), 4.81 (m, H3), 5.24 (dd, $J_{\text{H}_5,\text{H}_6}$ 5.4 Hz, $J_{\text{H}_5,\text{F}}$ 5.4 Hz, H5), 5.66 (dd, $J_{\text{H}_2,\text{F}}$ 12.7 Hz, $J_{\text{H}_2,\text{H}_3}$ 3.9 Hz, H2); assignments confirmed by double irradiation experiments. Nuclear Overhauser experiments gave the following results: irradiation at δ 3.60 gave an enhancement at δ 5.24 (6.5 %); irradiation at δ 4.74 gave an enhancement at δ 5.24 (1.6 %); irradiation at δ 4.81 gave an enhancement at δ 5.66 (2.0 %); irradiation at δ 5.24 gave enhancements at δ 3.60 (1.1 %) and at δ 4.74 (2.5 %); irradiation at δ 5.66 gave an enhancement at δ 4.82 (1.9 %). ^{13}C n.m.r. (CDCl_3) δ 44.4 (d, $J_{\text{C}_3,\text{F}}$ 8.4 Hz, C3), 55.6 (OMe),

61.4 (d, $J_{C_6,F}$ 28.2 Hz, C6), 96.2 (d, $J_{C_2,F}$ 27.1 Hz, C2), 100.6 (d, $J_{C_5,F}$ 9.4 Hz, C5), resonances for C1, C4 and $C(NO_2)_3$ were not observed; the above assignments were confirmed by reverse detected heteronuclear correlation spectra (HMQC).

Photochemistry of 4-fluoroanisole 615 in acetonitrile at 20° and the identification of the nitro phenol 627.

Reaction of 4-fluoroanisole-tetranitromethane in acetonitrile at 20°, as above, for 2 h resulted in partial conversion (ca. 40 %) into a product which was shown by 1H n.m.r. spectra to be a mixture of the aromatic compounds **624** (4 %), **625** (62 %), 4-fluoro-2-nitrophenol **627** (23 %) and unidentified aromatic compounds (total 10 %). Radial chromatography of this mixture on a silica gel Chromatotron plate gave:

4-Fluoro-2-nitrophenol 627, 1H n.m.r. ($CDCl_3$) δ 7.16 (dd, J_{H_6,H_5} 9.8 Hz, $J_{H_6,F}$ 4.4 Hz, H6), 7.37 (ddd, J_{H_5,H_6} 9.8 Hz, $J_{H_5,F}$ 7.3 Hz, J_{H_5,H_3} 2.9 Hz, H5), 7.82 (dd, $J_{H_3,F}$ 8.3 Hz, J_{H_3,H_5} 2.9 Hz, H3), 10.36 (s, OH); identical with literature⁵ values.

Photochemistry of 4-fluoroanisole 615 in 1,1,1,3,3,3-hexafluoropropan-2-ol (HFP) at 20°.

A solution of 4-fluoroanisole **615** (250 mg, 0.5 mol l^{-1}) and tetranitromethane (1.0 mol l^{-1}) in HFP at 20 °C was irradiated with filtered light ($\lambda_{cut-off} < 435$ nm) for 5 h. The conversion of 4-fluoroanisole **615** was low (ca. 18 %) and exclusively into 4-fluoro-2-nitroanisole **625**.

Photochemistry of 4-fluoroanisole 615 at 20 °C in dichloromethane containing trifluoroacetic acid (0.7 mol l^{-1}).

Reaction of 4-fluoroanisole-tetranitromethane in dichloromethane containing trifluoroacetic acid (0.7 mol l^{-1}) at 20°, as above, for 2h resulted in a relatively low conversion (ca. 29 %) into a mixture (1H n.m.r. spectra) of adducts **617** (5 %), **622** (2 %), **619** (2 %), **623** (1 %), **620** (8 %), aromatic compounds **624** (25 %), **625** (48 %), **626** (trace), **627** (2 %), and unidentified aromatic compounds (total 7 %).

General procedure for the photonitration of 4-fluoro-3-methylanisole 616 with tetranitromethane.

A solution of 4-fluoro-3-methylanisole **616** (500 mg, 0.45 mol l⁻¹) and tetranitromethane (0.9 mol l⁻¹) in dichloromethane (at 20°, -20° or -78°) or acetonitrile (20°, -20° or -50°) was irradiated with filtered light ($\lambda_{\text{cut-off}} < 435$ nm). Aliquots were withdrawn from the reaction mixture at appropriate time intervals, the volatile material removed under reduced pressure at $\leq 0^\circ$, and the product composition determined by n.m.r. spectral analysis (Tables 8.6.3 and 8.6.4). A similar reaction was carried out in 1,1,1,3,3,3-hexafluoropropan-2-ol.

Photochemistry of 4-fluoro-3-methylanisole 616 in dichloromethane at 20° and the identification of aromatic compounds 628-633.

Reaction of 4-fluoro-3-methylanisole-tetranitromethane in dichloromethane at 20°, as above, for 6 h resulted in partial conversion (ca. 75 %) into a product which was shown by ¹H n.m.r. spectra to be a mixture of the aromatic compounds **628** (3 %), **629** (1 %), **630** (64 %), **631** (5 %), **632** (6 %), and **633** (12 %), nitro-trinitromethyl adduct **634** (4 %) and unidentified adducts (total 2 %). The aromatic compounds (**628-633**) were separated by radial chromatography on a silica gel Chromatotron plate and gave in order of elution:

4-Fluoro-5-methyl-2-nitrophenol 628, isolated in low yield as an oil (Insufficient for elemental analysis. Found: M⁺ 171.0331. C₇H₆FNO₃ requires 171.0332). ¹H n.m.r. (CDCl₃) δ 2.34 (d, $J_{\text{Me,F}}$ 1.5 Hz, Me), 6.99 (d, $J_{\text{H6,F}}$ 6.3 Hz, H6), 7.74 (d, $J_{\text{H3,F}}$ 8.8 Hz, H3), 10.37 (s, OH).

4-Fluoro-5-methyl-3-trinitromethylanisole 629, isolated in low yield as an oil (Insufficient for elemental analysis. Found: M⁺ 289.0345. C₉H₈FN₃O₇ requires 289.0346). ¹H n.m.r. (CDCl₃) δ 2.34 (d, $J_{\text{Me,F}}$ 1.9 Hz, 5-Me), 3.80 (s, OMe), 6.76 (dd, $J_{\text{H2,F}}$ 5.4 Hz, $J_{\text{H2,H6}}$ 2.9 Hz, H2), 7.10 (dd, $J_{\text{H6,F}}$ 5.8 Hz, $J_{\text{H6,H2}}$ 2.9 Hz, H6). A nuclear Overhauser experiment gave the following result: irradiation at δ 2.34 gave an enhancement at δ 7.09 (3.7 %).

4-Fluoro-5-methyl-2-trinitromethylanisole **630**, m.p. 55-59° (X-ray crystal structure determined, see below). IR: ν_{\max} (KBr) 1624, 1593 cm^{-1} . ^1H n.m.r. (CDCl_3) δ 2.38 (d, $J_{\text{Me,F}}$ 2.0 Hz, 4-Me), 3.80 (s, OMe), 6.93 (d, $J_{\text{H}_6,\text{F}}$ 5.9 Hz, H6), 7.01 (d, $J_{\text{H}_3,\text{F}}$ 9.3 Hz, H3).

4-Fluoro-3-methyl-2-nitroanisole **631**, isolated in low yield as an oil (Insufficient for elemental analysis. Found: M^{++} 185.0488. $\text{C}_8\text{H}_8\text{FNO}_3$ requires 185.0488). ^1H n.m.r. (CDCl_3) δ 2.21 (d, $J_{\text{Me,F}}$ 1.9 Hz, Me), 3.85 (s, OMe), 6.82 (dd, $J_{\text{H}_6,\text{H}_5}$ 8.8 Hz, $J_{\text{H}_6,\text{F}}$ 4.4 Hz, H6), 7.10 (dd, $J_{\text{H}_5,\text{F}}$ 9.2 Hz, $J_{\text{H}_5,\text{H}_6}$ 8.8 Hz, H5).

4-Fluoro-3-methyl-2,6-dinitrophenol **632**, isolated in low yield as an oil (Insufficient for elemental analysis. Found: M^{++} 216.0183. $\text{C}_7\text{H}_5\text{FN}_2\text{O}_5$ requires 216.01825). ^1H n.m.r. (CDCl_3) δ 2.35 (d, $J_{\text{Me,F}}$ 1.9 Hz, 3-Me), 7.96 (d, $J_{\text{H}_5,\text{F}}$ 8.8 Hz, H5), 10.60 (br s, OH).

4-Fluoro-5-methyl-2-nitroanisole **633**, m.p. 84-85° (X-ray crystal structure determined, see below). IR: ν_{\max} (KBr) 1526 cm^{-1} . ^1H n.m.r. (CDCl_3) δ 2.35 (d, $J_{\text{Me,F}}$ 1.9 Hz, 5-Me), 3.93 (s, OMe), 6.89 (d, $J_{\text{H}_6,\text{F}}$ 6.4 Hz, H6), 7.62 (d, $J_{\text{H}_3,\text{F}}$ 8.8 Hz, H3).

The nitro-trinitromethyl adduct **634** was not eluted from the silica gel Chromatotron plate and it also decomposed during an attempted h.p.l.c. separation on a cyanopropyl column at -20° .

Photochemistry of 4-fluoro-3-methylanisole **616** in dichloromethane at -20° and the identification of nitro-trinitromethyl adducts (**634** and **635**).

Reaction of 4-fluoro-3-methylanisole-tetranitromethane in dichloromethane at -20° , as above, for 6 h resulted in partial conversion (ca. 73 %) into a product which was shown by ^1H n.m.r. spectra to be a mixture of the aromatic compounds **628** (2 %), **630** (62 %), **631** (3 %), and **633** (7 %), nitro-trinitromethyl adducts **634** (15 %), **635** (5 %), and **636** (2 %). None of the nitro-trinitromethyl adducts (**634-636**) could be isolated by h.p.l.c. using a cyanopropyl column even at -20° . Adducts **634** and **635** were identified

therefore by spectroscopic studies on this mixture of products, and adduct **636** by similar studies on a mixture of products from a reaction in acetonitrile at -20° (see below).

1-Fluoro-4-methoxy-6-methyl-c-6-nitro-r-3-trinitromethylcyclohexa-1,4-diene **634**. ^1H n.m.r. (CDCl_3) δ 1.89 (d, $J_{\text{Me,F}}$ 1.0 Hz, 6-Me), 3.63 (s, OMe), 4.96 (dd, $J_{\text{H}_3,\text{F}}$ 4.8 Hz, $J_{\text{H}_3,\text{H}_2}$ 3.9 Hz, H3), 5.26 (d, $J_{\text{H}_5,\text{F}}$ 6.4 Hz, H5), 6.01 (dd, $J_{\text{H}_2,\text{F}}$ 13.6 Hz, $J_{\text{H}_2,\text{H}_3}$ 3.9 Hz, H2). Nuclear Overhauser experiments gave the following results: irradiation at δ 1.89 gave an enhancement at δ 5.26 (6.7 %); irradiation at δ 3.63 gave an enhancement at δ 5.26 (11.5 %); irradiation at δ 4.96 gave an enhancement at δ 6.01 (2.8 %); irradiation at δ 5.26 gave enhancements at δ 1.89 (0.3 %) and at δ 3.63 (1.2 %); irradiation at δ 6.01 gave an enhancement at δ 4.96 (2.7 %). ^{13}C n.m.r. (CDCl_3) δ 44.7 (C3), 56.6 (OMe), 85.0 (C6), 100.2 (C2), 101.7 (C5), 150.4 (C4), 160.7 (C1), the resonance for $\text{C}(\text{NO}_2)_3$ was not observed; the above ^{13}C n.m.r. assignments were made from reverse detected heteronuclear correlation spectra (HMBC, HMQC).

1-Fluoro-4-methoxy-6-methyl-t-6-nitro-r-3-trinitromethylcyclohexa-1,4-diene **635**. ^1H n.m.r. (CDCl_3) δ 5.10 (br dd, $J_{\text{H}_3,\text{F}}$ 3.4 Hz, $J_{\text{H}_3,\text{H}_2}$ 3.4 Hz, $J_{\text{H}_3,\text{H}_5}$ ca. 1.0 Hz, H3), 5.15 (br d, $J_{\text{H}_5,\text{F}}$ 6.3 Hz, $J_{\text{H}_5,\text{H}_3}$ ca. 1.0 Hz, H5), 5.92 (dd, $J_{\text{H}_2,\text{F}}$ 14.2 Hz, $J_{\text{H}_2,\text{H}_3}$ 3.4 Hz, H2), resonances for -OMe and 6-Me not assigned. The above assignments were confirmed by double irradiation experiments.

Photochemistry of 4-fluoro-3-methylanisole **616** in acetonitrile at -20° and the identification of nitro-trinitromethyl adduct **636**.

Reaction of 4-fluoro-3-methylanisole-tetranitromethane in acetonitrile at -20° , as above, for 6 h resulted in partial conversion (ca. 72 %) into a product which was shown by ^1H n.m.r. spectra to be a mixture of the aromatic compounds **628** (13 %), **630** (17 %), **631** (14 %), **632** (3 %), **633** (32 %) and unidentified aromatic compounds (9 %), nitro-trinitromethyl adduct **636** (9 %) and unidentified adducts (total 2 %).

1-Fluoro-4-methoxy-2-methyl-r-5-nitro-c-6-trinitromethylcyclohexa-1,3-diene **636**. ^1H n.m.r. (CDCl_3) δ 1.91 (dd, $J_{\text{Me,F}}$ 1.9 Hz, $J_{\text{Me,H3}}$ 1.5 Hz, 3-Me), 3.61 (s, OMe), 4.66 (ddd, $J_{\text{H5,F}}$ 4.9 Hz, $J_{\text{H5,H6}}$ 4.4 Hz, $J_{\text{H5,H3}}$ 2.3 Hz, H5), 5.41 (br d, $J_{\text{H6,H5}}$ 4.4 Hz, H6), 6.07 (ddq, $J_{\text{H3,F}}$ 2.7 Hz, $J_{\text{H3,H5}}$ 2.3 Hz, $J_{\text{H3,Me}}$ 1.5 Hz, H3). Nuclear Overhauser experiments gave the following results: irradiation at δ 1.91 gave an enhancement at δ 6.07 (5.5 %); irradiation at δ 3.61 gave an enhancement at δ 4.66 (12.0 %). ^{13}C n.m.r. (CDCl_3) δ 44.4 (C6), 83.5 (C5), 128.1 (C3); these assignments were made from reverse detected heteronuclear correlation spectra (HMQC).

Photochemistry of 4-fluoro-3-methylanisole **616** at 20° in dichloromethane containing trifluoroacetic acid (0.7 mol l $^{-1}$).

Reaction of 4-fluoro-3-methylanisole-tetranitromethane at 20° in dichloromethane containing trifluoroacetic acid (0.7 mol l $^{-1}$), as above, for 4 h resulted in partial conversion (ca. 47 %) into a product which was shown by ^1H n.m.r. spectra to be a mixture of the aromatic compounds **628** (9 %), **630** (6 %), **631** (18 %), **632** (3 %), and **633** (60 %) and unidentified aromatic compounds (total 3 %).

Photochemistry of 4-fluoro-3-methylanisole **616** in 1,1,1,3,3,3-hexafluoropropan-2-ol (HFP) at 20°.

A solution of 4-fluoro-3-methylanisole **616** (250 mg, 0.5 mol l $^{-1}$) and tetranitromethane (1.0 mol l $^{-1}$) in HFP at 20° was irradiated with filtered light ($\lambda_{\text{cut-off}} < 435$ nm) for 4 h. The conversion of 4-fluoro-3-methylanisole **616** was low (ca. 18 %) and exclusively into 4-fluoro-3-methyl-2-nitroanisole **631** (26 %) and 4-fluoro-5-methyl-2-nitroanisole **633** (74 %).

Product Yield Data

Table 8.6.1 - Overview of product yields from the photolysis of 4-fluoroanisole **615** (0.46 mol l^{-1}) with tetranitromethane (0.92 mol l^{-1}) in dichloromethane.

t/h	Yields												
	617	618	619	620	621	622	623	Unknown Adducts	624	625	626	627	Unknown ArX
at 20°													
1	1.3	-	20.0	17.2	10.0	5.9	1.5	11.8	22.6	1.6	3.3	-	4.6
2	1.3	-	17.5	15.8	9.0	4.7	1.3	13.4	26.0	1.8	3.5	-	6.0
3	0.6	-	17.7	15.3	6.8	6.4	2.0	7.7	33.8	2.0	2.9	-	4.8
at -20°													
1	1.4	-	17.4	19.1	9.2	5.8	1.9	16.9	18.6	2.6	1.8	-	5.4
2	1.5	trace	16.6	20.3	8.7	6.0	1.5	19.5	17.0	2.3	1.5	-	4.9
3	1.2	trace	19.0	19.0	7.6	6.1	1.2	19.2	16.5	2.3	1.5	-	6.4
at -78°													
1	4.3	-	17.4	17.9	8.7	2.7	2.9	9.6	25.1	5.8	-	-	5.6
2	4.5	trace	16.7	19.2	8.6	4.2	3.1	7.9	24.7	4.2	1.1	-	5.8
3	5.7	trace	15.9	20.2	6.9	4.2	3.2	7.4	24.8	3.2	1.3	-	7.2

Table 8.6.2 - Overview of product yields from the photolysis of 4-fluoroanisole **615** (0.46 mol l^{-1}) with tetranitromethane (0.92 mol l^{-1}) in acetonitrile.

t/h	Yields												
	617	618	619	620	621	622	623	Unknown Adducts	624	625	626	627	Unknown ArX
at 20°													
1	-	-	-	1.1	-	-	-	3.1	8.1	61.3	-	14.5	11.9
2	-	-	-	-	-	-	-	-	4.3	62.2	-	23.0	10.4
at -20°													
1	-	-	-	4.4	3.1	-	-	12.3	16.2	33.9	-	24.0	6.1
2	-	-	-	3.5	2.2	-	-	8.7	16.8	39.9	-	20.2	9.7

Table 8.6.3 - Overview of product yields from the photolysis of 4-fluoro-3-methylanisole **616** (0.45 mol l^{-1}) with tetranitromethane (0.90 mol l^{-1}) in dichloromethane.

t/h	Yield (%)										
	628	629	630	631	632	633	Unknown Ar X	634	635	636	Unknown Adducts
20°											
2	2.5	-	61.8	-	0.3	7.6	5.0	13.9	1.3	2.0	5.6
4	2.8	0.5	64.9	3.4	3.4	11.3	2.0	9.1	-	0.2	2.3
6	2.6	1.4	64.0	5.2	5.9	12.3	2.0	4.2	-	-	2.5
-20°											
2	0.1	-	45.3	0.1	0.1	5.4	5.1	18.2	11.8	6.8	7.3
4	0.8	-	53.8	1.0	0.1	5.4	5.4	18.6	8.6	6.2	-
6	1.6	-	61.5	3.0	0.1	6.9	5.2	15.0	1.6	4.8	-
-78°											
2	6.7	-	36.8	5.9	1.9	22.6	2.4	6.1	3.5	11.7	2.4
4	6.5	-	24.3	10.0	1.9	35.3	0.8	4.2	1.2	14.9	0.8
6	6.1	-	23.1	9.8	3.1	39.3	-	3.3	-	12.9	2.3

Table 8.6.4 - Overview of product yields from the photolysis of 4-fluoro-3-methylanisole **616** (0.45 mol l^{-1}) with tetranitromethane (0.90 mol l^{-1}) in acetonitrile.

t/h	Yield (%)										
	628	629	630	631	632	633	Unknown		Unknown		
							Ar X	634	635	636	Adducts
20°											
4	9.5	4.0	7.3	19.1	10.9	45.5	-	-	-	3.6	0.2
6	8.3	4.8	6.8	19.7	13.3	44.2	-	-	-	2.0	0.8
-20°											
4	11.6	-	18.4	15.2	5.1	32.4	9.5	-	-	6.2	1.7
6	12.7	-	17.0	13.9	3.0	32.0	9.5	-	-	9.1	1.7
-78°											
4	6.0	0.1	13.3	14.0	3.2	37.6	2.2	-	-	23.7	-
6	7.7	0.1	11.2	13.5	2.9	36.7	1.9	-	-	26.1	-

Experimental Data Relating to Chapter 7

1-methoxynaphthalene was purchased from Aldrich.

General procedure for the photolysis of 1-methoxynaphthalene with tetranitromethane and ethanol.

A solution of 1-methoxynaphthalene **708**, (250mg, equal to 0.4 mol l⁻¹), tetranitromethane (0.8 mol l⁻¹), and ethanol (8 % v/v), in dichloromethane or acetonitrile at 20° were irradiated with filtered light (λ cut-off at 435 nm). Aliquots were withdrawn from the reaction mixture at appropriate time intervals, the volatile material removed rapidly under reduced pressure at $\leq 0^\circ$, and the product composition determined by ¹H n.m.r. spectral analysis (Table 8.7.1). All of the reaction products were identified by comparison of their ¹H n.m.r. spectral properties with authentic material (See Experimental data relating to Chapter 3 for details).

General procedure for the photolysis of 1,2-dimethoxybenzene with tetranitromethane.

A solution of 1,2-dimethoxybenzene **709**, (250mg, equal to 0.45 mol l⁻¹), tetranitromethane (0.9 mol l⁻¹), in dichloromethane or acetonitrile, was irradiated with filtered light (λ cut-off at 435 nm) at 20° and -20°. Aliquots were withdrawn from the reaction mixture at appropriate time intervals, the volatile material removed rapidly under reduced pressure at $\leq 0^\circ$, and the product composition determined by ¹H n.m.r. spectral analysis (Tables 8.7.2 and 8.7.3).

*Reaction in dichloromethane at -20° and the identification of 1,2-dimethoxy-4-trinitromethylbenzene **718** and 1,2-dimethoxy-4-nitrobenzene **719**.*

Reaction of 1,2-dimethoxybenzene in neat dichloromethane at -20°, as above, for 3 h gave a mixture of 1,2-dimethoxy-4-trinitromethylbenzene **718** (5 %), and 1,2-dimethoxy-4-nitrobenzene **719** (95 %) (Table 8.7.2). The trinitromethyl and nitro aromatic compounds **718** and **719** were isolated by radial chromatography on a silica gel Chromatotron plate using pentane-ether mixtures as the eluting solvent.

1,2-dimethoxy-4-trinitromethylbenzene **718**. Found $M^{+} - NO_2$ 241.04606, $C_9H_9N_2O_6$ requires 241.04606. 1H n.m.r. ($CDCl_3$) δ 7.19 (dd, $J_{H5,H6}$ 8.8 Hz, $J_{H5,H3}$ 2.9 Hz, H5), 7.04 (d, $J_{H3,H5}$ 2.9 Hz, H3), 6.97 (d, $J_{H6,H5}$ 8.8 Hz, H6), 3.97, 3.90 (s, 1-OMe and 2-OMe).

1,2-dimethoxy-4-nitrobenzene **719**, Identified by comparison of mass spectra with literature⁹ data. 1H n.m.r. ($CDCl_3$) δ 7.91 (dd, $J_{H5,H6}$ 8.8 Hz, $J_{H5,H3}$ 2.4 Hz, H5), 7.74 (d, $J_{H3,H5}$ 2.4 Hz, H3), 6.90 (d, $J_{H6,H5}$, H6), 3.97, 3.96 (s, 1-OMe and 2-OMe).

Reaction in dichloromethane and ethanol (8 % v/v) at 20°.

Reaction of 1,2-dimethoxybenzene in dichloromethane and ethanol (8 % v/v), as above, for 3 h gave a product, the composition of which was shown by 1H n.m.r. to be a mixture of 1,2-dimethoxy-4-trinitromethylbenzene **718** (62 %), 1,2-dimethoxy-4-nitrobenzene **719** (32 %), and ethyl 3,4-dimethoxybenzoate **720** (2 %) (Table 8.7.2).

Ethyl ester **720** was identified in the mixture by comparison of its 1H n.m.r. characteristics with authentic material.

General procedure for the photolysis of 1,4-dimethoxybenzene with tetranitromethane.

A solution of 1,4-dimethoxybenzene **710**, (250mg, equal to 0.45 mol l^{-1}), tetranitromethane (0.9 mol l^{-1}), in dichloromethane or acetonitrile, was irradiated with filtered light (λ cut-off at 435 nm) at 20°. Aliquots were withdrawn from the reaction mixture at appropriate time intervals, the volatile material removed rapidly under reduced pressure at $\leq 0^\circ$, and the product composition determined by 1H n.m.r. spectral analysis (Tables 8.7.4 and 8.7.5).

*Reaction of in dichloromethane with added ethanol (8 % v/v) and the identification of aromatic compounds **721** and **722** and adducts **724** and **725**.*

Reaction of 1,4-dimethoxybenzene **710** in dichloromethane and ethanol (8 % v/v and 4 % v/v) at 20°, as above for 5 h gave a product which was shown

by ^1H n.m.r. spectra to be a mixture of 1,4-dimethoxy-2-trinitromethylbenzene **721** (8.7 %), 1,2-dimethoxy-2-nitrobenzene **722** (82.5 %), 1,4-dimethoxy-*r*-3-nitro-*t*-6-trinitromethyl-cyclohexa-1,4-diene **724** (6.3 %), and 1,4-dimethoxy-*r*-3-nitro-*c*-6-trinitromethyl-cyclohexa-1,4-diene **725** (1.5 %) (Table 8.7.4). The aromatic compounds, 1,4-dimethoxy-2-trinitromethylbenzene **721**, and 1,2-dimethoxy-2-nitrobenzene **722** were isolated by radial chromatography of the reaction mixture on a silica gel Chromatotron plate using pentane-ether mixtures as the eluting solvent.

1,4-dimethoxy-2-trinitromethylbenzene **721**. Found M^{*+} 287.03896, $\text{C}_9\text{H}_9\text{N}_3\text{O}_8$ requires 287.03896. ^1H n.m.r. (CDCl_3) δ 7.23 (dd, $J_{\text{H}_5,\text{H}_6}$ 8.8 Hz, $J_{\text{H}_5,\text{H}_3}$ 2.9 Hz, H5), 7.04 (d, $J_{\text{H}_6,\text{H}_5}$ 8.8 Hz, H6), 6.82 (d, $J_{\text{H}_3,\text{H}_5}$ 2.9 Hz, H3), 3.79 and 3.78 (s, 1-OMe and 4-OMe).

1,4-dimethoxy-2-nitrobenzene **722**. Identified by comparison of mass spectra with literature data.⁹

Adducts **724** and **725** could not be isolated by h.p.l.c even at -20° and so were identified by n.m.r. spectroscopy performed on the crude reaction mixtures.

1,4-dimethoxy-*r*-3-nitro-*t*-6-trinitromethyl-cyclohexa-1,4-diene **724**. ^1H n.m.r. (CDCl_3) δ 5.59 (dd, $J_{\text{H}_3,\text{H}_6}$ 4.4 Hz, $J_{\text{H}_3,\text{H}_2}$ 4.4 Hz, H3), 5.20 (dd, $J_{\text{H}_2,\text{H}_3}$ 4.4 Hz, $J_{\text{H}_2,\text{H}_6}$ 1.0 Hz, H2), 5.14 (d, $J_{\text{H}_5,\text{H}_6}$ 3.9 Hz, H5), 5.06 (ddd, $J_{\text{H}_6,\text{H}_3}$ 4.4 Hz, $J_{\text{H}_6,\text{H}_5}$ 3.9 Hz, $J_{\text{H}_6,\text{H}_2}$ 1.0 Hz, H6), 3.63 (s, 4-OMe), 3.62 (s, 1-OMe). Nuclear Overhauser enhancement experiments gave the following results: irradiation at δ 5.59 gave enhancement at δ 5.20 (2.9 %); irradiation at δ 5.20 gave enhancement at δ 5.59 (4.2 %). ^{13}C n.m.r. δ 44.6 (C6), 55.9 (4-OCH₃ and 1-OCH₃), 83.1 (C3), 90.8 (C5), the remaining signals were not assigned in a very noisy spectrum. The above ^{13}C assignments were made by reverse detected heteronuclear correlation spectroscopy (HMQC).

1,4-dimethoxy-*r*-3-nitro-*c*-6-trinitromethyl-cyclohexa-1,4-diene **725**. ^1H n.m.r. (CDCl_3) δ 5.47 (dd, $J_{\text{H}_3,\text{H}_2}$ 5.3 Hz, $J_{\text{H}_3,\text{H}_6}$ 3.9 Hz, H3), 5.32 (d, $J_{\text{H}_2,\text{H}_3}$ 5.3 Hz, H2), 5.26 (d, $J_{\text{H}_5,\text{H}_6}$ 4.4 Hz, H5), 4.92 (br dd, $J_{\text{H}_6,\text{H}_5}$ 4.4 Hz, $J_{\text{H}_6,\text{H}_3}$ 3.9 Hz, H6). The $-\text{OCH}_3$ resonances were not able to be assigned from the mixture. These assignments were supported by double irradiation experiments where possible.

General procedure for the photolysis of 1,2-methylenedioxybenzene with tetranitromethane.

A solution of 1,2-methylenedioxybenzene **711**, (250mg, equal to 0.5 mol l^{-1}), tetranitromethane (1.0 mol l^{-1}), in dichloromethane or acetonitrile was irradiated with filtered light (λ cut-off at 435 nm). Aliquots were withdrawn from the reaction mixture at appropriate time intervals, the volatile material removed rapidly under reduced pressure at $\leq 0^\circ$, and the product composition determined by ^1H n.m.r. spectral analysis (Tables 8.7.6 and 8.7.7).

*Reaction in dichloromethane and the isolation of 1,2-methylenedioxy-4-trinitromethylbenzene **726** and 1,2-methylenedioxy-4-nitrobenzene **727**.*

Reaction of 1,2-methylenedioxybenzene in dichloromethane at 20° , as above, for 2 h, gave a mixture of products which were shown by ^1H n.m.r. spectra to be 1,2-methylenedioxy-4-trinitromethylbenzene **726** (32 %), 1,2-methylenedioxy-4-nitrobenzene **727** (65 %) and unknown aromatic compounds (3 %) (Table 8.7.6). The products were separated by radial chromatography on a silica gel Chromatotron plate using pentane-ether mixtures as the eluting solvent.

1,2-methylenedioxy-4-trinitromethylbenzene **726**. Found $\text{M}^{++} - \text{NO}_2$ 225.01476, $\text{C}_8\text{H}_5\text{N}_2\text{O}_6$ requires 225.01476. ^1H n.m.r. (CDCl_3) δ 7.13 (dd, $J_{\text{H}_5,\text{H}_6}$ 8.8 Hz, $J_{\text{H}_5,\text{H}_3}$ 2.4 Hz, H5), 7.05 (d, $J_{\text{H}_3,\text{H}_5}$ 2.4 Hz, H3), 6.94 (d, $J_{\text{H}_6,\text{H}_5}$ 8.8 Hz, H6), 6.14 (s, O- CH_2 -O).

1,2-methylenedioxy-4-nitrobenzene **727**. Found M^{++} 167.02186, $\text{C}_7\text{H}_5\text{NO}_4$ requires 167.02186. ^1H n.m.r. (CDCl_3) δ 7.89 (dd, $J_{\text{H}_5,\text{H}_6}$ 8.3 Hz, $J_{\text{H}_5,\text{H}_3}$

2.4 Hz, H5), 7.66 (d, $J_{\text{H3,H5}}$ 2.4 Hz, H3), 6.86 (d, $J_{\text{H6,H5}}$ 8.3 Hz, H6), 6.14 (s, O-CH₂-O).

Reaction in dichloromethane and ethanol (8 % v/v) and identification of the ester 728.

Reaction of 1,2-methylenedioxybenzene in dichloromethane and ethanol (8 % v/v) at 20°, as above, for 10h, gave a mixture which was shown by ¹H n.m.r. spectra to contain 1,2-methylenedioxy-4-trinitromethylbenzene **726** (60 %), 1,2-methylenedioxy-4-nitrobenzene **727** (19 %), 3,4-methylenedioxy-ethylbenzoate **728** (9 %), and unknown aromatic compounds (12 %) (Table 8.7.6).

3,4-methylenedioxy-ethylbenzoate **728** was identified by comparison of its ¹H n.m.r. characteristics with authentic material.

General procedure for the photolysis of 2-methylanisole with tetranitromethane in dichloromethane or acetonitrile with added ethanol.

A solution of 2-methylanisole **712**, (250mg, equal to 0.46 mol l⁻¹), tetranitromethane (0.92 mol l⁻¹), in dichloromethane or acetonitrile with added ethanol (8 % v/v) was irradiated with filtered light (λ cut-off at 435 nm). Aliquots were withdrawn from the reaction mixture at appropriate time intervals, the volatile material removed rapidly under reduced pressure at $\leq 0^\circ$, and the product composition determined by ¹H n.m.r. spectral analysis (Tables 8.7.8). All of the reaction products were identified by comparison of their ¹H n.m.r. characteristics with authentic material (see Experimental data relating to Chapter 5 for further details).

Table 8.7.1 - Overview of yields from the photolysis of 1-methoxynaphthalene (0.4 mol l^{-1}) and tetranitromethane (0.8 mol l^{-1}) in dichloromethane or acetonitrile at 20° , with added ethanol (8 % v/v).

t/h	Conversion(%)	Yield (%)						
		715	702	703	701	716	717	718
DCM/ 20° /EtOH								
0.16	19.0	tce	9.1	-	68.2	7.7	tce	14.1
0.33	41.7	2.8	10.4	-	64.0	6.0	0.9	15.8
0.5	50.9	2.4	8.8	-	66.8	4.7	1.1	16.2
0.75	59.0	1.6	10.8	-	66.9	4.3	1.0	13.4
1	75.3	1.9	7.9	-	70.5	3.5	0.8	15.4
AN/ 20° /EtOH								
0.33	20.7	0.9	31.1	-	56.9	-	-	11.1
0.5	25.2	1.6	34.1	-	53.1	-	-	11.2
0.75	36.4	1.4	30.6	-	56.0	-	-	12.0
1	41.3	1.6	30.1	-	53.8	-	-	14.5

Table 8.7.2 - Overview of yields from the photolysis of 1,2-dimethoxybenzene (0.45 mol l^{-1}) and tetranitromethane (0.9 mol l^{-1}) in dichloromethane with or without added ethanol.

Reaction conditions	t/h	Conversion (%)	Yields (%)		
			718	719	720
DCM/20°	1	21.3	11.4	88.6	-
	2	47.0	11.8	88.2	-
	3	63.9	9.6	90.4	-
DCM/-20°	1	23.1	10.8	89.2	-
	2	47.5	6.9	93.1	-
	3	67.1	4.8	95.2	-
DCM/20°/EtOH (8% v/v)	1	35.0	82.0	17.0	1.0
	2	55.0	71.0	27.0	1.0
	3	72.0	62.0	36.0	2.0
DCM/20°/EtOH (4% v/v)	1	42.6	71.1	28.4	0.5
	2	64.7	50.6	48.9	0.6
	3	84.7	42.9	55.8	1.3

Table 8.7.3 - Overview of yields from the photolysis of 1,2-dimethoxybenzene (0.45 mol l^{-1}) and tetranitromethane (0.9 mol l^{-1}) in acetonitrile with or without added ethanol.

Reaction conditions	t/h	Conversion (%)	Yields (%)		
			718	719	720
AN/20°	1	22.9	3.8	96.2	-
	2	40.6	3.4	96.6	-
	3	58.7	3.4	96.6	-
AN/-20°	1	16.5	4.5	95.5	-
	2	34.5	3.0	97.0	-
	3	50.1	2.9	97.1	-
AN/20°/EtOH (8% v/v)	1	27.9	30.9	67.6	1.5
	2	49.1	30.6	66.9	2.5
	3	64.0	26.4	70.8	2.8

Table 8.7.4 - Overview of yields from the photolysis of 1,4-dimethoxybenzene (0.45 mol l^{-1}) and tetranitromethane (0.9 mol l^{-1}) in dichloromethane with or without added ethanol.

Reaction conditions	t/h	Conversion	Yields (%)			
			721	722	724	725
20°	1	36.6	-	96.4	3.6	tce
	2	74.0	-	96.5	3.1	0.4
	3	96.0	-	96.8	2.7	0.5
20°/EtOH (8% v/v)	3	56.0	9.8	80.5	8.3	1.5
	5	84.0	8.7	82.5	6.3	1.5
20°/EtOH (4% v/v)	2	61.0	11.4	81.0	6.4	1.1
	3	88.0	8.7	83.1	5.7	1.5

Table 8.7.5 - Overview of yields from the photolysis of 1,4-dimethoxybenzene (0.45 mol l^{-1}) and tetranitromethane (0.9 mol l^{-1}) in acetonitrile with and without added ethanol.

Reaction conditions	t/h	Conversion	Yields (%)			
			721	722	724	725
20°	1	42.7	-	100	tce	tce
	2	71.8	-	99.5	0.5	tce
	3	90.9	-	99.3	0.7	tce
	4	100	-	99.1	0.9	tce
20°/EtOH (8% v/v)	1	23.1	-	100	tce	tce
	2	52.5	-	100	tce	tce
	3	71.5	-	99.5	0.5	tce
	4	85.7	-	99.1	0.9	tce

Table 8.7.6 - Overview of yields from the photolysis of 1,2-methylenedioxybenzene (0.5 mol l^{-1}) and tetranitromethane (1.0 mol l^{-1}) in dichloromethane with or without added ethanol.

Reaction conditions	t/h	Conversion (%)	Yields (%)			
			726	727	728	Unknowns
20°	1	35.9	31.7	65.3	-	3.0
	1.5	58.7	25.0	70.9	-	4.1
	2	66.1	19.2	75.3	-	5.5
-20° ^A	1	29.6	18.6	76.4	-	5.0
	1.5	41.8	12.1	83.5	-	4.4
	2	50.6	9.1	89.0	-	1.9
-40° ^A	1	32.2	10.3	86.2	-	3.4
	1.5	41.9	7.4	91.6	-	1.0
	2	39.4	9.9	87.9	-	2.2
20°/EtOH (8% v/v)	3	18.7	61.5	18.5	7.7	12.3
	6	29.3	56.3	19.4	8.7	14.6
	10	49.9	59.9	19.2	9.0	12.0
20°/EtOH (4% v/v)	3	32.4	74.5	11.8	3.9	9.8
	6	42.3	68.0	16.7	4.5	10.9
	10	58.8	51.7	33.1	5.1	10.1

^A Solid precipitated in the reaction mixture after t = 1h

Table 8.7.7 - Overview of yields from the photolysis of 1,2-methylenedioxybenzene (0.5 mol l^{-1}) and tetranitromethane (1.0 mol l^{-1}) in acetonitrile with or without added ethanol (8 % v/v).

Reaction conditions	t/h	Conversion (%)	Yields (%)			
			726	727	728	Unknowns
20°	1	26.2	-	100	-	-
	1.5	43.0	-	100	-	-
	2	61.5	-	100	-	-
-20° ^A	1	29.1	-	100	-	-
	1.5	38.9	-	100	-	-
	2	32.9	-	100	-	-
20°/EtOH (8% v/v)	3	27.7	10.5	75.6	2.9	11.0
	6	34.8	12.3	72.1	4.9	10.7
	10	54.8	6.3	81.3	8.3	4.2

^A Solid precipitated in the reaction mixture after t = 1h

Table 8.7.8 - Overview of yields from the photolysis of 2-methylanisole (0.46 mol l⁻¹) and tetranitromethane (0.92 mol l⁻¹) in dichloromethane or acetonitrile with added ethanol (8% v/v).

Reaction conditions	t/h	Conversion (%)	Yields (%)					
			Unknown			Unknown		
			729	730	Aromatics	731	732	Adducts
DCM/20°/EtOH	1	30.9	86.9	6.5	-	1.9	4.7	-
	2	60.0	87.6	7.0	-	1.2	4.1	-
	3	74.7	87.1	7.5	-	1.2	4.1	-
AN/20°/EtOH	1	16.6	81.2	12.6	-	1.1	5.0	-
	2	33.1	80.4	13.3	-	1.5	4.9	-
	3	49.2	73.7	21.2	-	1.5	3.6	-

Crystallography

Crystal data, established from precession photographs and measured accurately, by means of a Siemens R3m/V four-circle diffractometer [molybdenum X-radiation, $\lambda(\text{Mo K}\alpha)$ 0.71069 Å, or copper X-radiation, $\lambda(\text{Cu K}\alpha)$ 1.54180 Å, from a crystal monochromator] are given below. The space group was, in each case, determined unambiguously as a result of the structure analyses reported below, but initially indicated by conditions limiting possible reflections. ω -Scans were used to collect reflection intensities out to a maximum Bragg angle θ , given below. The cell parameters were determined by least-squares refinements for which the setting angles of 20-25 accurately centred high-angle reflections were used.

Crystal Data

4,8-Dimethyl-r-1-nitro-t-2-trinitromethyl-1,2-dihydronaphthalene 221. - $\text{C}_{13}\text{H}_{12}\text{N}_4\text{O}_8$, $M = 352.3$, orthorhombic, space group $Pbca$, $a = 9.316(1)$, $b = 12.868(2)$, $c = 24.695(4)$ Å, $V = 2960.4$ Å³, $D_c = 1.581$ g cm⁻³, $Z = 8$, $\mu(\text{Mo K}\alpha) = 1.34$ cm⁻¹. The crystal was colourless and of approximate dimensions 1.00 by 0.62 by 0.14 mm. Data were collected at 130 K out to a maximum Bragg angle $\theta = 22.50^\circ$. The number of independent reflections measured 1928, 885 with $I > 2\sigma(I)$; $g_1 = 0.0808$, $g_2 = 0.0000$; absorption corrections were not applied; $R_{(\text{obs})}$ -factor = 0.047, $wR_{(\text{all data})} = 0.148$.

1,5-Dimethyl-r-1-nitro-t-4-trinitromethyl-1,4-dihydronaphthalene 222. - $\text{C}_{13}\text{H}_{12}\text{N}_4\text{O}_8$, $M = 352.3$, orthorhombic, space group $Pbca$, $a = 27.496(5)$, $b = 24.468(4)$, $c = 8.949(2)$ Å, $V = 6021(2)$ Å³, $D_c = 1.555$ g cm⁻³, $Z = 16$, $\mu(\text{Mo K}\alpha) = 1.32$ cm⁻¹. The crystal was colourless and of approximate dimensions 0.80 by 0.24 by 0.12 mm. Data were collected at 130 K out to a maximum Bragg angle $\theta = 25.0^\circ$. The number of independent reflections measured 5302, 1082 with $I > 2\sigma(I)$; $g_1 = 0.0875$, $g_2 = 0.0000$; absorption corrections were not applied; $R_{(\text{obs})}$ -factor = 0.048, $wR_{(\text{all data})} = 0.182$.

Nitro cycloadduct 224. - $C_{13}H_{12}N_4O_8$, $M = 352.3$, monoclinic, space group $P 2_1/c$, $a = 10.904(2)$, $b = 6.704(1)$, $c = 19.41(1)$ Å, $\beta = 93.78(3)^\circ$, $V = 1415.5(8)$ Å³, $D_c = 1.653$ g cm⁻³, $Z = 4$, $\mu(\text{Mo K}\alpha) = 1.40$ cm⁻¹. The crystal was colourless and of approximate dimensions 1.00 by 0.57 by 0.46 mm. Data were collected at 130 K out to a maximum Bragg angle $\theta = 25.0^\circ$. The number of independent reflections measured 2129, 1737 with $I > 2\sigma(I)$; $g_1 = 0.0430$, $g_2 = 0.7400$; absorption corrections were not applied; $R_{(\text{obs})}$ -factor = 0.040, $wR_{(\text{all data})} = 0.094$.

Hydroxy cycloadduct 226. - $C_{13}H_{13}N_3O_7$, $M = 323.3$, monoclinic, space group $C 2/c$, $a = 14.610(5)$, $b = 15.110(5)$, $c = 12.430(4)$ Å, $\beta = 94.56(3)^\circ$, $V = 2735(2)$ Å³, $D_c = 1.570$ g cm⁻³, $Z = 8$, $\mu(\text{Cu K}\alpha) = 1.30$ cm⁻¹. The crystal was colourless and of approximate dimensions 0.70 by 0.37 by 0.24 mm. Data were collected at 130 K out to a maximum Bragg angle $\theta = 53.5^\circ$. The number of independent reflections measured 1622, 1401 with $I > 2\sigma(I)$; $g_1 = 0.0787$, $g_2 = 0.7400$; absorption corrections were not applied; $R_{(\text{obs})}$ -factor = 0.035, $wR_{(\text{all data})} = 0.104$.

Dinitro cycloadduct 231. - $C_{13}H_{11}N_5O_{10}$, $M = 397.3$, monoclinic, space group $P 2_1/c$, $a = 9.386(4)$, $b = 6.701(3)$, $c = 23.47(1)$ Å, $\beta = 95.34(2)^\circ$, $V = 1470(1)$ Å³, $D_c = 1.796$ g cm⁻³, $Z = 4$, $\mu(\text{Mo K}\alpha) = 1.58$ cm⁻¹. The crystal was colourless and of approximate dimensions 0.80 by 0.40 by 0.26 mm. Data were collected at 130 K out to a maximum Bragg angle $\theta = 25.0^\circ$. The number of independent reflections measured 2579, 1819 with $I > 2\sigma(I)$; $g_1 = 0.0562$, $g_2 = 0.0000$; absorption corrections were not applied; $R_{(\text{obs})}$ -factor = 0.031, $wR_{(\text{all data})} = 0.094$.

1-Methoxy-4-trinitromethylnaphthalene 309. $C_{12}H_9N_3O_7$, $M = 307.22$, orthorhombic, $P 2_12_12_1$, $a = 10.245(2)$, $b = 13.647(2)$, $c = 18.168$ Å; $V = 2540.1(7)$ Å³, $D_c = 1.607$ g cm⁻³, $Z = 8$, $\mu(\text{Mo K}\alpha) = 1.35$ cm⁻¹. The crystal was colourless and of approximate dimensions 0.60 by 0.36 by 0.26 mm. Data were collected at 130(2) K out to a maximum Bragg angle $\theta = 24.99^\circ$. Number of independent reflections measured 2001, 1543 with $I > 2\sigma(I)$. Absorption

corrections were not applied; $g_1 = 0.0387$, $g_2 = 0.0000$; $R_{(obs)}\text{-factor} = 0.037$, $wR_{(all\ data)} = 0.078$.

4,4'-Dimethoxy-1,1'-binaphthyl 319, $C_{22}H_{18}O_2$, $M = 314.36$, monoclinic, $C2/c$, $a = 25.902(7)$, $b = 6.463(2)$, $c = 9.572(3)$ Å, $\beta = 107.91(2)^\circ$; $V = 1524.7(8)$ Å³, $D_c = 1.369$ g cm⁻³, $Z = 4$, $\mu(\text{Mo K}\alpha) = 0.86$ cm⁻¹. The crystal was colourless and of approximate dimensions 0.56 by 0.20 by 0.06 mm. Data were collected at 132(2) K out to a maximum Bragg angle $\theta = 21.87^\circ$. Number of independent reflections measured = 820, 435 with $I > 2\sigma(I)$. Absorption corrections were not applied; $g_1 = 0.0474$, $g_2 = 0.0000$; $R_{(obs)}\text{-factor} = 0.041$, $wR_{(all\ data)} = 0.093$.

1-Methoxy-4-methyl-r-3-nitro-c-6-trinitromethylcyclohexa-1,4-diene 421, $C_9H_{10}N_4O_9$, $M = 318.21$, orthorhombic, space group $P 2_12_12_1$, $a = 6.786(1)$, $b = 11.817(5)$, $c = 16.180(2)$ Å; $V = 1297.5(6)$ Å³, $D_c = 1.629$ g cm⁻³, $Z = 4$, molybdenum X-radiation, $\mu(\text{Mo K}\alpha) = 0.71073$ Å, $\mu(\text{Mo K}\alpha) = 1.48$ cm⁻¹. The crystal was colourless and of approximate dimensions 0.70 by 0.68 by 0.28 mm. Data were collected at 130(2) K. Number of independent reflections measured 1945, 1823 with $I > 2\sigma(I)$. Absorption corrections were not applied; $g_1 = 0.0304$, $g_2 = 0.4404$; $R_{(obs)}\text{-factor} = 0.028$, $wR_{(all\ data)} = 0.066$.

1-Methoxy-6-methyl-c-6-nitro-r-3-trinitromethylcyclohexa-1,4-diene 519, $C_9H_{10}N_4O_9$, $M = 318.21$, triclinic, space group P_1 , $a = 6.097(2)$, $b = 10.290(2)$, $c = 11.188(2)$ Å, $\alpha = 73.23(1)$, $\beta = 86.80(2)$, $\gamma = 83.91(3)^\circ$; $V = 668.0(3)$ Å³, $D_c = 1.582$ g cm⁻³, $Z = 2$, $\mu(\text{Mo K}\alpha) = 1.44$ cm⁻¹. The crystal was colourless and of approximate dimensions 0.90 by 0.48 by 0.16 mm. Data were collected at 166(2) K. Number of independent reflections measured 2345, 1699 with $I > 2\sigma(I)$. Absorption corrections were not applied; $g_1 = 0.0531$, $g_2 = 0.4300$; $R_{(obs)}\text{-factor} = 0.054$, $wR_{(all\ data)} = 0.130$.

4-Fluoro-5-methyl-2-trinitromethylanisole 630, $C_9H_8FN_3O_7$, $M = 289.18$, monoclinic, space group $P 2_1/n$, $a = 7.646(1)$, $b = 7.272(2)$, $c = 21.196(9)$ Å, $\beta =$

94.28(2) °; $V = 1175.2(6) \text{ \AA}^3$, $D_c = 1.634 \text{ g cm}^{-3}$, $Z = 4$, $\mu(\text{Mo K}\alpha) = 1.52 \text{ cm}^{-1}$. The crystal was yellow in colour and of approximate dimensions 0.7 by 0.6 by 0.3 mm. Data were collected at 158(2) K out to a maximum Bragg angle $\theta = 24.0^\circ$. Number of independent reflections measured 1845, 1389 with $I > 2\sigma(I)$. Absorption corrections were not applied; $g_1 = 0.0463$, $g_2 = 0.6000$; $R_{(\text{obs})}$ -factor = 0.041, $wR_{(\text{all data})} = 0.107$.

4-Fluoro-5-methyl-2-nitroanisole **633**, $\text{C}_8\text{H}_8\text{FNO}_3$, $M = 185.15$, monoclinic, $P 2_1/n$, $a = 7.979(2)$, $b = 12.852(3)$, $c = 15.932(3) \text{ \AA}$, $\beta = 98.15(2)^\circ$; $V = 1617.3(6) \text{ \AA}^3$, $D_c = 1.521 \text{ g cm}^{-3}$, $Z = 8$, $\mu(\text{Mo K}\alpha) = 1.31 \text{ cm}^{-1}$. The crystal was colourless and of approximate dimensions 0.8 by 0.7 by 0.3 mm. Data were collected at 158(2) K out to a maximum Bragg angle $\theta = 22.5^\circ$. Number of independent reflections measured 2105, 1272 with $I > 2\sigma(I)$. Absorption corrections were not applied; $g_1 = 0.0516$, $g_2 = 1.3300$; $R_{(\text{obs})}$ -factor = 0.047, $wR_{(\text{all data})} = 0.142$.

Structure Determination

The structures were solved by direct methods and difference-Fourier syntheses. Full-matrix least-squares refinements (SHELXL-93)¹⁰ were employed. This program is based on intensities and uses all data. The observed threshold $I > 2\sigma(I)$ was used only for calculating $R_{(\text{obs})}$, shown here as a comparison for the refinements based on F . Reflection weights $1/[\sigma^2(F_o^2) + (g_1P)^2 + g_2P]$, where $P = (F_o + 2F_c^2)/3$, were used. All non-hydrogen atoms were assigned anisotropic thermal parameters. Methyl hydrogen atoms were included as rigid groups pivoting about their carbon atoms. Final Fourier syntheses show no abnormal discrepancies between observed and calculated structure factors.

Table 8.1 Atomic coordinates [$\times 10^4$] and equivalent isotropic displacement parameters [$\text{\AA}^2 \times 10^3$] for **221**. $U_{(\text{eq})}$ is defined as one third of the trace of the orthogonalised U_{ij} tensor.

	x/a	y/b	z/c	$U_{(\text{eq})}$
O(11)	5993(5)	4267(4)	1312(2)	58(2)
O(12)	4897(5)	3853(3)	575(2)	37(1)
O(21)	-709(5)	6338(4)	1251(2)	44(1)
O(22)	-301(5)	4693(5)	1057(2)	42(1)
O(31)	1745(5)	7285(4)	1446(2)	41(1)
O(32)	2550(5)	7420(3)	621(2)	34(1)
O(41)	2277(5)	5375(4)	-10(2)	40(1)
O(42)	213(4)	6152(3)	85(2)	32(1)
N(1)	5109(5)	4439(4)	958(2)	29(1)
N(2)	20(6)	5614(6)	1088(2)	34(2)
N(3)	1952(5)	6946(4)	993(2)	29(1)
N(4)	1327(6)	5793(4)	252(2)	27(1)
C(1)	4194(6)	5417(5)	993(2)	20(2)
C(2)	2637(6)	5044(5)	1085(2)	26(2)
C(3)	2380(7)	4801(5)	1681(2)	24(2)
C(4)	3091(6)	5272(5)	2076(2)	21(2)
C(4A)	4187(6)	6064(5)	1952(2)	21(2)
C(5)	4684(6)	6737(5)	2343(2)	22(2)
C(6)	5702(6)	7482(5)	2217(2)	27(2)
C(7)	6249(6)	7552(5)	1695(2)	24(2)
C(8)	5779(6)	6894(5)	1291(2)	20(2)
C(8A)	4741(6)	6145(4)	1419(2)	17(1)
C(9)	1545(6)	5823(5)	874(2)	22(2)
C(10)	2767(6)	5006(5)	2653(2)	26(2)
C(11)	6393(6)	6993(5)	725(2)	27(2)

Table 8.2 Atomic coordinates ($\times 10^4$) and equivalent isotropic displacement parameters ($\text{\AA}^2 \times 10^3$) for **222**. $U_{(\text{eq})}$ is defined as one third of the trace of the orthogonalised U_{ij} tensor.

	x/a	y/b	z/c	$U_{(\text{eq})}$
O(11)	3424(3)	1942(3)	24039(7)	75(2)
O(12)	3347(2)	1090(2)	23569(6)	40(2)
O(21)	4590(3)	1845(2)	18701(9)	91(3)
O(22)	5072(2)	1229(3)	19655(6)	53(2)
O(31)	4233(2)	657(2)	15926(7)	53(2)
O(32)	084(2)	1497(2)	16496(6)	43(2)
O(41)	5120(2)	507(2)	17365(7)	47(2)
O(42)	4633(2)	-16(2)	18612(7)	55(2)
O(11')	2085(2)	857(2)	15777(6)	40(2)
O(12')	1513(2)	380(2)	14729(6)	37(2)
O(21')	1650(2)	2119(2)	10877(7)	50(2)
O(22')	919(2)	2464(3)	11251(7)	66(2)
O(31')	914(2)	1342(2)	7549(6)	55(2)
O(32')	1596(2)	1740(2)	8172(6)	45(2)
O(41')	108(2)	1505(2)	10194(6)	47(2)
O(42')	365(2)	2193(3)	8883(8)	78(2)
N(1)	3516(2)	1537(3)	23334(7)	37(2)
N(2)	4731(2)	1389(3)	18894(7)	40(2)
N(3)	4232(2)	1054(3)	16749(8)	32(2)
N(4)	4750(2)	423(3)	18105(8)	37(2)
N(1')	1772(2)	789(2)	14834(7)	23(2)
N(2')	1215(3)	2129(2)	10767(7)	37(2)
N(3')	1192(3)	1571(3)	8418(7)	32(2)
N(4')	423(3)	1796(3)	9678(8)	42(2)
C(1)	3872(3)	1579(3)	21993(8)	25(2)
C(2)	4173(3)	1076(3)	22096(8)	27(2)
C(3)	4228(3)	722(3)	21013(9)	29(2)

C(4)	4002(2)	792(3)	19485(8)	22(2)
C(4A)	3585(2)	1200(3)	19483(8)	19(2)
C(5)	3221(3)	1165(3)	18386(8)	22(2)
C(6)	2863(2)	1549(3)	18375(8)	27(2)
C(7)	2854(3)	1953(3)	19440(9)	33(2)
C(8)	3180(3)	1973(3)	20572(9)	29(2)
C(8A)	3553(3)	1591(3)	20616(8)	20(2)
C(9)	4410(2)	916(3)	18349(8)	25(2)
C(10)	4159(3)	2095(3)	22193(10)	59(3)
C(11)	3181(2)	712(3)	17253(8)	26(2)
C(1')	1685(2)	1244(3)	13620(8)	21(2)
C(2')	1144(3)	1340(3)	13687(8)	26(2)
C(3')	839(3)	1284(3)	12545(8)	23(2)
C(4')	1015(2)	1116(3)	11013(8)	20(2)
C(4A')	1526(2)	868(3)	10988(8)	19(2)
C(5')	1675(3)	515(3)	9831(8)	24(2)
C(6')	2159(3)	344(3)	9821(9)	28(2)
C(7')	2479(3)	499(3)	10899(8)	27(2)
C(8')	2328(2)	802(3)	12079(8)	23(2)
C(8A')	1851(3)	979(2)	12160(8)	17(2)
C(9')	967(2)	1637(3)	9986(8)	22(2)
C(10')	1989(3)	1743(3)	14090(8)	33(2)
C(11')	1340(3)	272(3)	8683(8)	36(2)

Table 8.3 Atomic coordinates [$\times 10^4$] and equivalent isotropic displacement parameters [$\text{\AA}^2 \times 10^3$] for **224**. $U_{(\text{eq})}$ is defined as one third of the trace of the orthogonalised U_{ij} tensor.

	x/a	y/b	z/c	$U_{(\text{eq})}$
O(11)	3348(1)	14(2)	7080(1)	18(1)
O(12)	4563(1)	2584(2)	7360(1)	21(1)
O(21)	6444(2)	1711(3)	6292(1)	31(1)
O(22)	5554(2)	4165(3)	5738(1)	34(1)
O(31)	3694(2)	266(3)	5143(1)	26(1)
O(32)	4624(2)	-1618(2)	5922(1)	29(1)
O(41)	1635(2)	6345(3)	7096(1)	31(1)
O(42)	2036(2)	6957(2)	6035(1)	27(1)
N(1)	4456(2)	910(3)	6913(1)	18(1)
N(2)	5546(2)	2632(3)	6066(1)	21(1)
N(3)	4177(2)	-54(3)	5717(1)	20(1)
N(4)	2233(2)	6117(3)	6592(1)	21(1)
C(1)	3247(2)	3261(3)	6050(1)	17(1)
C(2)	3317(2)	4721(3)	6665(1)	17(1)
C(3)	3348(2)	3465(3)	7316(1)	18(1)
C(4)	2479(2)	1626(3)	7256(1)	18(1)
C(4A)	1533(2)	1750(3)	6647(1)	17(1)
C(5)	322(2)	1197(4)	6691(1)	23(1)
C(6)	-473(2)	1304(4)	6104(1)	28(1)
C(7)	-67(2)	1958(4)	5486(1)	26(1)
C(8)	1149(2)	2537(3)	5429(1)	20(1)
C(8A)	1949(2)	2404(3)	6021(1)	16(1)
C(9)	4271(2)	1740(3)	6207(1)	17(1)
C(10)	2010(2)	1068(4)	7943(1)	25(1)
C(11)	1536(2)	3315(4)	4749(1)	28(1)

Table 8.4 Atomic coordinates [$\times 10^4$] and equivalent isotropic displacement parameters [$\text{\AA}^2 \times 10^3$] for **226**. $U_{(\text{eq})}$ is defined as one third of the trace of the orthogonalised U_{ij} tensor.

	x/a	y/b	z/c	$U_{(\text{eq})}$
O(11)	2863(1)	444(1)	2062(1)	20(1)
O(12)	4232(1)	236(1)	1472(1)	21(1)
O(2)	3452(1)	1154(1)	-1103(1)	20(1)
O(21)	4137(1)	-1455(1)	-185(1)	28(1)
O(22)	3927(1)	-1928(1)	1421(1)	35(1)
O(31)	1920(1)	-1108(1)	1939(1)	27(1)
O(32)	1942(1)	-1738(1)	375(1)	29(1)
N(1)	3455(1)	-237(1)	1796(1)	19(1)
N(2)	3781(1)	-1427(1)	660(2)	22(1)
N(3)	2233(1)	-1226(1)	1078(2)	19(1)
C(1)	2858(1)	-154(2)	-221(2)	15(1)
C(2)	3663(2)	498(1)	-331(2)	15(1)
C(3)	3829(2)	924(2)	763(2)	18(1)
C(4)	2941(2)	1184(1)	1287(2)	19(1)
C(4A)	2082(2)	1128(2)	533(2)	19(1)
C(5)	1365(2)	1727(2)	561(2)	27(1)
C(6)	562(2)	1575(2)	-102(2)	31(1)
C(7)	482(2)	858(2)	-760(2)	29(1)
C(8)	1193(2)	246(2)	-815(2)	21(1)
C(8A)	2000(2)	395(1)	-159(2)	16(1)
C(9)	3071(1)	-700(2)	804(2)	16(1)
C(10)	3051(2)	2009(2)	1969(2)	30(1)
C(11)	1059(2)	-525(2)	-1568(2)	28(1)

Table 8.5 Atomic coordinates [$\times 10^4$] and equivalent isotropic displacement parameters [$\text{\AA}^2 \times 10^3$] for **227**. $U_{(\text{eq})}$ is defined as one third of the trace of the orthogonalised U_{ij} tensor.

	x/a	y/b	z/c	$U_{(\text{eq})}$
O(1)	5880(2)	5933(3)	6843(1)	19(1)
O(11)	7323(2)	2388(3)	6465(1)	25(1)
O(12)	6790(2)	537(3)	939(1)	31(1)
O(21)	3849(2)	1857(3)	6269(1)	18(1)
O(22)	4847(2)	470(3)	5730(1)	23(1)
O(32)	4961(2)	4380(3)	7985(1)	27(1)
O(31)	3747(2)	5404(3)	7474(1)	25(1)
C(4A)	3762(3)	4464(4)	6117(2)	13(1)
N(1)	6635(3)	1638(4)	6229(2)	22(1)
N(2)	4851(2)	1478(3)	6090(1)	17(1)
N(3)	4383(2)	4461(3)	7546(2)	18(1)
C(8A)	4676(3)	5213(4)	6042(2)	13(1)
C(1)	5629(3)	4841(4)	6407(2)	15(1)
C(2)	5516(3)	3419(4)	6763(2)	14(1)
C(3)	4487(3)	3280(4)	7074(2)	14(1)
C(4)	3672(3)	3258(4)	6583(2)	16(1)
C(5)	2922(3)	4807(4)	5758(2)	18(1)
C(6)	2980(3)	5914(4)	5339(2)	20(1)
C(7)	3877(3)	6677(4)	5271(2)	19(1)
C(8)	4735(3)	6342(4)	5612(2)	14(1)
C(9)	5625(3)	2169(4)	6342(2)	13(1)
C(10)	2605(3)	3017(4)	6839(2)	22(1)
C(11)	5703(3)	7189(4)	5515(2)	22(1)

Table 8.6 Atomic coordinates [$\times 10^4$] and equivalent isotropic displacement parameters [$\text{\AA}^2 \times 10^3$] for **231**. $U_{(\text{eq})}$ is defined as one third of the trace of the orthogonalised U_{ij} tensor.

	x/a	y/b	z/c	$U_{(\text{eq})}$
O(12)	9993(2)	5811(2)	6942(1)	17(1)
O(41)	6460(2)	1590(2)	6132(1)	21(1)
O(11)	8860(2)	8385(2)	6519(1)	15(1)
O(51)	8408(2)	6407(3)	4662(1)	25(1)
O(22)	7743(2)	3840(2)	7808(1)	21(1)
N(3)	6710(2)	8214(3)	7289(1)	16(1)
O(21)	8520(2)	6670(3)	8136(1)	28(1)
O(52)	7531(2)	9358(3)	4563(1)	31(1)
O(42)	8281(2)	2221(3)	5669(1)	27(1)
O(32)	7110(2)	9906(2)	7268(1)	22(1)
C(4A)	7357(2)	6740(3)	5811(1)	13(1)
N(2)	8025(2)	5569(3)	7760(1)	16(1)
N(5)	7665(2)	7769(3)	4807(1)	18(1)
N(4)	7592(2)	2407(3)	6079(1)	16(1)
C(7)	4426(2)	6923(3)	5515(1)	15(1)
O(31)	5549(2)	7649(3)	7416(1)	24(1)
N(1)	9096(2)	7429(3)	7052(1)	16(1)
C(8A)	6385(2)	6090(3)	6186(1)	13(1)
C(5)	6796(2)	7391(3)	5281(1)	14(1)
C(3)	9392(2)	5006(3)	6404(1)	16(1)
C(4)	8900(2)	6883(3)	6062(1)	14(1)
C(8)	4915(2)	6106(3)	6036(1)	14(1)
C(11)	3865(2)	5223(4)	6405(1)	19(1)
C(1)	7014(2)	5088(3)	6731(1)	13(1)
C(6)	5346(2)	7553(3)	5135(1)	16(1)
C(9)	7721(2)	6537(3)	7169(1)	14(1)
C(2)	8196(2)	3703(3)	6560(1)	15(1)
C(10)	10026(2)	7653(4)	5705(1)	18(1)

Table 8.7 Atomic coordinates [$\times 10^4$] and equivalent isotropic displacement parameters [$\text{\AA}^2 \times 10^3$] for **309**. $U_{(\text{eq})}$ is defined as one third of the trace of the orthogonalised U_{ij} tensor.

	x/a	y/b	z/c	$U_{(\text{eq})}$
O(1)	5134(4)	1138(2)	2213(2)	28(1)
O(11)	7026(4)	2230(2)	5870(2)	42(1)
O(12)	6191(4)	778(3)	5756(2)	40(1)
O(21)	8745(4)	139(2)	5788(2)	33(1)
O(22)	8678(4)	-351(2)	4655(2)	30(1)
O(31)	9913(4)	1794(2)	5214(2)	30(1)
O(32)	8560(4)	2778(2)	4665(2)	39(1)
O(1')	3100(4)	3618(2)	2532(2)	23(1)
O(11')	6057(4)	4516(2)	-565(2)	32(1)
O(12')	6782(4)	3040(2)	-732(2)	33(1)
O(21')	7921(4)	5276(2)	925(2)	32(1)
O(22')	8632(4)	4831(2)	-148(2)	34(1)
O(31')	7520(4)	2125(2)	544(2)	33(1)
O(32')	9222(5)	3067(3)	496(2)	36(1)
N(1')	6610(4)	3771(3)	-368(2)	24(1)
N(2')	7979(4)	4721(3)	403(2)	25(1)
N(3')	8067(6)	2912(3)	493(2)	24(1)
N(1)	6931(5)	1436(3)	5577(2)	29(1)
N(2)	8471(4)	231(3)	5146(2)	25(1)
N(3)	8868(5)	1997(3)	4943(2)	25(1)
C(1)	5725(6)	1144(3)	2879(2)	18(1)
C(2)	5076(5)	1163(3)	3530(2)	21(1)
C(3)	5781(6)	1180(3)	4189(2)	18(1)
C(4)	7106(6)	1181(3)	4202(2)	15(1)
C(5)	9190(6)	1133(3)	3468(2)	26(2)
C(6)	9791(6)	1113(4)	2799(3)	29(1)
C(7)	9089(7)	1093(4)	2145(3)	29(2)

C(8)	7762(7)	1101(3)	2177(2)	27(2)
C(8A)	7095(6)	1127(3)	2854(2)	17(1)
C(4A)	7809(6)	1156(3)	3524(2)	17(1)
C(9)	3743(7)	1143(4)	2191(3)	35(2)
C(10)	7802(5)	1203(3)	4918(2)	21(1)
C(1')	4032(6)	3663(3)	2001(2)	16(1)
C(2')	3772(5)	3681(3)	1266(2)	19(1)
C(3')	4806(5)	3730(3)	767(2)	19(1)
C(4')	6069(5)	3762(3)	982(2)	17(1)
C(5')	7666(6)	3713(4)	2047(2)	23(1)
C(6')	7883(6)	3677(3)	2786(2)	24(1)
C(7')	6846(6)	3650(3)	3281(2)	24(1)
C(8')	5597(6)	3642(3)	3029(2)	21(1)
C(4A')	6381(6)	3717(3)	1759(2)	16(1)
C(8A')	5338(6)	3673(3)	2262(2)	16(1)
C(9')	1778(6)	3590(4)	2306(3)	28(2)
C(10')	7116(5)	3795(3)	422(2)	20(1)

Table 8.8 Atomic coordinates [$\times 10^4$] and equivalent isotropic displacement parameters [$\text{\AA}^2 \times 10^3$] for **319**. $U_{(\text{eq})}$ is defined as one third of the trace of the orthogonalised U_{ij} tensor.

	x/a	y/b	z/c	$U_{(\text{eq})}$
O(1)	1957(1)	839(4)	3115(3)	23(1)
C(10)	1218(1)	2517(5)	3523(4)	15(1)
C(2)	1060(1)	-627(6)	2117(4)	20(1)
C(4)	295(1)	1110(5)	2569(4)	15(1)
C(7)	1381(1)	5691(6)	4934(4)	21(1)
C(9)	655(1)	2659(5)	3369(4)	15(1)
C(1)	1408(1)	836(6)	2892(4)	16(1)
C(3)	503(1)	-455(5)	1972(4)	20(1)
C(5)	479(1)	4344(6)	4047(4)	18(1)
C(6)	829(1)	5824(6)	4812(4)	22(1)
C(8)	1569(1)	4100(6)	4311(4)	18(1)
C(11)	2166(1)	-818(6)	2466(5)	29(1)

Table 8.9 Atomic coordinates [$\times 10^4$] and equivalent isotropic displacement parameters [$\text{\AA}^2 \times 10^3$] for **421**. $U_{(\text{eq})}$ is defined as one third of the trace of the orthogonalised U_{ij} tensor.

	x/a	y/b	z/c	$U_{(\text{eq})}$
O(1)	1476(2)	9513(1)	9488(1)	23(1)
O(11)	147(3)	13476(1)	11427(1)	48(1)
O(12)	2879(3)	12569(1)	11262(1)	46(1)
O(21)	6933(3)	8312(1)	11478(1)	40(1)
O(22)	4038(3)	7841(1)	11937(1)	38(1)
O(31)	6227(3)	9090(1)	9654(1)	35(1)
O(32)	4161(3)	7730(1)	9924(1)	34(1)
O(41)	5723(2)	10531(1)	11711(1)	34(1)
O(42)	5270(2)	10972(1)	10415(1)	34(1)
N(1)	1095(3)	12616(1)	11295(1)	29(1)
N(2)	5139(3)	8378(1)	11501(1)	27(1)
N(3)	4938(3)	8644(1)	10055(1)	25(1)
N(4)	5209(3)	10330(1)	11003(1)	24(1)
C(1)	1173(3)	10042(2)	10225(1)	18(1)
C(2)	291(3)	11028(2)	10339(1)	20(1)
C(3)	-71(3)	11504(2)	11182(1)	22(1)
C(4)	468(3)	10738(2)	11888(1)	19(1)
C(5)	1357(3)	9754(2)	11760(1)	18(1)
C(6)	1970(3)	9315(2)	10919(1)	18(1)
C(7)	634(3)	10049(2)	8771(1)	27(1)
C(9)	4229(3)	9198(2)	10863(1)	20(1)
C(8)	-131(3)	11132(2)	12733(1)	24(1)

Table 8.10 Atomic coordinates [$\times 10^4$] and equivalent isotropic displacement parameters [$\text{\AA}^2 \times 10^3$] for **519**. $U_{(\text{eq})}$ is defined as one third of the trace of the orthogonalised U_{ij} tensor.

	x/a	y/b	z/c	$U_{(\text{eq})}$
O1	1790(3)	-71(2)	1508(2)	32(1)
O42	-1357(3)	2999(2)	-875(2)	41(1)
O32	-888(3)	3822(3)	2623(2)	53(1)
N4	-664(4)	2408(2)	158(2)	31(1)
C1	2333(4)	1167(2)	1539(2)	24(1)
C2	3205(4)	1420(2)	2498(2)	25(1)
O22	4419(5)	1414(2)	4960(2)	56(1)
C3	3760(4)	2816(2)	2476(2)	24(1)
O12	1182(4)	5465(2)	3658(2)	56(1)
N3	73(4)	3126(2)	3535(2)	35(1)
C5	2526(4)	3582(3)	282(2)	28(1)
C4	3341(4)	3858(3)	1238(2)	27(1)
O21	2796(5)	2995(3)	5673(2)	66(1)
O31	-694(4)	2266(3)	4380(2)	61(1)
C6	1876(4)	2206(3)	308(2)	25(1)
N2	3328(4)	2482(2)	4847(2)	34(1)
N1	2799(5)	4760(2)	3481(2)	40(1)
O41	-1855(4)	2002(3)	1070(2)	58(1)
O11	4674(4)	5055(2)	3291(3)	60(1)
C8	2515(4)	3279(3)	3540(2)	27(1)
C9	2916(5)	1748(3)	-793(2)	36(1)
C7	1786(7)	-1106(3)	2684(3)	48(1)

Table 8.11 Atomic coordinates [$\times 10^4$] and equivalent isotropic displacement parameters [$\text{\AA}^2 \times 10^3$] for **630**. $U_{(\text{eq})}$ is defined as one third of the trace of the orthogonalised U_{ij} tensor.

	x/a	y/b	z/c	$U_{(\text{eq})}$
F1'	5349(3)	-3142(2)	-47(2)	40(1)
O11'	4587(4)	382(2)	1111(2)	47(1)
O12'	2235(4)	160(2)	1628(2)	44(1)
O4'	2759(4)	-1497(2)	2658(2)	34(1)
N1'	3507(5)	-179(3)	1366(2)	32(1)
C1'	4671(5)	-2743(3)	621(3)	28(1)
C2'	4454(5)	-1696(3)	660(3)	29(1)
C3'	3757(5)	-1304(3)	1338(3)	26(1)
C4'	3331(5)	-1946(3)	1982(3)	26(1)
C5'	3593(5)	-3004(3)	1909(3)	26(1)
C6'	4246(5)	-3429(3)	1222(3)	27(1)
C7'	2478(6)	-2168(3)	3345(3)	33(1)
C8'	4494(6)	-4582(3)	1138(3)	35(1)
F1	-312(3)	13214(2)	10018(2)	39(1)
O11	1640(4)	9736(2)	9391(2)	42(1)
O12	1549(4)	9701(2)	8034(2)	40(1)
O4	2255(4)	11453(2)	7339(2)	31(1)
N1	1511(4)	10162(3)	8697(3)	31(1)
C1	365(5)	12783(3)	9360(3)	28(1)
C2	636(5)	11736(3)	9360(3)	27(1)
C3	1268(5)	11294(3)	8678(3)	25(1)
C4	1638(5)	11906(3)	7998(3)	24(1)
C5	1380(5)	12977(3)	8048(3)	26(1)
C6	737(5)	13426(3)	8722(3)	27(1)
C7	2592(6)	12116(3)	6662(3)	33(1)
C8	430(6)	14586(3)	8751(3)	38(1)

Table 8.12 Atomic coordinates ($\times 10^4$) and equivalent isotropic displacement parameters ($\text{\AA}^2 \times 10^3$) for **633**. $U_{(\text{eq})}$ is defined as one third of the trace of the orthogonalised U_{ij} tensor.

	x/a	y/b	z/c	$U_{(\text{eq})}$
F(1)	2789(2)	8583(2)	2255(1)	37(1)
O(4)	-2330(2)	10005(2)	394(1)	27(1)
O(12)	-947(3)	13743(2)	629(1)	35(1)
O(11)	-3775(3)	13911(3)	634(1)	42(1)
O(32)	-4497(2)	10015(3)	1391(1)	34(1)
O(31)	-5028(2)	12725(3)	1763(1)	45(1)
C(3)	103(3)	8106(3)	796(1)	25(1)
N(2)	-1724(3)	13479(3)	1988(1)	32(1)
O(22)	-1188(3)	14991(3)	1867(1)	49(1)
N(3)	-4101(3)	11572(3)	1543(1)	29(1)
C(6)	398(3)	10310(4)	1860(1)	24(1)
O(21)	-1876(3)	12831(3)	2506(1)	42(1)
C(9)	-2204(3)	12182(4)	1439(1)	24(1)
C(2)	1431(3)	7758(4)	1266(1)	27(1)
C(1)	1514(3)	8886(4)	1784(1)	26(1)
N(1)	-2339(3)	13393(3)	839(1)	28(1)
C(8)	-2840(4)	8665(4)	-78(1)	32(1)
C(4)	-1059(3)	9541(3)	849(1)	22(1)
C(7)	2708(4)	6209(4)	1202(2)	40(1)
C(5)	-933(3)	10654(3)	1391(1)	23(1)

References

- ¹ Davies, A., and Warren, K. D., *J. Chem. Soc. B*, 1969, 873.
- ² Butts, C. P., Ebersson, L., Hartshorn, M. P., and Robinson, W. T., *Acta Chem. Scand.*, 1995, **49**, 389.
- ³ *Dictionary of Organic Compounds*, 5th Edn., Chapman and Hall, London, 1982.
- ⁴ (a) Bamsal, S. R., Nonhebel, D. C., and Mancilla, J. M., *Tetrahedron*, **29**, 1973, 993. (b) McKillop, A., Turrell, A. G., Young, D. W., and Taylor, E. C., *J. Am. Chem. Soc.*, **102**, 1980, 6504.
- ⁵ Sankararaman, S., and Kochi, J. K., *Recl. Trav. chim.*, 1986, **105**, 278.
- ⁶ Gibson, G. P., *J. Chem. Soc.*, 1925, **127**, 42.
- ⁷ Cross, G. G., Fischer, A., Henderson, G. N., and Smyth, T. A., *Can. J. Chem.*, 1984, **62**, 1446.
- ⁸ Clewley, R. G., Fischer, A., and Henderson, G. N., *Can. J. Chem.*, 1989, 1472.
- ⁹ NIST/NBS Mass spectral library.
- ¹⁰ Sheldrick, G. M., *J. Appl. Crystallogr.*, in preparation.

Acknowledgements

Well, two and a half years and here I am. My sincere thanks must go to all the members of staff who have given their time and expertise to help me in my work, in particular:-

- Bruce Clarke, for his glorious achievements in finding the compounds I wanted within the mixtures I gave him.
- Laurie Anderson and Bruce Whitfield who remembered my dry ice even when I forgot it.
- Ward Robinson, Mark Turnbull, and everyone else in X-ray who put up with an outsider until he learnt how to use the machine, and then still put up with him once he learnt how to break it!

All of my work has been made, not necessarily much easier, but certainly more enjoyable through the efforts of my fellow members of the Hartshorn tetranitromethane group, Dawson Young, Karen Fulton, Dave Timmerman-Vaughan, Bryan Wood and special thanks to Jane Calvert for teaching me everything I needed to know about photonitrating (including how to survive to tell this tale!).

To Professor Michael Hartshorn, well what can I say - please accept my heartfelt thanks and eternal gratitude for your tireless enthusiasm, encouragement and the occasional kick up the backside! Cheers Michael, it's been fun.

Finally to my parents who put up with me at home for twenty years and have now put up with my phone calls for the last three. You have given me the tools I need in life, let me choose my own path, and have never failed to support me all the way. Thank you.